U.PORTO
FC FACULDADE DE CIÊNCIAS
UNIVERSIDADE DO PORTO

Heteroclinic Dynamics in Game Theory

Liliana Sofia Garrido da Silva
Tese de Doutoramento apresentada à
Faculdade de Ciências da Universidade do Porto
Matemática
2018

PhD

Heteroclinic Dynamics in Game Theory

Liliana Sofia Garrido da Silva
Programa de Doutoramento em Matemática Aplicada
Departamento de Matemática
2018

Orientador
Sofia Balbina Santos Dias de Castro Gothen, Professora Catedrática, Faculdade de Economia da Universidade do Porto

Heteroclinic Dynamics in Game Theory

Liliana Sofia Garrido da Silva

MAP-PDMA | PhD in Applied Mathematics

Programa de Doutoramento em Matemática Aplicada

PhD Thesis | Tese de Doutoramento

Supervisor | **Orientador:** Sofia Balbina Santos Dias de Castro Gothen

September 2018

Acknowledgements

I would like to acknowledge the financial support of

- Fundação Portuguesa para a Ciência e a Tecnologia (FCT – Portugal) through a PhD grant number PD/BD/105731/2014 with national (MEC) and European structural funds (FEDER),
- Programa de Acções Integradas Luso-Alemãs 2017 resulting from an agreement between the Deutscher Akademischer Austauschdienst (DAAD) and Conselho de Reitores das Universidades Portuguesas (CRUP), and
- Centro de Matemática da Universidade do Porto (CMUP – UID/MAT/00144/2013), which is funded by FCT (Portugal) with national (MEC) and European structural funds (FEDER), under the partnership agreement PT2020.

I would like to express my deep sense of gratitude to my supervisor, Professor Sofia Castro, for proposing me a challenging research project, her patient guidance, enthusiastic encouragement, and all opportunities to meet researchers working across subjects linked to dynamical systems. It has been my proud privilege to share of her exceptional scientific knowledge and human qualities.

I am extremely thankful to Alexander Lohse for his valuable collaboration and constructive suggestions that helped to shape this work. His willingness to give his time so generously and receive me warmly in Hamburg has been very much appreciated.

My grateful thanks are extended to Alexandre Rodrigues for precious advices and discussions, and Professor Isabel Labouriau who was always available to help me.

My acknowledgement would never be complete without the special mention of my friends Pedro Soares and Juliane Oliveira for their moral support, motivation, and the enjoyable moments discussing interesting problems or laughing at terrible jokes.

Sometimes we need someone simply be there. Not to fix anything or do anything in particular, but just to let us feel we are supported and cared about. Thank you so much Cristiana Machado for being such a good friend.

From the bottom of my heart I want to thank to someone who really loves me, sees what a mess I can be, how moody I can get, how hard I am to handle but still wants me in his life: my darling and wonderful husband José António.

I dedicate this work to the memory of my eternal friend, Jacinta Brandão, who left me an important message that has become my motto of life

"Quanto maior for o sacrifício mais belo deve ser o sorriso!"

Abstract

The goal of this thesis is to understand the stability and the dynamics of robust heteroclinic cycles and networks made up of hyperbolic saddle equilibra and one-dimensional heteroclinic connections.

We start by presenting the essential background in heteroclinic dynamics. Accordingly, the stability of heteroclinic cycles can be obtained from the value of the local stability index along each heteroclinic connection. We develop a systematic method to compute the local stability index for a new class of robust heteroclinic cycles that we call *quasi-simple heteroclinic cycles*. A heteroclinic cycle is quasi-simple if the heteroclinic connections are one-dimensional and contained in flow-invariant spaces of equal dimension. They occur both in symmetric and non-symmetric contexts. We make one assumption on the dynamics along the heteroclinic connections to ensure that transition matrices to cross sections around the heteroclinic cycle exist and have a convenient form. Our results are constructive in the sense that we define a function whose images provide the value of the local stability index. Such a method applies to all simple heteroclinic cycles of type Z and to various heteroclinic cycles arising in game theory and population dynamics, namely non-simple heteroclinic cycles, as well as to heteroclinic cycles that are part of a heteroclinic network.

The dynamics near robust heteroclinic networks has been studied extensively due to its complexity. The occurrence of infinite switching near a heteroclinic network can induce chaotic behaviour. The mechanism seems to be related to transverse intersections between stable and unstable manifolds and/or rotating nodes (either with complex eigenvalues or periodic orbits). To our knowledge no consistent information is known about infinite switching near heteroclinic networks whose linearisation at equilibria has only real eigenvalues. We actually prove that there is no infinite switching.

We proceed with the illustration of our results for heteroclinic cycles in the heteroclinic network arising from a two-person parametrised Rock-Scissors-Paper game, and also for two abstract examples. We particularly survey the dynamics of the game because of the fact that those heteroclinic cycles are not simple in spite of the symmetry in the problem. We show that cyclic behaviour is a dominant feature of the dynamics. This follows from the *essential asymptotic stability* of the heteroclinic cycle where agents switch to best responses. We propose a first approach to an extension to two independent agents for two price setting models and interpret the results in light of empirical evidences.

Resumo

O propósito desta tese é compreender a estabilidade e dinâmica de ciclos e redes heteroclínicos formados por equilíbrios hiperbólicos do tipo sela e ligações heteroclínicas unidimensionais.

Começamos por apresentar as bases essenciais das dinâmicas heteroclínicas. Conformemente, a estabilidade de ciclos heteroclínicos pode ser obtida a partir do valor do índice de estabilidade local ao longo de cada ligação heteroclínica. Desenvolvemos um método sistemático de calcular o índice de estabilidade local para uma nova classe de ciclos heteroclínicos robustos que denominamos de *ciclos heteroclínicos quasi-simples*. Um ciclo heteroclínico é quasi-simples se as ligações heteroclínicas são unidimensionais e estão contidas em espaços invariantes pelo fluxo de igual dimensão. Os mesmos ocorrem em contextos simétricos e não simétricos. Estabelecemos um pressuposto sobre a dinâmica ao longo das ligações heteroclínicas para assegurar que matrizes de transição para secções transversais em torno do ciclo heteroclínico existam e tenham a forma conveniente. Os nossos resultados são construtivos no sentido em que definimos uma função cujas imagens fornecem o valor do índice de estabilidade local. Tal método aplica-se a todos os ciclos heteroclínicos simples do tipo Z e a vários ciclos heteroclínicos que surgem da teoria de jogos e dinâmica de populações, nomeadamente ciclos heteroclínicos não simples, assim como a ciclos heteroclínicos que fazem parte de redes heteroclínicas.

A dinâmica perto de redes heteroclínicas tem sido extensamente estudada devido à sua complexidade. A ocorrência de comutação infinita perto de uma rede heteroclínica pode induzir comportamento caótico. O mecanismo parece estar relacionado com intersecções transversais de variedades estável e instável e/ou selas de rotação (selas com valores próprios complexos ou órbitas periódicas). Até onde sabemos nenhuma informação consistente é conhecida sobre a comutação infinita perto de redes heteroclínicas cuja linearização nos equilíbrios apenas admite valores próprios reais. Na verdade provamos que aí não existe comutação infinita.

Prosseguimos com a ilustração dos nossos resultados para os ciclos heteroclínicos na rede heteroclínica que surge do jogo Pedra-Papel-Tesoura parametrizado para dois jogadores, e também para dois exemplos abstratos. Examinamos particularmente a dinâmica do jogo pelo facto daqueles ciclos heteroclínicos não serem simples apesar da simetria no problema. Mostramos que o comportamento ciclíco é uma característica dominante da dinâmica. Isto segue da *estabilidade assintótica essencial* do ciclo heteroclínico onde os agentes avançam para as suas melhores respostas. Propomos uma primeira abordagem para a extensão a dois agentes independentes em dois modelos de fixação de preços e interpretamos os resultados à luz das evidências empíricas.

Table of contents

List of figures

List of tables

Chapter 1

Introduction

1.1 Overview of Heteroclinic Dynamics

Heteroclinic objects (cycles and networks) have attracted the interest of researchers for playing a role in a wide range of applications. Some examples can be found in game theory and population models (e.g., [5, 32, 33]), neural circuits (e.g., [1, 2, 12]), geomagnetic field (e.g., [21, 49, 59]), and coupled cell structures (e.g., [4, 11, 25]). For our purpose we define a heteroclinic cycle as a collection of equilibria of a system of ordinary differential equations joined by sets of solution trajectories in a topological circle. Equilibria are therein called nodes. Refined definitions allow nodes to be any flow-invariant set. We do not consider this possibility here. All solution trajectories connecting consecutive nodes are contained in the non-trivial intersection of the unstable and stable manifolds of the connected nodes. A connected submanifold of this intersection outlines a heteroclinic connection. A heteroclinic orbit refers to an isolated connecting trajectory, always of dimension one. Heteroclinic connections and heteroclinic orbits are interchangeable terms when the former is one-dimensional. Ashwin and Chossat [10] name higher dimensional heteroclinic connections as continua of connections. In generic systems, heteroclinic connections are of saddle-saddle type and do not persist for small perturbations of the vector field. Since dos Reis [58] and Field [23] it is well known that systems preserving flow-invariant spaces[1] impart robustness to heteroclinic connections. In fact, restricted to a flow-invariant space the stable and unstable manifolds of nodes may intersect transversally. This holds in particular when a saddle connects to a sink inside the flow-invariant space. A heteroclinic cycle made up of robust heteroclinic connections is itself robust. Flow-invariant spaces appear naturally in symmetric systems as fixed-point subspaces for some symmetry group. Two other important class of examples are Lotka-Volterra-type models and coupled cell systems where invariance under the flow is controlled by biological and structural restrictions, respectively. An extensive review of early results on robust heteroclinic cycles is presented in Krupa [40].

One of the most popular robust heteroclinic cycle is first observed by May and Leonard [47] in a nonlinear model of competition among three species. Looking at the positive octant in $\mathbb{R}^3$ it consists of three nodes on the coordinate axes connected by three trajectories in the coordinate planes. The same heteroclinic cycle is discussed by Busse and Heikes [16] for a thermal convection in a rotating fluid layer. Guckenheimer and Holmes [30] further prove its existence in the setting of systems with

[1] Throughout this work, by *space* we mean any set with some added structure.

symmetry. Equivalent dynamics occur in the one-person Rock-Scissors-Paper (henceforth, RSP) game (e.g., [33]).

When various heteroclinic cycles coexist they may be put together comprising of a heteroclinic network. The study of robust heteroclinic cycles and networks has been focused on two subjects: stability and dynamics. The dynamic behaviour near a stable heteroclinic cycle is known by a mechanism of intermittency. Every solution approaching it spends a long time near nodes and makes fast transitions from one node to the next. The transition times increase monotonically and converge to infinity under asymptotic stability. Heteroclinic cycles that are not asymptotically stable can still be locally attracting. The strongest intermediate notion of stability is that of essencial asymptotic stability, e.a.s in the sequel. It is introduced in Melbourne [48] but reformulated accurately in Brannath [15]. An e.a.s. heteroclinic cycle attracts a full neighbourhood up to a thin cusp-shaped region. A form of weak attractiveness is equivalent to attracting any positive measure set. Podvigina [52] refers to it as fragmentarily asymptotic stability, f.a.s in the sequel. If a heteroclinic cycle is not f.a.s, then it is said to be completely unstable, c.u in the sequel. Within a heteroclinic network heteroclinic cycles are never asymptotically stable. The reason is that each heteroclinic cycle must have at least one node with an unstable direction to a node from a different heteroclinic cycle.

Krupa and Melbourne [41] derive a general sufficient criterion for asymptotic stability of heteroclinic cycles forced by symmetry. It is given in terms of the eigenvalues of the linearisation of the vector field about each node. These are divided into four classes depending on the geometry of their eigenspaces: radial, contracting, expanding and transverse. In most of the examples transverse eigenvalues are assumed to be negative when possible (e.g. [19, 39, 41, 43]). In Krupa and Melbourne [43] a robust heteroclinic cycle in $\mathbb{R}^4$ whose heteroclinic connections lie in two-dimensional fixed-point subspaces is called simple. The authors propose a classification into types A, B and C, and obtain sufficient and necessary conditions for asymptotic stability of such heteroclinic cycles. Optimal conditions for e.a.s and f.a.s of simple heteroclinic cycles in $\mathbb{R}^4$ are established in Podvigina and Ashwin [53]. Podvigina [52] extends the definition of simple heteroclinic cycle to $\mathbb{R}^n$ and groups them into two types: A as before, and Z. Asymptotic stability and f.a.s properties of type-Z cycles are examined herein.

Methods for stability computations have recourse to Lyapunov functions (e.g. [32, 35]) and return maps to cross sections to the flow (e.g. [41–43, 48]). Lyapunov functions have only been applied in the context of mathematical biology and game theory. The approach of return maps may be combined with the transition-matrix technique, rediscovered by Field and Swift [24], whenever the form of the return map is relatively simple. Podvigina and Ashwin [53] define a stability index that provides a relative measure of the basin of attraction for any compact invariant set. The local version of this index is particularly useful for characterising stability properties of robust heteroclinic cycles and networks.[2] The fact that it is constant along trajectories of the flow allows to keep track of a finite number of indices, one for each heteroclinic connection. Calculations in this respect have been performed for simple heteroclinic cycles in $\mathbb{R}^4$ by Podvigina and Ashwin [53] and, more recently, for non-simple heteroclinic cycles making up a heteroclinic network in a case study from Boussinesq convection by Podvigina et al. [54]. The greater the value of the stability index is, the stronger is the form of stability.

[2] See Keller [36] and Roslan and Ashwin [62] for distinct contexts of application.

Lohse [46] proves that e.a.s of a heteroclinic cycle or network is equivalent to positive local stability indices along its heteroclinic connections completing the results in Podvigina and Ashwin [53].

Stability of robust heteroclinic networks is of difficult treatment due to a greater number of possible visiting routes by nearby trajectories. Castro and Lohse [17] make use of the stability index and distinguish when it is computed with respect to a heteroclinic cycle (c-index) and the whole heteroclinic network (n-index). Comparison of both quantities says that along the same heteroclinic connection the n-index exceeds the c-index. Even so, the way by which the stability of individual heteroclinic cycles in a heteroclinic network may affect the stability of the whole heteroclinic network is not systematic. Kirk and Silber [39] address the competition between two heteroclinic cycles sharing a heteroclinic connection. According to their analysis the resulting heteroclinic network can be e.a.s while either one heteroclinic cycle is e.a.s and the other is f.a.s, or one of the two heteroclinic cycles is c.u. Other possible stability combinations for this example are explored in Castro and Lohse [17] by means of the violation of the assumption about transverse eigenvalues. They deduce that an e.a.s heteroclinic network can also be obtained from two f.a.s heteroclinic cycles. Besides, the co-existing of an e.a.s heteroclinic cycle is not sufficient to the entire network be e.a.s.

In another spirit, the interplay among various robust heteroclinic cycles in a heteroclinic network can produce increasingly complex dynamics. This raises the issue of determining the admissible sequences of visits to the nodes within each part of the heteroclinic network. The set of all such sequences describes switching behaviour in the vicinity of the heteroclinic network. There are different types of switching: at a node, along a heteroclinic connection, or infinite. The occurrence of infinite switching entails switching along every heteroclinic connection, which in turn entails switching at every node. Infinite switching actually ensures the existence of nearby trajectories following each infinite sequence of heteroclinic connections in the heteroclinic network in any prescribed order.

Aguiar et al. [6, 7], Homburg and Knobloch [34], Labouriau and Rodrigues [44], and Rodrigues and Labouriau [61] provide examples of heteroclinic networks for which infinite switching evolves to chaos and complicated structures, including suspended Smale horseshoes, that accumulate on them. The mechanisms for infinite switching are therein transverse intersections between stable and unstable manifolds combined with rotating nodes, either nodes with complex eigenvalues or periodic orbits. Kirk et al. [37] and Rodrigues [60] illustrate that the spiralling effect due to the presence of a pair of complex eigenvalues gives rise by itself to rich dynamics associated with infinite switching near a heteroclinic network. In the latter reference it is shown particularly that infinite switching holds without suspended horseshoes. Further constructions supporting infinite switching take the effect of noise and symmetry breaking as the main drivers behind it. See Armbruster et al. [8] and Kirk and Rucklidge [38], respectively.

Few results are known about the realisation of infinite switching for heteroclinic networks where all nodes are equilibria with real eigenvalues. On the contrary, it seems such heteroclinic networks are able to display solely simpler variants of switching. This is the case for Kirk and Silber [39] in which a nearby trajectory may switch from one heteroclinic cycle to the other but may not switch back again; for Postlethwaite and Dawes [57] near a heteroclinic network with three heteroclinic cycles unstable along a transversal direction, who found trajectories that visit all heteroclinic cycles sequentially, the number of loops around each being either constant or irregular. Aguiar [3] proves that infinite switching does not occur near a heteroclinic network with a Kirk and Silber subnetwork.

The argument is the absence of switching along the common heteroclinic connection in the Kirk and Silber subnetwork. Castro and Lohse [19] generalise it and have regard to the role of a heteroclinic connection or, more generally a finite sequence of heteroclinic connections, shared by two heteroclinic cycles within a heteroclinic network. As long as incoming and outgoing directions of the first and last nodes in the common part span the same space there is no switching along it. The works of Aguiar [3] and Aguiar and Castro [5] are apparently the only that establish conditions for infinite switching near edge heteroclinic networks in product of simplices for bimatrix games.

Game theory concerns interactions among agents. The dynamics of these interactions can be modelled using replicator dynamics through differential equations. In a two-person RSP game where the reward for ties is parametrised for each agent by a quantity strictly between -1 and $+1$, Aguiar and Castro [5] have shown the existence of a robust heteroclinic network in $\mathbb{R}^6$ nearby which long-term complex behaviour takes place. Such a heteroclinic network can be seen as made of two or three heteroclinic cycles. Heteroclinic connections are one-dimensional and contained in flow-invariant affine subspaces of equal dimension. Linearisation of the vector field about each node admits only real eigenvalues. By making use of the symmetry of the problem every node is identified with the group orbit. The heteroclinic network and its heteroclinic cycles are then restricted to the quotient space in $\mathbb{R}^4$. Stability properties of the individual quotient cycles add information to the dynamics. Those can be described by the local stability index along each heteroclinic connection with respect to the quotient cycle in question. It is important to note that the quotient cycles are not simple because heteroclinic connections do not belong to fixed-point spaces. They do not fit into the type A, B or C classification of Krupa and Melbourne [43], and calculations of the indices have to be explicit. The study of the stability and dynamics of non-simple robust heteroclinic cycles and networks like the ones of the two-person RSP game has been done on a case-by-case basis. The main features are one-dimensional heteroclinic connections and real eigenvalues at each node. Apart from simple heteroclinic cycles and networks these settings actually predominate in game theory and population dynamics. Heteroclinic dynamics in game theory as a motivation thus leads to two main research questions:

Q1. Is there a systematic way to compute local stability indices along one-dimensional heteroclinic connections between two hyperbolic non-resonant saddle equilibria?

Q2. Is there infinite switching near a robust heteroclinic network involving a finite number of hyperbolic non-resonant saddle equilibria whose linearisation has only real eigenvalues?

As we have reviewed the literature is scarce in this context reporting partial results confined to specific examples.

1.2 Organisation and Contributions

We outline the thesis organisation and research contributions in order to answer the questions raised above.

The thesis is divided into seven chapters. After this introduction and problem formulation, **Chapter 2** reviews the relevant background. In Section 2.1 we set up the definitions of a heteroclinic connection, a heteroclinic cycle and a heterocinic network, and list factors determining their robustness.

We classify the eigenvalues of the linearisation of the vector field about nodes composing a heteroclinic cycle based on the geometry of their eigenspaces. Section 2.2 distinguishes simple from pseudo-simple heteroclinic cycles in $\mathbb{R}^4$. We present the division of simple heteroclinic cycles in $\mathbb{R}^4$ into types A, B and C, and the respective generalisation to $\mathbb{R}^n$ grouping into types A and Z. We look at the attempt to characterise heteroclinic connections by types B and C for a simple heteroclinic cycle in $\mathbb{R}^n$ by Krupa and Melbourne [43]. Section 2.3 introduces the notions of e.a.s and f.a.s for an arbitrary compact flow-invariant set. The stability index and its local version are enunciated in Section 2.4. We describe their properties and relation with different forms of stability. Section 2.5 contains a brief summary of switching behaviour near a heteroclinic network. We clarify switching concepts at a node, along a heteroclinic connection and infinite.

Chapter 3 discusses our first question. In the motivation two-person RSP game the structure of the quotient cycles arising from the dynamics is relatively straightforward. This supports the need to define a new class of robust heteroclinic cycles that morally resemble simple heteroclinic cycles but whose existence is not solely restricted to systems with symmetry. We name it *quasi-simple* and give the precise definition in Section 3.1: a robust heteroclinic cycle in $\mathbb{R}^n$ is said to be quasi-simple if its heteroclinic connections are one-dimensional and contained in flow-invariant spaces of equal dimension. From the linearisation at each node of a quasi-simple heteroclinic cycle results one contracting and one expanding eigenvalues, and a constant number of radial (n_r) and transverse (n_t) eigenvalues such that $n = n_t + n_r + 2$. We are interested in the case of real eigenvalues (Assumption 3.1.4). Our purpose is to calculate the local stability index along each heteroclinic connection in a quasi-simple heteroclinic cycle. To this end, Section 3.2 is devoted to the construction of return maps (also called Poincaré maps), via the composition of local and global maps, for approximating the dynamics around the entire heteroclinic cycle. It is assumed that the global maps behave as permutations (Assumption 3.2.1). This has been largely taken in the literature. We observe that radial eigenvalues are irrelevant, which allows us to reduce the dimension of the problem to $N = n_t + 1$. Accordingly, we show in Section 3.3 that the transition between incoming cross sections at pairs of adjacent nodes can be described using basic transition matrices after a change of coordinates (Theorem 3.8). Section 3.4 considers separately the cases when transverse eigenvalues at nodes either are or are not all negative (Theorems 3.4.2 and 3.4.9). For instance, heteroclinic cycles in a heteroclinic network fall in the second case. From the former we deduce that f.a.s implies asymptotic stability. The latter requires the characterisation of the local basin of attraction of the heteroclinic cycle in a neighbourhood of any heteroclinic connection. Under some conditions expressed in terms of eigenvalues and eigenvectors of transition matrices we write it down as the intersection of suitable sets bounded by power curves (Lemma 3.4.6). To evaluate the stability of each set we construct the function F^{index} whose arguments are the exponents of a curve coming from rows of transition matrices with negative entries (Lemma 3.4.8). The local stability index along the heteroclinic connection is then the minimum of those measures. Section 3.5 concludes with an illustration of our results for the simplest non-simple heteroclinic cycle consisting of two nodes and two heteroclinic connections. It is obtained from the translation of the simple heteroclinic cycle of type B_2^+ through the cylinder realisation in Ashwin and Postlethwaite [13]. We join two of such heteroclinic cycles in a heteroclinic network by a common heteroclinic connection looking like the $\left(\mathrm{B}_2^+, \mathrm{B}_2^+\right)$-network of Castro and Lohse [17]. We calculate the local stability indices with respect to each heteroclinic cycle and see that they equal the ones concerning the B_2^+-cycles by Podvigina and Ashwin [53] (Lemma 3.5.1). Hence the value of the local stability index does not depend on the position of the node.

Chapter 4 addresses our second question. Aguiar and Castro [5] prove that the RSP quotient network exhibits infinite switching. We observe that the authors have not been considering an intrinsic permutation of axes into the global maps. The same occurs in Aguiar [3]. In order to show that effectively there is no infinite switching near heteroclinic networks whose linearisations at nodes have only real eigenvalues we start by investigating weaker forms of switching. Section 4.1 introduces two types of heteroclinic connections, contracting-to-expanding and contracting-to-transverse, generalising types B and C of Krupa and Melbourne [43]. We discuss the construction of building blocks of quasi-simple heteroclinic cycles in $\mathbb{R}^n$ such that the nodes lie on the coordinate axes and the heteroclinic connections occur in coordinate planes (Assumption 4.1.4). We examine the geometry of a quasi-simple heteroclinic cycle so obtained according to the type of its heteroclinic connections. The following two sections focus on heteroclinic networks made up of quasi-simple heteroclinic cycles satisfying the three Assumptions 3.1.4, 3.2.1 and 4.1.4. Section 4.2 establishes whether or not switching along a common heteroclinic connection takes place. We extend the result of Castro and Lohse [19] by relaxing their assumption on the global map near the common heteroclinic connection. In the first case we assume that there exists a single incoming direction at the first node in the common heteroclinic connection that is mapped by the global map into the outgoing space at the next node. The existence of switching along the common heteroclinic connection is controled by the ratios of the eigenvalues associated with the incoming directions at the first node and the eigenvalues associated with the outgoing directions at the next node (Theorem 4.2.4). The second case assumes that none of the incoming directions at the first node in the common heteroclinic connection is mapped by the global map into the outgoing space at the next node. We prove here that switching along the common heteroclinic connection always occurs (Theorem 4.2.6). Subsection 4.2.1 briefly looks at the House network as an illustrative example. Similar conclusions concerning switching along heteroclinic connections leading to a single common node are deduced in Subsection 4.2.2 (Propositions 4.2.9 and 4.2.10). Section 4.3 deals with switching along a heteroclinic cycle. We see that the type of a heteroclinic connection affects the way by which sets of points in an outgoing cross section hit the next one (Lemmas 4.3.1 and 4.3.3). Even so the image of the entire domain of a return map near a node is a topological cone-shaped region with its apex at the origin (Lemma 4.3.6). We give a sufficient condition depending on this set that precludes switching along a heteroclinic cycle (Lemma 4.3.8). Section 4.4 proves generally our claim through the form of stability of the heteroclinic cycles and the resulting heteroclinic network (Theorem 4.4.4).

Chapter 5 attends to the stability of cyclic behaviour in the dynamic two-person RSP game through the stability of the quotient cycles. Section 5.1 first gives a brief exposition of the two-person RSP game describing the original heteroclinic network and the one induced by symmetry. Section 5.2 surveys the stability properties of the quotient cycles. We check that these are quasi-simple heteroclinic cycles and calculate the local stability indices for the heteroclinic connections of every quotient cycle. To do this we employ directly the method developed in Chapter 3. Therefore we conclude that: the quotient cycle where agents never tie is e.a.s when the sum of payoffs for a tie is negative (Theorem 5.2.1); the two quotient cycles involving a tie and a loss by only one agent may be f.a.s when the sum of payoffs for a tie is positive (Theorems 5.2.3 and 5.2.4); and the two quotient cycles for which play goes through all possible combinations of outcomes in the two possible orders are always c.u (Theorems 5.2.5 and 5.2.6). Our results indicate that the two-person RSP game is a good tool for modelling cyclic dominance where agents change a winning position cyclically. Section 5.3 proposes an application of the two-person RSP game to price setting by extending the models of Noel [51] and Hopkins and Seymour [35]. For each case we define three choices for the actions of sellers and consumers in a retail market with the cyclical best-response structure of the RSP game. The dynamics of the gasoline retail market in [51] report that the major and independent firms alternate in setting the highest price. If we assume that consumers buy at the lowest price, then the major and independent firms alternate in winning and losing in an RSP game where the actions are "fix lowest price", "fix highest price" and "fix intermediate price". This corresponds to the win-loss cycle for which e.a.s is possible (Table 5.2). Considering the pricing model of [35] the two-person RSP game allows the introduction of consumers as active and independent agents by choosing to be "uninformed", "reasonably informed" and "fully informed" about prices. We show that the interaction between profit-maximising sellers and utility-maximising consumers can also be explained according to the dynamics near the win-loss cycle (Table 5.3).

Chapter 6 contains two abstract examples of heteroclinic networks comprising of two quasi-simple heteroclinic cycles connected by one node. Section 6.1 is devoted to the Bowtie network. We adopt the procedure in Chapter 3 in view of working out the local stability indices with respect to each heteroclinic cycle (Proposition 6.1.2). We also compute the local stability indices with respect to the whole heteroclinic network following [17] (Propositions 6.1.3–6.1.5). We prove that the heteroclinic cycle evolving in the weakest expanding direction at the common node, the L-cycle, is never e.a.s. However the entire heteroclinic network is e.a.s showing that trajectories that leave a neighbourhood of the L-cycle are attracted to the remaining heteroclinic cycle. We compare the results with those obtained for the Kirk and Silber network in [39]. In spite of some similarities we figure out, that unlike the Kirk and Silber network, the Bowtie network can be e.a.s even when both hetroclinic cycles are c.u. Section 6.2 presents the $\left(C_2^-,C_2^-\right)$-network. The possible stability properties of the heteroclinic cycles are analogously determined by means of the local stability indices (Proposition 6.2.1). None of the indices can be $+\infty$ as opposed to the $\left(B_2^+,B_2^+\right)$-network whose graph coincides with the one of the $\left(C_2^-,C_2^-\right)$-network. Moreover, we illustrate some results of Chapter 4, namely the existence of switching along a heteroclinic cycle (Lemma 6.2.2).

Chapter 7 concludes the thesis.

Chapter 2

Preliminaries

In this chapter we summarise the relevant material on stability and dynamics of heteroclinic objects.

2.1 Basic definitions

Consider a smooth vector field $f : \mathbb{R}^n \to \mathbb{R}^n$ described by a system of ordinary differential equations

$$\dot{x} = f(x), \quad x \in \mathbb{R}^n. \tag{2.1}$$

An *equilibrium*[1] $\xi \in \mathbb{R}^n$ of (2.1) satisfies $f(\xi) = 0$. The stable and unstable manifolds of ξ are denoted by $W^s(\xi)$ and $W^u(\xi)$ in the usual way. Let n_+ and n_- be the dimension of $W^s(\xi)$ and $W^u(\xi)$, respectively. We say that ξ is a *hyperbolic saddle* if $n = n_+ + n_-$ and $n_+ n_- \neq 0$.

For two hyperbolic saddles ξ_1 and ξ_2 of (2.1) the intersection $W^u(\xi_1) \cap W^s(\xi_2)$ provides the set of all solution trajectories of (2.1) from ξ_1 to ξ_2.

Definition 2.1.1. If $W^u(\xi_1) \cap W^s(\xi_2) \neq \emptyset$, then a *heteroclinic connection* from ξ_1 to ξ_2 is a connected flow-invariant manifold $\kappa_{1,2} = [\xi_1 \to \xi_2]$ contained in $W^u(\xi_1) \cap W^s(\xi_2)$.

Definition 2.1.2. A *heteroclinic cycle* is a flow-invariant set X in $\mathbb{R}^n$ consisting of an ordered collection of mutually distinct hyperbolic saddles $\{\xi_1, \ldots, \xi_m\}$ and heteroclinic connections $\kappa_{j,j+1} = [\xi_j \to \xi_{j+1}]$, $j = 1, \ldots, m$, where $\xi_{m+1} \equiv \xi_1$.

Definition 2.1.3. A *heteroclinic network* X in $\mathbb{R}^n$ is a connected union $X = \bigcup_i C_i$ of finitely many heteroclinic cycles $C_1, C_2, \ldots$.

Hyperbolic saddles making up a heteroclinic cycle are also called *nodes*. In the literature there are more complicated definitions where nodes can be any flow-invariant set other than equilibria, such as periodic orbis or chaotic saddles. We do not consider this for our purposes.

In generic dynamical systems heteroclinic cycles are unlikely to exist because heteroclinic connections between saddles are broken when f is slightly perturbed. They can however be robust (or structurally stable) to restricted perturbations that respect a specific set of flow-invariant spaces. Heteroclinic connections of saddle-sink or source-saddle type contained in flow-invariant spaces

[1] Equilibria are sometimes called fixed points or steady states.

Table 2.1 Types of flow-invariant spaces.

Systems	**Description**
Symmetric	Fixed-point subspace
Lotka-Volterra	Extinction affine subspace
Coupled cell	Synchrony subspace

ensure the robustness of these objects. The existence of flow-invariant spaces appears in vector fields with additional structure either inherited from symmetry (e.g. [41, 43]), or modelling assumptions required in Lotka-Volterra models in ecology and game dynamics (e.g. [32, 33]), or the realisation of coupled cell systems (e.g. [4]).

Throughout this work, by robust heteroclinic cycle we mean the following:

Definition 2.1.4. A heteroclinic cycle in $\mathbb{R}^n$ is *robust* if for all $j = 1, \ldots, m$ there exists a flow-invariant space $P_j \subset \mathbb{R}^n$ such that

- ξ_j is a saddle and ξ_{j+1} is a sink in P_j;
- $\kappa_{j,j+1}$ is contained in P_j.

Table 2.1 provides types of flow-invariant spaces P_j arising as an intrinsic feature of each application above.

Let $\mathbf{S} \subseteq \mathbb{R}^n$ be the state-space of (2.1). Whenever $\mathbf{S}$ is not Euclidean, $\mathbb{R}^n$ is naturally the Euclidean space of the smallest dimension containing the former. Without loss of generality we assume that $\mathbf{S}$ is an $\bar{n}$-manifold embedded in $\mathbb{R}^n$ for some $\bar{n} \leq n$.

Given two vector spaces $A, B \subset \mathbb{R}^n$, denote by $A \ominus B$ the orthogonal complement to B in A. For a manifold $M \subseteq \mathbb{R}^n$ we write $T_{\xi_j}M$ for the tangent space of M at ξ_j. As usual $\mathrm{d}f(\xi_j)$ is the Jacobian matrix of f evaluated at ξ_j.

The geometry of a robust heteroclinic cycle imposes constraints on the eigenvalues and associated eigenvectors of $\mathrm{d}f(\xi_j)$. Let $\hat{L}_j$ be the flow-invariant vector space connecting the node ξ_j to the origin in $\mathbb{R}^n$. We can group the eigenvalues into four classes according to the vector subspaces in which the eigenspaces lie, see Table 2.2. We refer to all non-radial eigenvalues in $T_{\xi_j}P_{j-1}$ and $T_{\xi_j}P_j$ as contracting and expanding, respectively. Define $-r_j$, $-c_j$, e_j and t_j to be the real part of a representative type of radial, contracting, expanding and transverse eigenvalue. Since ξ_j is a sink in P_{j-1} and a saddle in P_j, we have $-r_j < 0$, $-c_j < 0$ and at least one $e_j > 0$ while t_j can have either sign.

Note that there may be no radial eigenvalues depending on whether the origin belongs to $\mathbf{S}$ or not. In the same way, when the entire $\mathbb{R}^n$ is spanned by $T_{\xi_j}(P_{j-1} + P_j)$, transverse eigenvalues are inexistent. For example, a heteroclinic cycle for the dynamic one-player Rock-Scissors-Paper game in the two-dimensional simplex admits neither radial nor transverse eigenvalues.

The tangent space of $\mathbb{R}^n$ at ξ_j is trivially isomorphic to $\mathbb{R}^n$ and can be decomposed into

$$\mathbb{R}^n = \hat{L}_j \oplus V_j \oplus W_j \oplus T_j.$$

Table 2.2 Classification of eigenvalues of $\mathrm{d}f(\xi_j)$.

Eigenvalue class	Real part	Subspace
Radial	$-r_j < 0$	$\hat{L}_j$
Contracting	$-c_j < 0$	$V_j = T_{\xi_j}P_{j-1} \ominus \hat{L}_j$
Expanding	$e_j > 0$	$W_j = T_{\xi_j}P_j \ominus \hat{L}_j$
Transverse	$t_j \in \mathbb{R}$	$T_j = \mathbb{R}^n \ominus \left(T_{\xi_j}P_{j-1} + T_{\xi_j}P_j\right)$

2.2 Simple heteroclinic cycles

Robust heteroclinic cycles have been classified in low-dimensional vector spaces and in a symmetric setting, where f is *equivariant* under the action of a finite Lie group $\Gamma \subset \mathrm{O}(n)$, i.e

$$f(\gamma \cdot x) = \gamma \cdot f(x) \quad \text{for all } x \in \mathbb{R}^n, \quad \text{for all } \gamma \in \Gamma. \tag{2.2}$$

We say that $\gamma \in \Gamma$ satisfying (2.2) is a symmetry of f. Background on group theory and equivariant dynamis can be found in [22, 29]. We recall the following concepts.

A (linear) *representation* of Γ on $\mathbb{R}^n$ is a homomorphism $\rho : \Gamma \to \mathrm{GL}(\mathbb{R}^n)$ describing how a group element $\gamma \in \Gamma$ transforms the whole $\mathbb{R}^n$. A vector subspace $U \subseteq \mathbb{R}^n$ is Γ-*invariant* if $\gamma \cdot x \in U$ for all $x \in U$, $\gamma \in \Gamma$. We say that ρ is *irreducible* if the only Γ-invariant vector subspaces of $\mathbb{R}^n$ are the origin and $\mathbb{R}^n$. A vector subspace $U \subseteq \mathbb{R}^n$ is Γ-*irreducible* if U is Γ-invariant and the representation of Γ on U is irreducible.

One of the basic results in representation theory concerns the existence and uniqueness of the isotypic decomposition of a finite-dimensional vector space for a compact Lie group, which we state next

Lemma 2.2.1 (adapted from Theorem 2.5 in [29])**.** *Let Γ be a compact Lie group acting on $\mathbb{R}^n$.*

(a) For any representation of Γ on $\mathbb{R}^n$ there are a finite number of distinct Γ-irreducible vector subspaces of $\mathbb{R}^n$ up to isomorphism. Call these $U_1, \ldots, U_K$.

(b) Define $\hat{U}_i$ the sum of all Γ-irreducible vector subspaces of $\mathbb{R}^n$ isomorphic to U_i. Then,

$$\mathbb{R}^n = \hat{U}_1 \oplus \cdots \oplus \hat{U}_K. \tag{2.3}$$

The vector subspaces $\hat{U}_i$ are called the *isotypic components* of $\mathbb{R}^n$ of type U_i and (2.3) expresses the *isotypic decomposition* of $\mathbb{R}^n$ for Γ.

Definition 2.2.2 ([29])**.** Let $x \in \mathbb{R}^n$ and Σ be a subgroup of Γ.

- The Γ-*orbit* of x is the set $\Gamma(x) = \{\gamma \cdot x : \ \gamma \in \Gamma\}$.
- The *isotropy group* of x is the subgroup of Γ satisfying $\Sigma_x = \{\gamma \in \Gamma : \ \gamma \cdot x = x\}$.

- The *fixed-point subspace* of Σ is the vector subspace of $\mathbb{R}^n$ satisfying

$$\mathrm{Fix}\,(\Sigma) = \{x \in \mathbb{R}^n : \ \sigma \cdot x = x \ \text{ for all } \ \sigma \in \Sigma\}.$$

The elements in the Γ-orbit of an equilibrium ξ of (2.1) are also equilibria. We call to the group orbit $\Gamma(\xi)$ a *relative equilibrium*.

We now distinguish between homoclinic and heteroclinic cycles.

Definition 2.2.3. A heteroclinic cycle in $\mathbb{R}^n$ is called *homoclinic* if either $m = 1$ or $\xi_j \in \Gamma(\xi_1)$ for all $j = 1, \ldots, m$.

Krupa and Melbourne [41] propose the first classification of robust heteroclinic cycles in $\mathbb{R}^4$ introducing the so-called simple heteroclinic cycles. Suppose that an equivariant system (2.1) with finite $\Gamma \subset \mathrm{O}(4)$ possesses a robust heteroclinic cycle whose heteroclinic connections $\kappa_{j,j+1}$ lie in $P_j = \mathrm{Fix}\,(\Sigma_j)$ for a sequence of non-trivial isotropy groups $\Sigma_j \subset \Gamma$, $j = 1, \ldots, m$. We use the notation $L_j = P_{j-1} \cap P_j = \mathrm{Fix}\,(\Delta_j)$ where $\Delta_j \subset \Gamma$ is a subgroup.

Definition 2.2.4 ([41])**.** A robust heteroclinic cycle X in $\mathbb{R}^4$ is *simple* if for any j

- $\dim(P_j) = 2$;
- X intersects each connected component of $L_j \backslash \{0\}$ at most once.

Here L_j is a one-dimensional vector subspace of $\mathbb{R}^4$. Setting $\hat{L}_j = L_j$ the linearisation $\mathrm{d}f(\xi_j)$ has one real eigenvalue of each type. Such heteroclinic cycles are categorised into types A, B and C by Krupa and Melbourne [43] in line with the trichotomy of homoclinic cycles established by Chossat et al. [20].

Definition 2.2.5 ([43])**.** Let X be a simple robust heteroclinic cycle in $\mathbb{R}^4$.

1. X is of *type A* if $\Sigma_j \cong \mathbb{Z}_2$ for all j.
2. X is of *type B* if there is a fixed-point subspace Q with $\dim(Q) = 3$ and $X \subset Q$.
3. X is of *type C* if it is neither of type A nor of type B.

Krupa and Melbourne [43] enumerate simple heteroclinic cycles of types B and C according to the action of the symmetry group in $\mathbb{R}^4$. In their notation $\mathrm{B}_m^{\pm}$ and $\mathrm{C}_m^{\pm}$ indicate respectively heteroclinic cycles of type B and C with m different types of nodes and either $-\mathrm{Id} \in \Gamma$ (sign $-$) or not (sign $+$).

Theorem 2.2.6 ([43, 55])**.** *There are four different types of simple heteroclinic cycles of type B and three types of simple heteroclinic cycles of type C.*

1. B_2^+ *with* $\Gamma = \mathbb{Z}_2^3$ *consisting of the reflections* $(x_1, \pm x_2, \pm x_3, \pm x_4)$. *There are three different hyperplanes and in each of them, a heteroclinic cycle with two equilibria, one on each connected component of* $L_1 \setminus \{0\}$.
2. B_1^+ *with* $\Gamma = \mathbb{Z}_2 \ltimes \mathbb{Z}_2^3$ *where* $\mathbb{Z}_2^3$ *acts as above and* Z_2 *is generated by* $(-x_1, x_2, x_3, x_4)$. *The structure of the heteroclinic cycle is the same as above but* ξ_1 *and* ξ_2 *are interchanged by* $\mathbb{Z}_2$, *hence the cycle is homoclinic.*

3. B_3^- *with* $\Gamma = \mathbb{Z}_2^4$ *generated by reflexions through the four hyperplanes of coordinates. Similar heteroclinic cycles exist in each hyperplane. For example in the hyperplane* $(x_1, x_2, x_3, 0)$ *heteroclinic cycles connect the equilibria lying on any three axes* x_1*,* x_2*,* x_3 *and the heteroclinic connections lie in the corresponding planes of coordinates.*

4. B_1^- *with* $\Gamma = \mathbb{Z}_3 \ltimes \mathbb{Z}_2^4$ *where* $\mathbb{Z}_3$ *is generated by the circular permutation of* x_1*,* x_2*,* x_3*. Same as above but with all three equilibria in the same* Z_3*-orbit, hence the cycle is homoclinic.*

5. C_4^- *with* $\Gamma = \mathbb{Z}_2^4$ *acting as in 3. These cycles connect equilibria lying on the four coordinate axes.*

6. C_1^- *with* $\Gamma = \mathbb{Z}_4 \ltimes \mathbb{Z}_2^4$ *with* $\mathbb{Z}_4$ *acting by circular permutation of the coordinates. Same as above but with all equilibria in the same group orbit, hence the cycle is homoclinic.*

7. C_2^- *with* $\Gamma = \mathbb{Z}_2 \ltimes \mathbb{Z}_2^4$ *and* $\mathbb{Z}_2$ *generated by the permutation* $(x_1, x_2) \mapsto (x_3, x_4)$*. Same as above but the four equilibria are pairwise of the same type.*

Podvigina and Chossat [55] point out that Definition 2.2.4 implicitly assume the existence of distinct eigenvalues of $\mathrm{d}f(\xi_j)$ for every $j = 1, \ldots, m$. The authors show that this assumption is not generic. When it fails, at least one pair of consecutive nodes is such that the Jacobian matrix of f taken at these has, respectively, a double negative and positive eigenvalue. This prompts them to identify a new class of heteroclinic cycles in $\mathbb{R}^4$ called *pseudo-simple* by means of isotypic decomposition.

Lemma 2.2.7 (Lemma 1 in [55])**.** *Let a robust heteroclinic cycle in* $\mathbb{R}^4$ *be such that for all j: (i)* $dim(P_j) = 2$*, (ii) each connected component of* $L_j \backslash \{0\}$ *is intersected at most at one point by the heteroclinic cycle. Then, the isotypic decomposition of the representation of* Δ_j *in* $\mathbb{R}^4$ *is of one of the following types:*

1. $L_j \oplus V_j \oplus W_j \oplus T_j$*;*

2. $L_j \oplus V_j \oplus \widetilde{W}_j$ *where* $\widetilde{W}_j = W_j \oplus T_j$ *has dimension 2;*

3. $L_j \oplus V_j \oplus \widetilde{V}_j$ *where* $\widetilde{V}_j = V_j \oplus T_j$ *has dimension 2.*

In cases 2 and 3, Δ_j *acts in* $\widetilde{W}_j$ *(respectively,* $\widetilde{V}_j$*) as a dihedral group* $\mathbb{D}_m$ *in* $\mathbb{R}^2$ *for some* $m \geq 3$*. Note that the representations* $\widetilde{W}_j$ *and* $\widetilde{V}_j$ *are irreducible. Therefore, the respective eigenvalues have algebraic and geometric multiplicity 2, namely* $e_j = t_j$ *in case 2 and* $-c_j = t_j$ *in case 3.*

We notice that L_j is Δ_j-irreducible. Together with $\dim(L_j) = 1$, it follows that L_j is an isotypic component of $\mathbb{R}^4$ for Δ_j. Due to the uniqueness of both eigen and isotypic decompositions of the tangent space at ξ_j (here, $\mathbb{R}^4$), they must be the same.

Definition 2.2.8 ([55])**.** A robust heteroclinic cycle in $\mathbb{R}^4$ satisfying the conditions *(i)* and *(ii)* of Lemma 2.2.7 is called *simple* if case 1 holds true for all j, and *pseudo-simple* otherwise.

Krupa and Melbourne [43] generalise to higher dimensions the classification of heteroclinic cycles into types A, B and C. In particular, they provide an alternative local approach assigning a type to a heteroclinic connection in $\mathbb{R}^n$.

Definition 2.2.9 ([43])**.** Let X be a robust heteroclinic cycle in $\mathbb{R}^n$.

1. The jth connection is of *type B* if there are fixed-point subspaces Q_j, R_j such that

$$Q_j = P_j \oplus V_j = P_j \oplus W_{j+1} \quad \text{and} \quad R_j = P_j \oplus T_j = P_j \oplus T_{j+1}$$

2. The jth connection is of *type C* if there are fixed-point subspaces Q_j, R_j such that

$$Q_j = P_j \oplus V_j = P_j \oplus T_{j+1} \quad \text{and} \quad R_j = P_j \oplus T_j = P_j \oplus W_{j+1}.$$

Denote by $P^{\perp}$ the orthogonal complement to P in $\mathbb{R}^n$.

Definition 2.2.10 ([43])**.** For a robust heteroclinic cycle in $\mathbb{R}^n$, let λ_j^c and λ_j^t be, respectively, the contracting and transverse eigenvalues of $\mathrm{d}f(\xi_j)$ with the minimum real parts and λ_j^e the expanding eigenvalue with the maximum real part.

1. X is of *type A* if for any j
   - the eigenspaces corresponding to λ_j^c, λ_j^t, λ_{j+1}^e and λ_{j+1}^t lie in the same isotypic component in the decomposition of $P_j^{\perp}$ under Σ_j;
   - the eigenspaces corresponding to all transverse eigenvalues of $\mathrm{d}(\xi_j)$ with positive real part lie in the same isotypic component in the decomposition of $P_j^{\perp}$ under Σ_j.
2. X is of *type B* if each connection is of type B.
3. X is of *type C* if each connection is of type B or C and at least one connection is of type C.

The generalisation of type-A cycles comes directly from the description by Krupa and Melbourne [41]. In this regard Podvigina [52] extends explicitly to $\mathbb{R}^n$ the notion of simple heteroclinic cycle and presents type-Z cycles as the opposite to type-A cycles. Heteroclinic cycles of types B and C belong to type Z.

Definition 2.2.11 ([52])**.** A robust heteroclinic cycle in $\mathbb{R}^n$ is *simple* if for any j

- all eigenvalues of $\mathrm{d}f(\xi_j)$ are distinct;
- $\dim(P_{j-1} \ominus L_j) = 1$.

Definition 2.2.12 ([52])**.** A simple robust heteroclinic cycle in $\mathbb{R}^n$ is of *type Z* if for any j

- $\dim(P_j) = \dim(P_{j+1})$;
- the isotropy subgroup of P_j, Σ_j, decomposes $P_j^{\perp}$ into one-dimensional isotypic components.

2.3 Notions of stability

A robust heteroclinic cycle is asymptotically stable if all nearby trajectories remain close and converge to it. Numerical simulations show that certain heteroclinic cycles may be observable even though they are not asympotically stable. In this instance, intermediate measure-theoretic notions of stability have been developed with the contribution of Melbourne [48], Brannath [15], Podvigina and Ashwin [53] and Podvigina [52]. In [48] the author describes a stable heteroclinic cycle in the strong sense that it is asymptotically stable almost everywhere. Such property is termed therein as essential asymptotic stability and correctly formalised[2] in [15]. A weaker form of stability attracts any positive measure set in accordance with the concept fragmentarily asymptotic stability from [52]. If a heteroclinic cycle is not fragmentarily asymptotically stable, then it is completely unstable.

Consider now a compact set $X \subset \mathbb{R}^n$ invariant under the flow of (2.1) $\Phi_t(x)$, $t \in \mathbb{R}$, $x \in \mathbb{R}^n$. We use terminology of [52]. Given a metric d on $\mathbb{R}^n$ and $\varepsilon > 0$, denote an ε-neighbourhood of X by

$$B_\varepsilon(X) = \{x \in \mathbb{R}^n : d(x,X) < \varepsilon\}.$$

The (global) basin of attraction of X is

$$\mathscr{B}(X) = \left\{x \in \mathbb{R}^n : \lim_{t\to\infty} d(\Phi_t(x),X) = 0\right\}$$

and, for $\delta > 0$, its δ-local basin of attraction is

$$\mathscr{B}_\delta(X) = \left\{x \in \mathbb{R}^n : d(\Phi_t(x),X) < \delta \text{ for any } t \geq 0 \text{ and } \lim_{t\to\infty} d(\Phi_t(x),X) = 0\right\}.$$

Let $\ell(\cdot)$ be the Lebesgue measure in the appropriate dimension. The following defines the stability properties above for a more general set in terms of its local basin of attraction.

Definition 2.3.1 ([52])**.** Let $X \subset \mathbb{R}^n$ be a compact flow-invariant set.

1. X is *asymptotically stable (a.s)* if for any $\delta > 0$ there exists $\varepsilon > 0$ such that $B_\varepsilon(X) \subset \mathscr{B}_\delta(X)$.
2. X is *essentially asymptotically stable (e.a.s)* if $\lim_{\delta\to 0}\lim_{\varepsilon\to 0}\left[\frac{\ell(B_\varepsilon(X)\cap\mathscr{B}_\delta(X))}{\ell(B_\varepsilon(X))}\right] = 1$.
3. X is *fragmentarily asymptotically stable (f.a.s)* if $\ell(\mathscr{B}_\delta(X)) > 0$ for any $\delta > 0$.
4. X is *completely unstable (c.u)* if there exists $\delta > 0$ such that $\ell(\mathscr{B}_\delta(X)) = 0$.

The relation between different levels of stability is revisited in the next result.

Lemma 2.3.2. *Suppose that $X \subset \mathbb{R}^n$ is a compact invariant set for a continuous flow Φ_t.*

(a) If X is a.s, then it is e.a.s.

(b) If X is e.a.s, then it is f.a.s.

[2] Podvigina and Ashwin [53] distinguish Melbourne's [48] definition from the one of Brannath [15] by renaming the latter *predominant asymptotic stability*. We preserve the use of essentially asymptotically stability.

Proof. For (a) this immediately follows from Definition 2.3.1. For (b) suppose that X is e.a.s. Fix $\delta > 0$ small. Then, for any $\alpha > 0$, there exists $\varepsilon_0 > 0$ such that $\ell(B_\varepsilon(X) \cap \mathscr{B}_\delta(X)) > (1-\alpha)\ell(B_\varepsilon(X)) > 0$ for all $\varepsilon < \varepsilon_0$. Since $B_\varepsilon(X) \cap \mathscr{B}_\delta(X) \subset \mathscr{B}_\delta(X)$, we have $\ell(B_\varepsilon(X) \cap \mathscr{B}_\delta(X)) < \ell(\mathscr{B}_\delta(X))$. Hence $\ell(\mathscr{B}_\delta(X)) > 0$ for any $\delta > 0$ and X is f.a.s. □

2.4 The stability index

Podvigina and Ashwin [53] introduce a stability index in order to characterise the local geometry of basins of attraction of arbitrary compact flow-invariant sets. This can in turn be confined to a local stability index by taking the limit of stability indices of local basins of attraction. In practice, the two indices quantify respectively the level of attractivity and stability at some point of the set under study. Lohse [46], Castro and Lohse [17] and the authors themselves make use of such indices to examine the stability of simple heteroclinic cycles and networks. Other applications have arised in the framework of chaotically driven concave maps (see [36]) and riddled basins of attraction (see [62]).

Below we rewrite the definition of stability index and its local version from [53] for a compact flow-invariant set X in $\mathbb{R}^n$. Given $x \in X$ and $\varepsilon, \delta > 0$, set

$$\Sigma_\varepsilon(x) = \frac{\ell(B_\varepsilon(x) \cap \mathscr{B}(X))}{\ell(B_\varepsilon(x))}, \qquad \Sigma_{\varepsilon,\delta}(x) = \frac{\ell(B_\varepsilon(x) \cap \mathscr{B}_\delta(X))}{\ell(B_\varepsilon(x))}.$$

Definition 2.4.1 ([53])**.** Let $X \subset \mathbb{R}^n$ be a compact invariant set for a smooth flow Φ_t and $x \in X$. Define

$$\sigma_-(x) = \lim_{\varepsilon \to 0} \left[\frac{\ln(\Sigma_\varepsilon(x))}{\ln(\varepsilon)} \right], \qquad \sigma_+(x) = \lim_{\varepsilon \to 0} \left[\frac{\ln(1-\Sigma_\varepsilon(x))}{\ln(\varepsilon)} \right]$$

and

$$\sigma_{\mathrm{loc},-}(x) = \lim_{\delta \to 0} \lim_{\varepsilon \to 0} \left[\frac{\ln\left(\Sigma_{\varepsilon,\delta}(x)\right)}{\ln(\varepsilon)} \right], \qquad \sigma_{\mathrm{loc},+}(x) = \lim_{\delta \to 0} \lim_{\varepsilon \to 0} \left[\frac{\ln\left(1-\Sigma_{\varepsilon,\delta}(x)\right)}{\ln(\varepsilon)} \right].$$

The *stability index* of X at x is

$$\sigma(X,x) = \sigma_+(x) - \sigma_-(x)$$

and the *local stability index* of X at x is

$$\sigma_{\mathrm{loc}}(X,x) = \sigma_{\mathrm{loc},+}(x) - \sigma_{\mathrm{loc},-}(x).$$

We use the convenction that $\sigma_-(x) = \infty$ (resp. $\sigma_{\mathrm{loc},-}(x) = \infty$) if there is $\varepsilon_0 > 0$ such that $\Sigma_\varepsilon(x) = 0$ (resp. $\Sigma_{\varepsilon,\delta}(x) = 0$) for all $\varepsilon < \varepsilon_0$. Analogously, $\sigma_+(x) = \infty$ (resp. $\sigma_{\mathrm{loc},+}(x) = \infty$) if there is $\varepsilon_0 > 0$ such that $\Sigma_\varepsilon(x) = 1$ (resp. $\Sigma_{\varepsilon,\delta}(x) = 1$) for all $\varepsilon < \varepsilon_0$. Notice that $\sigma_\pm(x) > 0$ (resp. $\sigma_{\mathrm{loc},\pm}(x) > 0$) and hence $\sigma(X,x) \in [-\infty,\infty]$ (resp. $\sigma_{\mathrm{loc}}(X,x) \in [-\infty,\infty]$).

We say that near a point $x \in X$ the stability index $\sigma(X,x)$ quantifies the local extent of $\mathscr{B}(X)$ in the following sense: for $\sigma(X,x) > 0$ an increasingly large portion of points in small enough neighbourhoods of x converge to X as they shrink; for $\sigma(X,x) < 0$ the measure of the set of such

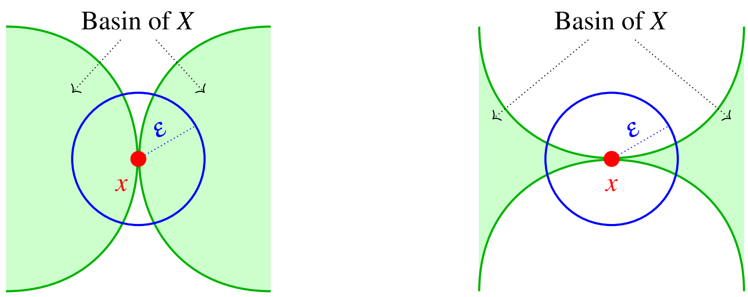

(a) $\sigma(X,x) > 0$ or $\sigma_{\mathrm{loc}}(X,x) > 0$ (b) $\sigma(X,x) < 0$ or $\sigma_{\mathrm{loc}}(X,x) < 0$

Fig. 2.1 Schematic illustration of the stability index (cf. [53, Figure 1]).

points relative to the measure of the neighbourhoods goes to zero. In the same way, the local index $\sigma_{\mathrm{loc}}(X,x)$ quantifies the local extent of $\mathscr{B}_\delta(X)$, see Figure 2.1.

We state the two main features of the stability index.

Theorem 2.4.2 (Theorems 2.2 and 2.4 in [53])**.** *Suppose that $X \subset \mathbb{R}^n$ is a compact invariant set for a C^1-smooth flow Φ_t. For any $x \in X$ let S be a codimension one surface that is transverse to the flow at x. Then,*

(a) the stability indices $\sigma(X,x)$ and $\sigma_{\mathrm{loc}}(X,x)$ are constant on trajectories, whenever they exist.

(b) the stability indices $\sigma(X,x)$ and $\sigma_{\mathrm{loc}}(X,x)$ can be computed on substituting $\Sigma_\varepsilon(x)$ and $\Sigma_{\varepsilon,\delta}(x)$ by

$$\Sigma_{\varepsilon,S}(x) = \frac{\ell(B_\varepsilon(x) \cap \mathscr{B}(X) \cap S)}{\ell(B_\varepsilon(x))} \quad \text{and} \quad \Sigma_{\varepsilon,\delta,S}(x) = \frac{\ell(B_\varepsilon(x) \cap \mathscr{B}_\delta(X) \cap S)}{\ell(B_\varepsilon(x))}.$$

Accordingly, the stability index is an invariant of the dynamics and can be calculated with respect to suitable transverse sections to the flow. From here stability properties of heteroclinic cycles are described through a finite number of local stability indices, namely the ones along the connecting trajectories.

Theorem 2.4.3 (Theorem 3.1(i) in [46])**.** *Let $X \subset \mathbb{R}^n$ be a heteroclinic cycle or network with finitely many equilibria and connecting trajectories. Suppose that for all $x \in X$ the local stability index $\sigma_{\mathrm{loc}}(X,x)$ exists and is not equal to zero. Then, generically, X is e.a.s if and only if $\sigma_{\mathrm{loc}}(X,x) > 0$ for x an arbitrary point on each connecting trajectory.*

Lemma 2.4.4. *Let $X \subset \mathbb{R}^n$ be a compact invariant set for a smooth flow Φ_t. Suppose that for all $x \in X$ the local stability index $\sigma_{\mathrm{loc}}(X,x) \in [-\infty,\infty]$ is defined.*

(a) If X is a.s, then $\sigma_{\mathrm{loc}}(X,x) = \infty$ for all $x \in X$.

(b) If there exists $x \in X$ such that $\sigma_{\mathrm{loc}}(X,x) > -\infty$, then X is f.a.s.

Proof. For (a) suppose that X is a.s. Pick $x \in X$ and $\delta > 0$. There is $\varepsilon_0 > 0$ such that $B_{\varepsilon_0}(X) \subset \mathscr{B}_\delta(X)$. Together with $B_{\varepsilon_0}(x) \subset B_{\varepsilon_0}(X)$, we have $\ell(B_{\varepsilon_0}(x) \cap \mathscr{B}_\delta(X)) = \ell(B_{\varepsilon_0}(x))$ so that $\Sigma_{\varepsilon,\delta}(x) = 1$ for all $\varepsilon < \varepsilon_0$. By the conjecture in Definition 2.4.1, it means that $\sigma_{\mathrm{loc}}(X,x) = \infty$. For (b) we note that $\sigma_{\mathrm{loc}}(X,x) > -\infty$ implies $\ell(\mathscr{B}_\delta(X)) > 0$ for small $\delta > 0$. This is just the definition of f.a.s. $\square$

Remark 2.4.5. The converse of Lemma 2.4.4(a) says $\sigma_{\text{loc}}(X,x) = -\infty$ for all $x \in X$ if X is c.u.

The next two lemmas allow to determine stability indices with respect to heteroclinic networks as a whole.

Lemma 2.4.6 (Lemma 2.4. in [17]). *Let X be a heteroclinic network and $C \subset X$ a heteroclinic cycle. Then, for all $x \in C$, we have $\sigma(X,x) \geq \sigma(C,x)$.*

Lemma 2.4.7 (Lemma 2.5 in [17]). *Let $X \subset R^n$ be a heteroclinic cycle (or network) and $x \in X$ a point on a connecting trajectory. Suppose that for all points $y = (y_1, \ldots, y_n) \in B_\varepsilon(x)$, stability with respect to X depends only on their (y_1, y_2)-components. Furthermore, assume that*

$$\mathscr{B}(X) \cap B_\varepsilon(x) = B_\varepsilon(x) \setminus \bigcap_{m \in \mathbb{N}} \mathscr{E}_m,$$

where $\mathscr{E}_m$ are non-empty, disjoint sets of the form

$$\mathscr{E}_m = \left\{ y \in B_\varepsilon(x) : \ k_m y_1^{\alpha_m} \leq y_2 \leq \hat{k}_m y_1^{\alpha_m} \right\},$$

with constants $k_m, \hat{k}_m > 0$. Suppose that $(\alpha_m)_{m \in \mathbb{N}}$ is bounded away from 1 and not all α_m are negative. Then, with $\alpha_{\max} := \max\{\alpha_m : \ 0 < \alpha_m < 1\}$ and $\alpha_{\min} := \min\{\alpha_m : \ \alpha_m > 1\}$, we have

$$\sigma(X,x) = -1 + \min\left\{ \frac{1}{\alpha_{\max}}, \alpha_{\min} \right\} > 0.$$

The results for the local stability index follow in the same way.

2.5 Switching

The interaction among various heteroclinic cycles composing a heteroclinic network can produce increasingly complex dynamics that range from intermittency to chaos. An interesting phenomenon is characterised by the way how nearby trajectories visit parts of the network, which is known as *switching*. A heteroclinic network can exhibit different forms of switching as described below.

Consider a heteroclinic network $X \subset \mathbb{R}^n$ with a finite set of nodes for the flow Φ_t of (2.1). Reordering if necessary, a (finite) *heteroclinic path* on X is a sequence of $k < \infty$ heteroclinic connections $(\kappa_{j,j+1})_{j \in \{1,\cdots,k\}}$ such that $\kappa_{j,j+1} = [\xi_j \to \xi_{j+1}]$ for consecutive nodes ξ_j and ξ_{j+1}. An infinite path takes $j \in \mathbb{N}$.

Given an initial condition $x \in \mathbb{R}^n$, the trajectory $\Phi_t(x)$ *follows* (or *shadows*) a heteroclinic path on X if, for every neighbourhood U of the path, there exists a time interval $I \subset \mathbb{R}^0_+$ such that $\Phi_t(x) \in U$ for all $t \in I$ (see Figure 2.2).

Definition 2.5.1 ([6]). We say there is *switching at a node* ξ_j of X if, for any neighbourhood of a point in any connection leading to ξ_j and sufficiently close to it, trajectories starting in that neighbourhood follow along all the possible connections forward from ξ_j.

Definition 2.5.2 ([6]). We say there is *switching along a heteroclinic connection* $\kappa_{i,j}$ of X if, for any neighbourhood of a point in any connection leading to ξ_i and sufficiently close to it, trajectories starting in that neighbourhood follow along $\kappa_{i,j}$ and then along all the possible connections forward from ξ_j.

Definition 2.5.3 ([6])**.** We say there is *finite* (resp. *infinite*) *switching* near X if, for each finite (resp. infinite) path on X, there exists a trajectory that follows it.

Of course, the existence of infinite switching implies switching along the heteroclinic connections, which in turn implies switching at all nodes of the heteroclinic network.

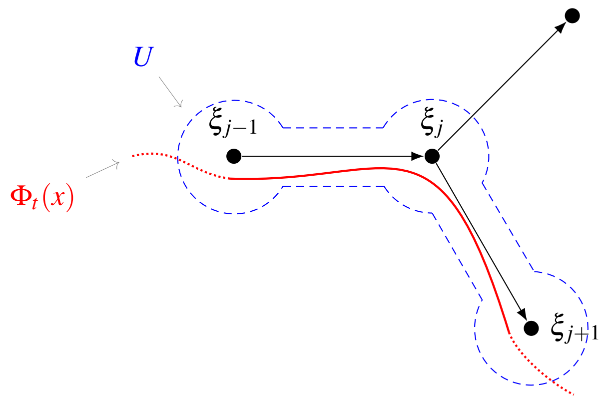

Fig. 2.2 Solution trajectory following an heteroclinic path: given a neighbourhood U of the heteroclinic path $[\xi_{j-1} \to \xi_j \to \xi_{j+1}]$, the trajectory $\Phi_t(x)$ follows it in U.

Chapter 3

Stability of quasi-simple heteroclinic cycles

[1]

Stability properties of heteroclinic cycles and networks can be quantified by the local stability index of Podvigina and Ashwin [53]. Such an index has been defined for an arbitrary invariant set. To the best of our knowledge, in the context of heteroclinic dynamics it has only been computed for some types of simple heteroclinic cycles in [53] and [46], and used by [17] in simple heteroclinic networks.

The aim of this chapter is to extend the calculations of the local stability index to quasi-simple heteroclinic cycles, a much wider collection of heteroclinic cycles. These include all simple heteroclinic cycles of type Z, various non-simple heteroclinic cycles arising from a straightforward generalisation of a construction method in [13], and heteroclinic cycles with heteroclinic connections contained in flow-invariant spaces which are not vector spaces, as those arising from population dynamics.

The chapter is organised as follows. In Section 3.1 we introduce the notion of quasi-simple heteroclinic cycle in $\mathbb{R}^n$. Section 3.2 describes the construction of local and global maps used to approximate the flow near the heteroclinic cycle. We make one assumption on global maps to ensure that basic transition matrices exist. These are presented in Section 3.3. In Section 3.4 we investigate the properties of suitable products of basic transition matrices required for the calculation of the local stability index along heteroclinic connections. The main achievements are the definition of a function whose images provide the local stability index in Lemma 3.4.8, and Theorems 3.4.2 and 3.4.9. Section 3.5 illustrates our results with a heteroclinic network in $\mathbb{R}^4$ made of two quasi-simple (non-simple) heteroclinic cycles.

[1] The content of this chapter is published in Garrido-da-Silva and Castro [28]. Definition 3.8 and Lemma 3.9 correspond here to Lemma 3.4.8 and Definition 3.4.7, respectively. We believe that this slight change helps the reader to better understand the construction of the function F^{index}.

3.1 Quasi-simple heteroclinic cycles

We define quasi-simple heteroclinic cycles so as to include all simple heteroclinic cycles and mainly to be useful in a non-symmetric context. Recall that $\hat{L}_j$ is the vector space connecting the node ξ_j to the origin in $\mathbb{R}^n$.

Definition 3.1.1 (Definition 2.1 in [28])**.** A robust heteroclinic cycle in $\mathbb{R}^n$ is *quasi-simple* if for any $j = 1,\dots,m$

- $\xi_j \in P_{j-1} \cap P_j$ where P_{j-1} and P_j are flow-invariant spaces;
- $\dim(P_j) = \dim(P_{j+1})$;
- $\dim\left(P_j \ominus \hat{L}_j\right) = 1$.

The condition $\dim\left(P_j \ominus \hat{L}_j\right) = 1$ means that for any j the dimension of the expanding eigenspace at ξ_j is one. This ensures that each heteroclinic connection $\kappa_{j,j+1} \subset P_j$ is one-dimensional.

Set $\hat{Q}_j = \hat{L}_j \oplus \left(T_{\xi_j} P_j \ominus \hat{L}_j\right)$. We can certainly assume that $T_{\xi_j} P_j \subseteq \hat{Q}_j$, since otherwise $T_{\xi_j} P_j$ has to comprise at least one transverse direction at ξ_j. In addition, $\hat{Q}_j$ is the smallest vector subspace in $\mathbb{R}^n$ locally coordinatised near ξ_j that contains P_j when this is not itself a vector space. We can rewrite $\hat{Q}_j = \hat{L}_{j+1} \oplus \left(T_{\xi_{j+1}} P_j \ominus \hat{L}_{j+1}\right)$ near ξ_{j+1}.

Lemma 3.1.2. *Let X be a quasi-simple heteroclinic cycle in R^n. Then,* $\dim\left(\hat{Q}_j\right) = \dim\left(\hat{Q}_{j+1}\right)$ *for all $j = 1,\dots,m$.*

Proof. As X is a quasi-simple heteroclinic cycle $\dim\left(T_{\xi_j} P_j \ominus \hat{L}_j\right) = 1$ for all $j = 1,\dots,m$. On account of the types of eigenvalues, the dimension of the contracting eigenspace at ξ_j is always greater than or equal to one. We thus get

$$\dim\left(T_{\xi_j} P_{j-1} \ominus \hat{L}_j\right) \geq 1 = \dim\left(T_{\xi_j} P_j \ominus \hat{L}_j\right).$$

Taking $\hat{Q}_{j-1} = \hat{L}_j \oplus \left(T_{\xi_j} P_{j-1} \ominus \hat{L}_j\right)$ and $\hat{Q}_j = \hat{L}_j \oplus \left(T_{\xi_j} P_j \ominus \hat{L}_j\right)$ near ξ_j yields

$$\dim\left(\hat{Q}_{j-1}\right) = \dim\left(\hat{L}_j\right) + \dim\left(T_{\xi_j} P_{j-1} \ominus \hat{L}_j\right) \geq \dim\left(\hat{L}_j\right) + \dim\left(T_{\xi_j} P_j \ominus \hat{L}_j\right) = \dim\left(\hat{Q}_j\right).$$

Now $\dim\left(\hat{Q}_1\right) \geq \dim\left(\hat{Q}_2\right) \geq \cdots \geq \dim\left(\hat{Q}_m\right) \geq \dim\left(\hat{Q}_1\right)$ forces the equality of all terms. □

Let us mention a straightforward consequence of the lemma.

Corollary 3.1.3. *Let X be a quasi-simple heteroclinic cycle in $\mathbb{R}^n$. Then, for all $j = 1,\dots,m$, (i)* $\dim\left(T_{\xi_j} P_{j-1} \ominus \hat{L}_j\right) = 1$*; (ii)* $\dim\left(\hat{L}_j\right) = \dim\left(\hat{L}_{j+1}\right)$*; and (iii)* $\dim(T_j) = \dim(T_{j+1})$.

Define n_r and n_t to be respectively the number of radial and transverse eigenvalues at each node. Corollary 3.1.3 states these are the same for every node in a quasi-simple heteroclinic cycle while contracting and expanding eigenvalues are simple. Thus $n = n_r + n_t + 2$. We make the following assumption:

Assumption 3.1.4. *Transverse, contracting and expanding eigenvalues are real and distinct.*

We focus on vector fields whose eigenvalues of the Jacobian matrix at the nodes are all real and distinct. However, having complex radial eigenvalues does not change stability results in which we are interested (see [52, Footnote 1]).

We denote the radial eigenvalues of $\mathrm{d}f(\xi_j)$ by $-r_{j,l}$ $(l = 1,\dots,n_r)$, the contracting one by $-c_j$, the expanding one by e_j and the transverse ones by $t_{j,s}$ $(s = 1,\dots,n_t)$. The constants $r_{j,l}$, c_j and e_j are positive but $t_{j,s}$ can have either sign.

3.2 Maps between cross sections

The standard way to address the dynamics of a heteroclinic cycle is to look at the return maps (also called Poincaré maps) from and to cross sections to the flow close to each node around the entire heteroclinic cycle.

Consider a neighbourhood of ξ_j where Ruelle's [63] sufficient condition for linearisation of the vector field f is satisfied. We choose local coordinates $(\boldsymbol{u},v,w,\boldsymbol{z}) \in \mathbb{R}^n$ in the basis of eigenvectors where the radial direction comes first, followed by the contracting, expanding and transverse directions. In particular, $\boldsymbol{u} = (u_1,\dots,u_{n_r})$ and $\boldsymbol{z} = (z_1,\dots,z_{n_t})$ are vectors.[2] The linearised system about ξ_j is given by

$$\begin{aligned}
\dot{u}_l &= -r_{j,l}u_l, \qquad l=1,\dots,n_r\\
\dot{v} &= -c_j v\\
\dot{w} &= e_j w\\
\dot{z}_s &= t_{j,s}z_s, \qquad s=1,\dots,n_t.
\end{aligned} \tag{3.1}$$

We introduce $(n-1)$-dimensional cross sections to the flow near ξ_j with the notation H_j^{in} along the incoming heteroclinic connection from ξ_{j-1} and H_j^{out} along the outgoing heteroclinic connection to ξ_{j+1}. Locally at ξ_j the heteroclinic connection $\kappa_{j-1,j}$ is tangent to the subspace $\{\boldsymbol{u} = \boldsymbol{0}, w = 0, \boldsymbol{z} = \boldsymbol{0}\}$ whereas the heteroclinic connection $\kappa_{j,j+1}$ is tangent to the subspace $\{\boldsymbol{u} = \boldsymbol{0}, v = 0, \boldsymbol{z} = \boldsymbol{0}\}$ so that[3]

$$\begin{aligned}
H_j^{in} &= \{(\boldsymbol{u},1,w,\boldsymbol{z}) : 0 \le u_l, w, z_s < 1 \text{ for all } l = 1,\dots,n_r,\ s = 1,\dots,n_t\}\\
H_j^{out} &= \{(\boldsymbol{u},\, v,\, 1,\boldsymbol{z}) : 0 \le u_l,\, v,\, z_s < 1 \text{ for all } l = 1,\dots,n_r,\ s = 1,\dots,n_t\}.
\end{aligned}$$

Now we construct a *local map* $\phi_j : H_j^{in} \to H_j^{out}$ to approximate the behaviour of trajectories passing close to ξ_j. Integrating (3.1) the local flow at time t takes the form

$$\mathscr{F}_t(\boldsymbol{u},v,w,\boldsymbol{z}) = \left(\left\{u_l\,\mathrm{e}^{-r_{j,l}t}\right\}_{l=1,\dots,n_r}, v\,\mathrm{e}^{-c_j t}, w\,\mathrm{e}^{e_j t}, \left\{z_s\,\mathrm{e}^{t_{j,s}t}\right\}_{s=1,\dots,n_t}\right).$$

A trajectory with initial condition $(\boldsymbol{u},v,w,\boldsymbol{z}) \in H_j^{in}$ hits H_j^{out} when it satisfies $w\mathrm{e}^{e_j t} = 1$. The associated transit time is then

$$t = -\frac{\ln(w)}{e_j}.$$

[2] Here and subsequently, we use boldtype to indicate a vector.

[3] Because all points in each orthant of $\mathbb{R}^{n-1}$ of H_j^{in} follow the same path (see [52, p. 1894]), we only consider the dynamics in the positive orthant.

To leading order we find

$$\phi_j(\boldsymbol{u},w,\boldsymbol{z}) = \left(\left\{ u^0_{j,l}\, w^{\frac{r_{j,l}}{e_j}} \right\}_{l=1,\ldots,n_r}, v^0_j\, w^{\frac{c_j}{e_j}}, \left\{ z_s\, w^{-\frac{t_{j,s}}{e_j}} \right\}_{s=1,\ldots,n_t} \right), \tag{3.2}$$

where $\boldsymbol{u}^0_j = \left(u^0_{j,1},\ldots,u^0_{j,n_r}\right)$ and v^0_j account for the coordinates of a point $\left(\boldsymbol{u}^0_j, v^0_j, 0, \boldsymbol{0}\right) \in P_{j-1}$ sufficiently close to the intersection of $\kappa_{j-1,j}$ with H^{in}_j. If $t_{j,s}$ is positive for some $s=1,\ldots,n_t$, the domain of definition of ϕ_j in H^{in}_j is constrained by the inequalities[4]

$$0 \le z_s < w^{\frac{t_{j,s}}{e_j}}.$$

A *global map* (also called *connecting diffeomorphism*) $\psi_j : H^{out}_j \to H^{in}_{j+1}$ further approximates the flow along each heteroclinic connection $\kappa_{j,j+1}$. We label the points at which $\kappa_{j,j+1}$ crosses H^{out}_j and H^{in}_{j+1} as $\left(\boldsymbol{u}^\bullet,0,1,\boldsymbol{0}\right)$ near ξ_j and $\left(\boldsymbol{u}^\star,1,0,\boldsymbol{0}\right)$ near ξ_{j+1}. Accordingly, ψ_j maps neighbourhoods of $\left(\boldsymbol{u}^\bullet,0,1,\boldsymbol{0}\right)$ in H^{out}_j homeomorphically onto neighbourhoods of $\left(\boldsymbol{u}^\star,1,0,\boldsymbol{0}\right)$ in H^{in}_{j+1}. Write ψ_j in components

$$\psi_j = \left(\left\{ \psi^{u_l}_j \right\}_{l=1,\ldots,n_r}, \psi^w_j, \left\{ \psi^{z_s}_j \right\}_{s=1,\ldots,n_t} \right).$$

The flow-invariance of P_j enables us to assert $\psi_j\left(P_j \cap H^{out}_j\right) \subset P_j \cap H^{in}_{j+1}$, which in turn implies

$$\begin{aligned} &\psi^w_j(\boldsymbol{u},0,\boldsymbol{0}) = 0 \\ &\psi^{z_s}_j(\boldsymbol{u},0,\boldsymbol{0}) = 0, \quad s=1,\ldots,n_t. \end{aligned}$$

Using a Taylor series expansion we obtain up to linear terms

$$\psi_j \begin{pmatrix} \boldsymbol{u} \\ v \\ \boldsymbol{z} \end{pmatrix} = \begin{pmatrix} \boldsymbol{u}^\star \\ 0 \\ \boldsymbol{0} \end{pmatrix} + \left(\begin{array}{c|c} C^{\|}_j & D_j \\ \hline \boldsymbol{0} & C_j \end{array} \right) \begin{pmatrix} \boldsymbol{u} \\ v \\ \boldsymbol{z} \end{pmatrix}.$$

Here the upper triangular block matrix comprises two squares blocks[5] $C^{\|}_j$ and C_j of order n_r and n_t+1, respectively, and an $n_r \times (n_t+1)$ block D_j such that $\det\left(C^{\|}_j\right) \neq 0$ and $\det(C_j) \neq 0$.

Set $g_j = \psi_j \circ \phi_j : H_j \to H_{j+1}$. A *return* or *Poincaré map* for a heteroclinic cycle connecting m nodes is constructed by appropriately composing these maps

$$\pi_j : H^{in}_j \to H^{in}_j, \qquad \pi_j = g_{j-1} \circ \cdots \circ g_1 \circ g_m \circ \cdots \circ g_{j+1} \circ g_j.$$

Notice that ϕ_j in (3.2) is independent of $\boldsymbol{u}$ and v. Therefore only the w and z_s components of ψ_j are sent through ϕ_j whenever the composition $g_j = \psi_j \circ \phi_j$ is taken in the return maps. It means that the relevant dimension of the maps is equal to the number of transverse eigenvalues plus one. We

---

[4]Strictly speaking, the maps are defined for $z_s < K(1-\varepsilon)\, w^{\frac{t_{j,s}}{e_j}}$, where K is a constant and ε is small. For more details we refer the reader to [39] and [53, Footnote 5].

[5]The notation $C^{\|}_j$ comes from [52].

can thus restrict the cross sections above to an (n_t+1)-dimensional subspace. The coordinates $(w,\boldsymbol{z})$ and $(v,\boldsymbol{z})$ are respectively used in the incoming and outgoing cross sections. From now on we always work in the significant subspaces preserving the notation in order to keep things simple. We write $\mathbb{R}^{n_t+1}$ or $\mathbb{R}^N$ $(N=n_t+1)$ in place of a cross section when no constrains are applied and no confusion arises. The restricted local and global maps are then given by

$$\phi_j\begin{pmatrix} w \\ \boldsymbol{z} \end{pmatrix} = \begin{pmatrix} v_j^0 w^{\frac{c_j}{e_j}} \\ \left\{ z_s w^{-\frac{t_{j,s}}{e_j}} \right\}_{s=1,\dots,n_t} \end{pmatrix}, \qquad \psi_j\begin{pmatrix} v \\ \boldsymbol{z} \end{pmatrix} = C_j \begin{pmatrix} v \\ \boldsymbol{z} \end{pmatrix}. \tag{3.3}$$

We need the following assumption:

Assumption 3.2.1 (Assumption 3.1 in [28])**.** *The global maps consist of a rescaled permutation of the local coordinate axes.*

This assumption holds for simple heetroclinic cycles of types B and C in $\mathbb{R}^4$ (see [43]) and more generally for simple heteroclinic cycles of type Z in $\mathbb{R}^n$ (see [52]). In the context of non-simple heetroclinic cycles, a remark in [5, p.1603] argues that global maps are permutations without rescaling.

In Section 2.3 stability properties of a flow-invariant set are described in terms of its δ-local basin of attraction. Now we see that the δ-local basin of attraction of a heteroclinic cycle can be related to that of a fixed point of a suitable collection of return maps. In fact, each return map $\pi_j : \mathbb{R}^N \to \mathbb{R}^N$ generates a discrete dynamical system through the relation $\boldsymbol{x}_{k+1} = \pi_j(\boldsymbol{x}_k)$ where $\boldsymbol{x}_k = (w_k, \boldsymbol{z}_k)$ denotes the state at the discrete time k. By construction the origin in $\mathbb{R}^N$ is a fixed point of π_j. In this way stability of a heteroclinic cycle follows from stability of the fixed point at the origin of return maps around the heteroclinic cycle.

We call *partial turns* to the maps

$$g_{(l,j)} : H_j^{in} \to H_{l+1}^{in}, \qquad g_{(l,j)} = \begin{cases} g_l \circ \cdots \circ g_j, & l > j \\ g_l \circ \cdots \circ g_1 \circ g_m \circ \cdots \circ g_j, & l < j \\ g_l, & l = j. \end{cases}$$

For $\delta > 0$ let $\mathscr{B}_\delta^{\pi_j}$ be the δ-local basin of attraction of $\mathbf{0} \in \mathbb{R}^N$ for the map π_j. Roughly speaking, $\mathscr{B}_\delta^{\pi_j}$ is the set of all initial conditions near ξ_j whose trajectories remain in a δ-neighbourhood of the heteroclinic cycle and converge to it. We use $\|\cdot\|$ to denote the Euclidean norm in $\mathbb{R}^N$. According to Definition 10 in [52], we have

$$\begin{aligned} \mathscr{B}_\delta^{\pi_j} = \Big\{ (w,\boldsymbol{z}) \in \mathbb{R}^N : \left\| g_{(l,j)} \circ \pi_j^k(w,\boldsymbol{z}) \right\| < \delta \text{ for all } l = 1,\dots,m, \text{ and } k \in \mathbb{N}_0 \\ \text{and } \lim_{k\to\infty} \left\| g_{(l,j)} \circ \pi_j^k(w,\boldsymbol{z}) \right\| = 0 \text{ for all } l = 1,\dots,m \Big\}. \end{aligned} \tag{3.4}$$

3.3 Transition matrices

From (3.3) the maps $g_j : H_j^{in} \to H_{j+1}^{in}$ may conveniently be written in matrix form as

$$g_j(w,\boldsymbol{z}) = C_j \begin{pmatrix} v_j^0 w^{\frac{c_j}{e_j}} \\ \left\{ z_s w^{-\frac{t_{j,s}}{e_j}} \right\}_{s=1,\dots,n_t} \end{pmatrix}.$$

Under Assumption 3.2.1, each matrix C_j in (3.3) is the product of a permutation matrix A_j with a diagonal matrix

$$B_j = \begin{pmatrix} a_{j,1} & 0 & \dots & 0 \\ 0 & a_{j,2} & \dots & 0 \\ . & . & \dots & . \\ 0 & 0 & \dots & a_{j,N} \end{pmatrix}.$$

The constants $a_{j,i}$, $i = 1,\dots,N$, are all positive due to the flow-invariance of P_j and uniqueness of solutions. Formally, B_j represents the rescaling of $(v,\boldsymbol{z})$ in the basis of eigenvectors of $\mathrm{d}f(\xi_j)$ and A_j is the transformation of $(v,\boldsymbol{z})$ in the basis of eigenvectors of $\mathrm{d}f(\xi_j)$ to $(w,\boldsymbol{z})$ in the basis of eigenvectors of $\mathrm{d}f(\xi_{j+1})$. There is no loss of generality in assuming ψ_j in (3.3) as orientation preserving because the change of direction of some vector is actually irrelevant in the study of stability (see [52, Footnote 3]).

Remark 3.3.1. When the global map in Assumption 3.2.1 is the identity, the matrix A_j need not be the identity since it also accounts for the permutation between the local bases in H_j^{out} and H_{j+1}^{in}. By way of illustration, for simple heteroclinic cycles of type B the matrix A_j is the identity; however, for simple heteroclinic cycles of type C, it is not. In general, if the heteroclinic cycle is simple and $n_t = 1$, then Proposition 4.1 in [43] provides the form of the global maps.

As in [52], take new coordinates of the form

$$\boldsymbol{\eta} = (\ln(w), \ln(z_1), \dots, \ln(z_{n_t})). \tag{3.5}$$

The maps $g_j : \boldsymbol{\eta} \mapsto \boldsymbol{\eta}$ become linear. We denote them by $\mathscr{M}_j$ where

$$\mathscr{M}_j \boldsymbol{\eta} = M_j \boldsymbol{\eta} + F_j \tag{3.6}$$

such that

$$M_j = A_j \begin{pmatrix} b_{j,1} & 0 & 0 & \dots & 0 \\ b_{j,2} & 1 & 0 & \dots & 0 \\ b_{j,3} & 0 & 1 & \dots & 0 \\ . & . & . & \dots & . \\ b_{j,N} & 0 & 0 & \dots & 1 \end{pmatrix}, \qquad F_j = A_j \begin{pmatrix} \ln\left(v_j^0\right) + \ln(a_{j,1}) \\ \ln(a_{j,2}) \\ \ln(a_{j,3}) \\ \vdots \\ \ln(a_{j,N}) \end{pmatrix}. \tag{3.7}$$

Since the matrix A_j is a permutation it naturally remains the same in (3.7). The entries of M_j depend exclusively on the contracting, expanding and transverse eigenvalues at node ξ_j with

$$b_{j,1} = \frac{c_j}{e_j}, \qquad b_{j,s+1} = -\frac{t_{j,s}}{e_j}, \qquad s = 1,\dots,n_t,\ \ j = 1,\dots,m.$$

In [52] the matrices M_j are called *basic transition matrices* of the maps g_j. Based on the expressions of the maps in (3.3) and the new coordinates (3.5) we have just proved the following

Theorem 3.3.2 (Theorem 3.1 in [28])**.** *For a quasi-simple heteroclinic cycle satisfying Assumption 3.2.1, the transition between incoming sections at consecutive equilibria can be described using basic transition matrices of the form* (3.7)*.*

This matrix representation is essential for our results. In fact, if a heteroclinic cycle is neither quasi-simple nor does it satisfy Assumption 3.2.1 but such a representation exists, then our results are still true. Note that the dimension of a transition matrix is determined by the dimension of the state-space, while the layout of its entries does not.

Transition matrices of the maps π_j and $g_{(j,l)}$ are respectively the products of basic transition matrices

$$M^{(j)} = M_{j-1}\cdots M_1 M_m \cdots M_{j+1} M_j \tag{3.8}$$

and

$$M_{(l,j)} = \begin{cases} M_l \cdots M_j, & l > j \\ M_l \cdots M_1 M_m \cdots M_j, & l < j \\ M_j, & l = j. \end{cases}$$

The definition of the local stability index requires asymptotically small w and z_s for any $s = 1,\dots,n_t$, which is equivalent to asymptotically large negative $\boldsymbol{\eta}$. As noticed in [53, p. 903], because F_j in (3.6) is finite we can ignore it[6] so that the map g_j asymptotically to leading order is described by the matrix M_j. The same holds true for their compositions. Then, the limit in (3.4) in coordinates (3.5) becomes for all $l = 1,\dots,m$

$$\lim_{k\to\infty} M_{(l,j)} \left(M^{(j)}\right)^k \boldsymbol{\eta} = -\boldsymbol{\infty}. \tag{3.9}$$

Setting $M = M^{(j)}$, we see that the points in $\mathscr{B}_\delta^{\pi_j}$ are a subset of

$$U^{-\infty}(M) = \left\{ \boldsymbol{y} \in \mathbb{R}^N_- : \lim_{k\to\infty} M^k \boldsymbol{y} = -\boldsymbol{\infty} \right\}. \tag{3.10}$$

Assume that M has eigenvalues $\lambda_1,\dots,\lambda_N$ and corresponding linearly independent eigenvectors $\boldsymbol{w}_1,\dots,\boldsymbol{w}_N$. Let $\lambda_{\max}$ be the maximum, in absolute value, eigenvalue of M such that $|\lambda_{\max}| \neq 1$ and $\boldsymbol{w}^{\max} = (w_1^{\max},\dots,w_N^{\max})$ the associated eigenvector.

[6] Alternatively, we may proceed as in [56] and rescale the coordinates such that all the coefficients of the map g_j are one yielding $F_j = \boldsymbol{0}$.

Podvigina [52] claims that Lemma 3 provides only sufficient conditions in terms of $\lambda_{\max}$ and $\boldsymbol{w}^{\max}$ that guarantee $\ell\left(U^{-\infty}(M)\right) > 0$ for an arbitrary $N \times N$ real matrix M (regardless of whether or not $|\lambda_{\max}| \neq 1$). However, it is straightforward to check that these are also necessary. For ease of reference, we state the necessary and sufficient conditions in next lemma.

First observe that any vector $\boldsymbol{y} = (y_1, \ldots, y_N) \in \mathbb{R}^N_-$ can be written as a linear combination of the eigenvectors of M as

$$\boldsymbol{y} = \sum_{i=1}^{N} a_i \boldsymbol{w}_i = P\boldsymbol{a}, \tag{3.11}$$

where P is the matrix whose columns are $\boldsymbol{w}_i$, $i = 1, \ldots, N$, and $\boldsymbol{a} = (a_1, \ldots, a_N) \in \mathbb{R}^N$ is some vector. For each $k \in \mathbb{N}$ the k^{th} iterate of $\boldsymbol{y}$ under M is

$$M^k \boldsymbol{y} = \sum_{i=1}^{N} \lambda_i^k a_i \boldsymbol{w}_i. \tag{3.12}$$

Lemma 3.3.3 (adapted from Lemma 3 in [52])**.** *The measure $\ell\left(U^{-\infty}(M)\right)$ is positive if and only if the three following conditions are satisfied:*

(i) $\lambda_{\max}$ *is real;*

(ii) $\lambda_{\max} > 1$*;*

(iii) $w_q^{\max} w_p^{\max} > 0$ *for all* $q, p = 1, \ldots, N$.

Proof. Suppose that at least one of the conditions *(i)–(iii)* is violated. It follows from Lemma 3(i)–(iv) in [52] that $\ell\left(U^{-\infty}(M)\right) = 0$.

The converse is already shown in Lemma 3(v) of [52]. □

Since the transformation (3.5) can turn a set of finite measure into one of infinite measure we preserve the convention of [52, p. 1900] that the measure of a set is always its measure in the original variables.

3.4 Calculation of stability indices

For $R \in \mathbb{R}$ let us introduce the subset of $\mathbb{R}^N$

$$U_R = \left\{ \boldsymbol{y} \in \mathbb{R}^N : \max_{i=1,\ldots,N} y_i < R \right\}. \tag{3.13}$$

Recall that the change of coordinates (3.5) transforms the origin into $-\boldsymbol{\infty}$. Together with (3.9), an alternative way of describing $\mathscr{B}_\delta^{\pi_j}$ for $S = \ln(\delta)$ is

$$\begin{aligned} \mathscr{U}_S^{M^{(j)}} = \Big\{ \boldsymbol{y} \in \mathbb{R}^N_- : M_{(l,j)} \left(M^{(j)}\right)^k \boldsymbol{y} \in U_S \text{ for all } l = 1, \ldots, m, \text{ and } k \in \mathbb{N}_0 \\ \text{and } \lim_{k\to\infty} M_{(l,j)} \left(M^{(j)}\right)^k \boldsymbol{y} = -\boldsymbol{\infty} \text{ for all } l = 1, \ldots, m \Big\}. \end{aligned} \tag{3.14}$$

The set $\mathscr{U}_S^{M^{(j)}}$ is the S-local basin of attraction of the fixed point $-\boldsymbol{\infty}$ in $\mathbb{R}^N$ for the matrix $M^{(j)}$ representing the map π_j.

Calculation of local stability indices is divided into two cases: when transverse eigenvalues at all nodes are negative and when, for at least one node, there is one positive transverse eigenvalue. In terms of transition matrices, this corresponds to basic transition matrices with only non-negative entries and with at least one negative entry, respectively. The latter occurs naturally whenever the cycle is part of a heteroclinic network. The two cases are addressed in Theorems 3.4.2 and 3.4.9.

The following is a useful auxiliary result for the proof of Theorem 3.4.2.

Lemma 3.4.1 (Lemma 3.3 in [28]). *Let M be a transition matrix* (3.8) *with non-negative entries and $\lambda_{\max} > 1$. Then, generically, $U^{-\infty}(M) = \mathbb{R}^N_-$.*

Proof. Since $|\lambda_{\max}| > 1$, Theorem 3 in [52] guarantees that generically all components of the eigenvector $\boldsymbol{w}^{\max}$ are non-zero. Therefore $U^{-\infty}(M) = \mathbb{R}^N_-$ by Lemma 4(iii) in [52]. □

We point out that, in view of Lemma 4(i) in [52], the hypothesis $\lambda_{\max} > 1$ is equivalent to $|\lambda_{\max}| > 1$.

Denote by σ_j the local stability index along the heteroclinic connection leading to ξ_j.

Theorem 3.4.2 (Theorem 3.4 in [28]). *Let M_j, $j = 1,\ldots,m$, be basic transition matrices of a collection of maps associated with a heteroclinic cycle. Suppose that for all $j = 1,\ldots,,m$ all entries of the matrices are non-negative. Then:*

(a) If the transition matrix $M^{(1)} = M_m \ldots M_1$ satisfies $|\lambda_{\max}| > 1$, then $\sigma_j = +\infty$ for all $j = 1,\ldots,m$, and the cycle is asymptotically stable.

(b) Otherwise, $\sigma_j = -\infty$ for all $j = 1,\ldots,m$ and the cycle is not an attractor.

Proof. We treat each statement separately.

(a) Suppose that the matrix $M \equiv M^{(1)}$ satisfies $|\lambda_{\max}| > 1$. Similarity of the matrices $M^{(j)}$ ensures that the same holds for all $j = 1,\ldots,m$.

The product of matrices with non-negative entries also has non-negative entries. This is the case for $M^{(j)}$ and $M_{(l,j)}$ with $j,l = 1,\ldots,m$. By Lemma 3.4.1, $U^{-\infty}(M^{(j)}) = \mathbb{R}^N_-$. Then, for any $\boldsymbol{y} \in \mathbb{R}^N_-$,

$$M_{(l,j)}\left(M^{(j)}\right)^k \boldsymbol{y} \in \mathbb{R}^N_- \qquad \text{for all } j,l = 1,\ldots,m, \text{ and } k \in \mathbb{N}_0$$

and

$$\lim_{k\to\infty} M_{(l,j)}\left(M^{(j)}\right)^k \boldsymbol{y} = -\boldsymbol{\infty} \qquad \text{for all } j,l = 1,\ldots,m.$$

Given $S < 0$ and the linearity of maps M_j it follows that $U_R \cap \mathscr{U}_S^{M^{(j)}}$ is reduced to U_R for an R-neighbourhood U_R of $-\boldsymbol{\infty}$ with $R < S$. Taking the respective measures in original coordinates, $\sigma_{j,+} = \infty$ and $\sigma_{j,-} = 0$ for all $j = 1,\ldots,m$ by the convention in Definition 2.4.1. In addition $U_R \subset \mathscr{U}_S^{M^{(j)}}$ and, by Definition 2.3.1, the heteroclinic cycle is a.s.

(b) If the matrix $M \equiv M^{(1)}$ satisfies $|\lambda_{\max}| \leq 1$, then $U^{-\infty}(M)$ is empty as proved in [52, Lemma 3(i)]. Hence $\sigma_{1,+} = 0$ and $\sigma_{1,-} = \infty$. Since the inequality $|\lambda_{\max}| \leq 1$ is satisfied for any $M^{(j)}$ we get $\sigma_{j,+} = 0$ and $\sigma_{j,-} = \infty$ for all $j = 1, \ldots, m$.

□

Irrespectively of the sign of the entries of the basic transition matrices we have the following generalisation of Corollary 4.1 in [53] to quasi-simple heteroclinic cycles.

Lemma 3.4.3 (Lemma 3.5 in [28])**.** *Let M_j, $j = 1, \ldots, m$, be basic transition matrices of a collection of maps associated with a heteroclinic cycle. If $\ell\left(U^{-\infty}\left(M^{(j)}\right)\right) = 0$ for some $j \in \{1, \ldots, m\}$ then $\ell\left(\mathscr{U}_S^{M^{(j)}}\right) = 0$ for all $j = 1, \ldots, m$ and $S < 0$.*

Proof. The contrapositive of Lemma 3.3.3 asserts that $\ell\left(U^{-\infty}\left(M^{(j)}\right)\right) = 0$ if and only if $M^{(j)}$ violates at least one condition *(i)* to *(iii)*.

Recall that all matrices $M^{(j)}$ are similar so that *(i)–(ii)* of Lemma 3.3.3 either are, or are not, simultaneously satisfied for all $j = 1, \ldots, m$. If either *(i)* or *(ii)* fail, we trivially get $\ell\left(U^{-\infty}\left(M^{(j)}\right)\right) = 0$ for all $j = 1, \ldots, m$. As $\mathscr{U}_S^{M^{(j)}} \subset U^{-\infty}\left(M^{(j)}\right)$ the result is $\ell\left(\mathscr{U}_S^{M^{(j)}}\right) = 0$ for all $j = 1, \ldots, m$ and $S < 0$.

Let $\boldsymbol{w}^{\max,j} = \left(w_1^{\max,j}, \ldots, w_N^{\max,j}\right)$ be the eigenvector of the matrix $M^{(j)}$ associated with the eigenvalue $\lambda_{\max}$. Suppose now that *(i)–(ii)* hold for all $j = 1, \ldots, m$ while *(iii)* is not satisfied for some $j \in \{1, \ldots, m\}$. That is, $\lambda_{\max}$ is real and greater than one and there exist $q, p \in \{1, \ldots, N\}$ such that $w_q^{\max,j} w_p^{\max,j} \leq 0$. For a vector $\boldsymbol{y} \in \mathbb{R}^N$ expressed as in (3.11) the iterates $\left(M^{(j)}\right)^k \boldsymbol{y}$ become asymptotically close to $a_{\max} \lambda_{\max}^k \boldsymbol{w}^{\max,j}$ when $k \to \infty$ (see (3.12)). Hence $\left(M^{(j)}\right)^k \boldsymbol{y}$ are not in $\mathbb{R}_-^N$ for sufficiently large k and any $\boldsymbol{y} \in \mathbb{R}^N$. The same reasoning applies to the iterates of $M_{(j-1,l)}\boldsymbol{y}$ under $M^{(j)}$ so that for all $l = 1, \ldots, m$

$$\lim_{k \to \infty} \left(M^{(j)}\right)^k M_{(j-1,l)} \boldsymbol{y} = \lim_{k \to \infty} M_{(j-1,l)} \left(M^{(l+1)}\right)^k \boldsymbol{y} \notin \mathbb{R}_-^N.$$

On account of (3.14), we have $\ell\left(\mathscr{U}_S^{M^{(l+1)}}\right) = 0$ for all $l = 1, \ldots, m$ and $S < 0$. □

Concerning local stability indices for quasi-simple heteroclinic cycles in general, we are led to Theorem 3.4.9. Assume next that at least one entry of some basic transition matrix M_j is negative. It means that at least one transverse eigenvalue at ξ_j is positive.

We need a couple of auxiliary results and notation as follows. Define the set

$$U_R(\boldsymbol{\alpha}_1; \boldsymbol{\alpha}_2; \ldots; \boldsymbol{\alpha}_N) = \left\{ \boldsymbol{y} \in U_R : \sum_{i=1}^N \alpha_{si} y_i < 0 \text{ for } \boldsymbol{\alpha}_s \neq \boldsymbol{0},\ s = 1, \ldots, N \right\} \tag{3.15}$$

where $\boldsymbol{\alpha}_s = (\alpha_{s1}, \ldots, \alpha_{sN}) \in \mathbb{R}^N$ and $R < 0$. If $\alpha_{si} > 0$ for all $s = 1, \ldots, N$, then $\sum_{i=1}^N \alpha_{si} y_i < 0$ trivially.

Regard $\boldsymbol{y} \in \mathbb{R}_-^N$ as a linear combination of the eigenvectors of $M^{(j)}$ such in (3.11). Hence

$$\boldsymbol{a} = \left(P^{(j)}\right)^{-1} \boldsymbol{y}. \tag{3.16}$$

Let

$$\boldsymbol{v}^{\max,j} = \left(v_1^{\max,j}, v_2^{\max,j}, \ldots, v_N^{\max,j}\right) \tag{3.17}$$

be the line of $\left(P^{(j)}\right)^{-1}$ corresponding to the position associated with $\lambda_{\max}$.

Lemma 3.4.4. *If $\ell\left(U^{-\infty}\left(M^{(j)}\right)\right) > 0$, then $U^{-\infty}\left(M^{(j)}\right)$ is either $\mathbb{R}^N_-$ or given by $U_0\left(\boldsymbol{v}^{\max,j};\boldsymbol{0};\ldots;\boldsymbol{0}\right)$ such that $v_i^{\max,j} > 0$ for some $i = 1,\ldots,N$.*

Proof. Suppose that the matrix $M \equiv M^{(j)}$ meets $\ell\left(U^{-\infty}(M)\right) > 0$. Lemma 3.3.3 provides that

$$U^{-\infty}(M) = \left\{\boldsymbol{y} \in \mathbb{R}^N_- : \ a_{\max} < 0\right\} \neq \emptyset \tag{3.18}$$

where $a_{\max}$ is the coefficient in front of $\boldsymbol{w}^{\max}$ in expansion (3.11) for $\boldsymbol{y}$. If $a_{\max} < 0$ for any $\boldsymbol{y} \in \mathbb{R}^N_-$, then $U^{-\infty}(M) = \mathbb{R}^N_-$. Otherwise we make use of (3.16) and the fact that $U_0 = \mathbb{R}^N_-$, which establishes

$$U^{-\infty}(M) = \left\{\boldsymbol{y} \in U_0 : \sum_{i=1}^{N} v_i^{\max,j} y_i < 0\right\} = U_0\left(\boldsymbol{v}^{\max,j};\boldsymbol{0};\ldots;\boldsymbol{0}\right). \tag{3.19}$$

Of course $U^{-\infty}(M) \neq \emptyset$ whenever there is some $i = 1,\ldots,N$ for which $v_i^{\max,j} > 0$. $\square$

Lemma 3.4.5 (Lemma 3.6 in [28])**.** *Let $q = j_1,\ldots,j_L$, $L \geq 1$, denote all the indices for which M_q has at least one negative entry. Then, $\ell\left(U^{-\infty}\left(M^{(j)}\right)\right) > 0$ for all $j = 1,\ldots,m$ if and only if $\ell\left(U^{-\infty}\left(M^{(j)}\right)\right) > 0$ for all $j = j_p + 1$, $p = 1,\ldots,L$, such that $j_p + 1 \notin \{j_1,\ldots,j_L\}$.*

Proof. The implication $\Rightarrow$ is trivial.

For the implication $\Leftarrow$, notice that $\ell\left(U^{-\infty}\left(M^{(j)}\right)\right) > 0$ if and only if $M^{(j)}$ satisfies *(i)–(iii)* of Lemma 3.3.3. Conditions *(i)–(ii)* hold simultaneously for every $j = 1,\ldots,m$ since all matrices $M^{(j)}$ are similar.

Suppose that for each $p = 1,\ldots,L$ such that $j_p + 1 \notin \{j_1,\ldots,j_L\}$ the matrix $M^{(j_p+1)}$ satisfies *(iii)* of Lemma 3.3.3. Without loss of generality, we assume that all entries of M_j with $j = j_p+1, j_p+2,\ldots,j_{p+1}-1$ are non-negative. As a consequence, the product $M_{(j-1,j_p+1)} = M_{j-1}\cdots M_{j_p+2}M_{j_p+1}$ has non-negative entries for any $j = j_p+2,\ldots,j_{p+1}$. Now $M_{(j-1,j_p+1)}M^{(j_p+1)} = M^{(j)}M_{(j-1,j_p+1)}$ and[7]

$$\boldsymbol{w}^{\max,j} = M_{(j-1,j_p+1)}\boldsymbol{w}^{\max,j_p+1}.$$

Therefore if all components of $\boldsymbol{w}^{\max,j_p+1}$ have the same sign, then all components of $\boldsymbol{w}^{\max,j}$ have similarly the same sign for all remaining $j \in \cup_{p=1}^{L}\{j_p+2,\ldots,j_{p+1}\}$. $\square$

For each $l = 1,\ldots,m$ denote by $\boldsymbol{\alpha}_s^l = \left(\alpha_{s1}^l,\ldots,\alpha_{sN}^l\right)$, $s = 1,\ldots,N$, the s^{th} row of the matrix $M_{(l,j)}$. Note that this implies $\boldsymbol{\alpha}_s^l \neq \boldsymbol{0}$ for all $s = 1,\ldots,N$.

Lemma 3.4.6 (Lemma 3.7 in [28])**.** *Let $q = j_1,\ldots,j_L$, $L \geq 1$, denote all the indices for which M_q has at least one negative entry. Suppose that the matrices $M^{(j)}$ satisfy conditions (i)–(iii) of Lemma 3.3.3 for all $j = j_p+1$, $p = 1,\ldots,L$, such that $j_p+1 \notin \{j_1,\ldots,j_L\}$. Then, $\boldsymbol{y} \in \mathbb{R}^N_-$ such that for all $l = 1,\ldots,m$*

$$\lim_{k\to\infty} M_{(l,j)}\left(M^{(j)}\right)^k \boldsymbol{y} = -\boldsymbol{\infty} \tag{3.20}$$

[7] If $\boldsymbol{w}$ is an eigenvector of $M^{(j)}$, that is, $M^{(j)}\boldsymbol{w} = \lambda\boldsymbol{w}$ for some scalar λ, then $M^{(l)}M_{(l-1,j)}\boldsymbol{w} = M_{(l-1,j)}M^{(j)}\boldsymbol{w} = \lambda M_{(l-1,j)}\boldsymbol{w}$. It means that $M_{(l-1,j)}\boldsymbol{w}$ is an eigenvector for $M^{(l)}$ associated to the same eigenvalue λ.

is equivalent to

$$\boldsymbol{y} \in U^{-\infty}\left(M^{(j)}\right) \cap \left(\bigcap_{p=1}^{L} U_0\left(\boldsymbol{\alpha}_1^{j_p};\boldsymbol{\alpha}_2^{j_p};\ldots;\boldsymbol{\alpha}_N^{j_p}\right)\right).$$

Proof. Take $\boldsymbol{y} \in \mathbb{R}_-^N$. For any $l = 1,\ldots,m$ and $k \in \mathbb{N}_0$ we can write $M_{(l,j)}\left(M^{(j)}\right)^k = \left(M^{(l+1)}\right)^k M_{(l,j)}$ so that

$$\lim_{k\to\infty} M_{(l,j)}\left(M^{(j)}\right)^k \boldsymbol{y} = \lim_{k\to\infty}\left(M^{(l+1)}\right)^k M_{(l,j)}\boldsymbol{y}.$$

From (3.10) the limit $\lim_{k\to\infty}\left(M^{(l+1)}\right)^k M_{(l,j)}\boldsymbol{y} = -\boldsymbol{\infty}$ is true if and only if

$$M_{(l,j)}\boldsymbol{y} \in U^{-\infty}\left(M^{(l+1)}\right).$$

By virtue of Lemma 3.4.5, $\ell\left(U^{-\infty}\left(M^{(j)}\right)\right) > 0$ for all $j = 1,\ldots,m$ and $U^{-\infty}\left(M^{(j)}\right)$ are of the form (3.18). Considering $\boldsymbol{y} = P^{(j)}\boldsymbol{a}$ yields $M_{(l,j)}\boldsymbol{y} = M_{(l,j)}P^{(j)}\boldsymbol{a} = P^{(l+1)}\boldsymbol{a}$ (see Footnote 7). Hence the component $a_{\max}$ is the same in the description of $\boldsymbol{y} \in U^{-\infty}\left(M^{(j)}\right)$ and of $M_{(l,j)}\boldsymbol{y} \in U^{-\infty}\left(M^{(l+1)}\right)$. Based on (3.18), if $\boldsymbol{y} \in U^{-\infty}\left(M^{(j)}\right)$, it suffices to demand $M_{(l,j)}\boldsymbol{y} \in U_0 = \mathbb{R}_-^N$ in order to guarantee that $M_{(l,j)}\boldsymbol{y}$ belongs to $U^{-\infty}\left(M^{(l+1)}\right)$. We see at once that

$$M_{(l,j)}\boldsymbol{y} \in U_0 \Leftrightarrow \sum_{i=1}^{N} \alpha_{si}^{l} y_i < 0 \qquad \text{for all } s = 1,\ldots,N$$

is equivalent to $\boldsymbol{y} \in U_0\left(\boldsymbol{\alpha}_1^l,\ldots,\boldsymbol{\alpha}_N^l\right)$ on account of (3.15).

We do not need all the m sets $U_0\left(\boldsymbol{\alpha}_1^l,\ldots,\boldsymbol{\alpha}_N^l\right)$. In fact, when $M_{(q,j)}$ is the product of matrices with only non-negative entries, $\lim_{k\to\infty} M_{(q,j)}\left(M^{(j)}\right)^k \boldsymbol{y} = -\boldsymbol{\infty}$ holds naturally for any $\boldsymbol{y} \in U^{-\infty}\left(M^{(j)}\right)$. Suppose that the basic transition matrix M_{q+1} with $M_{q+1}M_{(q,j)} = M_{(q+1,j)}$ has at least one negative entry. Then, $\lim_{k\to\infty} M_{(q+1,j)}\left(M^{(j)}\right)^k \boldsymbol{y} = -\boldsymbol{\infty}$ for any $\boldsymbol{y} \in U^{-\infty}\left(M^{(j)}\right) \cap U_0\left(\boldsymbol{\alpha}_1^{q+1},\ldots,\boldsymbol{\alpha}_N^{q+1}\right)$ as before. The set of points satisfying (3.20) for all $l = 1,\ldots,m$ gets restricted to

$$U^{-\infty}\left(M^{(j)}\right) \cap \left(\bigcap_{p=1}^{L} U_0\left(\boldsymbol{\alpha}_1^{j_p};\boldsymbol{\alpha}_2^{j_p};\ldots;\boldsymbol{\alpha}_N^{j_p}\right)\right).$$

□

We compute the local stability index by means of the function F^{index}, the analogue of the function f^{index} of [53, p. 905].

Definition 3.4.7 (Lemma 3.9 in [28])**.** Let the intersection of the local basin of attraction of a compact flow-invariant set X with a cross section transverse to the flow at $x \in X$ be given in coordinates (3.5) by $U_R(\boldsymbol{\alpha};\mathbf{0};\ldots;\mathbf{0})$ for some $\boldsymbol{\alpha} = (\alpha_1,\alpha_2,\ldots,\alpha_N) \in \mathbb{R}^N$ and $R < 0$. The function $\boldsymbol{\alpha} \mapsto F^{\text{index}}(\boldsymbol{\alpha})$ is the local stability index for X at x relative to this intersection, i.e. $F^{\text{index}}(\boldsymbol{\alpha}) = \sigma_{\text{loc}}(X,x)$.

Lemma 3.4.6 and Theorem 3.4.9 show that in coordinates (3.5) the set $\mathscr{B}_\delta^{\pi_j}$ in H_j^{in} is of the form $U_R(\boldsymbol{\alpha}_1;\boldsymbol{\alpha}_2;\ldots;\boldsymbol{\alpha}_N)$. By (3.15) we can set

$$U_R(\boldsymbol{\alpha}_1;\boldsymbol{\alpha}_2;\ldots;\boldsymbol{\alpha}_N) = \bigcap_{i=1}^{N} U_R(\boldsymbol{\alpha}_i;\mathbf{0};\ldots;\mathbf{0}).$$

The local stability index for the heteroclinic connection that intersects H_j^{in} enables us to characterise the local geometry of $\mathscr{B}_\delta^{\pi_j}$. From Definition 3.4.7 its value is given by

$$\min_{i=1,\ldots,N} \left\{F^{\text{index}}\left(\boldsymbol{\alpha}_i\right)\right\}.$$

The function F^{index} is used to determine the local stability index at any point of a heteroclinic cycle through two components, F^- and F^+, related respectively to $\sigma_{\text{loc},-}$ and $\sigma_{\text{loc},+}$ in Definition 2.4.1.

Lemma 3.4.8 (Definition 3.8 in [28])**.** *Let* $\boldsymbol{\alpha} = (\alpha_1, \ldots, \alpha_N) \in \mathbb{R}^N$ *and* $\alpha_{\min} = \min_{i=1,\ldots,N}\{\alpha_i\}$*. The values of the function* $F^{\text{index}} : \mathbb{R}^N \to \mathbb{R}$ *are*

$$F^{\text{index}}\left(\boldsymbol{\alpha}\right) = F^+\left(\boldsymbol{\alpha}\right) - F^-\left(\boldsymbol{\alpha}\right)$$

where $F^-\left(\boldsymbol{\alpha}\right) = F^+\left(-\boldsymbol{\alpha}\right)$ *and*

$$F^+\left(\boldsymbol{\alpha}\right) = \begin{cases} +\infty, & \text{if } \alpha_{\min} \geq 0 \\ 0, & \text{if } \sum_{i=1}^N \alpha_i \leq 0 \\ -\dfrac{1}{\alpha_{\min}} \sum_{i=1}^N \alpha_i, & \text{if } \alpha_{\min} < 0 \text{ and } \sum_{i=1}^N \alpha_i \geq 0. \end{cases}$$

See Appendix A for the detailed construction of F^{index} as well as its explicit values when $N = 3$.

Theorem 3.4.9 (Theorem 3.10 in [28])**.** *Let* M_j*,* $j = 1, \ldots, m$*, be basic transition matrices of a collection of maps associated with a heteroclinic cycle. Denote by* $q = j_1, \ldots, j_L$*,* $L \geq 1$*, all the indices for which* M_q *has at least one negative entry.*

(a) If, for at least one j*, the matrix* $M^{(j)}$ *does not satisfy conditions (i)–(iii) of Lemma 3.3.3, then* $\sigma_j = -\infty$ *for all* $j = 1, \ldots, m$ *and the cycle is not an attractor.*

(b) If the matrices $M^{(j)}$ *satisfy conditions (i)–(iii) of Lemma 3.3.3 for all* $j = j_p + 1$*,* $p = 1, \ldots, L$*, such that* $j_p + 1 \notin \{j_1, \ldots, j_L\}$*, then the cycle is f.a.s. Furthermore, for each* $j = 1, \ldots, m$*, there exist vectors* $\boldsymbol{\beta}_1, \boldsymbol{\beta}_2, \ldots, \boldsymbol{\beta}_K \in \mathbb{R}^N$ *such that*

$$\sigma_j = \min_{i=1,\ldots,K} \left\{F^{\text{index}}\left(\boldsymbol{\beta}_i\right)\right\}. \tag{3.21}$$

Proof. Statement (a) follows immediately from Lemma 3.4.3.

(b) Under the hypotheses, Lemma 3.4.5 gives $\ell\left(U^{-\infty}\left(M^{(j)}\right)\right) > 0$ for all $j = 1, \ldots, m$. The cycle is then f.a.s.[8]

By Definition 2.4.1 the local stability index is computed for $\delta > 0$ small leading to large negative $S = \ln(\delta)$. We derive the S-local basin of attraction in (3.14) from (3.19) together with

[8] The implication is handled in much the same way as in [52, Theorem 5(b)]. The arguments therein involve exclusively the maps associated with the heteroclinic cycle, which coincide with ours.

Lemma 3.4.6 so that

$$\begin{aligned}\mathscr{U}_S^{M^{(j)}} = U_0\left(\boldsymbol{v}^{\max,j};\mathbf{0};\ldots;\mathbf{0}\right) \cap \left(\bigcap_{p=1}^{L} U_0\left(\boldsymbol{\alpha}_1^{j_p};\boldsymbol{\alpha}_2^{j_p};\ldots;\boldsymbol{\alpha}_N^{j_p}\right)\right)\\ \cap \left\{\boldsymbol{y}\in\mathbb{R}_-^N : \, M_{(l,j)}\left(M^{(j)}\right)^k \boldsymbol{y}\in U_S \text{ for all } l=1,\ldots,m, \text{ and } k\in\mathbb{N}_0\right\}.\end{aligned} \tag{3.22}$$

As S approaches $-\infty$ the condition defining the third set above becomes redundant in the sense that it holds true for all $\boldsymbol{y}\in U_R$ with $R<S$. Therefore $U_R\cap\mathscr{U}_S^{M^{(j)}}$ is reduced to

$$U_R\left(\boldsymbol{v}^{\max,j};\mathbf{0};\ldots;\mathbf{0}\right)\cap\left(\bigcap_{p=1}^{L} U_R\left(\boldsymbol{\alpha}_1^{j_p};\boldsymbol{\alpha}_2^{j_p};\ldots;\boldsymbol{\alpha}_N^{j_p}\right)\right).$$

The local stability index relative to $U_R\left(\boldsymbol{v}^{\max,j};\mathbf{0};\ldots;\mathbf{0}\right)$ is $F^{\text{index}}\left(\boldsymbol{v}^{\max,j}\right)$. Similarly, the local stability index relative to $U_R\left(\boldsymbol{\alpha}_1^{j_p};\boldsymbol{\alpha}_2^{j_p};\ldots;\boldsymbol{\alpha}_N^{j_p}\right)$ is given by

$$\min_{i=1,\ldots,N}\left\{F^{\text{index}}\left(\boldsymbol{\alpha}_i^{j_p}\right)\right\}$$

for any $p=1,\ldots,L$, and the local stability index relative to $\bigcap_{p=1}^{L}U_R\left(\boldsymbol{\alpha}_1^{j_p};\boldsymbol{\alpha}_2^{j_p};\ldots;\boldsymbol{\alpha}_N^{j_p}\right)$ is given by

$$\min_{p=1,\ldots,L}\left\{\min_{i=1,\ldots,N}\left\{F^{\text{index}}\left(\boldsymbol{\alpha}_i^{j_p}\right)\right\}\right\}.$$

We thus get, for each $j=1,\ldots,m$,

$$\sigma_j=\min\left\{F^{\text{index}}\left(\boldsymbol{v}^{\max,j}\right),\min_{p=1,\ldots,L}\left\{\min_{i=1,\ldots,N}\left\{F^{\text{index}}\left(\boldsymbol{\alpha}_i^{j_p}\right)\right\}\right\}\right\}.$$

□

Remark 3.4.10. Equality $U^{-\infty}(M^{(j)})=\mathbb{R}_-^N$ implies $v_q^{\max,j}v_p^{\max,j}>0$ for all $q,p=1,\ldots,N$ by virtue of (3.19). Applying Lemma 3.4.8 we find $F^{\text{index}}\left(\boldsymbol{v}^{\max,j}\right)=+\infty$, and the above expression can be simplified.

We have shown that the local basin of attraction of heteroclinic cycles in $\mathbb{R}^n$ for which a representation using basic transition matrices (3.8) exists is generically bounded by power curves.

Lemma 3.4.11. *Let M_j, $j=1,\ldots,m$, be basic transition matrices of a collection of maps associated with a heteroclinic cycle. Denote by $q=j_1,\ldots,j_L$, $L\geq 1$, all the indices for which M_q has at least one negative entry. Suppose that the matrices $M^{(j)}$ satisfy conditions (i)–(iii) of Lemma 3.3.3 for all $j=j_p+1$, $p=1,\ldots,L$, such that $j_p+1\notin\{j_1,\ldots,j_L\}$. Then, $\sigma_j>-\infty$ for all $j=1,\ldots,m$.*

Proof. According to Theorem 3.4.9 the heteroclinic cycle is f.a.s. Suppose, contrary to the first statement, that there is some j such that $\sigma_j=-\infty$. By (3.21) there is some vector $\boldsymbol{\beta}=(\beta_1,\ldots,\beta_N)\in\mathbb{R}^N$ such that $F^{\text{index}}(\boldsymbol{\beta})=-\infty$. From Lemma 3.4.8 this occurs when $\beta_{\max}=\max_{i=1,\ldots,N}\{\beta_i\}\leq 0$, which implies $\beta_i\leq 0$ for all $i=1,\ldots,N$. Then, $U_0(\boldsymbol{\beta};\mathbf{0};\ldots;\mathbf{0})=\emptyset$. Considering (3.22) we know that $\mathscr{U}_S^{M^{(j)}} \subset U_0(\boldsymbol{\beta};\mathbf{0};\ldots;\mathbf{0})$ for $S<0$ sufficiently large negative. Hence $\ell\left(\mathscr{U}_S^{M^{(j)}}\right)=0$ and the heteroclinic cycle is c.u by Definition 2.3.1. The proof is complete. □

We thus extend Corollary 4.1 in [53] for simple heteroclinic cycles in $\mathbb{R}^4$.

Corollary 3.4.12. *Let M_j, $j=1,\ldots,m$, be basic transition matrices of a collection of maps associated with a heteroclinic cycle. Then, $\sigma_j=-\infty$ for some $j\in\{1,\ldots,m\}$ if and only if $\sigma_j=-\infty$ for all $j=1,\ldots,m$.*

Theorems 3.4.2 and 3.4.9, and Lemma 3.4.11 together with Lemma 2.4.4 imply the next corollary:

Corollary 3.4.13. *Let X be a quasi-simple heteroclinic cycle in $\mathbb{R}^n$ satisfying Assumption 3.2.1. Suppose that for all $x\in X$ the local stability index $\sigma_{\text{loc}}(X,x)\in[-\infty,\infty]$ is defined.*

(a) X is a.s if and only if $\sigma_{\text{loc}}(X,x)=\infty$ for all $x\in X$.

(b) X is f.a.s if and only if there exists $x\in X$ such that $\sigma_{\text{loc}}(X,x)>-\infty$.

(b) X is c.u if and only if $\sigma_{\text{loc}}(X,x)=-\infty$ for all $x\in X$.

The section finishes with a relation of the local stability index along a heteroclinic connection shared by two quasi-simple heteroclinic cycles.

Lemma 3.4.14. *Let $\kappa_{1,2}=[\xi_1\to\xi_2]$ be a common heteroclinic connection between two quasi-simple heteroclinic cycles satisfying Assumption 3.2.1. Then, the local stability index along $\kappa_{1,2}$ is negative with respect to the heteroclinic cycle whose the expanding eigenvalue at ξ_2 is the weakest.*

Proof. Consider two quasi-simple heteroclinic cycles C_1 and C_2 with sequences $[\xi_a\to\xi_1\to\xi_2\to\xi_b]$ and $\left[\xi_\alpha\to\xi_1\to\xi_2\to\xi_\beta\right]$, see Figure 4.9. Under Assumption 3.2.1, Theorem 3.3.2 ensures that dynamics around C_1 and C_2 can be represented by basic transition matrices of the form (3.8). We use the notation e_{2k} for the eigenvalue at ξ_2 to the unstable direction $\kappa_{2,k}$, $k\in\{b,\beta\}$. Near ξ_2, the eigenvalue e_{2b} (resp. $e_{2\beta}$) is expanding with respect to C_1 (resp. C_2) and transverse with respect to C_2 (resp. C_1). Assume that $e_{2b}>e_{2\beta}$ and $M_2: H_2^{in,1}\to H_2^{in,\beta}$ is the basic transition matrix for C_2 from ξ_2 to ξ_β. By (3.8) one of the rows of M_2 is a permutation of the N-tuple

$$\left(-\frac{e_{2b}}{e_{2\beta}},1,0,\ldots,0\right).$$

Denote by σ_2 the local stability index along $\kappa_{1,2}$ with respect to C_2. From Theorem 3.4.9 either $\sigma_2=-\infty$ or $\sigma_2>-\infty$ depending whether or not the transition matrix $M^{(2)}: H_2^{in,1}\to H_2^{in,1}$ around C_2 satisfies conditions *(i)–(iii)* of Lemma 3.3.3. The latter calculations take into account the rows of M_2 with negative entries since $M^{(2)}$ is the product of basic transition matrices wherein M_2 is the first factor (from right to left). We observe that F^{index} is invariant under permutations so that

$$\sigma_2=\min\left\{F^{\text{index}}\left(-\frac{e_{2b}}{e_{2\beta}},1,0,\ldots,0\right),\ \ldots\ \right\}.$$

Lemma 3.4.8 yields

$$F^{\text{index}}\left(-\frac{e_{2b}}{e_{2\beta}},1,0,\ldots,0\right)=-\frac{e_{2b}}{e_{2\beta}}+1<0.$$

Therefore, in either case, $\sigma_2 < 0$ as claimed. □

3.5 The simplest non-simple heteroclinic cycle

We illustrate the application of Theorem 3.4.9 by calculating the local stability indices for the heteroclinic connections of two non-simple heteroclinic cycles in a heteroclinic network in $\mathbb{R}^4$. Each heteroclinic cycle is made of two nodes and two heteroclinic connections. The heteroclinic network is obtained from the so-called simple $\left(\mathrm{B}_2^+, \mathrm{B}_2^+\right)$-network in $\mathbb{R}^4$ by a translation along the axis containing the nodes. The simple $\left(\mathrm{B}_2^+, \mathrm{B}_2^+\right)$-network consists of two simple heteroclinic cycles of type B_2^+ with a common heteroclinic connection. For more details we refer the reader to [17]. The translated heteroclinic cycles are non-simple because the second condition in Definition 2.2.4 fails to hold. They do satisfy Definition 3.1.1 and are therefore quasi-simple (see Figure 3.1).

In order to prove the existence of such a network we provide a vector field that supports it. Based on the *cylinder realisation* in [13], for $(\boldsymbol{x}, p)$ with $\boldsymbol{x} = (x_1, x_2, x_3) \in \mathbb{R}^3$ and $p \in \mathbb{R}$ we write

$$\begin{aligned} \dot{x}_i &= -x_i G_i(\boldsymbol{x}, p), \qquad && i = 1,2,3 \\ \dot{p} &= -\sin(2\pi p) + F(\boldsymbol{x}, p) && \end{aligned} \tag{3.23}$$

where $F, G_i : \mathbb{R}^3 \times \mathbb{R} \to \mathbb{R}$ are smooth functions and even in each of the x_i, and $F(\mathbf{0}, p) = 0$ for any $p \in \mathbb{R}$. See Proposition 2 in [13] for specific forms for F and G_i, $i = 1,2,3$. The vector field (3.23) is equivariant under the action of $\mathbb{Z}_2^3(\gamma_1, \gamma_2, \gamma_3)$ such that $\gamma_i : x_i \mapsto -x_i$. We check at once that for each $i = 1,2,3$

$$P_i = \mathrm{Fix}\left(\mathbb{Z}_2^2(\gamma_{i+1}, \gamma_{i+2})\right) = \{(\boldsymbol{x}, p) : x_{i+1} = x_{i+2} = 0\} \pmod 3$$

and

$$L = \mathrm{Fix}\left(\mathbb{Z}_2^3(\gamma_1, \gamma_2, \gamma_3)\right) = \{(\boldsymbol{x}, p) : \boldsymbol{x} = \mathbf{0}\}$$

are flow-invariant spaces. In particular, equilibria of (3.23) are all on the axis L at $p = n$ for every $n \in \mathbb{Z}$. We can choose the parameters appropriately so there are robust heteroclinic connections between $\xi_a = (\mathbf{0}, a)$ and $\xi_b = (\mathbf{0}, b)$ for some $0 < a < b$ with

$$\kappa_{a,b} = [\xi_a \to \xi_b] \subset P_1, \qquad \tilde{\kappa}_{b,a} = [\xi_b \to \xi_a] \subset P_2, \qquad \kappa_{b,a} = [\xi_b \to \xi_a] \subset P_3.$$

We obtain two identical heteroclinic cycles sharing a heteroclinic connection in P_1 as in the $\left(\mathrm{B}_2^+, \mathrm{B}_2^+\right)$ simple network. Set

$$\begin{aligned} C_2 &= [\xi_a \to \xi_b \to \xi_a] \subset P_1 \cup P_2 \\ C_3 &= [\xi_a \to \xi_b \to \xi_a] \subset P_1 \cup P_3. \end{aligned}$$

Near each ξ_j, $j = a,b$, denote by $-c_{jk}$ the negative eigenvalue in the stable x_k-direction and by e_{jl} the positive eigenvalue in the unstable x_l-direction, $k \neq l \in \{1,2,3\}$. We further write H_{jk}^{in} and H_{jl}^{out} for the cross sections to the flow approaching and leaving ξ_j, respectively.

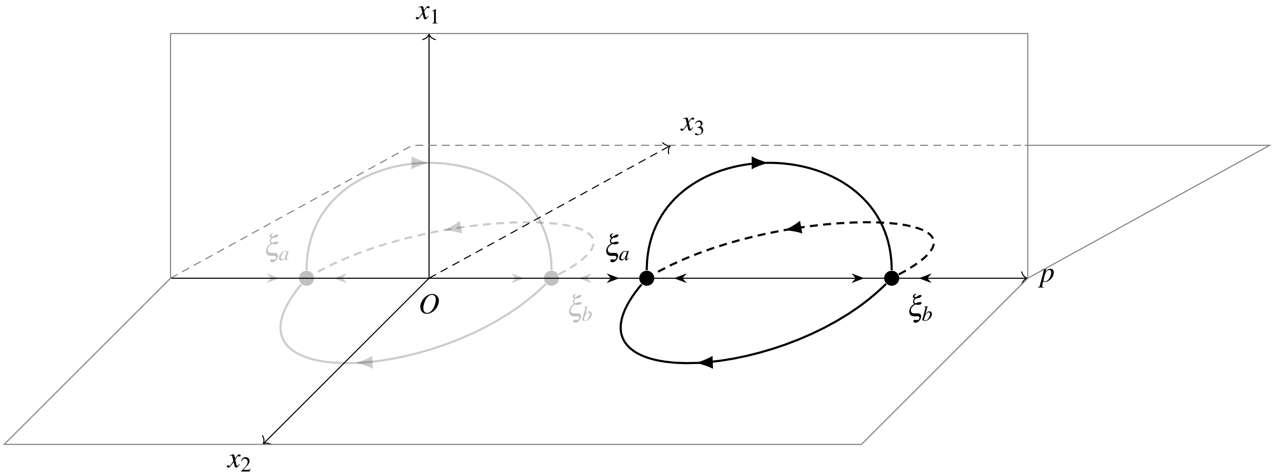

Fig. 3.1 A non-simple heteroclinic network in $\mathbb{R}^4$ constructed by an adaptation of the cylinder realisation in [13].

Assumption 3.2.1 is satisfied due to the $\mathbb{Z}_2^3$-symmetry which must be preserved by the global maps. In coordinates (3.5) the basic transition matrices are then: for C_2

$$\widetilde{M}_a : H_{a2}^{in} \to H_{b1}^{in}, \qquad \widetilde{M}_b : H_{b1}^{in} \to H_{a2}^{in}$$

where

$$\widetilde{M}_a = \begin{bmatrix} \frac{c_{a2}}{e_{a1}} & 0 \\ \frac{c_{a3}}{e_{a1}} & 1 \end{bmatrix} = \begin{bmatrix} \tilde{a}_1 & 0 \\ \tilde{b}_1 & 1 \end{bmatrix}, \qquad \widetilde{M}_b = \begin{bmatrix} \frac{c_{b1}}{e_{b2}} & 0 \\ -\frac{e_{b3}}{e_{b2}} & 1 \end{bmatrix} = \begin{bmatrix} \tilde{a}_2 & 0 \\ \tilde{b}_2 & 1 \end{bmatrix}$$

and, for C_3,

$$M_a : H_{a3}^{in} \to H_{b1}^{in}, \qquad M_b : H_{b1}^{in} \to H_{a3}^{in}$$

where

$$M_a = \begin{bmatrix} \frac{c_{a3}}{e_{a1}} & 0 \\ \frac{c_{a2}}{e_{a1}} & 1 \end{bmatrix} = \begin{bmatrix} a_1 & 0 \\ b_1 & 1 \end{bmatrix}, \qquad M_b = \begin{bmatrix} \frac{c_{b1}}{e_{b3}} & 0 \\ -\frac{e_{b2}}{e_{b3}} & 1 \end{bmatrix} = \begin{bmatrix} a_2 & 0 \\ b_2 & 1 \end{bmatrix}.$$

The product of the matrices above in the appropriate order yields the transition matrices of the full return maps associated to each cycle: for C_2

$$\begin{aligned} \widetilde{M}^{(a)} &: H_{a2}^{in} \to H_{a2}^{in}, \qquad \widetilde{M}^{(a)} = \widetilde{M}_b \widetilde{M}_a = \begin{bmatrix} \tilde{a}_1\tilde{a}_2 & 0 \\ \tilde{b}_2\tilde{a}_1 + \tilde{b}_1 & 1 \end{bmatrix} \\ \widetilde{M}^{(b)} &: H_{b1}^{in} \to H_{b1}^{in}, \qquad \widetilde{M}^{(b)} = \widetilde{M}_a \widetilde{M}_b = \begin{bmatrix} \tilde{a}_1\tilde{a}_2 & 0 \\ \tilde{b}_1\tilde{a}_2 + \tilde{b}_2 & 1 \end{bmatrix} \end{aligned} \tag{3.24}$$

and, for C_3,

$$M^{(a)}: H^{in}_{a3} \to H^{in}_{a3}, \qquad M^{(a)} = M_b M_a = \begin{bmatrix} a_1 a_2 & 0 \\ b_2 a_1 + b_1 & 1 \end{bmatrix}$$
$$M^{(b)}: H^{in}_{b1} \to H^{in}_{b1}, \qquad M^{(b)} = M_a M_b = \begin{bmatrix} a_1 a_2 & 0 \\ b_1 a_2 + b_2 & 1 \end{bmatrix}. \tag{3.25}$$

With this notation we have $b_1, \tilde{b}_1 > 0$ and $b_2, \tilde{b}_2 < 0$. The local stability indices follow from Theorem 3.4.9. Here the function F^{index} coincides with f^{index} of [53]. We use $\sigma_{jk,i}$ to denote the local stability index at a point on $\kappa_{j,k}$ with respect to the cycle C_i, $j \neq k \in \{a,b\}$ and $i = 2,3$.

Lemma 3.5.1. *Suppose that $e_{b2} > e_{b3}$.*

(a) The local stability indices for the cycle C_2 are:

- *if either $\tilde{a}_1\tilde{a}_2 < 1$ or $\tilde{b}_2\tilde{a}_1 + \tilde{b}_1 < 0$, then $\sigma_{ab,2} = \sigma_{ba,2} = -\infty$;*
- *if $\tilde{a}_1\tilde{a}_2 > 1$ and $\tilde{b}_2\tilde{a}_1 + \tilde{b}_1 > 0$, then*

$$\sigma_{ba,2} = +\infty, \qquad \sigma_{ab,2} = F^{\text{index}}(\tilde{b}_2, 1) = \frac{e_{b2}}{e_{b3}} - 1 > 0.$$

(b) The local stability indices for the cycle C_3 are:

- *if either $a_1 a_2 < 1$ or $b_2 a_1 + b_1 < 0$, then $\sigma_{ab,3} = \sigma_{ba,3} = -\infty$;*
- *if $a_1 a_2 > 1$ and $b_2 a_1 + b_1 > 0$, then*

$$\sigma_{ba,3} = +\infty, \qquad \sigma_{ab,3} = F^{\text{index}}(b_2, 1) = -\frac{e_{b2}}{e_{b3}} + 1 < 0.$$

Proof. We give the proof only for case (a); the remaining is similar.

Transition matrices in (3.24) are lower triangular making conditions *(i)–(iii)* of Lemma 3.3.3 of easy verification. Their eigenvalues are $\lambda_1 = \tilde{a}_1\tilde{a}_2$ and $\lambda_2 = 1$. The associated eigenvectors for $\widetilde{M}^{(a)}$ are $\boldsymbol{w}^{1,a} = \left(\tilde{a}_1\tilde{a}_2 - 1, \tilde{b}_2\tilde{a}_1 + \tilde{b}_1\right)$ and $\boldsymbol{w}^{2,a} = (0,1)$, respectively. It suffices to use $\widetilde{M}^{(a)}$ according to Lemma 3.4.5. Since the eigenvalues are all real the matrix $\widetilde{M}^{(a)}$ does not satisfy either *(ii)* or *(iii)* when either $\tilde{a}_1\tilde{a}_2 < 1$ or $\tilde{b}_2\tilde{a}_1 + \tilde{b}_1 < 0$. In both cases we get $\sigma_{ab,2} = \sigma_{ba,2} = -\infty$ from part (a) of Theorem 3.4.9.

Conversely, the hypotheses of part (b) of Theorem 3.4.9 hold if $\tilde{a}_1\tilde{a}_2 > 1$ and $\tilde{b}_2\tilde{a}_1 + \tilde{b}_1 > 0$. Then, $\lambda_{\max} = \lambda_1$ and $\boldsymbol{w}^{\max,a} = \boldsymbol{w}^{1,a}$. The arguments employed in the proof of Theorem 3.4.9(b) yield

$$\sigma_{ba,2} = \min\left\{F^{\text{index}}\left(\boldsymbol{v}^{\max,a}\right), \min\left\{F^{\text{index}}\left(\tilde{a}_1\tilde{a}_2, 0\right), F^{\text{index}}\left(\tilde{b}_2\tilde{a}_1 + \tilde{b}_1, 1\right)\right\}\right\}$$
$$\sigma_{ab,2} = \min\left\{F^{\text{index}}\left(\boldsymbol{v}^{\max,b}\right), \min\left\{F^{\text{index}}\left(\tilde{a}_2, 0\right), F^{\text{index}}\left(\tilde{b}_2, 1\right)\right\}\right\}.$$

By simple algebra we see that $\boldsymbol{v}^{\max,a}$ and $\boldsymbol{v}^{\max,b}$ in (3.19) are multiple of the vector

$$\left(0, \frac{1}{\tilde{a}_1\tilde{a}_2 - 1}\right)$$

whose entries are all non-negative. Lemma 3.4.8 states

$$F^{\text{index}}\left(\boldsymbol{v}^{\max,a}\right) = F^{\text{index}}\left(\boldsymbol{v}^{\max,b}\right) = +\infty.$$

In the same manner

$$F^{\text{index}}\left(\tilde{a}_2, 0\right) = F^{\text{index}}\left(\tilde{a}_1\tilde{a}_2, 0\right) = F^{\text{index}}\left(\tilde{b}_2\tilde{a}_1 + \tilde{b}_1, 1\right) = +\infty.$$

Hence

$$\sigma_{ab,2} = +\infty$$

and

$$\sigma_{ba,2} = F^{\text{index}}\left(\tilde{b}_2, 1\right) = F^{+}\left(\tilde{b}_2, 1\right) = -\frac{1}{\tilde{b}_2} - 1 = \frac{e_{b2}}{e_{b3}} - 1 > 0.$$

□

Comparison with the corresponding maps in [17] shows that the transition matrices remain unchanged. The content of Lemma 3.5.1 meets the results of [53] and [17] for simple heteroclinic cycles of type B_2^+. Indeed, the systems realising the two heteroclinic networks, simple and non-simple, are C^1-conjugated. The values of the local stability index must be equal by the comment after Theorem 2.2 in [53]. We provide here an alternative and direct way of calculating those indices.

An original application of Theorem 3.4.9 can be found in Chapter 5.

Chapter 4

Switching in heteroclinic networks

The study of the dynamics near heteroclinic networks has been of interest because of its degree of complexity. A way of evaluate the complexity is through the occurrence of switching, which discloses how nearby trajetories follow sequences of heteroclinic connections within a heteroclinic network. Random-like visits to all nodes characterise infinite switching. For noise-free systems the general features inducing infinite switching in the neighbourhood of a heteroclinic network are so far related to transverse intersections of invariant manifolds and rotating nodes.

The aim of the chapter is to examine the existence of infinite switching near heteroclinic networks whose linearisation of the vector field at nodes has no complex eigenvalues.

The chapter is organised as follows. Section 4.1 presents some results on the construction of quasi-simple heteroclinic cycles. We proceed with the study of various types of switching near a heteroclinic network comprising of two quasi-simple heteroclinic cycles, from switching along a heteroclinic connection in Section 4.2 to switching along a heteroclinic cycle in Section 4.3. We treat infinite switching near an arbitrary heteroclinic network with real eigenvalues in Section 4.4. The main achievements are Theorems 4.2.4, 4.2.4 and 4.4.4.

4.1 Construction of quasi-simple heteroclinic cycles

We divide individual heteroclinic connections of quasi-simple heteroclinic cycles into two types according to the transformation of the global map defined therein. Recall that a local map near ξ_j and a global map near $\kappa_{j,j+1} = [\xi_j \to \xi_{j+1}]$ are respectively such that

$$\phi_j : H_j^{in} \to H_j^{out} \qquad \text{and} \qquad \psi_j : H_j^{out} \to H_{j+1}^{in}.$$

Definition 4.1.1. Let X be a quasi-simple heteroclinic cycle in $\mathbb{R}^n$.

1. The jth connection is of *type contracting-to-expanding* if ψ_j maps v to w.

2. The jth connection is of *type contracting-to-transverse* if ψ_j maps v to z where z is spanned by z_s for $s = 1, \ldots, n_t$.

Remark 4.1.2. Regarding the types of eigenvalues in Table 2.2 a quasi-simple heteroclinic cycle is subject to $\dim(T_j) = n_t$ for all j. Based on Assumption 3.1.4 we can write $T_j = \oplus_{s=1}^{n_t} T_j^s$

where T_j^s is the generalised eigenspace for the transverse eigenvalue $t_{j,s}$ with $\dim\left(T_j^s\right) = 1$. When Assumption 3.2.1 is in turn fulfilled, Definition 4.1.1 may be summarised by saying that: the jth connection is of type contracting-to-expanding if $V_j = W_{j+1}$ and $T_j = T_{j+1}$; the jth connection is of type contracting-to-transverse if $V_j = T_{j+1}^{s_1}$ and $T_j^{s_2} = W_{j+1}$ for some $s_1, s_2 \in \{1, \dots, n_t\}$.

Definition 2.2.9 distinguishes between type-B and type-C connections by means of fixed-point subspaces. We further observe that a type-B connection is contracting-to-expanding and a type-C connection is contracting-to-transverse.

It is worth pointing out that the local characterisation of individual heteroclinic connections depends on which heteroclinic cycles one considers. Of course this gains in significance if heteroclinic cycles coexist in a heteroclinic network. In particular a common heteroclinic connection may adopt both types with respect to different heteroclinic cycles. Figure 4.1 represents the graph of the simple $\left(\mathrm{B}_3^-, \mathrm{C}_4^-\right)$-network as in [18, Figure 3]. The heteroclinic connections $\kappa_{1,2}$ and $\kappa_{2,3}$ are of type contracting-to-expanding from the point of view of the B_3^--cycle and of type contracting-to-transverse from the point of view of the C_4^--cycle. See also [45, Remark 2.10].

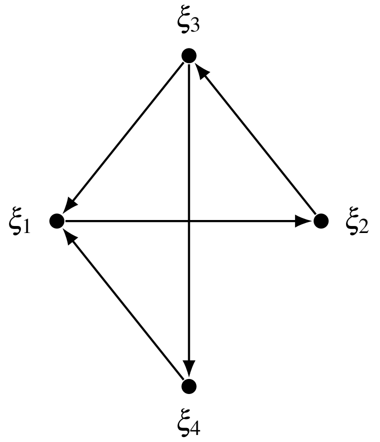

Fig. 4.1 The simple $\left(\mathrm{B}_3^-, \mathrm{C}_4^-\right)$-network. The C_4^--cycle is $[\xi_1 \to \xi_2 \to \xi_3 \to \xi_4 \to \xi_1]$ and the B_3^--cycle is $[\xi_1 \to \xi_2 \to \xi_3 \to \xi_1]$.

We look at minimal sequences of robust heteroclinic connections that makes up a quasi-simple heteroclinic cycle. It meets the notion of *building block*. Under a symmetry group $\Gamma \subset \mathrm{O}(n)$ a *building bock*, see [55, Definition 7], is a sequence of connections $[\xi_1 \to \cdots \to \xi_m \to \xi_{m+1}]$ where $\xi_{m+1} = \gamma\xi_1$ for some $\gamma \in \Gamma$ and $\xi_i \notin \Gamma\xi_1$ for all $i = 2, \dots, m$. According to [18, p.3680] a building block is called *elementary* if $\gamma = Id$ and no two of the nodes $\xi_1, \dots, \xi_m$ belong to the same group orbit. In non-symmetric settings any heteroclinic cycle can be naturally regarded as an unique elementary building block.

The next result is an extension of Lemma 3.2 in [18] to quasi-simple heteroclinic cycles. When $n_r = \dim\left(\hat{L}_j\right) = 1$ we recover the latter (see Figure 4.2).

Proposition 4.1.3. *Let X be a quasi-simple heteroclinic cycle in $\mathbb{R}^n$ with only two nodes. Then, these nodes belong to the same n_r-dimensional vector subspace and all heteroclinic connections are of type contracting-to-expanding.*

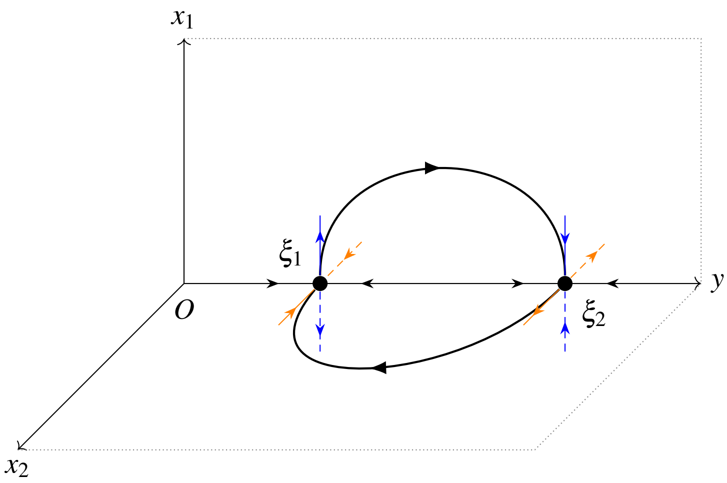

Fig. 4.2 A quasi-simple heteroclinic cycle with two nodes.

Proof. Suppose that ξ_1 and ξ_2 are the nodes of the quasi-simple cycle $[\xi_1 \to \xi_2 \to \xi_1]$. By definition $\kappa_{1,2} \subset P_1$ and $\kappa_{2,1} \subset P_2$ such that each P_j is contained in an (n_r+1)-dimensional vector subspace $\hat{Q}_j$ represented either by $\hat{L}_j \oplus \left(T_{\xi_j}P_j \ominus \hat{L}_j\right)$ in the local coordinates near ξ_j or by $\hat{L}_{j+1} \oplus \left(T_{\xi_{j+1}}P_j \ominus \hat{L}_{j+1}\right)$ near ξ_{j+1}, $j=1,2$. Now $\hat{Q}_1 \cap \hat{Q}_2 = \hat{L}_1$ and $\hat{Q}_1 \cap \hat{Q}_2 = \hat{L}_2$ since $P_1 \neq P_2$. As $\xi_1, \xi_2 \in \hat{L}_1 = \hat{L}_2$ the first claim follows. Due to Assumption 3.2.1, radial and expanding directions near ξ_j must be respectively in one-to-one correspondence with radial and contracting directions near ξ_{j+1}, $j=1,2$. Hence $\kappa_{1,2}$ and $\kappa_{2,1}$ are of type contracting-to-expanding. $\square$

The realisation of arbitrary directed graps as robust heteroclinic cycles and networks in the phase space of coupled cells has recently been adressed by Ashwin and Postlethwaite [13, 14] and Field [25, 26]. The authors present methods for designing coupled dynamical systems that embed a prescribed one- or two-cycle free graph as a flow-invariant set. By making use of symmetry the result is a robust heteroclinic object within an attractor.

Section 3.5 has shown that simple and quasi-simple (non-simple) heteroclinic cycles may have an identical structure determined by the constraints and dimension of the system. Unless otherwise stated we then adopt

Assumption 4.1.4.

(i) All nodes in the heteroclinic cycle are on the coordinate axes.

(ii) All heteroclinic connections in the heteroclinic cycle are contained in coordinate planes.

The simplex and cylinder realisations in [13] generate quasi-simple heteroclinic cycles in $\mathbb{R}^n$ with the desired properties. Hence $\dim\left(\hat{L}_j\right) = 1$ and $\dim\left(P_j\right) = 2$ for any j. We take P_j to be the smallest possible flow-invariant vector space in order to achieve a clear geometric construction. Moreover, this permits a comparison with the well-known simple heteroclinic cycles.

Let $(x_1,\dots,x_n)$ denote the Euclidean coordinates in $\mathbb{R}^n$. Under Assumptions 3.1.4, 3.2.1 and 4.1.4, we study the ways in which heteroclinic connections can be put together to form a quasi-simple heteroclinic cycle according to their type.

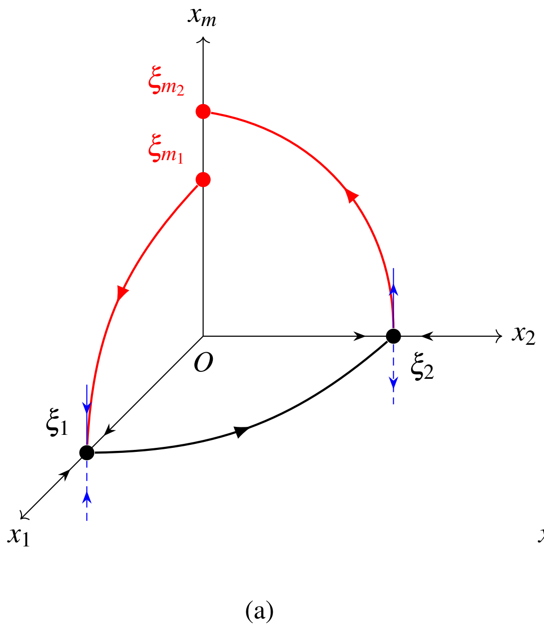

Fig. 4.3 Construction of a quasi-simple heteroclinic cycle with contracting-to-expanding connections. (a) If $\kappa_{1,2} \subset P_1 = \{(x_1, x_2)\}$ is of type contracting-to-expanding, then there are nodes ξ_{m_1} and ξ_{m_2} on the x_m-axis such that $\kappa_{m_1,1} \subset P_m = \{(x_m, x_1)\}$ and $\kappa_{2,m_2} \subset P_2 = \{(x_2, x_m)\}$; (b) If the nodes are all on different axes, then $\xi_{m_1} = \xi_{m_2} \equiv \xi_3$.

Proposition 4.1.5. *Let X be a quasi-simple heteroclinic cycle in $\mathbb{R}^n$ fulfilling Assumptions 3.1.4, 3.2.1 and 4.1.4. Suppose that the nodes of X are all on different coordinate axes. Then, the heteroclinic connections of X are all either of type contracting-to-expanding or of type contracting-to-transverse.*

Proof. Suppose that $X = [\xi_1 \to \cdots \to \xi_m \to \xi_1]$ is a quasi-simple heteroclinic cycle such that ξ_j is on the x_j-axis and $\kappa_{j,j+1} \subset P_j$ where P_j is the flow-invariant (x_j, x_{j+1})-plane, $j = 1, \dots, m$. Then, $n \geq m \geq 3$ from Proposition 4.1.3.

Assume that at least one heteroclinic connection, say $\kappa_{1,2}$, is of type contracting-to-expanding. It follows that the expanding direction near ξ_2 corresponds to the contracting direction near ξ_1, which is x_m. Hence there is a node ξ_m on the x_m-axis connected to either of ξ_1 and ξ_2 with $\kappa_{m,1} \subset P_m$ and $\kappa_{2,m} \subset P_2$ (see Figure 4.3). We have $m = 3$ given the condition that all nodes belong to different axes. From here the coordinate x_1 spans the contracting eigenspace at ξ_2 and the expanding eigenspace at ξ_3. In the same manner the coordinate x_2 spans the contracting eigenspace at ξ_3 and the expanding eigenspace at ξ_1. Thus $\kappa_{2,3}$ and $\kappa_{3,1}$ are also of type contracting-to-expanding.

Let now $\kappa_{1,2}$ be of type contracting-to-transverse and assume that $\kappa_{m,1}$ is of type contracting to-expanding. Thus ξ_m is in a transverse direction to ξ_2 and ξ_2 is in the contracting direction at ξ_m. So ξ_2 does not connect to ξ_m (see Figure 4.4). Another node in the x_2-axis is required, contradicting the assumption that nodes are on different coordinate axes.

□

As a direct consequence of the last proof we derive the number of nodes comprising of the quasi-simple heteroclinic cycles under consideration.

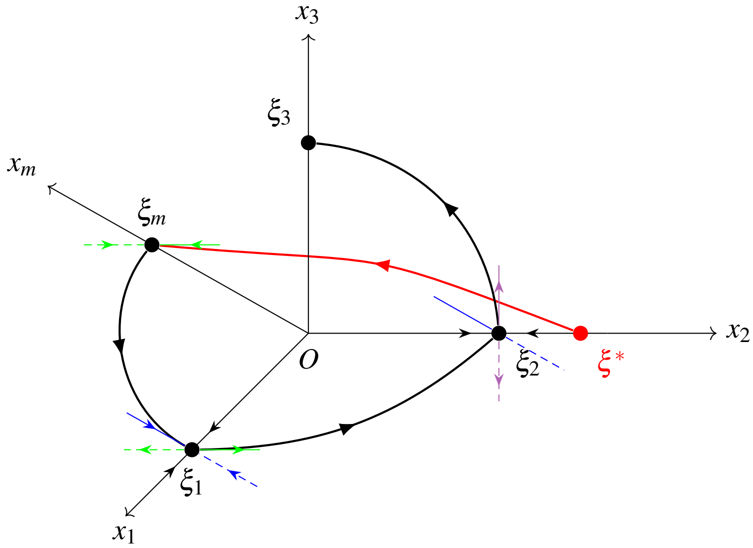

Fig. 4.4 Construction of a quasi-simple heteroclinic cycle with contracting-to-transverse connections. If $\kappa_{1,2} \subset P_1 = \{(x_1,x_2)\}$ is of type contracting-to transverse and $\kappa_{m,1} \subset P_m = \{(x_m,x_1)\}$ is of type contracting-to-expanding, then there must be a node ξ^* on the x_2-axis such that $[\xi^* \to \xi_m]$ is contained in the (x_2,x_m)-plane.

Corollary 4.1.6. *Let X be a quasi-simple heteroclinic cycle in $\mathbb{R}^n$ fulfilling Assumptions 3.1.4, 3.2.1 and 4.1.4. Suppose that the nodes of X are all on different coordinate axes.*

(a) The heteroclinic connections of X are all of type contracting-to-expanding if and only if X has three nodes.

(b) The heteroclinic connections of X are all of type contracting-to-transverse if and only if X has at least four nodes.

Every simple heteroclinic cycle in $\mathbb{R}^4$ lying in a three-dimensional vector space is of type B from the classification of [43], see Definition 2.2.5. Their generalisation of heteroclinic cycles of type B to higher dimensions implies the same property taking into account the Definition 2.2.9 of type-B connection. We prove, more generally, that this also applies to quasi-simple heteroclinic cycles.

Proposition 4.1.7. *Let X be a quasi-simple heteroclinic cycle in $\mathbb{R}^n$ fulfilling Assumptions 3.1.4, 3.2.1 and 4.1.4. The heteroclinic connections of X are all of type contracting-to-expanding if and only if there exists a three-dimensional vector subspace Q such that $X \subset Q$.*

Proof. Suppose that $X = [\xi_1 \to \cdots \to \xi_m \to \xi_1]$ is a quasi-simple heteroclinic cycle such that each ξ_j is on a coordinate axis and $\kappa_{j,j+1}$ lies in a flow-invariant coordinate plane P_j. Then, $P_j = \hat{L}_j \oplus W_j = \hat{L}_{j+1} \oplus V_{j+1}$ for all $j = 1,\ldots,m$.

Assume that $\kappa_{j,j+1}$ is of type contracting-to-expanding for all $j = 1,\ldots,m$. Set $Q_j = P_j \oplus V_j$. Of course Q_j is a three-dimensional vector subspace wherein $P_j \subset Q_j$. Because $V_j = W_{j+1}$, see Remark 4.1.2, we have $P_{j+1} = \hat{L}_{j+1} \oplus W_{j+1} \subset Q_j$. Moreover, for all $j = 1,\ldots,m$,

$$Q_j = P_j \oplus V_j = \hat{L}_j \oplus W_j \oplus V_j = \hat{L}_{j+1} \oplus V_{j+1} \oplus W_{j+1} = P_{j+1} \oplus V_{j+1} = Q_{j+1}$$

and consequently $Q = Q_j$.

Assume that $X \subset Q$ for some three-dimensional vector subspace Q. We must have $Q = \hat{L}_j \oplus W_j \oplus V_j$ for all $j = 1, \dots, m$ according to the prescribed conditions. If there is $j \in \{1, \dots, m\}$ such that $\kappa_{j,j+1}$ is of type contracting-to-transverse, then $P_j \subset Q$ and $P_{j+1} \not\subset Q$. This means that $\kappa_{j+1,j+2} \subset P_{j+1} \not\subset Q$, which is absurd. □

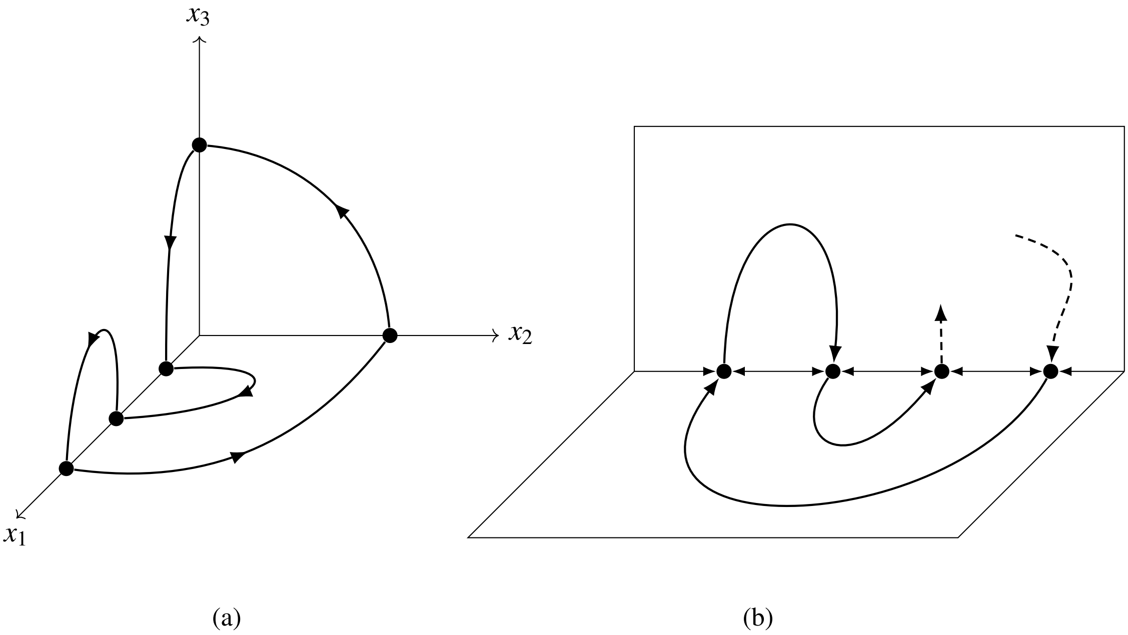

Fig. 4.5 Examples of quasi-simple heteroclinic cycles (a) in [31]; (b) in [25]. The heteroclinic cycle in (a) is not robust provided there are no extra non-trivial equilibria.

Figure 4.5 reproduces two examples of quasi-simple heteroclinic cycles by Hawker and Ashwin [31, Figure 4] and Field [25, Figure 7]. Both are contained in $\mathbb{R}^3$ and so their heteroclinic connections are all of type contracting-to-expanding following Proposition 4.1.7. Notice that the heteroclinic cycle in (a) is not robust unless there exist non-trivial equilibria that are not part of the heteroclinic cycle. Considering as usual that the origin is a source, the trajectory within the (x_1, x_2)-plane connecting two nodes in the x_1-axis is of saddle-saddle type. On the other hand, the heteroclinic cycle in (b) evidences the existence of extra equilibria between each two nodes.

We have been working under the condition of nodes being on different coordinate axes. Now suppose that this is no longer so and nodes are all on the same coordinate axis.

Proposition 4.1.8. *Let X be a quasi-simple heteroclinic cycle in $\mathbb{R}^n$ fulfilling Assumptions 3.1.4, 3.2.1 and 4.1.4. Suppose that the nodes of X line up along the same coordinate axis and its heteroclinic connections are all on different coordinate planes.*

(a) The heteroclinic connections of X are all of type contracting-to-expanding if and only if X has two nodes.

(b) The heteroclinic connections of X are all of type contracting-to-transverse if and only if X has at least three nodes.

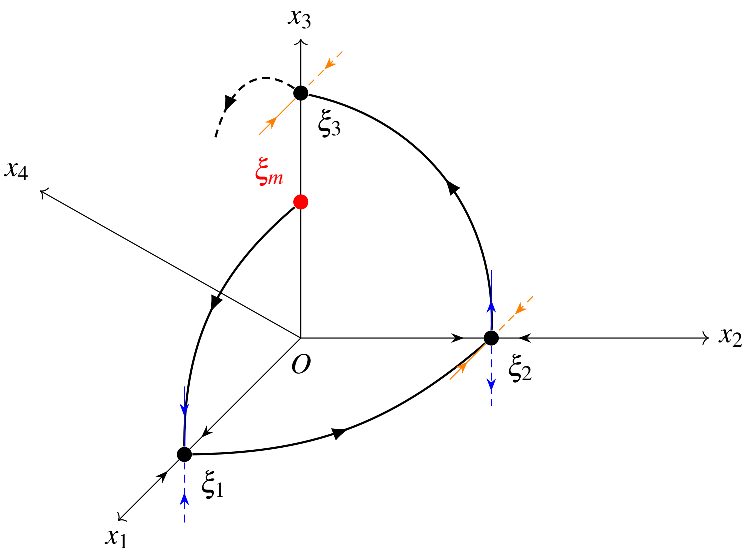

Fig. 4.6 Construction of a quasi-simple heteroclinic cycle with both types of heteroclinic connections. If $\kappa_{1,2} \subset P_1 = \{(x_1, x_2)\}$ is of type contracting-to-expanding and $\kappa_{2,3} \subset P_2 = \{(x_2, x_3)\}$ is of type contracting-to-transverse, then the node ξ_m is on the x_3-axis such that $\kappa_{m,1}$ is contained in the (x_1, x_3)-plane and $\xi_m \neq \xi_3$.

Proof. Suppose that $X = [\xi_1 \to \cdots \to \xi_m \to \xi_1]$ is a quasi-simple heteroclinic cycle such that all ξ_j are on the same axis, say y, and $\kappa_{j,j+1} \subset P_j$ where P_j is the flow-invariant (y, x_j)-plane, $j = 1, \cdots, m$. In particular $X \subset P_1 + \cdots + P_m$ with $m \leq n$. We denote by $\hat{L}$ the line parametrised by y.

(a) The implication $\Leftarrow$ comes directly from Proposition 4.1.3. Assume that $\kappa_{j,j+1}$ are of type contracting-to-expanding for all $j = 1, \cdots, m$. By Proposition 4.1.7 we get $X \subset Q$ for some three-dimensional vector subspace. This forces $Q = P_1 + P_2$, each P_j supporting one heteroclinic connection between exactly two nodes.

(b) We first assume that X has at least three nodes i.e. $m \geq 3$. There are at least two distinct heteroclinic connections: $\kappa_{m,1} \subset P_m$, $\kappa_{1,2} \subset P_1$ and $\kappa_{2,3} \subset P_2$. To obtain a contradiction let $\kappa_{1,2}$ be of type contracting-to-expanding. By definition, $V_1 = W_2$ (see Remark 4.1.2) and

$$P_m = \hat{L} \oplus W_m = \hat{L} \oplus V_1 = \hat{L} \oplus W_2 = P_2.$$

Therefore $\kappa_{m,1}$ and $\kappa_{2,3}$ belong to the same plane, which is absurd.

Assume that $\kappa_{j,j+1}$ are of type contracting-to-transverse for all $j = 1, \cdots, m$. Proposition 4.1.7 implies that $X \not\subset P_j + P_{j+1}$. Since all heteroclinic connections are contained in coordinate planes, X has at least three nodes and $m \geq 3$.

□

Next we prove that, by relaxing the hypothesis that nodes are on different axes, it is possible to construct quasi-simple heteroclinic cycles with heteroclinic connections of both types. For simple heteroclinic cycles, Krupa and Melbourne [43] suggest that types-B and -C connections may coexist in dimensions greater than four. Definition 2.2.10 actually classifies such a heteroclinic cycle as type C. As far as we know there are no examples in the literature capable of realising it.

Proposition 4.1.9. *Let X be a quasi-simple heteroclinic cycle in $\mathbb{R}^n$ fulfilling Assumptions 3.1.4, 3.2.1 and 4.1.4. If X comprises heteroclinic connections of each type, then at least two nodes are on the same coordinate axis.*

Proof. Suppose that $X = [\xi_1 \to \cdots \to \xi_m \to \xi_1]$ is a quasi-simple heteroclinic cycle such that each ξ_j is on a coordinate axis and $\kappa_{j,j+1}$ lies in a flow-invariant coordinate plane P_j with $P_j \neq P_{j+1}$ for all $j = 1, \cdots, m$. As X involves heteroclinic connections of both types we have $m \geq 3$ by Proposition 4.1.3. We can assume that ξ_i is on the x_i-axis, $i = 1,2,3$, with $x_1 \neq x_2 \neq x_3$, since otherwise the assertion follows trivially. In this case P_1 and P_2 are respectively the (x_1,x_2)- and (x_2,x_3)-plane.

Consider $\kappa_{1,2}$ is of type contracting-to-expanding while $\kappa_{2,3}$ is of type contracting-to-transverse. The contracting eigenspace at ξ_1 and the expanding eigenspace at ξ_2 are spanned by the same coordinate, say x_3. It means that $\kappa_{m,1}$ must belong to the (x_1,x_3)-plane with ξ_m on the x_3-axis. From Corollary 4.1.6 we get $\xi_m \neq \xi_3$ as depicted in Figure 4.6. □

In order to describe the dynamics near a heteroclinic cycle we find the form of the global maps $\psi_j : H_j^{in} \to H_{j+1}^{in}$ determined by each type of the heteroclinic connection $\kappa_{j,j+1}$. Recall that for quasi-simple heteroclinic cycles we have deduced in (3.3) that restrictions of ψ_j to the relevant $(v,\mathbf{z})$-subspace are linear. To be specific these express rescaled permutations under Assumption 3.2.1. However, constants arising from the rescaling can be ignored as argued in Section 3.3.

Proposition 4.1.10. *Let X be a quasi-simple heteroclinic cycle in $\mathbb{R}^n$ fulfilling Assumptions 3.1.4, 3.2.1 and 4.1.4 and $\mathbb{R}^{\bar{m}}$ be the Euclidean space of the smallest dimension containing X where $\bar{m} \leq n$.*

(a) If the heteroclinic connection $\kappa_{j,j+1}$ is of type contracting-to-expanding, then ψ_j is represented in the local coordinates $(v,\mathbf{z})$ by the identity.

(b) If the heteroclinic connection $\kappa_{j,j+1}$ is of type contracting-to-transverse, then ψ_j is represented in the local coordinates $(v,\mathbf{z})$ by a block diagonal matrix

$$\left(\begin{array}{c|c} A & \mathbf{0} \\ \hline \mathbf{0} & \mathrm{Id} \end{array}\right), \qquad A = \begin{pmatrix} 0 & 0 & \dots & 0 & 1 \\ 1 & 0 & \dots & 0 & 0 \\ 0 & 1 & \dots & 0 & 0 \\ . & . & \dots & . & . \\ 0 & 0 & \cdots & 1 & 0 \end{pmatrix}$$

in which A is a permutation matrix of size $\bar{m}-2$ and Id *is the identity matrix of size $n_t - \bar{m} + 3$.*

Proof. Suppose that $X = [\xi_1 \to \cdots \to \xi_m \to \xi_1]$ is a quasi-simple heteroclinic cycle such that ξ_j is on a coordinate axis and $\kappa_{j,j+1}$ lies in a flow-invariant coordinate plane P_j, $j = 1, \dots, m$.

We use Remark 4.1.2. Assume that $\kappa_{j,j+1}$ is of type contracting-to-expanding. We have $V_j = W_{j+1}$ and $T_j = T_{j+1}$. Relabelling transverse eigenvalues if necessary enables us to write

$$\psi_j(v,\mathbf{z}) = (v,\mathbf{z}).$$

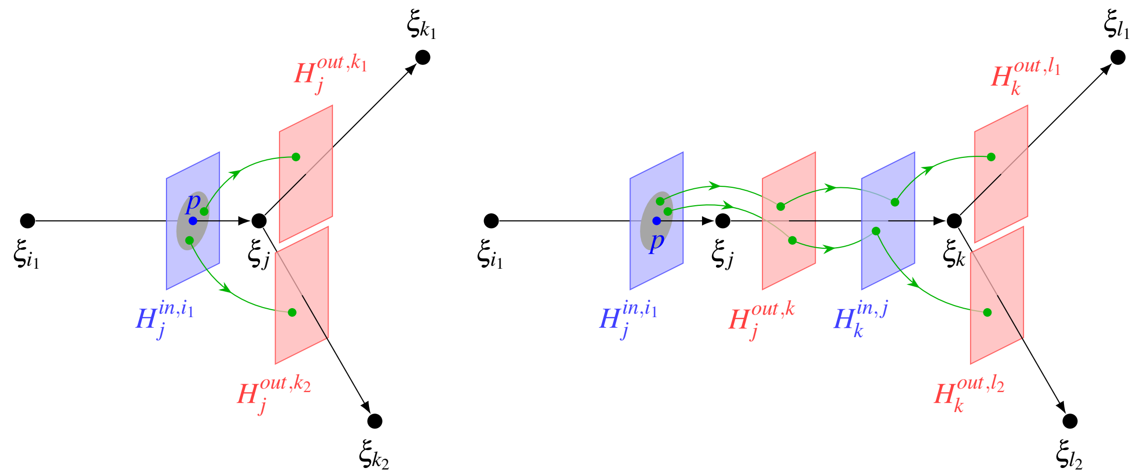

Fig. 4.7 Behaviour of trajectories inducing switching dynamics (a) at a node ξ_j; (b) along a heteroclinic connection $\kappa_{j,k} = [\xi_j \to \xi_k]$.

Assume that $\kappa_{j,j+1}$ is of type contracting-to-transverse. There exist $s_1, s_2 \in \{1,\dots,n_t\}$ such that $V_j = T_{j+1}^{s_1}$ and $T_j^{s_2} = W_{j+1}$. Moreover $T_j \backslash T_j^{s_2} = T_{j+1} \backslash T_{j+1}^{s_1}$. Restricted to $\mathbb{R}^{\bar{m}}$ each node ξ_j admits $\bar{m}-3$ transverse eigenvalues. We can always reorder them where $V_j = T_{j+1}^1$, $T_j^{\bar{m}-3} = W_{j+1}$ and $T_j^i = T_j^{i+1}$ for every $i = 2,\dots,\bar{m}-4$. This choice guarantees that X is contained in the whole $\mathbb{R}^{\bar{m}}$, $\bar{m}$ being the smallest dimension. The remaining $n_t - \bar{m} + 3$ transverse eigenvalues at ξ_j are handled as the case before. We thus get

$$\psi_j(v,z) = \left(z_{\bar{m}-3},\, v,\, z_1,\dots,z_{\bar{m}-4}, z_{\bar{m}-2}, z_{\bar{m}-1},\dots,z_{n_t}\right).$$

$\square$

4.2 Switching along common heteroclinic connections

In order to establish the setup for our study we use the notation from [19]. When a heteroclinic cycle is part of a heteroclinic network and nodes have more than one incoming and/or outgoing connection, it is convenient to distinguish cross sections by adding a second index. Near ξ_j we set $H_j^{in,i}$ to be a section transverse to the heteroclinic connection $\kappa_{i,j} = [\xi_i \to \xi_j]$ and $H_j^{out,k}$ to be a section transverse to the heteroclinic connection $\kappa_{j,k} = [\xi_j \to \xi_k]$. With this notation $\phi_{i,j,k} : H_j^{in,i} \to H_j^{out,k}$ stands for a local map near ξ_j and $\psi_{j,k} : H_j^{out,k} \to H_k^{in,j}$ for a global map[1] near $\kappa_{j,k}$. Write $C_{i,j,k}$ and $F_{i,j,k}$ for the domain and range of definition of $\phi_{i,j,k}$, respectively.

Trajectories in the vicinity of a heteroclinic cycle are accurately approximated by the composition of local and global maps in the correct order. In this sense, Aguiar and Castro [5] make Definitions 2.5.1 and 2.5.2 of switching at nodes and along heteroclinic connections more technical as follows.

[1]Local and global maps are generically defined in Section 3.2

- There is switching at a node ξ_j if for any neighbourhood U_p of a point $p \in \kappa_{i,j}$ there exists $q_k \in U_p \cap H_j^{in,i}$ such that $\phi_{i,j,k}(q_k) \in H_j^{out,k}$ for all the possible i and k. See Figure 4.7(a).
- There is switching along a heteroclinic connection $\kappa_{j,k}$ if for any neighbourhood U_p of a point $p \in \kappa_{i,j}$ there exists $q_l \in U_p \cap H_j^{in,i}$ such that $\phi_{j,k,l} \circ \psi_{j,k} \circ \phi_{i,j,k}(q_l) \in H_k^{out,l}$ for all the possible i and l. See Figure 4.7(b).

Switching dynamics near a heteroclinic network involving nodes with real eigenvalues have been explicitly addressed in [3], [5] and [19]. These works attend in particular to heteroclinic networks comprising one-dimensional heteroclinic connections. The first two are interested in the so-called *edge networks* in a simplex or product of simplices. One of the main results is Theorem 1 of [3] excluding infinite switching near a heteroclinic network with a Kirk and Silber subnetwork because there is no switching along the common heteroclinic connection (see Figure 4.8). Theorem 3.4 of [19] gives general sufficient conditions for the absence of switching along a heteroclinic connection shared by two simple heteroclinic cycles (see Figure 4.9).

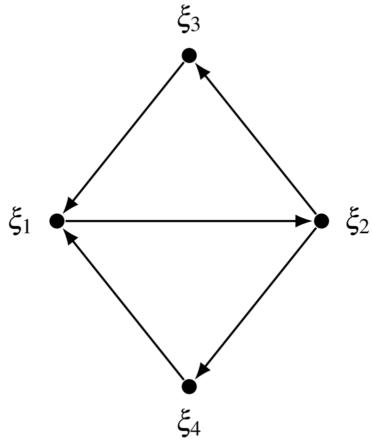

Fig. 4.8 A Kirk and Silber network.

For ease of reference we reproduce the latter:

Theorem 4.2.1 (Theorem 3.4 in [19]). *Consider a simple heteroclinic network in $\mathbb{R}^n$, $n \geq 4$, with sequences $[\xi_\alpha \to \xi_1 \to \xi_2 \to \xi_\beta]$ and $[\xi_a \to \xi_1 \to \xi_2 \to \xi_b]$ such that each ξ_j lies on the x_j-axis. Suppose that the (x_a, x_α)-plane is mapped into the (x_b, x_β)-plane by the global map $\psi_{1,2}$ along the common connection $\kappa_{1,2}$. Then, there is no switching along $\kappa_{1,2}$.*

From now on we are concerned with heteroclinic networks in $\mathbb{R}^n$, $n \geq 4$, made up of quasi-simple heteroclinic cycles satisfying the standing Assumptions 3.1.4, 3.2.1 and 4.1.4. Nodes are labelled accordingly where each ξ_j lies on the x_j-axis. Evidently $\hat{L}_j$ is the vector subspace spanned by x_j. We allow $\xi_i \neq \xi_j$ and $\hat{L}_i = \hat{L}_j$ for $i \neq j$.

We first investigate the presence of various type of switching near heteroclinic networks having a common heteroclinic connection. For this purpose, the hypothesis of Theorem 4.2.1 is broken so that in line with Assumption 3.2.1 one of two cases prevails:

Case 4.2.2. *there exists a direction* $x_\gamma \neq x_\alpha$ *such that the* (x_a, x_γ)*-plane is mapped into the* (x_b, x_β)*-plane by* $\psi_{1,2}$.

Case 4.2.3. *there exist directions* $x_d \neq x_a$ *and* $x_\gamma \neq x_\alpha$ *such that the* (x_d, x_γ)*-plane that is mapped into the* (x_b, x_β)*-plane by* $\psi_{1,2}$.

We adapt the description in [19]: suppose that two quasi-simple heteroclinic cycles

$$[\xi_\alpha \to \boldsymbol{\xi_1} \to \boldsymbol{\xi_2} \to \xi_\beta \to \cdots \to \xi_\alpha] \qquad \text{and} \qquad [\xi_a \to \boldsymbol{\xi_1} \to \boldsymbol{\xi_2} \to \xi_b \to \cdots \to \xi_a]$$

share a heteroclinic connection $\kappa_{1,2}$ in a heteroclinic network with $\xi_\alpha \neq \xi_a$ and $\xi_\beta \neq \xi_b$ as illustrated in Figure 4.9.

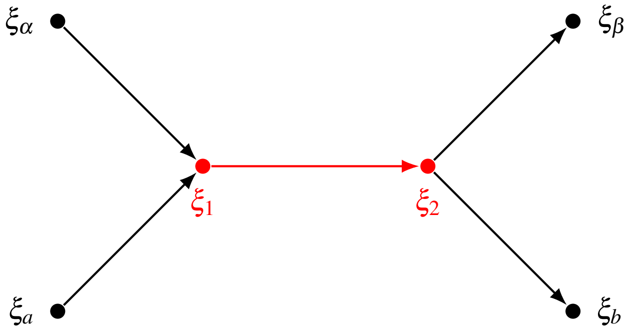

Fig. 4.9 A common heteroclinic connection $\kappa_{1,2} = [\xi_1 \to \xi_2]$.

Locally at ξ_j denote by $-c_{ji} < 0$ the eigenvalue in the stable x_i-direction and by $e_{jk} > 0$ the eigenvalue in the unstable x_k-direction. The type of the eigenvalues depends on the heteroclinic cycle under consideration. Contracting or expanding eigenvalues with respect to one heteroclinic cycle may be transverse with respect to another. Recall that the number of radial and transverse eigenvalues is the same at every node in a quasi-simple heteroclinic cycle, say n_r and n_t, respectively. Assumption 4.1.4 *(i)* asserts $n_r = \dim(\hat{L}_j) = 1$ and so $n = n_t + 3$.

We recover the construction of suitable maps between cross sections in Section 3.2. We can omit the radial direction and choose local coordinates $(y_1, \ldots, y_{n-1})$ such that the linearisation of the flow about ξ_j, $j = 1, 2$, is given by

$$\begin{aligned} \xi_1 : \quad & \dot{y}_1 = e_{12}\, y_1 & \qquad \xi_2 : \quad & \dot{y}_1 = -c_{21}\, y_1 \\ & \dot{y}_2 = -c_{1a}\, y_2 & & \dot{y}_2 = e_{2b}\, y_2 \\ & \dot{y}_3 = -c_{1\alpha}\, y_3 & & \dot{y}_3 = e_{2\beta}\, y_3 \\ & \dot{y}_s = t_{1s}\, y_s, \qquad s = 4, \ldots, n-1, & & \dot{y}_s = t_{2s}\, y_s, \qquad s = 4, \ldots, n-1. \end{aligned}$$

The constants t_{js} are the remaining $n_t - 1$ transverse eigenvalues at ξ_j to either heteroclinic cycle. As usual we require that transverse eigenvalues at nodes are negative whenever possible.[2] Take then $t_{1s} = -c_{1s} < 0$ and $t_{2s} = -c_{2s} < 0$ for all $s = 4, \ldots, n-1$.

[2]This requirement is widely accepted in the literature. See for instance [19, 39, 41, 43].

Consider a neighbourhood of $\xi_j,\ j=1,2$, where the flow can be linearised and define a cross section for each of the three heteroclinic connections as follows

$$\begin{aligned} H_1^{in,a} &= \{(y_1,1,y_3,\dots,y_{n-1}):\ 0\le y_i<1 \text{ for all } i\neq 2\}\\ H_1^{in,\alpha} &= \{(y_1,y_2,1,\dots,y_{n-1}):\ 0\le y_i<1 \text{ for all } i\neq 3\}\\ H_1^{out,2} &= \{(1,u_2,u_3,\dots,u_{n-1}):\ 0\le u_i<1 \text{ for all } i\neq 1\}\end{aligned} \tag{4.1}$$

and

$$\begin{aligned} H_2^{out,b} &= \{(u_1,1,u_3,\dots,u_{n-1}):\ 0\le u_i<1 \text{ for all } i\neq 2\}\\ H_2^{out,\beta} &= \{(u_1,u_2,1,\dots,u_{n-1}):\ 0\le u_i<1 \text{ for all } i\neq 3\}\\ H_2^{in,1} &= \{(1,y_2,y_3,\dots,y_{n-1}):\ 0\le y_i<1 \text{ for all } i\neq 1\}.\end{aligned} \tag{4.2}$$

As in (3.3) we obtain

$$\begin{aligned} \phi_{a,1,2} :& H_1^{in,a}\to H_1^{out,2}\\ &\phi_{a,1,2}\left(y_1,y_3,\{y_s\}_{s=4,\dots,n-1}\right)=\left(y_1^{\frac{c_{1a}}{e_{12}}},\, y_3\,y_1^{\frac{c_{1\alpha}}{e_{12}}},\, \left\{y_s\,y_1^{\frac{c_{1s}}{e_{12}}}\right\}_{s=4,\dots,n-1}\right)\\ \phi_{\alpha,1,2} :& H_1^{in,\alpha}\to H_1^{out,2}\\ &\phi_{\alpha,1,2}\left(y_1,y_2,\{y_s\}_{s=4,\dots,n-1}\right)=\left(y_2\,y_1^{\frac{c_{1a}}{e_{12}}},\, y_1^{\frac{c_{1\alpha}}{e_{12}}},\, \left\{y_s\,y_1^{\frac{c_{1s}}{e_{12}}}\right\}_{s=4,\dots,n-1}\right)\end{aligned}$$

and

$$\begin{aligned} \phi_{1,2,b} :& H_2^{in,1}\to H_2^{out,b}\\ &\phi_{1,2,b}\left(y_2,y_3,\{y_s\}_{s=4,\dots,n-1}\right)=\left(y_2^{\frac{c_{21}}{e_{2b}}},\, y_3\,y_2^{-\frac{e_{2\beta}}{e_{2b}}},\, \left\{y_s\,y_2^{\frac{c_{2s}}{e_{2b}}}\right\}_{s=4,\dots,n-1}\right)\\ \phi_{1,2,\beta} :& H_2^{in,1}\to H_2^{out,\beta}\\ &\phi_{1,2,\beta}\left(y_2,y_3,\{y_s\}_{s=4,\dots,n-1}\right)=\left(y_3^{\frac{c_{21}}{e_{2\beta}}},\, y_2\,y_3^{-\frac{e_{2b}}{e_{2\beta}}},\, \left\{y_s\,y_3^{\frac{c_{2s}}{e_{2\beta}}}\right\}_{s=4,\dots,n-1}\right).\end{aligned}$$

The domains of definition of $\phi_{1,2,k}$, $k\in\{b,\beta\}$, are the sets $C_{1,2,k}$ described in the respective local coordinates by

$$\begin{aligned} C_{1,2,b} &= \left\{(y_1,\dots,y_{n-1})\in H_2^{in,1}:\ y_3<y_2^{\frac{e_{2\beta}}{e_{2b}}}\right\}\\ C_{1,2,\beta} &= \left\{(y_1,\dots,y_{n-1})\in H_2^{in,1}:\ y_2<y_3^{\frac{e_{2b}}{e_{2\beta}}}\right\}.\end{aligned} \tag{4.3}$$

Here $C_{1,2,\beta}$ is taken as the complement of $C_{1,2,b}$ and the other way around (recall Footnote 4 in Chapter 3). An easy computation shows that the ranges of $\phi_{i,1,2}$, $i\in\{a,\alpha\}$, turn out to be the sets

$F_{i,1,2}$ where

$$F_{a,1,2} = \left\{ (u_1, \ldots, u_{n-1}) \in H_1^{out,2} : \; u_3 < u_2^{\frac{c_{1\alpha}}{c_{1a}}} \text{ and } u_s < u_2^{\frac{c_{1s}}{c_{1a}}} \text{ for all } s = 4, \ldots, n-1 \right\}$$
$$F_{\alpha,1,2} = \left\{ (u_1, \ldots, u_{n-1}) \in H_1^{out,2} : \; u_2 < u_3^{\frac{c_{1a}}{c_{1\alpha}}} \text{ and } u_s < u_3^{\frac{c_{1s}}{c_{1\alpha}}} \text{ for all } s = 4, \ldots, n-1 \right\}. \tag{4.4}$$

The surface $y_3 = y_2^{\frac{e_{2\beta}}{e_{2b}}}$ divides $H_2^{in,1}$ into the region of points that go from ξ_1 to ξ_b and the region of points that go from ξ_1 to ξ_β. The surface $u_3 = u_2^{\frac{c_{1\alpha}}{c_{1a}}}$ in $H_1^{out,2}$ separates points coming from ξ_a to ξ_2 from those coming from ξ_α to ξ_2.

We observe that the local coordinates (y_2, y_3) in $H_2^{in,1}$ correspond to (x_b, x_β) in the original coordinate system and (u_2, u_3) in $H_1^{out,2}$ correspond to (x_a, x_α).

Theorem 4.2.4. *Let X be a heteroclinic network in $\mathbb{R}^n$ with sequences $[\xi_\alpha \to \xi_1 \to \xi_2 \to \xi_\beta]$ and $[\xi_a \to \xi_1 \to \xi_2 \to \xi_b]$ fulfilling Assumptions 3.1.4, 3.2.1 and 4.1.4. Suppose that Case 4.2.2 holds. Then, there is no switching along $\kappa_{1,2}$ if and only if*

$$\frac{e_{2\beta}}{e_{2b}} < \frac{c_{1\gamma}}{c_{1a}}. \tag{4.5}$$

Proof. Switching along $\kappa_{1,2}$ occurs if and only if $\psi_{1,2}(F_{i,1,2}) \cap C_{1,2,k} \neq \emptyset$ for all $i \in \{a, \alpha\}$ and $k \in \{b, \beta\}$. Below we prove that $\psi_{1,2}\left(\hat{F}_{a,1,2}\right) \cap \hat{C}_{1,2,\beta}$ may be empty.

For the points to be in $F_{i,1,2}$ the relevant directions are x_a and x_α while for the points to be in $C_{1,2,k}$ the relevant directions are x_b and x_β.

Suppose that $\psi_{1,2} : H_1^{out,2} \to H_2^{in,1}$ maps respectively the x_a- and x_γ-axes with $x_\gamma \neq x_\alpha$ into the x_b- and x_β-axes. Hence the x_α-axis must be mapped by $\psi_{1,2}$ into an axis other than x_b and x_β, say the x_δ-axis with $\delta \neq \{b, \beta\}$. We can therefore reduce $H_1^{out,2}$ to the $(x_a, x_\alpha, x_\gamma)$-subspace and $H_2^{in,1}$ to the (x_b, x_β, x_δ)-subspace. These are locally coordinatised[3] by (u_2, u_3, u_γ) and (y_2, y_3, y_δ).

We use a "hat" for labelling sets restricted to the relevant coordinates so that

$$\hat{F}_{a,1,2} = \left\{ (u_2, u_3, u_\gamma) \in \hat{H}_1^{out,2} : \; u_3 < u_2^{\frac{c_{1\alpha}}{c_{1a}}} \text{ and } u_\gamma < u_2^{\frac{c_{1\gamma}}{c_{1a}}} \right\}$$
$$\hat{F}_{\alpha,1,2} = \left\{ (u_2, u_3, u_\gamma) \in \hat{H}_1^{out,2} : \; u_2 < u_3^{\frac{c_{1a}}{c_{1\alpha}}} \text{ and } u_\gamma < u_3^{\frac{c_{1\gamma}}{c_{1\alpha}}} \right\} \tag{4.6}$$

and

$$\hat{C}_{1,2,b} = \left\{ (y_2, y_3, y_\delta) \in \hat{H}_2^{in,1} : \; y_3 < y_2^{\frac{e_{2\beta}}{e_{2b}}} \right\}$$
$$\hat{C}_{1,2,\beta} = \left\{ (y_2, y_3, y_\delta) \in \hat{H}_2^{in,1} : \; y_2 < y_3^{\frac{e_{2b}}{e_{2\beta}}} \right\}. \tag{4.7}$$

[3] When no confusion arises we keep the same subscript to designate new axes in original and local coordinates.

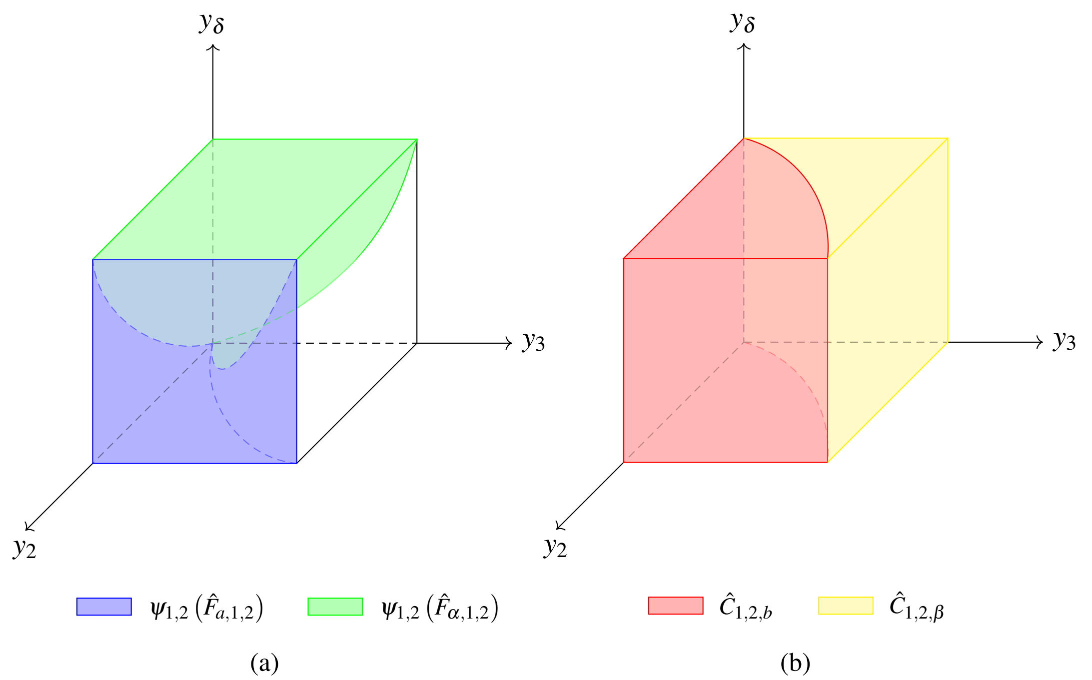

Fig. 4.10 Representation of the sets (a) $\psi_{1,2}\left(\hat{F}_{i,1,2}\right)$, $i \in \{a, \alpha\}$; (b) $\hat{C}_{1,2,k}$, $k \in \{b, \beta\}$, inside $\hat{H}_2^{in,1}$.

Up to rescaling constants the convenient restriction of $\psi_{1,2}$ in local coordinates takes the form

$$\psi_{1,2}\left(u_2, u_3, u_\gamma\right) = \left(u_2, u_\gamma, u_3\right) = \left(y_2, y_3, y_\delta\right).$$

Geometric representations of $\psi_{1,2}\left(\hat{F}_{i,1,2}\right)$ and $\hat{C}_{1,2,k}$ for all $i \in \{a, \alpha\}$ and $k \in \{b, \beta\}$ are pictured in Figure 4.10. It is sufficient to check the intersection $\psi_{1,2}\left(\hat{F}_{a,1,2}\right) \cap \hat{C}_{1,2,\beta}$. The image of $\hat{F}_{a,1,2}$ under $\psi_{1,2}$ is

$$\psi_{1,2}\left(\hat{F}_{a,1,2}\right) = \left\{ \left(y_2, y_3, y_\delta\right) \in \hat{H}_2^{in,1} : \; y_\delta < y_2^{\frac{c_{1\alpha}}{c_{1a}}} \text{ and } y_3 < y_2^{\frac{c_{1\gamma}}{c_{1a}}} \right\}$$

and hence

$$\psi_{1,2}\left(\hat{F}_{a,1,2}\right) \cap \hat{C}_{1,2,\beta} = \left\{ \left(y_2, y_3, y_\delta\right) \in \hat{H}_2^{in,1} : \; y_\delta < y_2^{\frac{c_{1\alpha}}{c_{1a}}} \text{ and } y_2^{\frac{e_{2\beta}}{e_{2b}}} < y_3 < y_2^{\frac{c_{1\gamma}}{c_{1a}}} \right\}.$$

We see at once that $\psi_{1,2}\left(\hat{F}_{a,1,2}\right) \cap \hat{C}_{1,2,\beta} = \emptyset$ whenever

$$y_2^{\frac{e_{2\beta}}{e_{2b}}} > y_2^{\frac{c_{1\gamma}}{c_{1a}}} \Leftrightarrow \frac{e_{2\beta}}{e_{2b}} < \frac{c_{1\gamma}}{c_{1a}} \tag{4.8}$$

which is the desired conclusion, see Figure 4.11. □

Remark 4.2.5. Combining Case 4.2.2 with Assumption 3.2.1 in Theorem 4.2.4 we know that the global map $\psi_{1,2}$ sends coordinate axes into coordinate axes. The statement (4.5) implicitly considers that the x_a- and x_γ-axes are respectively in one-to-one correspondence with the x_b- and x_β-axes. When

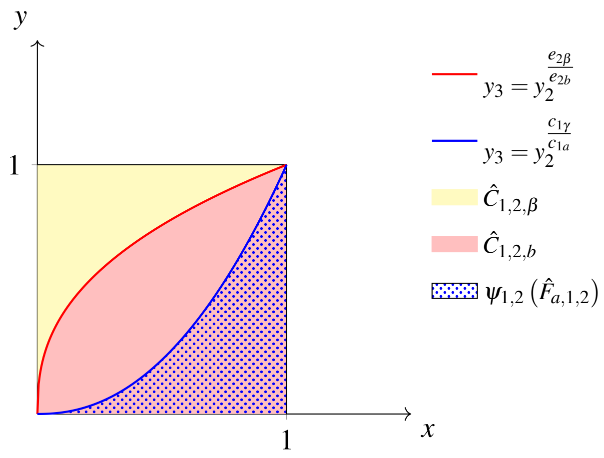

Fig. 4.11 Restriction of $\psi_{1,2}\left(\hat{F}_{a,1,2}\right) \cap \hat{C}_{1,2,k}$ to the (y_2, y_3)-plane, for $k \in \{b, \beta\}$. The plot suggests $\psi_{1,2}\left(\hat{F}_{a,1,2}\right) \subset \hat{C}_{1,2,b}$ and $\psi_{1,2}\left(\hat{F}_{a,1,2}\right) \cap \hat{C}_{1,2,\beta} = \emptyset$.

$\psi_{1,2}$ is assumed to map respectively the x_a- and x_γ-axes into the x_β- and x_b-axes, the subscripts "γ" and "a" must interchange in (4.5).

Theorem 4.2.6. *Let X be a heteroclinic network in $\mathbb{R}^n$ with sequences $\left[\xi_\alpha \to \xi_1 \to \xi_2 \to \xi_\beta\right]$ and $[\xi_a \to \xi_1 \to \xi_2 \to \xi_b]$ fulfilling Assumptions 3.1.4, 3.2.1 and 4.1.4. Suppose that Case 4.2.3 holds. Then, there is switching along $\kappa_{1,2}$.*

Proof. Suppose that $\psi_{1,2} : H_1^{out,2} \to H_2^{in,1}$ maps respectively the x_d- and x_γ-axes with $d \neq a$ and $\gamma \neq \alpha$ into the x_b- and x_β-axes. It means the x_a- and x_α-axes are mapped by $\psi_{1,2}$ into axes other than x_b and x_β, say the x_f- and x_δ-axes with $f, \delta \neq \{b, \beta\}$.

We now restrict $H_1^{out,2}$ to the $\left(x_a, x_\alpha, x_d, x_\gamma\right)$-subspace and $H_2^{in,1}$ to the $\left(x_b, x_\beta, x_f, x_\delta\right)$-subspace. These are expressed in local coordinates by $\left(u_2, u_3, u_d, u_\gamma\right)$ and $(y_2, y_3, y_f, y_\delta)$. Accordingly,

$$\hat{F}_{a,1,2} = \left\{ \left(u_2, u_3, u_d, u_\gamma\right) \in \hat{H}_1^{out,2} \, : \, u_3 < u_2^{\frac{c_{1\alpha}}{c_{1a}}} \text{ and } u_d < u_2^{\frac{c_{1d}}{c_{1a}}} \text{ and } u_\gamma < u_2^{\frac{c_{1\gamma}}{c_{1a}}} \right\}$$
$$\hat{F}_{\alpha,1,2} = \left\{ \left(u_2, u_3, u_d, u_\gamma\right) \in \hat{H}_1^{out,2} \, : \, u_2 < u_3^{\frac{c_{1a}}{c_{1\alpha}}} \text{ and } u_d < u_3^{\frac{c_{1d}}{c_{1\alpha}}} \text{ and } u_\gamma < u_3^{\frac{c_{1\gamma}}{c_{1\alpha}}} \right\}.$$

and

$$\hat{C}_{1,2,b} = \left\{ (y_2, y_3, y_f, y_\delta) \in \hat{H}_2^{in,1} \, : \, y_3 < y_2^{\frac{e_{2\beta}}{e_{2b}}} \right\}$$
$$\hat{C}_{1,2,\beta} = \left\{ (y_2, y_3, y_f, y_\delta) \in \hat{H}_2^{in,1} \, : \, y_2 < y_3^{\frac{e_{2b}}{e_{2\beta}}} \right\}.$$

Up to rescaling constants we further write

$$\psi_{1,2}\left(u_2, u_3, u_d, u_\gamma\right) = \left(u_d, u_\gamma, u_2, u_3\right) = (y_2, y_3, y_f, y_\delta)$$

such that

$$\psi_{1,2}\left(\hat{F}_{a,1,2}\right) = \left\{ (y_2,y_3,y_f,y_\delta) \in \hat{H}_2^{in,1} \,:\, y_\delta < y_f^{\frac{c_{1\alpha}}{c_{1a}}} \text{ and } y_2 < y_f^{\frac{c_{1d}}{c_{1a}}} \text{ and } y_3 < y_f^{\frac{c_{1\gamma}}{c_{1a}}} \right\}$$

$$\psi_{1,2}\left(\hat{F}_{\alpha,1,2}\right) = \left\{ (y_2,y_3,y_f,y_\delta) \in \hat{H}_2^{in,1} \,:\, y_f < y_\delta^{\frac{c_{1a}}{c_{1\alpha}}} \text{ and } y_2 < y_\delta^{\frac{c_{1d}}{c_{1\alpha}}} \text{ and } y_3 < y_\delta^{\frac{c_{1\gamma}}{c_{1\alpha}}} \right\}.$$

It follows that

$$\psi_{1,2}\left(\hat{F}_{a,1,2}\right) \cap \hat{C}_{1,2,b} = \left\{ (y_2,y_3,y_f,y_\delta) \in \hat{H}_2^{in,1} \,:\, y_\delta < y_f^{\frac{c_{1\alpha}}{c_{1a}}} \text{ and } y_2 < y_f^{\frac{c_{1d}}{c_{1a}}} \text{ and } y_3 < \min\left\{ y_f^{\frac{c_{1\gamma}}{c_{1a}}}, y_2^{\frac{e_{2\beta}}{e_{2b}}} \right\} \right\}$$

$$\psi_{1,2}\left(\hat{F}_{a,1,2}\right) \cap \hat{C}_{1,2,\beta} = \left\{ (y_2,y_3,y_f,y_\delta) \in \hat{H}_2^{in,1} \,:\, y_\delta < y_f^{\frac{c_{1\alpha}}{c_{1a}}} \text{ and } y_2 < \min\left\{ y_f^{\frac{c_{1d}}{c_{1a}}}, y_3^{\frac{e_{2b}}{e_{2\beta}}} \right\} \text{ and } y_3 < y_f^{\frac{c_{1\gamma}}{c_{1a}}} \right\}$$

and

$$\psi_{1,2}\left(\hat{F}_{\alpha,1,2}\right) \cap \hat{C}_{1,2,b} = \left\{ (y_2,y_3,y_f,y_\delta) \in \hat{H}_2^{in,1} \,:\, y_f < y_\delta^{\frac{c_{1a}}{c_{1\alpha}}} \text{ and } y_2 < y_\delta^{\frac{c_{1d}}{c_{1\alpha}}} \text{ and } y_3 < \min\left\{ y_\delta^{\frac{c_{1\gamma}}{c_{1\alpha}}}, y_2^{\frac{e_{2\beta}}{e_{2b}}} \right\} \right\}$$

$$\psi_{1,2}\left(\hat{F}_{\alpha,1,2}\right) \cap \hat{C}_{1,2,\beta} = \left\{ (y_2,y_3,y_f,y_\delta) \in \hat{H}_2^{in,1} \,:\, y_f < y_\delta^{\frac{c_{1a}}{c_{1\alpha}}} \text{ and } y_2 < \min\left\{ y_\delta^{\frac{c_{1d}}{c_{1\alpha}}}, y_3^{\frac{e_{2b}}{e_{2\beta}}} \right\} \text{ and } y_3 < y_\delta^{\frac{c_{1\gamma}}{c_{1\alpha}}} \right\}.$$

Clearly $\psi_{1,2}\left(\hat{F}_{k,1,2}\right) \cap \hat{C}_{1,2,k} \neq \emptyset$ for all $i \in \{a,\alpha\}$ and $k \in \{b,\beta\}$, so there is switching along $\kappa_{1,2}$. $\square$

4.2.1 Switching in the House network

The House network consists of two heteroclinic cycles, a B_3^-- and a C_4^--cycles each with an extra transverse dimension, linked together via a heteroclinic connection, see Figure 4.12. We can use the simplex realisation from [13] to generate it in $\mathbb{R}^5$ by choosing suitable parameters.[4]

The House network has five nodes arranged in the heteroclinic cycles $[\xi_1 \to \xi_2 \to \xi_3 \to \xi_1]$ (B_3^--cycle) and $[\xi_1 \to \xi_2 \to \xi_4 \to \xi_5 \to \xi_1]$ (C_4^--cycle). The heteroclinic connection $\kappa_{1,2} = [\xi_1 \to \xi_2]$ is common to both heteroclinic cycles.

Castro and Lohse [19] examine the House network as an example of illustrating the role of their assumption with regard to the common heteroclinic connection. Recall Theorem 4.2.1.

Denote by (x_1,x_2,x_3,x_4,x_5) the standard basis in $\mathbb{R}^5$. From Figure 4.9 and Theorem 4.2.1 the (x_a,x_α) incoming directions at ξ_1 correspond to (x_3,x_5). The $\left(x_b,x_\beta\right)$ outgoing directions at ξ_2 are now (x_3,x_4). The system is equivariant under the $\mathbb{Z}_2^5$-symmetry and the above-mentioned heteroclinic cycles are naturally of type Z within $\mathbb{R}^5$. Global maps can be assumed to equal the identity.[5] Each cross section $H_j^{out,k}$ in the relevant local coordinates is freely identified with $H_k^{in,j}$. In particular the global map $\psi_{1,2} : H_1^{out,2} \to H_2^{in,1}$ along $\kappa_{1,2}$ does not transform the (x_a,x_α)-plane into the $\left(x_b,x_\beta\right)$-plane but satisfies Case 4.2.2. Applying Theorem 4.2.4 we state

[4] A brief description of an application of the simplex realisation can be found in Section 6.1.

[5] For more details we refer the reader to [43] and [52].

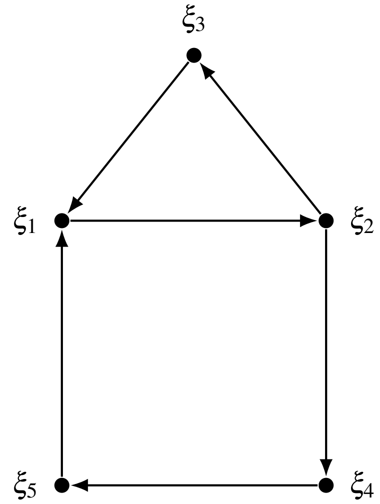

Fig. 4.12 The House network. The B_3^--cycle is $[\xi_1 \to \xi_2 \to \xi_3 \to \xi_1]$ and the C_4^--cycle is $[\xi_1 \to \xi_2 \to \xi_4 \to \xi_5 \to \xi_1]$.

Corollary 4.2.7. *There is no switching along the common heteroclinic connection $\kappa_{1,2}$ in the House network if and only if*

$$\frac{e_{24}}{e_{23}} < \frac{c_{14}}{c_{13}}.$$

Proof. Ignoring the radial direction every cross section is viewed as a cube in $\mathbb{R}^3$. We can write

$$H_1^{out,2} \equiv H_2^{in,1} = \{(x_3, x_4, x_5) : 0 \leq x_3, x_4, x_5 < 1\}.$$

On the one hand, the cross section $H_1^{out,2}$ is split into the set $F_{3,1,2}$ whose points come from ξ_3 and the set $F_{5,1,2}$ whose points come from ξ_5. A trivial verification from (4.6) shows that

$$F_{3,1,2} = \left\{ (x_3, x_4, x_5) \in H_1^{out,2} : \ x_4 < x_3^{\frac{c_{14}}{c_{13}}} \text{ and } x_5 < x_3^{\frac{c_{15}}{c_{13}}} \right\}$$
$$F_{5,1,2} = \left\{ (x_3, x_4, x_5) \in H_1^{out,2} : \ x_3 < x_5^{\frac{c_{13}}{c_{15}}} \text{ and } x_4 < x_5^{\frac{c_{14}}{c_{15}}} \right\}.$$

On the other hand, the cross section $H_2^{in,1}$ is split into the set $C_{1,2,3}$ whose points go to ξ_3 and the set $C_{1,2,4}$ whose points go to ξ_4. By (4.7) we get

$$C_{1,2,3} = \left\{ (x_3, x_4, x_5) \in H_2^{in,1} : \ x_4 < x_3^{\frac{e_{24}}{e_{23}}} \right\}$$
$$C_{1,2,4} = \left\{ (x_3, x_4, x_5) \in H_2^{in,1} : \ x_3 < x_4^{\frac{e_{23}}{e_{24}}} \right\}.$$

The F- and C-sets are represented in Figure 4.13. The shape of the boundary surfaces depends on the relative magnitudes of the eigenvalues. Since $H_1^{out,2}$ and $H_2^{in,1}$ are indistinguishable we can directly intersect the indicated sets, see Figure 4.14. Using the same reasoning as in the proof of Theorem 4.2.4 we only need to look at the intersections $F_{i,1,2} \cap C_{1,2,k}$, $i = 3, 5$, $k = 3, 4$, restricted to the (x_3,x_4)-plane. The delimiting curves are $x_4 = x_3^{\frac{c_{14}}{c_{13}}}$ for the F-sets and $x_4 = x_3^{\frac{e_{24}}{e_{23}}}$ for the C-sets. Thus switching along $\kappa_{1,2}$ does not occurs if and only if

$$x_3^{\frac{e_{24}}{e_{23}}} > x_3^{\frac{c_{14}}{c_{13}}} \Leftrightarrow \frac{e_{24}}{e_{23}} < \frac{c_{14}}{c_{13}}.$$

□

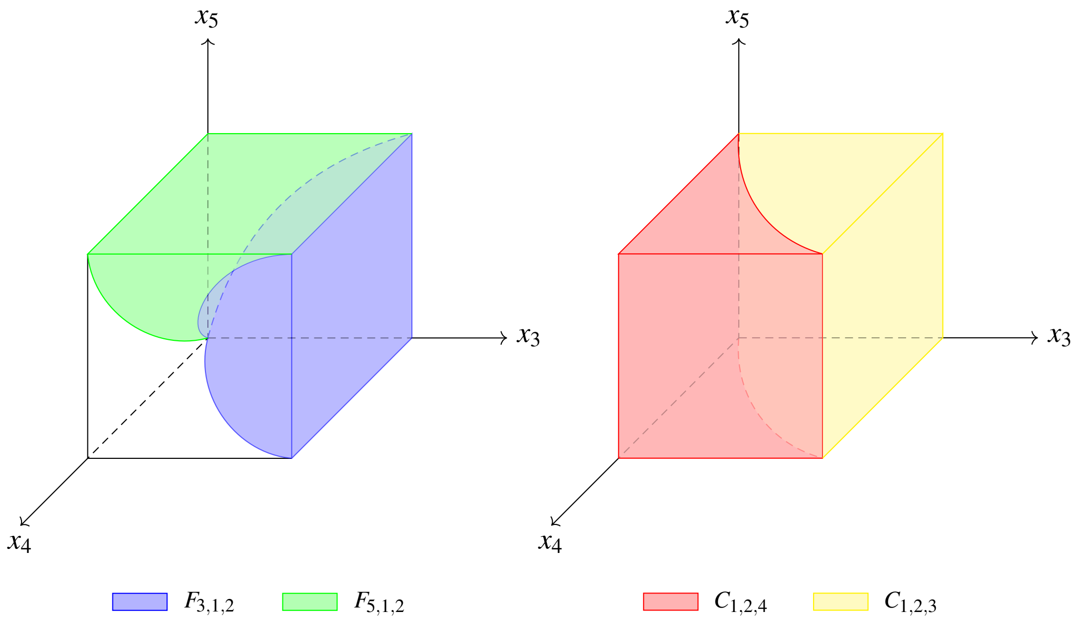

(a) (b)

Fig. 4.13 Splitting of the cross sections (a) $H_1^{out,2}$ into the set $F_{3,1,2}$ of points coming from ξ_3 and the set $F_{5,1,2}$ of points coming from ξ_5; (b) $H_2^{in,1}$ into the set $C_{1,2,3}$ of points going to ξ_3 and the set $C_{1,2,4}$ of points going to ξ_4.

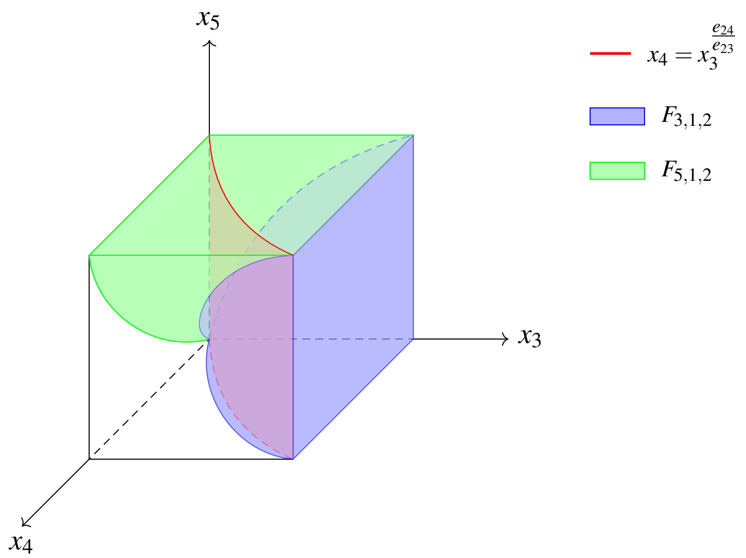

Fig. 4.14 Intersection of the F-sets with the splitting boundary of the C-sets in $H_2^{in,1}$.

Contrary to our claim, Lemma 3.7 in [19] asserts there is always switching along the common heteroclinic connection in the House network. The proof has been supported by the Figure 6 therein, which is incorrect in view of Figure 4.13(a).

4.2.2 A single common node

We proceed to show that the presence of a single common node instead of the whole heteroclinic connection in Figure 4.9 can provide switching dynamics in much the same way as switching along heteroclinic connections.

Consider a heteroclinic network in $\mathbb{R}^n$ with two quasi-simple heteroclinic cycles connected at a node ξ_2 as in Figure 4.15. We name the heteroclinic cycles

$$[\xi_\alpha \to \boldsymbol{\xi_2} \to \xi_\beta \to \cdots \to \xi_\alpha] \qquad \text{and} \qquad [\xi_1 \to \boldsymbol{\xi_2} \to \xi_b \to \cdots \to \xi_1]$$

where $\xi_1 \neq \xi_\alpha$ and $\xi_\beta \neq \xi_b$, the L-cycle (left) and the R-cycle (right), respectively. Notice that the lowest dimension for this construction is five. As before we linearise the flow about ξ_2 in non-radial directions $(y_1, \ldots, y_{n-1})$ to obtain

$$\begin{aligned}
\dot{y}_1 &= -c_{21}\, y_1 \\
\dot{y}_2 &= e_{2b}\, y_2 \\
\dot{y}_3 &= e_{2\beta}\, y_3 \\
\dot{y}_4 &= -c_{2\alpha}\, y_4 \\
\dot{y}_s &= -c_{2s}\, y_s, \quad s = 5, \ldots, n-1.
\end{aligned}$$

Recall that the constants $-c_{2s} < 0$, $s = 5, \ldots, n-1$, are assumed to be negative transverse eigenvalues at ξ_2 to either heteroclinic cycle.

We introduce four cross sections near ξ_2: $H_2^{out,b}$, $H_2^{out,\beta}$ and $H_2^{in,1}$ as in (4.2), and

$$H_2^{in,\alpha} = \{(y_1, y_2, y_3, 1, \ldots, y_{n-1}) : \ 0 \leq y_i < 1 \text{ for all } i \neq 4\}.$$

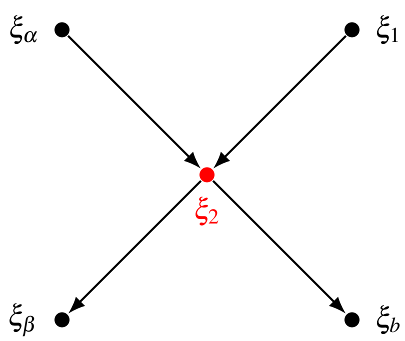

Fig. 4.15 A common node of a heteroclinic network comprising of two heteroclinic cycles: L (left) and R (right). The L-cycle involves the nodes ξ_2 and those to its left. The R-cycle involves the nodes ξ_2 and those to its right.

In a small neighbourhood of ξ_2 the behaviour of trajectories is approximated by the local maps

$$
\begin{aligned}
\phi_{1,2,b} :& H_2^{in,1} \to H_2^{out,b} \\
& \phi_{1,2,b}\left(y_2, y_3, y_4 \{y_s\}_{s=5,\dots,n-1}\right) = \left(y_2^{\frac{c_{21}}{e_{2b}}}, y_3 y_2^{-\frac{e_{2\beta}}{e_{2b}}}, y_4 y_2^{\frac{c_{2\alpha}}{e_{2b}}}, \left\{ y_s y_2^{\frac{c_{2s}}{e_{2b}}} \right\}_{s=5,\dots,n-1} \right) \\
\phi_{1,2,\beta} :& H_2^{in,1} \to H_2^{out,\beta} \\
& \phi_{1,2,\beta}\left(y_2, y_3, y_4, \{y_s\}_{s=5,\dots,n-1}\right) = \left(y_3^{\frac{c_{21}}{e_{2\beta}}}, y_2 y_3^{-\frac{e_{2b}}{e_{2\beta}}}, y_4 y_3^{\frac{c_{2\alpha}}{e_{2\beta}}}, \left\{ y_s y_3^{\frac{c_{2s}}{e_{2\beta}}} \right\}_{s=5,\dots,n-1} \right) \\
\phi_{\alpha,2,b} :& H_2^{in,\alpha} \to H_2^{out,b} \\
& \phi_{\alpha,2,b}\left(y_1, y_2, y_3, \{y_s\}_{s=5,\dots,n-1}\right) = \left(y_1 y_2^{\frac{c_{21}}{e_{2b}}}, y_3 y_2^{-\frac{e_{2\beta}}{e_{2b}}}, y_2^{\frac{c_{2\alpha}}{e_{2b}}}, \left\{ y_s y_2^{\frac{c_{2s}}{e_{2b}}} \right\}_{s=5,\dots,n-1} \right) \\
\phi_{\alpha,2,\beta} :& H_2^{in,\alpha} \to H_2^{out,\beta} \\
& \phi_{\alpha,2,\beta}\left(y_1, y_2, y_3, \{y_s\}_{s=5,\dots,n-1}\right) = \left(y_1 y_3^{\frac{c_{21}}{e_{2\beta}}}, y_2 y_3^{-\frac{e_{2b}}{e_{2\beta}}}, y_3^{\frac{c_{2\alpha}}{e_{2\beta}}}, \left\{ y_s y_3^{\frac{c_{2s}}{e_{2\beta}}} \right\}_{s=5,\dots,n-1} \right).
\end{aligned}
\tag{4.9}
$$

Points in $H_2^{in,1}$ for which $\phi_{1,2,k}$, $k \in \{b, \beta\}$, are well defined constitute the set $C_{1,2,k}$ in (4.3). The sets $C_{\alpha,2,k}$ describing the domains of definition of $\phi_{\alpha,2,k}$ in $H_2^{in,\alpha}$ are constrained by identical inequalities such that

$$
\begin{aligned}
C_{\alpha,2,b} &= \left\{ (y_1, \dots, y_{n-1}) \in H_2^{in,\alpha} : \; y_3 < y_2^{\frac{e_{2\beta}}{e_{2b}}} \right\} \\
C_{\alpha,2,\beta} &= \left\{ (y_1, \dots, y_{n-1}) \in H_2^{in,\alpha} : \; y_2 < y_3^{\frac{e_{2b}}{e_{2\beta}}} \right\}.
\end{aligned}
$$

Moreover, we find $F_{i,2,k} = \phi_{i,2,k}(C_{i,2,k})$ for every $i \in \{1, \alpha\}$ and $k \in \{b, \beta\}$ where

$$
\begin{aligned}
F_{1,2,b} &= \left\{ (u_1, \dots, u_{n-1}) \in H_2^{out,b} : \; u_4 < u_1^{\frac{c_{2\alpha}}{c_{21}}} \text{ and } u_s < u_1^{\frac{c_{2s}}{c_{21}}} \text{ for all } s = 5, \dots, n-1 \right\} \\
F_{1,2,\beta} &= \left\{ (u_1, \dots, u_{n-1}) \in H_2^{out,\beta} : \; u_4 < u_1^{\frac{c_{2\alpha}}{c_{21}}} \text{ and } u_s < u_1^{\frac{c_{2s}}{c_{21}}} \text{ for all } s = 5, \dots, n-1 \right\} \\
F_{\alpha,2,b} &= \left\{ (u_1, \dots, u_{n-1}) \in H_2^{out,b} : \; u_1 < u_4^{\frac{c_{21}}{c_{2\alpha}}} \text{ and } u_s < u_4^{\frac{c_{2s}}{c_{2\alpha}}} \text{ for all } s = 5, \dots, n-1 \right\} \\
F_{\alpha,2,\beta} &= \left\{ (u_1, \dots, u_{n-1}) \in H_2^{out,\beta} : \; u_1 < u_4^{\frac{c_{21}}{c_{2\alpha}}} \text{ and } u_s < u_4^{\frac{c_{2s}}{c_{2\alpha}}} \text{ for all } s = 5, \dots, n-1 \right\}.
\end{aligned}
\tag{4.10}
$$

Lemma 4.2.8. *Let X be a heteroclinic network in $\mathbb{R}^n$ with sequences $[\xi_1 \to \xi_2 \to \xi_b]$ and $[\xi_\alpha \to \xi_2 \to \xi_\beta]$ fulfilling Assumption 3.1.4. Then, there is switching at ξ_2.*

Proof. It suffices to note that around ξ_2 the sets $C_{i,2,k}$ and $F_{i,2,k}$ for all $i \in \{1, \alpha\}$ and $k \in \{b, \beta\}$ have all positive measure. Points in $H_2^{in,1}$ are thus sent through a suitable local map to both $H_2^{out,b}$ and $H_2^{out,\beta}$ depending on whether they belong to either $C_{1,2,b}$ or $C_{1,2,\beta}$. The same is true for points in $H_2^{in,\alpha}$. $\square$

Without loss of generality we assume that the sequence $[\xi_a \to \xi_1 \to \xi_2 \to \xi_b]$ is part of the R-cycle but allow $\xi_a = \xi_b$. The flow linearised about ξ_1 in non-radial coordinates is given by

$$\begin{aligned}\dot{y}_1 &= e_{12}\, y_1 \\ \dot{y}_2 &= -c_{1a}\, y_2 \\ \dot{y}_s &= -c_{1s}\, y_s, \quad s = 3, \dots, n-1.\end{aligned}$$

The coordinates y_1, y_2 and y_s are respectively expanding, contracting and transverse at ξ_1. Taking $H_1^{in,a}$ and $H_1^{out,2}$ in (4.1) we write down the local map $\phi_{a,1,2} : H_1^{in,a} \to H_1^{out,2}$ with

$$\phi_{a,1,2}\left(y_1, \{y_s\}_{s=3,\dots,n-1}\right) = \left(y_1^{\frac{c_{1a}}{e_{12}}}, \left\{y_s\, y_1^{\frac{c_{1s}}{e_{12}}}\right\}_{s=3,\dots,n-1}\right).$$

Such a map is defined in the whole $H_1^{in,a}$ and its image yields

$$F_{a,1,2} = \left\{(u_1, \dots, u_{n-1}) \in H_1^{out,2} : \; u_s < u_2^{\frac{c_{1s}}{c_{1a}}} \text{ for all } s = 3, \dots, n-1\right\}. \tag{4.11}$$

Proposition 4.2.9. *Let X be a heteroclinic network in $\mathbb{R}^n$ with sequences $[\xi_a \to \xi_1 \to \xi_2 \to \xi_b]$ and $\left[\xi_\alpha \to \xi_2 \to \xi_\beta\right]$ fulfilling Assumptions 3.1.4, 3.2.1 and 4.1.4. Suppose that the x_a-axis is mapped by the global map $\psi_{1,2}$ within the $\left(x_b, x_\beta\right)$-plane. Then, there is no switching along $\kappa_{1,2}$ if and only if*

$$\frac{e_{2\beta}}{e_{2b}} < \frac{c_{1\gamma}}{c_{1a}}.$$

Proof. We employ the arguments in the proof of Theorem 4.2.4: switching along $\kappa_{1,2}$ occurs if and only if $\psi_{1,2}\left(F_{a,1,2}\right) \cap C_{1,2,k} \neq \emptyset$ for all $k \in \{b, \beta\}$.

Only the coordinates $\left(x_b, x_\beta\right)$ in $C_{1,2,k} \subset H_2^{in,k}$ for $k \in \{b, \beta\}$ are important. Suppose that $\psi_{1,2} : H_1^{out,2} \to H_2^{in,1}$ maps respectively the x_a- and x_γ-axes for some $x_\gamma \neq x_a$ into the x_b- and x_β-axes. Restricting $H_1^{out,2}$ to the $\left(x_a, x_\gamma\right)$-subspace and $H_2^{in,1}$ to the $\left(x_b, x_\beta\right)$-subspace we have in local coordinates

$$\hat{F}_{a,1,2} = \left\{\left(u_2, u_\gamma\right) \in \hat{H}_1^{out,2} : \; u_\gamma < u_2^{\frac{c_{1\gamma}}{c_{1a}}}\right\}$$

and

$$\begin{aligned}\hat{C}_{1,2,b} &= \left\{(y_2, y_3) \in \hat{H}_2^{in,1} : \; y_3 < y_2^{\frac{e_{2\beta}}{e_{2b}}}\right\} \\ \hat{C}_{1,2,\beta} &= \left\{(y_2, y_3) \in \hat{H}_2^{in,1} : \; y_2 < y_3^{\frac{e_{2b}}{e_{2\beta}}}\right\}.\end{aligned}$$

The restriction of $\psi_{1,2}$ to the relevant plane is the identity up to a rescaling, and therefore

$$\psi_{1,2}\left(\hat{F}_{a,1,2}\right) = \left\{(y_2, y_3) \in \hat{H}_2^{in,1} : \; y_3 < y_2^{\frac{c_{1\gamma}}{c_{1a}}}\right\}.$$

Now

$$\psi_{1,2}\left(\hat{F}_{a,1,2}\right) \cap \hat{C}_{1,2,b} = \left\{ (y_2, y_3) \in \hat{H}_2^{in,1} \, : \, y_3 < \min\left\{ y_2^{\frac{c_{1\gamma}}{c_{1a}}}, y_2^{\frac{e_{2\beta}}{e_{2b}}} \right\} \right\}$$
$$\psi_{1,2}\left(\hat{F}_{a,1,2}\right) \cap \hat{C}_{1,2,\beta} = \left\{ (y_2, y_3) \in \hat{H}_2^{in,1} \, : \, y_2^{\frac{e_{2\beta}}{e_{2b}}} < y_3 < y_2^{\frac{c_{1\gamma}}{c_{1a}}} \right\}.$$

We conclude that $\psi_{1,2}\left(\hat{F}_{a,1,2}\right) \subset \hat{C}_{1,2,b}$ and the intersection of $\psi_{1,2}\left(\hat{F}_{a,1,2}\right)$ and $\hat{C}_{1,2,\beta}$ is always empty provided

$$y_2^{\frac{e_{2\beta}}{e_{2b}}} > y_2^{\frac{c_{1\gamma}}{c_{1a}}} \Leftrightarrow \frac{e_{2\beta}}{e_{2b}} < \frac{c_{1\gamma}}{c_{1a}}.$$

This excludes the occurrence of switching along $\kappa_{1,2}$. □

Proposition 4.2.10. *Let X be a heteroclinic network in $\mathbb{R}^n$ with sequences $[\xi_a \to \xi_1 \to \xi_2 \to \xi_b]$ and $[\xi_\alpha \to \xi_2 \to \xi_\beta]$ fulfilling Assumptions 3.1.4, 3.2.1 and 4.1.4. Suppose that the x_a-axis is not mapped by the global map $\psi_{1,2}$ within the (x_b, x_β)-plane. Then, there is switching along $\kappa_{1,2}$.*

Proof. Suppose that $\psi_{1,2} : H_1^{out,2} \to H_2^{in,1}$ maps respectively the x_a-, x_d- and x_γ-axes into the x_δ-, x_b- and x_β-axes for some $x_d \neq x_\gamma \neq x_a$ and $x_\delta \neq \{x_b, x_\beta\}$. The (x_a, x_d, x_γ)-subspace corresponds locally to (u_2, u_d, u_γ) in $\hat{H}_1^{out,2}$ and the (x_b, x_β, x_δ)-subspace to (y_2, y_3, y_δ) in $\hat{H}_2^{in,1}$. We thus get

$$\psi_{1,2}\left(u_2, u_d, u_\gamma\right) = \left(u_d, u_\gamma, u_2\right) = (y_2, y_3, y_\delta).$$

From

$$\hat{F}_{a,1,2} = \left\{ \left(u_2, u_d, u_\gamma\right) \in \hat{H}_1^{out,2} \, : \, u_d < u_2^{\frac{c_{1d}}{c_{1a}}} \text{ and } u_\gamma < u_2^{\frac{c_{1\gamma}}{c_{1a}}} \right\}$$

it follows that

$$\psi_{1,2}\left(\hat{F}_{a,1,2}\right) = \left\{ (y_2, y_3, y_\delta) \in \hat{H}_2^{in,1} \, : \, y_2 < y_\delta^{\frac{c_{1d}}{c_{1a}}} \text{ and } y_3 < y_\delta^{\frac{c_{1\gamma}}{c_{1a}}} \right\}.$$

Together with (4.7) we assert that

$$\psi_{1,2}\left(\hat{F}_{a,1,2}\right) \cap \hat{C}_{1,2,b} = \left\{ (y_2, y_3, y_\delta) \in \hat{H}_2^{in,1} \, : \, y_2 < y_\delta^{\frac{c_{1d}}{c_{1a}}} \text{ and } y_3 < \min\left\{ y_\delta^{\frac{c_{1\gamma}}{c_{1a}}}, y_2^{\frac{e_{2\beta}}{e_{2b}}} \right\} \right\}$$
$$\psi_{1,2}\left(\hat{F}_{a,1,2}\right) \cap \hat{C}_{1,2,\beta} = \left\{ (y_2, y_3, y_\delta) \in \hat{H}_2^{in,1} \, : \, y_2 < \min\left\{ y_\delta^{\frac{c_{1d}}{c_{1a}}}, y_3^{\frac{e_{2b}}{e_{2\beta}}} \right\} \text{ and } y_3 < y_\delta^{\frac{c_{1\gamma}}{c_{1a}}} \right\}.$$

Because $\psi_{1,2}\left(\hat{F}_{a,1,2}\right) \cap \hat{C}_{1,2,k} \neq \emptyset$ for all $k \in \{b, \beta\}$ there is switching along $\kappa_{1,2}$. □

Remark 4.2.11. The analogue of Propositions 4.2.9 and 4.2.10 can be stated in terms of the heteroclinic connection $\kappa_{\alpha,2}$ for the L-cycle.

We have shown that a heteroclinic connection leading to a singular common node that makes up a heteroclinic network contributes likewise to the dynamics near the heteroclinic network as any heteroclinic connection shared by two heteroclinic cycles. Indeed, the behaviour of trajectories in the vicinity of a heteroclinic network are controlled by the non-radial eigenvalues at the entrance and exit of each node.

4.3 Switching along a heteroclinic cycle

We continue our study by describing the dynamics near the R- and L-cycles together in a heteroclinic network in $\mathbb{R}^n$ by means of at least one node. Based on the comment at the end of the previous section all the following results will hold whether there is a common heteroclinic connection or just a common node.

Castro and Lohse [19] introduce the notion of *switching along a cycle* in the context of the Bowtie network in $\mathbb{R}^5$ pictured in Figure 4.16. This consists of switching along a sequence of heteroclinic connections forming a heteroclinic cycle.

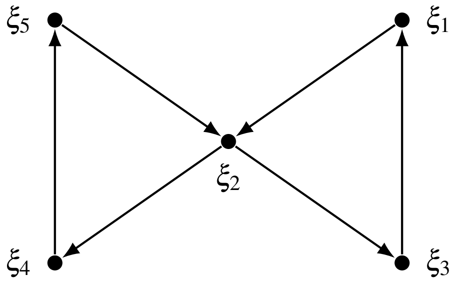

Fig. 4.16 The Bowtie network. The node ξ_2 is common to the R and L-cycles. The R-cycle is $[\xi_1 \to \xi_2 \to \xi_3 \to \xi_1]$ and the L-cycle is $[\xi_5 \to \xi_2 \to \xi_4 \to \xi_5]$.

Figure 4.15 exhibits the common node in a generalisation of the Bowtie network to any heteroclinic network with two quasi-simple heteroclinic cycles each with arbitrary length. It is this figure that illustrates the lemmas in the present section. To establish switching along the R-cycle we determine how the sets $C_{1,2,k}$, $k \in \{b, \beta\}$, in $H_2^{in,1}$ are sent through composite maps around the heteroclinic cycle and returned to $H_2^{in,1}$. Let us denote by $\pi_R : H_2^{in,1} \to H_2^{in,1}$ the return map around the entire R-cycle where

$$\pi_R = \psi_{1,2} \circ \phi_{a,1,2} \circ \cdots \circ \psi_{2,b} \circ \phi_{1,2,b}. \tag{4.12}$$

First we check what exactly happens to the cusps defining the boundary of $F_{1,2,b}$ within $H_2^{out,b}$ in (4.10) when they move along the heteroclinic connection $\kappa_{2,b}$ until they hit $H_b^{out,d}$. This is described by the composition of maps $\phi_{2,b,d} \circ \psi_{2,b} : H_2^{out,b} \to H_b^{out,d}$. We require that ξ_d succeeds ξ_b such that ξ_d might be ξ_a, and in turn ξ_1. Near $H_2^{out,b}$ the local coordinates (u_1, u_4) match the original ones (x_1, x_α). The result depends on the type of $\kappa_{2,b}$.

Lemma 4.3.1. *Let X be a heteroclinic network in $\mathbb{R}^n$ composed of two quasi-simple heteroclinic cycles R and L with sequences $[\xi_a \to \xi_1 \to \xi_2 \to \xi_b \to \xi_d]$ and $[\xi_\alpha \to \xi_2 \to \xi_\beta]$. Suppose that both R and L-cycles satisfy Assumptions 3.1.4, 3.2.1 and 4.1.4. Suppose that*

(i) x_i is a transverse coordinate at ξ_2 with respect to the R-cycle such that $x_i \neq x_\beta$;

(ii) the heteroclinic connection $\kappa_{2,b}$ is of type contracting-to-expanding.

The image of $F_{1,2,b}$ *in* (4.10) *under* $\phi_{2,b,d} \circ \psi_{2,b}$ *is such that:*

(a) the (x_α, x_β)*-face is mapped into the origin of* $\mathbb{R}^{n-2}$*.*

(b) every (x_1, x_i)*-face is mapped into a cuspoidal region bounded by the curve* $x_\gamma = x_2^{\frac{c_{b\gamma}}{c_{b2}}}$ *in the* (x_2, x_γ)*-face for some transverse coordinate* x_γ *at* ξ_b*. Moreover, the image of the curve* $x_i = x_1^{\frac{c_{2i}}{c_{21}}}$ *is the curve defined by* $x_\gamma = x_2^{\frac{e_{b1}}{c_{b2}}\frac{c_{2i}}{c_{21}}+\frac{c_{b\gamma}}{c_{b2}}}$*.*

(c) the (x_1, x_β)*-face is mapped into a cuspoidal region bounded by the curve* $x_\delta = x_2^{\frac{c_{b\delta}}{c_{b2}}}$ *in the* (x_2, x_δ)*-face for some transverse coordinate* x_δ *at* ξ_b*.*

Proof. We look at the R-cycle and assume that $\kappa_{2,b}$ is a contracting-to-expanding connection. The expanding direction at ξ_b coincides with the contracting direction at ξ_2, that is, x_1. Transverse directions at ξ_2 and ξ_b are in one-to-one correspondence.

(a) The directions spanned by x_α and x_β are transverse at ξ_2 regarding the R-cycle. The (x_α, x_β)-plane is first mapped by $\psi_{2,b} : H_2^{out,b} \to H_b^{int,2}$ into the $(x_{\gamma_1}, x_{\gamma_2})$-plane for some coordinates, x_{γ_1} and x_{γ_2}, transverse at ξ_b. The image of the whole (x_1, x_α, x_β)-subspace under $\psi_{2,b}$ is the $(x_1, x_{\gamma_1}, x_{\gamma_2})$-subspace. Let $(y_1, y_2, y_3, \ldots, y_{n-1})$ be the local non-radial coordinates near ξ_b in the associated eigenbasis where the expanding and the contracting directions are followed by the transverse ones. The local flow near ξ_b

$$\begin{aligned} \dot{y}_1 &= e_{b1} y_1 \\ \dot{y}_2 &= -c_{b2} y_2 \\ \dot{y}_s &= -c_{bs} y_s, \quad s = 3, \ldots, n-1, \end{aligned} \tag{4.13}$$

induces the map $\phi_{2,b,d} : H_b^{in,2} \to H_b^{out,d}$, which takes the form

$$\phi_{2,b,d}\left(y_1, \{y_s\}_{s=3,\ldots,n-1}\right) = \left(y_1^{\frac{c_{b2}}{e_{b1}}}, \left\{y_s y_1^{\frac{c_{bs}}{e_{b1}}}\right\}_{s=3,\ldots,n-1}\right) = \left(u_2, \{u_s\}_{s=3,\ldots,n-1}\right). \tag{4.14}$$

The (x_α, x_β)-face in $H_2^{out,b}$ belongs to the hyperplane $x_1 = 0$. Therefore the $(x_{\gamma_1}, x_{\gamma_2})$-face in $H_b^{in,2}$ belongs to the hyperplane $x_1 = 0$ locally coordinatised by $y_1 = 0$. This forces the former to be sent through $\phi_{2,b,d} \circ \psi_{2,b}$ to the origin of $\mathbb{R}^{n-2}$.

(b) Pick a transverse coordinate x_i at ξ_2 with respect to the R-cycle. There exists a transverse coordinate x_γ at ξ_b for which $\psi_{2,b}$ maps the (x_1, x_i)-face into the (x_1, x_γ)-face. The image of the curve $x_i = x_1^{\frac{c_{2i}}{c_{21}}}$ under $\psi_{2,b}$ yieds the curve $x_\gamma = x_1^{\frac{c_{2i}}{c_{21}}}$.

We restrict the local map $\phi_{2,b,d}$ in (4.14) to the (x_1, x_γ)-face so that it returns values in the (x_2, x_γ)-face and

$$\phi_{2,b,d}(y_1, y_\gamma) = \left(y_1^{\frac{c_{b2}}{e_{b1}}}, y_\gamma y_1^{\frac{c_{b\gamma}}{e_{b1}}}\right) = (u_2, u_\gamma).$$

In the local coordinates near ξ_b the (x_1, x_γ)-face in $H_b^{in,2}$ is expressed as the (y_1, y_γ)-face and the (x_2, x_γ)-face in $H_b^{out,d}$ is expressed as the (u_2, u_γ)-face. The curve $x_\gamma = x_1^{\frac{c_{2i}}{c_{21}}}$ is mapped by $\phi_{2,b,d}$ into the parametric curve

$$\phi_{2,b,d}\left(y_1, y_1^{\frac{c_{2i}}{c_{21}}}\right) = \left(y_1^{\frac{c_{b2}}{e_{b1}}}, y_1^{\frac{c_{2i}}{c_{21}} + \frac{c_{b\gamma}}{e_{b1}}}\right)$$

leading to

$$\begin{cases} y_1^{\frac{c_{b2}}{e_{b1}}} = u_2 \\ y_1^{\frac{c_{2i}}{c_{21}} + \frac{c_{b\gamma}}{e_{b1}}} = u_\gamma \end{cases} \Leftrightarrow \begin{cases} y_1 = u_2^{\frac{e_{b1}}{c_{b2}}} \\ \text{———} \end{cases} \Leftrightarrow \begin{cases} \text{———} \\ u_2^{\frac{e_{b1}}{c_{b2}}\frac{c_{2i}}{c_{21}} + \frac{c_{b\gamma}}{c_{b2}}} = u_\gamma. \end{cases}$$

On the other hand, the (y_1, y_γ)-face is delimited by four edges: $(0, y_\gamma)$, $(y_1, 0)$, $(1, y_\gamma)$, $(y_1, 1)$. In determining their images under $\phi_{2,b,d}$

$$\phi_{2,b,d}(0, y_\gamma) = (0,0), \qquad \phi_{2,b,d}(y_1, 0) = \left(y_1^{\frac{c_{b2}}{e_{b1}}}, 0\right),$$

$$\phi_{2,b,d}(1, y_\gamma) = (1, y_\gamma), \qquad \phi_{2,b,d}(y_1, 1) = \left(y_1^{\frac{c_{b2}}{e_{b1}}}, y_1^{\frac{c_{b\gamma}}{e_{b1}}}\right),$$

we find that the edge $(y_1, 1)$ is transformed into the curve

$$\begin{cases} y_1^{\frac{c_{b2}}{e_{b1}}} = u_2 \\ y_1^{\frac{c_{b\gamma}}{e_{b1}}} = u_\gamma \end{cases} \Leftrightarrow \begin{cases} y_1 = u_2^{\frac{e_{b1}}{c_{b2}}} \\ \text{———} \end{cases} \Leftrightarrow \begin{cases} \text{———} \\ u_2^{\frac{c_{b\gamma}}{c_{b2}}} = u_\gamma. \end{cases}$$

(c) The (x_1, x_β)-face is mapped by $\psi_{2,b}$ into the (x_1, x_δ)-face where x_δ is some transverse coordinate at ξ_b. The rest of the proof runs as before.

□

Example 4.3.2. By construction, all heteroclinic connections in the Bowtie network in Figure 4.16 are of type contracting-to-expanding. Global maps coincide with the identity so that $H_j^{out,k}$ can be freely identified with $H_k^{in,j}$ (recall Proposition 4.1.10). The sets $F_{1,2,3}$ and $F_{5,2,3}$ separate $H_2^{out,3}$ into points leaving $H_2^{in,1}$ from points leaving $H_2^{in,5}$; these are divided by the surface $x_5 = x_1^{\frac{c_{25}}{c_{21}}}$. The transition $\phi_{2,3,1} \circ \psi_{2,3} : H_2^{out,3} \to H_3^{out,1}$ equates to $\tilde{g}_3 : H_3^{in,2} \to H_1^{in,3}$ where $H_2^{out,3} \equiv H_3^{in,2} = \{(x_1, x_4, x_5)\}$ and $H_3^{out,1} \equiv H_1^{in,3} = \{(x_2, x_4, x_5)\}$. See Appendix C.1 for the maps near the Bowtie network.

Each square $[ABCD]$ on the intersection of $H_2^{out,3}$ with a plane $x_1 = k$ for a constant $k < 1$ is shrunk by $\phi_{2,3,1} \circ \psi_{2,3}$ into another square $[A'B'C'D']$ on the plane $x_2 = k'$, see Figure 4.17 (a) and (b).

Each square $[EFGH]$ on the intersection of $H_2^{out,3}$ with a plane $x_4 = k$ for a constant $k < 1$ is transformed by $\phi_{2,3,1} \circ \psi_{2,3}$ into a cuspoidal surface $[E'F'G']$, see Figure 4.17 (c) and (d).

From the point of view of the R-cycle the transverse directions at ξ_2 are spanned by x_4 and x_5. We show that a visit to the R-cycle through $\phi_{2,3,1} \circ \psi_{2,3}$ ends up in the origin of $H_3^{out,1}$ for any initial condition in the boundary face $(0, x_4, x_5)$ of $H_2^{out,3}$ contained in the plane $x_1 = 0$. In general, the whole

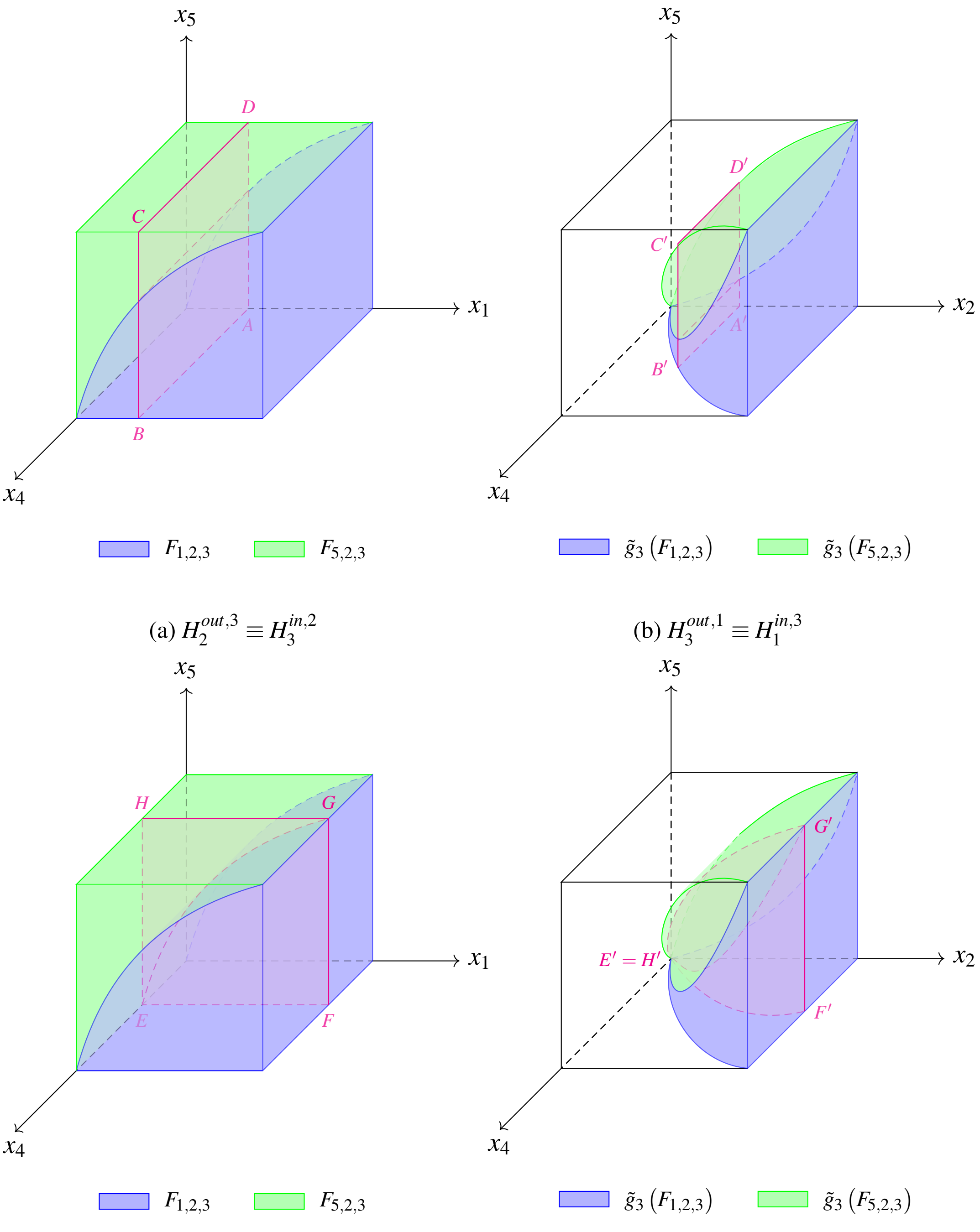

(a) $H_2^{out,3} \equiv H_3^{in,2}$

(b) $H_3^{out,1} \equiv H_1^{in,3}$

(c) $H_2^{out,3} \equiv H_3^{in,2}$

(d) $H_3^{out,1} \equiv H_1^{in,3}$

Fig. 4.17 Transformation of the F-sets near ξ_2 under $\phi_{2,3,1} \circ \psi_{2,3} \equiv \tilde{g}_3 : H_3^{in,2} \to H_1^{in,3}$ for the R-cycle in the Bowtie network: the set $F_{1,2,3}$ of points coming from ξ_1 and the $F_{5,2,3}$ of points coming from ξ_5 on the left side, and their images under $\tilde{g}_3$ on the right side. (a) and (b) each square $[ABCD]$ on $x_1 = k$ is shrunk and transformed into another square $[A'B'C'D']$; (c) and (d) each square $[EFGH]$ on $x_4 = k$ is shrunk and transformed into a cuspoidal surface $E'F'G'$.

$H_2^{out,3} \equiv H_3^{in,2}$ becomes a topological cone-shaped region fixed to the origin in $H_3^{out,1} \equiv H_1^{in,3}$, and the remaining conclusions of Lemma 4.3.1 follow.

Lemma 4.3.3. *Let X be a heteroclinic network in $\mathbb{R}^n$ composed of two quasi-simple heteroclinic cycles R and L with sequences $[\xi_a \to \xi_1 \to \xi_2 \to \xi_b \to \xi_d]$ and $[\xi_\alpha \to \xi_2 \to \xi_\beta]$. Suppose that both R- and L-cycles satisfy Assumptions 3.1.4, 3.2.1 and 4.1.4. Suppose that*

(i) x_i is a transverse coordinate at ξ_2 with respect to the R-cycle;

(ii) x_d is the expanding coordinate at ξ_b with respect to the R-cycle;

(iii) the heteroclinic connection $\kappa_{2,b}$ is of type contracting-to-transverse.

The image of $F_{1,2,b}$ in (4.10) *under $\phi_{2,b,d} \circ \psi_{2,b}$ is such that:*

(a) for every $x_i \neq x_d$ the (x_1, x_i)-face is mapped into the origin of $\mathbb{R}^{n-2}$.

(b) for $x_i = x_d$ the cuspoidal region bounded by the curve $x_d = x_1^{\frac{c_{2d}}{c_{21}}}$ and the edges $x_1 = 1$ and $x_d = 0$ in the (x_1, x_d)-face is mapped into the conic region bounded by the curves $x_2 = x_\gamma^{\frac{e_{bd}}{c_{b2}}\frac{c_{21}}{c_{2d}}+\frac{c_{b\gamma}}{c_{b2}}}$ and $x_2 = x_\gamma^{\frac{c_{b\gamma}}{c_{b2}}}$ in the (x_2, x_γ)-face for some transverse coordinate x_γ at ξ_b.

Proof. Assume that $\kappa_{2,b}$ is a contracting-to-transverse connection. The expanding direction x_d at ξ_b thus spans a transverse direction at ξ_2 regarding the R-cycle.

(a) When $x_i \neq x_d$ there are transverse coordinates $x_{\gamma_1}, x_{\gamma_2} \neq x_i$ at ξ_b such that $\psi_{2,b} : H_2^{out,b} \to H_b^{in2}$ assigns axis by axis the (x_1, x_i, x_d)-subspace to the $(x_{\gamma_1}, x_{\gamma_2}, x_d)$-subspace. On substituting e_{b1} with e_{bd} in (4.13) the local coordinate y_1 near ξ_2 agrees with x_d. Because the (x_1, x_i)-face in $H_2^{out,b}$ lies in the hyperplane $x_d = 0$ the $(x_{\gamma_1}, x_{\gamma_2})$-face in $H_b^{in,2}$ lies in the hyperplane $x_d = 0$ by virtue of the form of $\psi_{2,b}$. We apply $\phi_{2,b,d} : H_b^{in,2} \to H_b^{out,d}$ and the $(x_{\gamma_1}, x_{\gamma_2})$-face is further mapped into the origin of $\mathbb{R}^{n-2}$.

(b) Suppose that $x_i = x_d$. Now $\psi_{2,b}$ maps the (x_1, x_d)-face into the (x_γ, x_d)-face where x_γ is some transverse coordinate at ξ_b. Restricting to these faces the curve $x_d = x_1^{\frac{c_{2d}}{c_{21}}}$ and the edges $x_1 = 1$ and $x_d = 0$ in $H_2^{out,b}$ become $x_d = x_\gamma^{\frac{c_{2d}}{c_{21}}}$, $x_\gamma = 1$ and $x_d = 0$ in $H_b^{in,2}$, respectively. The restriction of $\phi_{2,b,d}$ to the (x_d, x_γ)-face is in turn recovered from (4.14) replacing e_{b1} by e_{bd}. The (x_d, x_γ)-face in $H_b^{in,2}$ is equipped with the local coordinates (y_1, y_γ). We calculate the image of the curve $x_d = x_\gamma^{\frac{c_{2d}}{c_{21}}}$ under $\phi_{2,b,d}$ by means of

$$\phi_{2,b,d}\left(y_\gamma^{\frac{c_{2d}}{c_{21}}}, y_\gamma\right) = \left(y_\gamma^{\frac{c_{2d}}{c_{21}}\frac{c_{b2}}{e_{bd}}}, y_\gamma^{1+\frac{c_{2d}}{c_{21}}\frac{c_{b\gamma}}{e_{bd}}}\right) = (u_2, u_\gamma).$$

Coordinates (u_2, u_γ) parameterise locally the (x_2, x_γ)-face in $H_b^{out,d}$ and we obtain the curve

$$\begin{cases} y_\gamma^{\frac{c_{b2}}{e_{bd}}\frac{c_{2d}}{c_{21}}} = u_2 \\ y_\gamma^{1+\frac{c_{b\gamma}}{e_{bd}}\frac{c_{2d}}{c_{21}}} = u_\gamma \end{cases} \Leftrightarrow \begin{cases} y_\gamma = u_2^{\frac{e_{bd}}{c_{b2}}\frac{c_{21}}{c_{2d}}} \\ \rule{4em}{0.4pt} \end{cases} \Leftrightarrow \begin{cases} \rule{4em}{0.4pt} \\ u_2^{\frac{e_{bd}}{c_{b2}}\frac{c_{21}}{c_{2d}}+\frac{c_{b\gamma}}{c_{b2}}} = u_\gamma. \end{cases}$$

In the same manner the edges $x_d = 0$ and $x_\gamma = 1$ are transformed by $\phi_{2,b,d}$ into

$$\phi_{2,b,d}\left(0, y_\gamma\right) = (0,0) \quad \text{and} \quad \phi_{2,b,d}\left(y_1, 1\right) = \left(y_1^{\frac{c_{b2}}{e_{bd}}}, y_1^{\frac{c_{b\gamma}}{e_{bd}}}\right),$$

the last equality resulting in the curve

$$\begin{cases} y_1^{\frac{c_{b2}}{e_{bd}}} = u_2 \\ y_1^{\frac{c_{b\gamma}}{e_{bd}}} = u_\gamma \end{cases} \Leftrightarrow \begin{cases} y_1 = u_2^{\frac{e_{bd}}{c_{b2}}} \\ \text{———} \end{cases} \Leftrightarrow \begin{cases} \text{———} \\ u_2^{\frac{c_{b\gamma}}{c_{b2}}} = u_\gamma. \end{cases}$$

□

Remark 4.3.4. Lemmas 4.3.1 and 4.3.3 apply analogously if we replace the heteroclinic connection $\kappa_{2,b}$ by the heteroclinic connection $\kappa_{2,\beta}$ with respect to the L-cycle. They can also be reformulated in order to describe what happens to $F_{\alpha,2,b}$ in $H_2^{out,b}$ when it is similarly transformed under $\phi_{2,b,d} \circ \psi_{2,b}$.

Consider a set $D \subset \mathbb{R}^n$ and a map $g : D \to \mathbb{R}^n$. For $A \subset D$ and $B \subset g(D)$ we define

$$\begin{aligned} g^*(A) &= \left\{\boldsymbol{x} \in \mathbb{R}^n : \ g^{-1}(\boldsymbol{x}) \in A\right\} \\ \left(g^{-1}\right)^*(B) &= \{\boldsymbol{x} \in \mathbb{R}^n : \ g(\boldsymbol{x}) \in B\} \end{aligned}$$

such that $g(A) = g(D) \cap g^*(A)$ and $g^{-1}(B) = D \cap \left(g^{-1}\right)^*(B)$.

Set $\tilde{g}_j = \psi_{j,k} \circ \phi_{i,j,k} : H_j^{in,i} \to H_k^{in,j}$ for the pairwise composite maps concerning the R-cycle.

Corollary 4.3.5. *Let R be a quasi-simple heteroclinic cycle in $\mathbb{R}^n$ fulfilling Assumption 3.2.1. The domain and the range of definition for the map $\tilde{g}_j$ are given by the sets $C_{i,j,k}$ and $\psi_{j,k}\left(F_{i,j,k}\right)$, respectively.*

Proof. Consider the global map $\psi_{j,k} : H_j^{out,k} \to H_k^{in,j}$ for which Assumption 3.2.1 is true. Therefore the domain and the range of $\psi_{j,k}$ are respectively the whole cross sections $H_j^{out,k}$ and $H_k^{in,j}$. Composing $\psi_{j,k}$ after $\phi_{i,j,k} : H_j^{in,i} \to H_j^{out,k}$ we have that the domain of $\tilde{g}_j$ is

$$\begin{aligned} \operatorname{dom}(\tilde{g}_j) &= \operatorname{dom}\left(\phi_{i,j,k}\right) \cap \left(\phi_{i,j,k}^{-1}\right)^* \left(\operatorname{dom}\left(\psi_{j,k}\right)\right) \\ &= C_{i,j,k} \cap \left(\phi_{i,j,k}^{-1}\right)^* \left(H_j^{out,k}\right) \\ &= C_{i,j,k}. \end{aligned}$$

The range of $\tilde{g}_j$ is

$$\begin{aligned} \operatorname{im}(\tilde{g}_j) &= \operatorname{im}\left(\psi_{j,k}\right) \cap \psi_{j,k}^*\left(\operatorname{im}\left(\phi_{i,j,k}\right)\right) \\ &= H_k^{in,j} \cap \psi_{j,k}^*\left(F_{i,j,k}\right) \\ &= \psi_{j,k}\left(F_{i,j,k}\right). \end{aligned}$$

□

The return map $\pi_R : H_2^{in,1} \to H_2^{in,1}$ around the R-cycle can be written as $\pi_R = \tilde{g}_1 \circ \tilde{g}_a \circ \cdots \circ \tilde{g}_b \circ \tilde{g}_2$. Assuming that all transverse eigenvalues are negative whenever possible, the domain of definition C_R

of the map π_R coincides with $C_{1,2,b}$ in (4.3). We call F_R to the range of π_R. Although the shape of the set F_R may depend on the type of heteroclinic connections (see Figures 4.18 and 6.5) we find that it has in general a topological cone-shaped form with its apex at the origin.

Lemma 4.3.6. *Let X be a heteroclinic network in $\mathbb{R}^n$ composed of two quasi-simple heteroclinic cycles R and L with sequences $[\xi_a \to \xi_1 \to \xi_2 \to \xi_b \to \xi_d]$ and $\left[\xi_\alpha \to \xi_2 \to \xi_\beta\right]$. Suppose that the R-cycle satisfies Assumptions 3.1.4, 3.2.1 and 4.1.4. Then, the origin in $\mathbb{R}^{n-2}$ belongs to the boundary of F_R.*

Proof. By definition of π_R it follows that

$$F_R = (\tilde{g}_1 \circ \tilde{g}_a \circ \cdots \circ \tilde{g}_b)(\mathrm{im}(\tilde{g}_2)) = \mathrm{im}(\tilde{g}_1) \cap \tilde{g}_1^*(\mathrm{im}(\tilde{g}_a)) \cap \cdots \cap (\tilde{g}_1 \circ \tilde{g}_a \circ \cdots \circ \tilde{g}_b)^*(\mathrm{im}(\tilde{g}_2)).$$

We begin by proving the claim for $\mathrm{im}(\tilde{g}_1)$, i.e the range of $\tilde{g}_1$. Corollary 4.3.5 states that $\mathrm{im}(\tilde{g}_1)$ equals $\psi_{1,2}(F_{a,1,2})$. From (4.11) the set $F_{a,1,2}$ contains the origin of $\mathbb{R}^{n-2}$ in its boundary around the x_a-axis in $H_1^{out,2}$. Since $\psi_{1,2} : H_1^{out,2} \to H_2^{in,1}$ can be simply regarded as a permutation of the local coordinate axes in $H_1^{out,2}$, the set $\psi_{1,2}(F_{a,1,2})$ also contains the origin of $\mathbb{R}^{n-2}$ in its boundary around the image of the x_a-axis under $\psi_{1,2}$ in $H_2^{in,1}$.

The same reasoning applies to $\mathrm{im}(\tilde{g}_j)$ for every j. Regardless of the type of the heteroclinic connection we deduce from Lemmas 4.3.1 and 4.3.3 that the origin belongs to the boundary of $\tilde{g}_{j+1}(\mathrm{im}(\tilde{g}_j)) = \mathrm{im}(\tilde{g}_{j+1}) \cap \tilde{g}_{j+1}^*(\mathrm{im}(\tilde{g}_j))$. We proceed by induction on consecutive nodes of the heteroclinic cycle. Assume that the claim holds for some k with

$$\left(\tilde{g}_{j+k} \circ \tilde{g}_{j+k-1} \circ \cdots \circ \tilde{g}_{j+1}\right)(\mathrm{im}(\tilde{g}_j)).$$

Then,

$$\left(\tilde{g}_{j+k+1} \circ \tilde{g}_{j+k} \circ \cdots \circ \tilde{g}_{j+1}\right)(\mathrm{im}(\tilde{g}_j)) = \tilde{g}_{j+k+1}\left[\left(\tilde{g}_{j+k} \circ \tilde{g}_{j+k-1} \circ \cdots \circ \tilde{g}_{j+1}\right)(\mathrm{im}(\tilde{g}_j))\right].$$

Combining the induction hypothesis and Lemmas 4.3.1 and 4.3.3 the claim also holds for $k+1$. □

Example 4.3.7. Consider the transitions near the Bowtie network detailed in Appendix C.1. The return map $\pi_R : H_2^{in,1} \to H_2^{in,1}$ around the R-cycle coincides with $\tilde{\pi}_2 = \tilde{g}_1 \circ \tilde{g}_3 \circ \tilde{g}_2$ for which $\tilde{g}_j = \psi_{j,j+1} \circ \phi_{j-1,j,j+1} : H_j^{in,j-1} \to H_{j+1}^{in,j}$, $j = 1,2,3 \pmod 3$. We write $F_{j-1,j,j+1}$ instead of $\psi_{j,j+1}(F_{j-1,j,j+1})$ because the global maps $\psi_{j,j+1}$ are the identity. We check at once that

$$F_R = (\tilde{g}_1 \circ \tilde{g}_3)(F_{1,2,3}) = F_{3,1,2} \cap \tilde{g}_1^*(F_{2,3,1}) \cap (\tilde{g}_1 \circ \tilde{g}_3)^*(F_{1,2,3})$$

where

$$F_{3,1,2} = \left\{ (x_3, x_4, x_5) \in H_2^{in,1} : x_4 < x_3^{\frac{c_{14}}{c_{13}}} \text{ and } x_5 < x_3^{\frac{c_{15}}{c_{13}}} \right\}$$

$$\tilde{g}_1^*(F_{2,3,1}) = \left\{ (x_3, x_4, x_5) \in H_2^{in,1} : x_4 < x_3^{\frac{c_{14}}{c_{13}} + \frac{e_{12}}{c_{13}}\frac{c_{34}}{c_{32}}} \text{ and } x_5 < x_3^{\frac{c_{15}}{c_{13}} + \frac{e_{12}}{c_{13}}\frac{c_{35}}{c_{32}}} \right\}$$

$$(\tilde{g}_1 \circ \tilde{g}_3)^*(F_{1,2,3}) = \left\{ (x_3, x_4, x_5) \in H_2^{in,1} : x_5 < x_3^{\frac{c_{15}}{c_{13}} + \frac{e_{12}}{c_{13}}\frac{c_{35}}{c_{32}} + \frac{e_{12}}{c_{13}}\frac{e_{31}}{c_{32}}\frac{c_{25}}{c_{21}}} \right\}$$

leading to

$$F_R = \left\{ (x_3, x_4, x_5) \in H_2^{in,1} : x_4 < x_3^{\frac{c_{14}}{c_{13}} + \frac{e_{12}}{c_{13}} \frac{c_{34}}{c_{32}}} \text{ and } x_5 < x_3^{\frac{c_{15}}{c_{13}} + \frac{e_{12}}{c_{13}} \frac{c_{35}}{c_{32}} + \frac{e_{12}}{c_{13}} \frac{e_{31}}{c_{32}} \frac{c_{25}}{c_{21}}} \right\}. \tag{4.15}$$

Given the parameters in (C.7) we can simplify

$$\frac{c_{14}}{c_{13}} + \frac{e_{12}}{c_{13}} \frac{c_{34}}{c_{32}} = \frac{\tilde{\nu} + \frac{e_{23}}{e_{24}}}{\tilde{\rho}} \quad \text{and} \quad \frac{c_{15}}{c_{13}} + \frac{e_{12}}{c_{13}} \frac{c_{35}}{c_{32}} + \frac{e_{12}}{c_{13}} \frac{e_{31}}{c_{32}} \frac{c_{25}}{c_{21}} = \frac{\tilde{\mu}}{\tilde{\rho}}.$$

Figure 4.18 illustrates the inequalities constraining the set F_R. Its boundary is delimited by branches of cuspoidal surfaces typically attached to the origin. The interior surrounds the image of the contracting axis at ξ_1 under $\psi_{1,2}$, here the x_3-axis, when extended to negative coordinates.

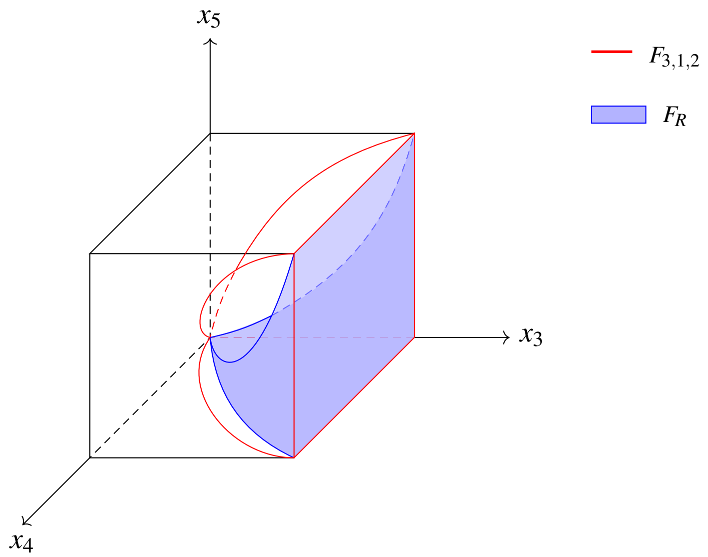

Fig. 4.18 The set F_R in $H_2^{in,1}$ for the Bowtie network.

Lemma 4.3.8. *Let X be a heteroclinic network in $\mathbb{R}^n$ composed of two heteroclinic cycles R and L with sequences $[\xi_1 \to \xi_2 \to \xi_b]$ and $[\xi_\alpha \to \xi_2 \to \xi_\beta]$. Suppose that $\pi_R : H_2^{in,1} \to H_2^{in,1}$ is the return map around R. If the domain C_R of π_R is mapped into itself, that is $F_R \subseteq C_R$, then there is no switching along R.*

Proof. Assume that $\pi_R = \tilde{g}_1 \circ \cdots \circ \tilde{g}_b \circ \tilde{g}_2$. The cross section $H_2^{out,b}$ is split into the set of points $F_{1,2,b}$ coming from ξ_1 and the set of points $F_{\alpha,2,b}$ coming from ξ_α. The cross section $H_2^{in,1}$ is split into the set of points $C_{1,2,b}$ going to ξ_b and the set of points $C_{1,2,\beta}$ going to ξ_β. We have now to look how $F_{i,2,b}$, $i = 1, \alpha$, are sent to $H_2^{in,1}$. This is described by the composition $(\tilde{g}_1 \circ \cdots \circ \tilde{g}_b)(\psi_{2,b}(F_{i,2,b}))$. We have defined $C_R = C_{1,2,b}$ and so $F_R = (\tilde{g}_1 \circ \cdots \circ \tilde{g}_b)(\psi_{2,b}(F_{1,2,b}))$. Because $F_R \subseteq C_R$ it implies $F_R \cap C_{1,2,\beta} = \emptyset$, which inhibits switching along the R-cycle. □

Example 4.3.9. For the Bowtie network, switching along the R-cycle occurs if and only if $\tilde{g}_1 \circ \tilde{g}_3 (F_{i,2,3}) \cap C_{1,2,k} \neq \emptyset$ with $i = 1, 5$ and $k = 3, 4$. The sets $C_{1,2,3}$ and $\tilde{g}_1 \circ \tilde{g}_3 (F_{1,2,3})$ correspond respectively to the domain C_R and the range F_R of the return map $\pi_R \equiv \tilde{\pi}_2 = \tilde{g}_1 \circ \tilde{g}_3 \circ \tilde{g}_2$ around R. From Appendix C.1 we derive

$$C_{1,2,3} = \left\{ (x_3, x_4, x_5) \in H_2^{in,1} : x_4 < x_3^{\frac{e_{24}}{e_{23}}} \right\} (= C_R)$$
$$C_{1,2,4} = \left\{ (x_3, x_4, x_5) \in H_2^{in,1} : x_3 < x_4^{\frac{e_{23}}{e_{24}}} \right\}.$$

Together with (4.15) gives

$$\tilde{g}_1 \circ \tilde{g}_3 \left(F_{1,2,3}\right) \cap C_{1,2,3} = \left\{ (x_3, x_4, x_5) \in H_2^{in,1} : x_4 < \min \left\{ x_3^{\frac{\tilde{\nu} + \frac{e_{23}}{e_{24}}}{\tilde{\rho}}}, x_3^{\frac{e_{24}}{e_{23}}} \right\} \text{ and } x_5 < x_3^{\frac{\tilde{\mu}}{\tilde{\rho}}} \right\}$$
$$\tilde{g}_1 \circ \tilde{g}_3 \left(F_{1,2,3}\right) \cap C_{1,2,4} = \left\{ (x_3, x_4, x_5) \in H_2^{in,1} : x_3^{\frac{e_{24}}{e_{23}}} < x_4 < x_3^{\frac{\tilde{\nu} + \frac{e_{23}}{e_{24}}}{\tilde{\rho}}} \text{ and } x_5 < x_3^{\frac{\tilde{\mu}}{\tilde{\rho}}} \right\}.$$

It follows that $F_R \subseteq C_R$, i.e $\tilde{g}_1 \circ \tilde{g}_3 \left(F_{1,2,3}\right) \subseteq C_{1,2,3}$, provided

$$\begin{aligned} x_3^{\frac{\tilde{\nu} + \frac{e_{23}}{e_{24}}}{\tilde{\rho}}} < x_3^{\frac{e_{24}}{e_{23}}} &\Leftrightarrow \tilde{\nu} + \frac{e_{23}}{e_{24}} > \frac{e_{24}}{e_{23}} \tilde{\rho} \\ &\Leftrightarrow 0 > \frac{e_{23}}{e_{24}} (\tilde{\rho} - 1) - \tilde{\nu} = -\frac{c_{21}}{e_{23}} \tilde{\delta} \\ &\Leftrightarrow \tilde{\delta} > 0. \end{aligned}$$

Under this inequality $\tilde{g}_1 \circ \tilde{g}_3 \left(F_{1,2,3}\right) \cap C_{1,2,4} = \emptyset$, and the absence of switching along the R-cycle is ensured. An equivalent formulation is to say:

Lemma 4.3.10. *There is switching along each heteroclinic cycle in the Bowtie network if and only if* $\tilde{\delta}, \delta < 0$.

Proof. Based on previous considerations about the R-cycle we have seen $\tilde{g}_1 \circ \tilde{g}_3 \left(F_{1,2,3}\right) \cap C_{1,2,k} \neq \emptyset$, $k = 3, 4$ as long as $\tilde{\delta} < 0$. The respective proof is completed by showing that the same conclusion is true for $\tilde{g}_1 \circ \tilde{g}_3 \left(F_{5,2,3}\right) \cap C_{1,2,k}$. Accordingly,

$$\tilde{g}_1 \circ \tilde{g}_3 \left(F_{5,2,3}\right) = F_{3,1,2} \cap \tilde{g}_1^* \left(F_{2,3,1}\right) \cap \left(\tilde{g}_1 \circ \tilde{g}_3\right)^* \left(F_{5,2,3}\right).$$

We determine

$$\left(\tilde{g}_1 \circ \tilde{g}_3\right)^* \left(F_{5,2,3}\right) = \left\{ (x_3, x_4, x_5) \in H_2^{in,1} : x_3^{\frac{\tilde{\mu}}{\tilde{\rho}}} < x_5 < x_3^{\frac{\tilde{\mu} - \frac{c_{25}}{e_{23}}}{\tilde{\rho}}} \right\}$$

so that

$$\tilde{g}_1 \circ \tilde{g}_3 \left(F_{5,2,3}\right) = \left\{ (x_3, x_4, x_5) \in H_2^{in,1} : x_4 < x_3^{\frac{\tilde{\nu} + \frac{e_{23}}{e_{24}}}{\tilde{\rho}}} \text{ and } x_3^{\frac{\tilde{\mu}}{\tilde{\rho}}} < x_5 < x_3^{\frac{\tilde{\mu} - \frac{c_{25}}{e_{23}}}{\tilde{\rho}}} \right\}.$$

The condition that establishes whether or not the intersection $\tilde{g}_1 \circ \tilde{g}_3 \left(F_{5,2,3}\right) \cap C_{1,2,k}$ is empty is exactly the one for $\tilde{g}_1 \circ \tilde{g}_3 \left(F_{1,2,3}\right) \cap C_{1,2,k}$, $k = 3, 4$. $\square$

The result improves Lemma 4.1 in [19] that suggests the existence of switching along each heteroclinic cycle in the Bowtie network regardless of the parameter values.

4.4 Infinite switching

Infinite switching is characterised by shadowing all possible heteroclinic paths on a heteroclinic network. We investigate the (in)existence of infinite switching near the heteroclinic networks that have been a subject of study throughout this chapter and, more generally, near an arbitrary heteroclinic network involving equilibria whose linearisation satisfies Assumption 3.1.4. To this end we identify the stability properties for which *visible* switching dynamics may prevail. By visible we mean there exists a positive Lebesgue measure set of nearby initial conditions on a section transverse to the heteroclinic network exhibiting switching. This description intends to enhance the pratical effects of switching capable of being observed in numerical experiments.

Corollary 4.4.1. *Let X be a heteroclinic network in $\mathbb{R}^n$ and $C \subset X$ a quasi-simple heteroclinic cycle. If X is c.u, then C is c.u.*

Proof. Suppose that X is c.u. Remark 2.4.5 asserts that $\sigma_{\text{loc}}(X,x) = -\infty$ for all $x \in X$. Since $C \subset X$, $\sigma_{\text{loc}}(X,x) = -\infty$ for all $x \in C$. Therefore $\sigma_{\text{loc}}(C,x) = -\infty$ for all $x \in C$ by Lemma 2.4.6. From Corollary 3.4.13 we deduce that C is c.u. □

Lemma 4.4.2. *Let X be a heteroclinic network in $\mathbb{R}^n$. If X is c.u, then there is no infinite switching near X almost everywhere.*

Proof. Suppose that X is c.u. By definition, there are a neighbourhood V of X and a set D with $\ell(D) = 0$ such that all trajectories starting in $V \setminus D$ leave V from some positive time onwards. As trajectories do not stay near X any longer they can not follow every feasible heteroclinic path. □

Lemma 4.4.3. *Let X be a heteroclinic network in $\mathbb{R}^n$ and $C \subset X$ a heteroclinic cycle. If C is c.u, then there is no infinite switching near X almost everywhere.*

Proof. Since C is c.u. there are a neighbourhood U of C and a set D with $\ell(D) = 0$ such that no trajectory starting in $U \setminus D$ remains in U from some positive time onwards. Take a neighbourhood V of X such that $U \subset V$. The heteroclinic path described by infinite turns around C is not followed by any trajectory with initial condition on V. This excludes infinite switching. □

What is left is to show that infinite switching does not occur near a f.a.s heteroclinic network whose heteroclinic cycles are f.a.s. Recover now Figure 4.15 where the common element between the L- and the R-cycle is reduced to a node.

Theorem 4.4.4. *Let ξ_2 be a common node between two heteroclinic cycles R and L constituting a heteroclinic network X in $\mathbb{R}^n$. Suppose that Assumption 3.1.4 holds. If both R- and L-cycles are f.a.s, then there is no infinite switching near X almost everywhere.*

Proof. Suppose that the R- and L-cycles are f.a.s. Now X is either c.u or f.a.s. By Lemma 4.4.2 the assertion follows immediately when X is c.u. We then assume that X is f.a.s. The procedure is to find a heteroclinic path and a neighbourhood V of X such that any trajectory does not follow it in V.

Consider the return map $\pi_R : H_2^{in,1} \to H_2^{in,1}$ around the R-cycle as in (4.12). Recall that its domain of definition is denoted by C_R. We write the set of points taking at least $k \in \mathbb{N}$ turns around R as

$$\tilde{\mathscr{E}}_k = \left\{ \mathbf{y} \in H_2^{in,1} : \mathbf{y} \in \mathrm{dom}\left(\pi_R^{k-1}\right) \text{ and } \pi_R^{k-1}(\mathbf{y}) \in C_R \right\} \tag{4.16}$$

It is easy to check that $\tilde{\mathscr{E}}_k$ coincides with the domain of definition of the iterate π_R^k and $\tilde{\mathscr{E}}_{k+1} \subseteq \tilde{\mathscr{E}}_k$ for all $k \in \mathbb{N}$. In particular, $\tilde{\mathscr{E}}_1 = C_R$.

Let $\pi_{RL} : H_2^{in,1} \to H_2^{in,\alpha}$ be the map modelling the dynamics of trajectories that visit the L-cycle from a neighbourhood of the R-cycle, see Figure 4.19. We call C_{RL} the set of points in $H_2^{in,1}$ for which π_{RL} is well defined. Since trajectories that get lost once they hit $H_2^{in,1}$ are not relevant here we can assume that $C_{RL} = H_2^{in,1} \setminus C_R$. For each $k \in \mathbb{N}$, the set $\tilde{\mathscr{E}}_k \setminus \tilde{\mathscr{E}}_{k+1}$ corresponds to the domain of definition of $\pi_{RL} \circ \pi_R^k$. Indeed,

$$\begin{aligned}
\mathbf{y} \in \tilde{\mathscr{E}}_k \setminus \tilde{\mathscr{E}}_{k+1} &\Leftrightarrow \mathbf{y} \in \tilde{\mathscr{E}}_k \text{ and } \mathbf{y} \notin \tilde{\mathscr{E}}_{k+1} \\
&\Leftrightarrow \mathbf{y} \in \mathrm{dom}\left(\pi_R^k\right) \text{ and } \pi_R^k(\mathbf{y}) \in H_2^{in,1} \setminus C_R \\
&\Leftrightarrow \mathbf{y} \in \mathrm{dom}\left(\pi_R^k\right) \text{ and } \pi_R^k(\mathbf{y}) \in C_{RL} \\
&\Leftrightarrow \mathbf{y} \in \mathrm{dom}\left(\pi_{RL} \circ \pi_R^k\right).
\end{aligned}$$

By construction, $\left(\tilde{\mathscr{E}}_k\right)_{k\in\mathbb{N}}$ is a nested decreasing sequence of sets and converges to

$$\lim_{k\to\infty} \tilde{\mathscr{E}}_k = \bigcap_{k=1}^{\infty} \tilde{\mathscr{E}}_k.$$

We can express

$$\bigcup_{k=1}^{\infty} \left(\tilde{\mathscr{E}}_k \setminus \tilde{\mathscr{E}}_{k+1}\right) = C_R \setminus \bigcap_{k=1}^{\infty} \tilde{\mathscr{E}}_k.$$

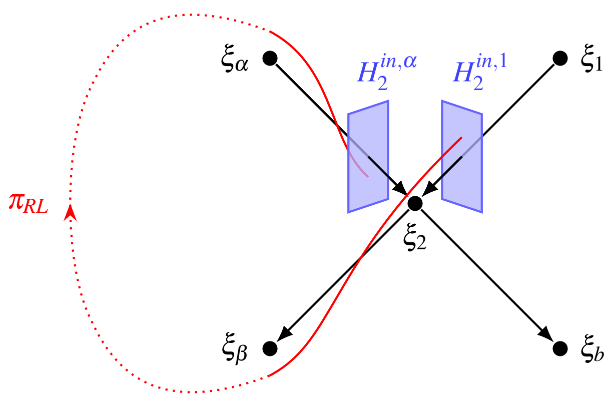

Fig. 4.19 The map π_{RL} from $H_2^{in,1}$ (near R) to $H_2^{in,\alpha}$ (near L).

Next we show that

$$\lim_{k\to\infty} \tilde{\mathscr{E}}_k \setminus \tilde{\mathscr{E}}_{k+1} = \emptyset.$$

Define

$$\liminf_{k\to\infty} \tilde{\mathscr{E}}_k \setminus \tilde{\mathscr{E}}_{k+1} = \bigcup_{k=1}^{\infty}\bigcap_{j=k}^{\infty} \tilde{\mathscr{E}}_j \setminus \tilde{\mathscr{E}}_{j+1}$$

$$\limsup_{k\to\infty} \tilde{\mathscr{E}}_k \setminus \tilde{\mathscr{E}}_{k+1} = \bigcap_{k=1}^{\infty}\bigcup_{j=k}^{\infty} \tilde{\mathscr{E}}_j \setminus \tilde{\mathscr{E}}_{j+1}.$$

The sets in $\left(\tilde{\mathscr{E}}_k \setminus \tilde{\mathscr{E}}_{k+1}\right)_{k\in\mathbb{N}}$ are mutually disjoint. It is immediate that for any $k \in \mathbb{N}$

$$\bigcap_{j=k}^{\infty} \tilde{\mathscr{E}}_j \setminus \tilde{\mathscr{E}}_{j+1} = \emptyset$$

and hence

$$\bigcup_{k=1}^{\infty}\bigcap_{j=k}^{\infty} \tilde{\mathscr{E}}_j \setminus \tilde{\mathscr{E}}_{j+1} = \emptyset.$$

On the other hand,

$$\bigcup_{j=k}^{\infty} \tilde{\mathscr{E}}_j \setminus \tilde{\mathscr{E}}_{j+1} = \tilde{\mathscr{E}}_k \setminus \bigcap_{i=1}^{\infty} \tilde{\mathscr{E}}_i$$

yielding

$$\bigcap_{k=1}^{\infty}\bigcup_{j=k}^{\infty} \tilde{\mathscr{E}}_j \setminus \tilde{\mathscr{E}}_{j+1} = \bigcap_{k=1}^{\infty}\left(\tilde{\mathscr{E}}_k \setminus \bigcap_{i=1}^{\infty} \tilde{\mathscr{E}}_i\right) = \left(\bigcap_{k=1}^{\infty} \tilde{\mathscr{E}}_k\right) \setminus \left(\bigcap_{i=1}^{\infty} \tilde{\mathscr{E}}_i\right) = \emptyset.$$

Then,

$$\liminf_{k\to\infty} \tilde{\mathscr{E}}_k \setminus \tilde{\mathscr{E}}_{k+1} = \limsup_{k\to\infty} \tilde{\mathscr{E}}_k \setminus \tilde{\mathscr{E}}_{k+1} = \emptyset.$$

The limit of $\left(\tilde{\mathscr{E}}_k \setminus \tilde{\mathscr{E}}_{k+1}\right)_{k\in\mathbb{N}}$ exists and equals

$$\lim_{k\to\infty} \tilde{\mathscr{E}}_k \setminus \tilde{\mathscr{E}}_{k+1} = \liminf_{k\to\infty} \tilde{\mathscr{E}}_k \setminus \tilde{\mathscr{E}}_{k+1} = \limsup_{k\to\infty} \tilde{\mathscr{E}}_k \setminus \tilde{\mathscr{E}}_{k+1} = \emptyset. \tag{4.17}$$

The proof falls naturally into two cases depending on the measure[6] of $\bigcap_{k=0}^{\infty} \tilde{\mathscr{E}}_k$. Accordingly, if $\ell\left(\bigcap_{k=1}^{\infty} \tilde{\mathscr{E}}_k\right) = 0$, the heteroclinic path moving infinite turns around R is not followed by trajectories with initial condition on $C_R \setminus \bigcap_{k=0}^{\infty} \tilde{\mathscr{E}}_k$. Otherwise, there is $k_0 \in \mathbb{N}$ such that $\ell\left(\bigcap_{k=1}^{\infty} \tilde{\mathscr{E}}_k\right) > 0$ together with (4.17) rule out the heteroclinic path that takes k_0 turns around the R-cycle before visiting the L-cycle. We thus choose the neighbourhood $\tilde{\mathscr{E}}_{k_0}$ provided $\tilde{\mathscr{E}}_{k_0} = \bigcap_{k=0}^{\infty} \tilde{\mathscr{E}}_k$ or else $\tilde{\mathscr{E}}_{k_0} \setminus \bigcap_{k=0}^{\infty} \tilde{\mathscr{E}}_k$. Figure 4.20 illustrates the accumulation of the sets $\tilde{\mathscr{E}}_k$ on the plane. Notice that every path of the form

$$\underbrace{R\cdots R}_{k_0+j}L\cdots$$

for $j \geq 1$ is not followed by any trajectory either.

□

[6]We refer $\ell(\cdot)$ to the Lebesgue measure in the appropriate context and dimension.

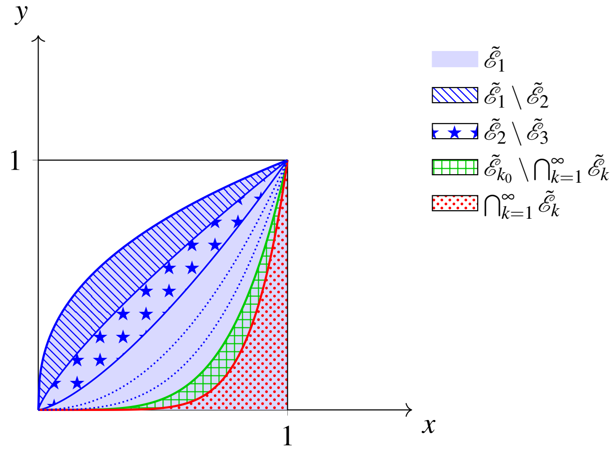

Fig. 4.20 Accumulation of the sets $\tilde{\mathscr{E}}_k$ as k tends to infinity.

Example 4.4.5. Proposition 4.3 in [19] asserts that infinite switching does not occur near the Bowtie network if $\tilde{\delta}, \delta < 0$. Sequences of visits turning infinitely many times around the same heteroclinic cycle are not followed by any trajectory with initial condition either in $C_R = \mathrm{dom}\,(\pi_R) \subset H_2^{in,1}$ or in $C_L = \mathrm{dom}\,(\pi_L) \subset H_2^{in,5}$. The proof consists of showing that $\bigcap_{k=1}^{\infty} \tilde{\mathscr{E}}_k = \bigcap_{k=1}^{\infty} \mathscr{E}_k = \emptyset$ where $\tilde{\mathscr{E}}_k = \mathrm{dom}\left(\pi_R^k\right)$ and $\mathscr{E}_k = \mathrm{dom}\left(\pi_L^k\right)$. But when $\tilde{\delta}, \delta < 0$ both heteroclinic cycles are c.u by virtue of Proposition 6.1.2. The result in question is further a direct consequence of Lemma 4.4.3.

Chapter 5

Cyclic dominance in a two-person Rock-Scissors-Paper game

[1]

The Rock-Scissors-Paper game (henceforth, RSP) has been used to understand competition issues in both economics and life sciences. In the context of one-person or population, it provides a good model for convergent and oscillating dynamics, the type being determined by the parameters. In life sciences, a classic example is that of the evolution of three color morphs of male side-blotched lizards *Uta Stansburiana*. See Sinervo and Lively [65]. In economics, market pricing drives a dynamic RSP game attempting to explain why prices vary among different sellers and over time. Cyclic dominance of prices are empirically reported by Noel [50, 51] in retail gasoline markets. Hopkins and Seymour [35] introduce the search behaviour of consumers and show its influence in the equilibrium price distribution. Accordingly, the evidence of price dispersion persists when the amount of information held by consumers is sufficiently small.

Social and economic dilemmas between consumers and sellers, or firms and workers are examples of strategic interactions where agents frequently adopt asymmetric positions. We are then interested in investigating cyclic dominance in a two-person parametrised RSP game and its application to price dispersion modelling. The parameters are the agents' payoffs when there is a tie. They range from the penalty for losing to the reward for winning. Asymptotic behaviour in the RSP version with two independent agents can be very complex. Numerical simulations by Sato et al. [64] provide various types of low-dimensional chaos due to the existence of a heteroclinic network. Aguiar and Castro [5] give the theoretical proof by reducing to the study of the dynamics near a heteroclinic network with three nodes in a suitable quotient space. This can be regarded as made of three or two heteroclinic cycles depending on convenient combinations of outcomes the agents go through.

The aim of this chapter is to address the stability of the heteroclinic cycles comprising of the RSP network. We observe they are quasi-simple (non-simple) and make use of the explicit stability index achieved in Chapter 3. The resulting conclusions allow us to discuss the contribution of the two-person RSP game in a concrete economics problem.

[1] The content of this chapter appears in Garrido-da-Silva and Castro [27].

The chapter is organised as follows. Section 5.1 describes the two-person RSP game and the heteroclinic cycles arising from the dynamics. In Section 5.2 we proceed with a thorough study of the stability properties of such heteroclinic cycles. The main results are Theorems 5.2.1 to 5.2.6, which state sufficient conditions for various types of stability. Section 5.3 suggests a possible first approach to an extension to two agents of the price setting models by Noel [51] and by Hopkins and Seymour [35].

5.1 A two-person Rock-Scissors-Paper game

We examine the long-term dynamics for the two-person Rock-Scissors-Paper (RSP) game. Three possible actions R (rock), S (scissors) and P (paper) engage in a cyclic relation where R beats S, S beats P, P beats R. Our description of the RSP interaction is based on [5] and [64]: two agents, say X and Y, choose simultaneously one action among $\{$R, S, P$\}$. The payoff of the winning action is $+1$ while the payoff of the losing action is -1. If a tie occurs with both agents choosing the same action, the respective payoffs are parametrised by quantities $\varepsilon_x, \varepsilon_y \in (-1,1)$. The normal form representation of the game is given by two normalised payoff matrices

$$A = \begin{pmatrix} 0 & 1-\varepsilon_x & -1-\varepsilon_x \\ -1-\varepsilon_x & 0 & 1-\varepsilon_x \\ 1-\varepsilon_x & -1-\varepsilon_x & 0 \end{pmatrix}, \qquad B = \begin{pmatrix} 0 & 1-\varepsilon_y & -1-\varepsilon_y \\ -1-\varepsilon_y & 0 & 1-\varepsilon_y \\ 1-\varepsilon_y & -1-\varepsilon_y & 0 \end{pmatrix},$$

whose columns and rows respect the order of actions R, S, P. Each element of the matrix A (resp. B) is the payoff of the row agent X (resp. Y) playing against the column agent Y (resp. X).

The agents' choices are expressed in the form of state probabilities of playing R, S and P. At time $t \geq 0$, these are $\boldsymbol{x}^T = (x_1, x_2, x_3) \in \Delta_X$ for agent X and $\boldsymbol{y}^T = (y_1, y_2, y_3) \in \Delta_Y$ for agent Y, where Δ_X and Δ_Y denote the unit simplex in $\mathbb{R}^3$ associated to each agent.[2] We define $\boldsymbol{x}$ and $\boldsymbol{y}$ as column vectors.

The three vertices of each Δ_X and Δ_Y correspond to the choice of a pure strategy. We then refer to those only as R, S and P.

The pair $(\boldsymbol{x}, \boldsymbol{y}) \in \Delta = \Delta_X \times \Delta_Y \subset \mathbb{R}^6$ stands for the state of the game at a particular time. The game dynamics evolves according to the reinforcement learning governed by the coupled replicator equations

$$\begin{aligned} \frac{dx_i}{dt} &= x_i \left[(A\boldsymbol{y})_i - \boldsymbol{x}^T A \boldsymbol{y} \right], \quad i = 1,2,3, \\ \frac{dy_j}{dt} &= y_j \left[(B\boldsymbol{x})_j - \boldsymbol{y}^T B \boldsymbol{x} \right], \quad j = 1,2,3. \end{aligned} \tag{5.1}$$

Here $(A\boldsymbol{y})_i$ and $(B\boldsymbol{y})_j$ are respectively the ith and jth element of the vectors $A\boldsymbol{y}$ and $B\boldsymbol{x}$.

The unique Nash equilibrium is $(\boldsymbol{x}^*, \boldsymbol{y}^*) = \left(\frac{1}{3}, \frac{1}{3}, \frac{1}{3}; \frac{1}{3}, \frac{1}{3}, \frac{1}{3}\right)$ at which both agents are indiferent among all three actions. This is also a steady state of the dynamics. There are nine additional steady states corresponding to the vertices of Δ. All steady states are saddles.

The nine vertices together with the edges of Δ form a heteroclinic network. Aguiar and Castro [5] analitically prove its existence. This heteroclinic network can be described both as the union of three

[2] The superscript T indicates the transpose of a matrix in general.

heteroclinic cycles C_0, C_1 and C_2, with

$$
\begin{aligned}
C_0 &= [(\mathrm{R},\mathrm{P}) \to (\mathrm{S},\mathrm{P}) \to (\mathrm{S},\mathrm{R}) \to (\mathrm{P},\mathrm{R}) \to (\mathrm{P},\mathrm{S}) \to (\mathrm{R},\mathrm{S}) \to (\mathrm{R},\mathrm{P})] \\
C_1 &= [(\mathrm{R},\mathrm{S}) \to (\mathrm{R},\mathrm{R}) \to (\mathrm{P},\mathrm{R}) \to (\mathrm{P},\mathrm{P}) \to (\mathrm{S},\mathrm{P}) \to (\mathrm{S},\mathrm{S}) \to (\mathrm{R},\mathrm{S})] \\
C_2 &= [(\mathrm{S},\mathrm{R}) \to (\mathrm{R},\mathrm{R}) \to (\mathrm{R},\mathrm{P}) \to (\mathrm{P},\mathrm{P}) \to (\mathrm{P},\mathrm{S}) \to (\mathrm{S},\mathrm{S}) \to (\mathrm{S},\mathrm{R})] \,,
\end{aligned}
$$

and as the union of two heteroclinic cycles C_3 and C_4, with

$$
\begin{aligned}
C_3 = [&(\mathrm{R},\mathrm{S}) \to (\mathrm{R},\mathrm{R}) \to (\mathrm{R},\mathrm{P}) \to (\mathrm{S},\mathrm{P}) \to (\mathrm{S},\mathrm{S}) \to (\mathrm{S},\mathrm{R}) \to (\mathrm{P},\mathrm{R}) \\
&\to (\mathrm{P},\mathrm{P}) \to (\mathrm{P},\mathrm{S}) \to (\mathrm{R},\mathrm{S})] \\
C_4 = [&(\mathrm{S},\mathrm{R}) \to (\mathrm{R},\mathrm{R}) \to (\mathrm{P},\mathrm{R}) \to (\mathrm{P},\mathrm{S}) \to (\mathrm{S},\mathrm{S}) \to (\mathrm{R},\mathrm{S}) \to (\mathrm{R},\mathrm{P}) \\
&\to (\mathrm{P},\mathrm{P}) \to (\mathrm{S},\mathrm{P}) \to (\mathrm{S},\mathrm{R})] \,.
\end{aligned}
$$

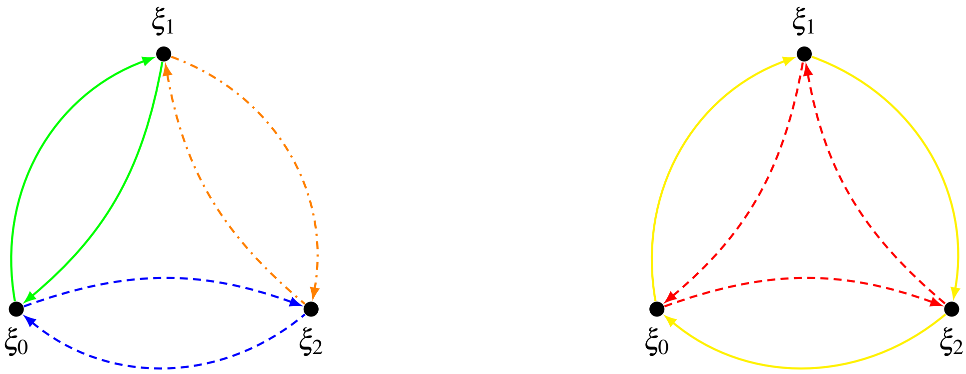

(a) $C_0 \cup C_1 \cup C_2$ (b) $C_3 \cup C_4$

Fig. 5.1 Heteroclinic cycles in the quotient network. Each style identifies a quotient cycle: (a) C_0 is represented by a solid green line, C_1 by a dash-dot orange line, and C_2 by a dashed blue line; (b) C_3 is represented by a solid yellow line, and C_4 by a dashed red line.

The vector field associated to (5.1) is equivariant under the action of the symmetry group $\Gamma = \mathbb{Z}_3$ generated by

$$\gamma : (x_1, x_2, x_3; y_1, y_2, y_3) \mapsto (x_3, x_1, x_2; y_3, y_1, y_2) \,.$$

The Γ-orbits of the steady states (R,P), (R,S) and (R,R) are the following relative steady states:

$$
\begin{aligned}
\xi_0 &\equiv \Gamma(\mathrm{R},\mathrm{P}) = \{(\mathrm{R},\mathrm{P}), (\mathrm{S},\mathrm{R}), (\mathrm{P},\mathrm{S})\} \\
\xi_1 &\equiv \Gamma(\mathrm{R},\mathrm{S}) = \{(\mathrm{R},\mathrm{S}), (\mathrm{S},\mathrm{P}), (\mathrm{P},\mathrm{R})\} \\
\xi_2 &\equiv \Gamma(\mathrm{R},\mathrm{R}) = \{(\mathrm{R},\mathrm{R}), (\mathrm{S},\mathrm{S}), (\mathrm{P},\mathrm{P})\} \,.
\end{aligned}
$$

These represent the three possible outcomes: loss, win and tie. For instance, agent X loses at ξ_0, wins at ξ_1 and ties at ξ_2.

Due to symmetry the dynamics of (5.1) can be studied from the dynamics on a quotient space. The restricted flow to this space contains the quotient network with one-dimensional heteroclinic connections between every pair of relative steady states: ξ_0, ξ_1 and ξ_2. The quotient cycles are defined by the sequences (see Figure 5.1)

$$\begin{aligned} C_0 &= [\xi_0 \to \xi_1 \to \xi_0] \\ C_1 &= [\xi_1 \to \xi_2 \to \xi_1] \\ C_2 &= [\xi_0 \to \xi_2 \to \xi_0] \end{aligned} \quad \text{and} \quad \begin{aligned} C_3 &= [\xi_0 \to \xi_1 \to \xi_2 \to \xi_0] \\ C_4 &= [\xi_0 \to \xi_2 \to \xi_1 \to \xi_0]\,. \end{aligned}$$

In the context of the game, the C_0-cycle involves alternate win-loss of both agents; the C_1- and C_2-cycles involve a tie and a loss by one agent; the C_3- and C_4-cycles go through all possible outcomes (loss, win, tie) in the two possible orders.

Notice that the coordinate hyperplanes as well as all sub-simplices of Δ are flow-invariant spaces. In particular, every heteroclinic connection $\kappa_{i,j} = [\xi_i \to \xi_j]$, $i \neq j = 0,1,2$, is of saddle-sink type in a two-dimensional face boundary of Δ. Denote this face boundary by P_{ij}. Evidently, P_{ij} is not a vector subspace of $\mathbb{R}^6$. For convenience we find a three-dimensional vector subspace Q_{ij} of $\mathbb{R}^6$ invariant under the flow such that $P_{ij} \subset Q_{ij}$ and $\kappa_{i,j}$ persists in a robust way. Representatives of all heteroclinic connections in the quotient network and respective flow-invariant spaces are listed in Table 5.1.

Connection	Representative	2-dim space P_{ij}	3-dim vector space Q_{ij}
$[\xi_0 \to \xi_1]$	$[(\mathrm{R,P}) \to (\mathrm{S,P})]$	$\{(x_1,x_2,0;0,0,1)\}$	$\{(x_1,x_2,0;0,0,y_3)\}$
$[\xi_1 \to \xi_0]$	$[(\mathrm{S,P}) \to (\mathrm{S,R})]$	$\{(0,1,0;y_1,0,y_3)\}$	$\{(0,x_2,0;y_1,0,y_3)\}$
$[\xi_1 \to \xi_2]$	$[(\mathrm{R,S}) \to (\mathrm{R,R})]$	$\{(1,0,0;y_1,y_2,0)\}$	$\{(x_1,0,0;y_1,y_2,0)\}$
$[\xi_2 \to \xi_1]$	$[(\mathrm{R,R}) \to (\mathrm{P,R})]$	$\{(x_1,0,x_3;1,0,0)\}$	$\{(x_1,0,x_3;y_1,0,0)\}$
$[\xi_0 \to \xi_2]$	$[(\mathrm{S,R}) \to (\mathrm{R,R})]$	$\{(x_1,x_2,0;1,0,0)\}$	$\{(x_1,x_2,0;y_1,0,0)\}$
$[\xi_2 \to \xi_0]$	$[(\mathrm{R,R}) \to (\mathrm{R,P})]$	$\{(1,0,0;y_1,0,y_3)\}$	$\{(x_1,0,0;y_1,0,y_3)\}$

Table 5.1 Flow-invariant spaces and representatives for the heteroclinic connections in the quotient network.

5.2 Stability of the RSP cycles

In this section we establish the stability properties of the (quotient) heteroclinic cycles C_k, $k = 0,\dots,4$, by looking at the stability of the individual heteroclinic connections. For this purpose the behaviour of trajectories passing close to each heteroclinic cycle is captured by return maps defined on suitable cross sections to the heteroclinic connections. Due to an appropriate change of coordinates such maps are the product of basic transition matrices. Appendix B provides all details.

For every C_k, $k = 0,\dots,4$, we compute the local stability indices along its heteroclinic connections. First observe that the C_k-cycles are not simple heteroclinic cycles: although the heteroclinic connections lie in two-dimensional flow-invariant spaces, these are not fixed-point spaces. A trivial verification confirms that C_k are in turn quasi-simple heteroclinic cycles. We then make use of the results of Section 3.4. The main tool is the function $F^{\text{index}} : \mathbb{R}^3 \to [-\infty,\infty]$, which is related to the local stability index in Definition 3.4.7. For $\boldsymbol{\alpha} = (\alpha_1, \alpha_2, \alpha_3) \in \mathbb{R}^3$ we employ the explicit form of $F^{\text{index}}(\boldsymbol{\alpha})$ in Appendix A.2.

Let us denote by σ_{ij} the local stability index along the heteroclinic connection $\kappa_{i,j} = [\xi_i \to \xi_j]$.

Theorem 5.2.1. *Suppose that $\varepsilon_x, \varepsilon_y \in (-1,1)$. The local stability indices for the C_0-cycle are:*

(i) if $\varepsilon_x + \varepsilon_y > 0$, then $\sigma_{10} = \sigma_{01} = -\infty$;

(ii) if $\varepsilon_x + \varepsilon_y < 0$, then

$$\sigma_{10} = \min\left\{\frac{1-\varepsilon_x}{1+\varepsilon_x}, \frac{(1-\varepsilon_y)^2}{2(1+\varepsilon_y)}\right\} > 0$$
$$\sigma_{01} = \min\left\{\frac{1-\varepsilon_y}{1+\varepsilon_y}, \frac{(1-\varepsilon_x)^2}{2(1+\varepsilon_x)}\right\} > 0.$$

Proof. In Step 1, we establish that Lemma 3.3.3 holds if and only if $\varepsilon_x + \varepsilon_y < 0$. This is enough to prove part (i) according to Theorem 3.4.9(a). In Step 2, when $\varepsilon_x + \varepsilon_y < 0$, we apply the function F^{index} to evaluate the local stability index for each heteroclinic connection in the C_0-cycle.

Step 1: Consider the transition matrices $M^{(0)}$ and $M^{(1)}$ in (B.7) associated with the C_0-cycle. Since they are similar[3], conditions *(i)–(ii)* of Lemma 3.3.3 are satisfied, or not, for either matrices. Set $M \equiv M^{(0)}$. The eigenvalues of M are the roots of the characteristic polynomial

$$p(\lambda) = -\lambda^3 + \mathrm{Tr}(M)\lambda^2 - \mathrm{B}(M)\lambda + \mathrm{Det}(M), \tag{5.2}$$

where $\mathrm{Tr}(M)$ and $\mathrm{Det}(M)$ are respectively the trace and the determinant of M, and

$$\mathrm{B}(M) = \begin{vmatrix} \frac{-1-3\varepsilon_x-\varepsilon_y+\varepsilon_x\varepsilon_y}{4} & \frac{1-\varepsilon_x}{2} \\ \frac{3+\varepsilon_y^2}{4} & -\frac{1+\varepsilon_y}{2} \end{vmatrix} + \begin{vmatrix} -\frac{1+\varepsilon_y}{2} & 0 \\ 1 & 0 \end{vmatrix} + \begin{vmatrix} \frac{-1-3\varepsilon_x-\varepsilon_y+\varepsilon_x\varepsilon_y}{4} & 1 \\ \frac{1-\varepsilon_y}{2} & 0 \end{vmatrix}.$$

The Fundamental Theorem of Algebra states that $p(\lambda) = 0$ has precisely three roots $\lambda_1, \lambda_2, \lambda_3 \in \mathbb{C}$ such that

$$\mathrm{Tr}(M) = \lambda_1 + \lambda_2 + \lambda_3 = \frac{-3-3\varepsilon_x-3\varepsilon_y+\varepsilon_x\varepsilon_y}{4}, \tag{5.3}$$
$$\mathrm{B}(M) = \lambda_1\lambda_2 + \lambda_1\lambda_3 + \lambda_2\lambda_3 = \frac{-3+3\varepsilon_x+3\varepsilon_y+\varepsilon_x\varepsilon_y}{4}, \tag{5.4}$$
$$\mathrm{Det}(M) = \lambda_1\lambda_2\lambda_3 = 1.$$

By virtue of the Routh-Hurwitz Criterion (see [9]), the number of roots with positive real part equals the number of sign changes of the sequence

$$-1, \quad \mathrm{Tr}(M), \quad \frac{1-\mathrm{B}(M)\,\mathrm{Tr}(M)}{\mathrm{Tr}(M)}, \quad 1.$$

[3] We say that two square matrices of the same order, A and B, are similar if there exists an invertible matrix P such that $B = P^{-1}AP$. In particular, similar matrices have the same characteristic polynomial.

For all $\varepsilon_x, \varepsilon_y \in (-1,1)$ we have

$$\operatorname{Tr}(M)\operatorname{B}(M) = \frac{1}{16}(3-\varepsilon_x\varepsilon_y)^2 - \frac{9}{16}(\varepsilon_x+\varepsilon_y)^2 \in (-2,1),$$

yielding

$$sgn\left(\frac{1-\operatorname{B}(M)\operatorname{Tr}(M)}{\operatorname{Tr}(M)}\right) = sgn(\operatorname{Tr}(M)).$$

Hence, there is a single root with positive real part. It is, in fact, purely real because $p(\lambda)$ admits only three roots. Let $\lambda_1 \in \mathbb{R}$ and $\lambda_1 > 0$. We make the following

Claim: The characteristic polynomial $p(\lambda)$ has one real root, λ_1, and a pair of complex roots, $\alpha \pm \beta i$.

Let $\lambda_{\max}$ be the maximum root in absolute value of $p(\lambda)$. Since

$$\det(M) = \lambda_1(\alpha^2+\beta^2) = 1 \Leftrightarrow \lambda_1 = \frac{1}{\alpha^2+\beta^2} > 0$$

it follows that

$$\lambda_1 = \lambda_{\max} \Leftrightarrow \lambda_1 > 1.$$

We then prove that $\varepsilon_x + \varepsilon_y > 0$ is equivalent to $\lambda_1 \neq \lambda_{\max}$. Given that

$$\operatorname{B}(M) > 0 \Rightarrow \varepsilon_x+\varepsilon_y > 0 \Rightarrow \operatorname{tr}(M) < 0$$

and

$$\operatorname{tr}(M) > 0 \Rightarrow \varepsilon_x+\varepsilon_y < 0 \Rightarrow \operatorname{B}(M) < 0$$

one of three possible situations takes place:

<u>Case 1</u>: suppose that $\operatorname{Tr}(M) < 0$ and $\operatorname{B}(M) > 0$, that is, $\varepsilon_x+\varepsilon_y > 0$; thus

$$\begin{aligned}\operatorname{Tr}(M) &= \lambda_1 + 2\alpha < 0 \Leftrightarrow 2\alpha\lambda_1 < -\lambda_1^2 \\ \operatorname{B}(M) &= 2\alpha\lambda_1 + \alpha^2+\beta^2 > 0.\end{aligned}$$

Replacing the first in the second equation we obtain $\lambda_1^2 < \alpha^2+\beta^2$, and therefore $\lambda_1 \neq \lambda_{\max}$.

<u>Case 2</u>: suppose that $\operatorname{tr}(M) > 0$ and $\operatorname{B}(M) < 0$, that is, $\varepsilon_x+\varepsilon_y < 0$; a procedure analogous to the one above shows now that $\lambda_1 = \lambda_{\max}$.

<u>Case 3</u>: suppose that $\operatorname{Tr}(M) < 0$ and $\operatorname{B}(M) < 0$; from (5.3) and (5.4), we can write

$$\operatorname{B}(M) - \operatorname{Tr}(M) = 2\alpha(\lambda_1-1) + \alpha^2+\beta^2-\lambda_1 = \frac{3}{2}(\varepsilon_x+\varepsilon_y),$$

and proceed by contradiction.

(a) if $\varepsilon_x+\varepsilon_y > 0$ and $\lambda_1 > 1$, then $\lambda_1 = \lambda_{\max}$ and

$$2\alpha(\lambda_1-1) > \lambda_1 - (\alpha^2+\beta^2) > 0.$$

However, the left-hand side is negative as $\alpha < 0$, which is absurd. Accordingly, if $\varepsilon_x + \varepsilon_y > 0$, then $\lambda_1 \neq \lambda_{\max}$.

(b) if $\varepsilon_x + \varepsilon_y < 0$ and $0 < \lambda_1 < 1$, then $|\lambda_{\max}| = \alpha^2 + \beta^2$ and

$$2\alpha(\lambda_1 - 1) < \lambda_1 - (\alpha^2 + \beta^2) < 0.$$

But the left-hand side is positive as $\alpha < 0$. Hence, if $\varepsilon_x + \varepsilon_y < 0$, then $\lambda_1 = \lambda_{\max}$.

We have seen that *(i)* and *(ii)* of Lemma 3.3.3 are true if and only if $\varepsilon_x + \varepsilon_y < 0$. Next we prove that *(i)–(ii)* guarantee condition *(iii)* of Lemma 3.3.3 for every $M^{(j)}$, $j = 0, 1$. Let $\boldsymbol{w}^{\max,j}$ be the eigenvector of $M^{(j)}$ corresponding to $\lambda_{\max}$. In particular, *(iii)* holds if all the coordinates of $\boldsymbol{w}^{\max,j}$ have the same sign. Note that we need to check *(iii)* for both $\boldsymbol{w}^{\max,j}$ because every basic transition matrix M_q, $q = 0, 1$, in (B.6) has one negative entry.

Assume that $M \equiv M^{(0)}$ satisfies *(i)–(ii)* with $\lambda_{\max} = \lambda_1$, i.e., $\lambda_1 \in \mathbb{R}$ and $\lambda_1 > 1$. Again, by similarity, the same remains valid for $M^{(1)}$. Direct computation reveals that $\boldsymbol{w}^{\max,0}$ has coordinates multiple of

$$\left(\lambda_1 + \frac{1+\varepsilon_y}{2},\ \frac{3+\varepsilon_y^2}{4},\ \lambda_1^2 - \mathrm{Tr}\,(M)\,\lambda_1 + \mathrm{B}\,(M) + \frac{1-\varepsilon_y}{2}\right).$$

Due to $\lambda_1 > 1$ and $\varepsilon_y \in (-1, 1)$ the first two coordinates have positive signs. From $\mathrm{Det}\,(M) = 1$ and $p(\lambda_1) = 0$ we get $\lambda_1 \left(\lambda_1^2 - \mathrm{Tr}\,(M)\,\lambda_1 + \mathrm{B}\,(M)\right) = 1$, and therefore the third coordinate is also positive. The coordinates of $\boldsymbol{w}^{\max,1}$ can be obtained from those for $\boldsymbol{w}^{\max,0}$ if we replace ε_y by ε_x. All coordinates of $\boldsymbol{w}^{\max,1}$ are analogously positive.

We prove the claim. The discriminant of $p\,(\lambda)$ in (5.2), being a real cubic polynomial, is

$$\begin{aligned}
&\Delta(\varepsilon_x, \varepsilon_y) \\
&\quad = 18\mathrm{Tr}\,(M)\,\mathrm{B}\,(M) - 4\mathrm{Tr}\,(M)^3 + \mathrm{Tr}\,(M)^2\,\mathrm{B}\,(M)^2 - 4\mathrm{B}\,(M)^3 - 27 \\
&\quad = \frac{1}{256}\Big[\left(\varepsilon_x^2 - 9\right)^2 \varepsilon_y^4 + \left(-80\varepsilon_x^3 - 432\varepsilon_x\right)\varepsilon_y^3 \\
&\qquad + \left(-18\varepsilon_x^4 - 396\varepsilon_x^2 - 162\right)\varepsilon_y^2 + \left(-432\varepsilon_x^3 - 3024\varepsilon_x\right)\varepsilon_y \\
&\qquad + 81\varepsilon_x^4 - 162\varepsilon_x^2 - 3375\Big].
\end{aligned}$$

For each value of $\varepsilon_x \in (-1, 1)$ we can regard $\Delta(\varepsilon_x, \cdot)$ as a real quartic polynomial in the variable ε_y. Its discriminant is in turn given by

$$-\frac{59049}{67108864}\left(\varepsilon_x^2 + 15\right)^3\left(\varepsilon_x^2 + 3\right)^8.$$

This is negative for every $\varepsilon_x \in (-1, 1)$ and hence $\Delta\,(\varepsilon_x, \cdot)$ has two distinct real roots and two complex conjugate non-real roots. The coefficient of the leading term of $\Delta\,(\varepsilon_x, \cdot)$ is positive. Together with

$$\begin{aligned}
\Delta\,(\varepsilon_x, -1) &= -\frac{1}{4}\,(1 - \varepsilon_x)\left(\varepsilon_x^3 + 9\varepsilon_x^2 + 54\right) < 0 \\
\Delta\,(\varepsilon_x, 1) &= -\frac{1}{4}\,(1 + \varepsilon_x)\left(-\varepsilon_x^3 + 9\varepsilon_x^2 + 54\right) < 0
\end{aligned}$$

for all $\varepsilon_x \in (-1,1)$ implies

$$\Delta(\varepsilon_x, \varepsilon_y) < 0$$

for all $\varepsilon_x, \varepsilon_y \in (-1,1)$. Accordingly, $p(\lambda)$ has one real root and two complex conjugate non-real roots.

Step 2: From (3.14) the local basin $\mathscr{B}_\delta^{\pi_0}$ for points near ξ_0 in coordinates (3.5) is defined by the sequences $\left(M^{(0)}\right)^k \boldsymbol{\eta}$ and $M_0\left(M^{(0)}\right)^k \boldsymbol{\eta}$ with $k \in \mathbb{N}_0$. Theorem 3.4.9 says that

$$\begin{aligned}\sigma_0 = \min\Bigg\{ & F^{\text{index}}\left(\boldsymbol{v}^{\max,0}\right), \\ & \min\left\{F^{\text{index}}\left(\frac{1-\varepsilon_y}{2},1,0\right), F^{\text{index}}\left(-\frac{1+\varepsilon_x}{2},0,1\right), F^{\text{index}}(1,0,0)\right\}, \\ & \min\Bigg\{F^{\text{index}}\left(\frac{-1-3\varepsilon_x-\varepsilon_y+\varepsilon_x\varepsilon_y}{4}, \frac{1-\varepsilon_x}{2},1\right), \\ & \quad F^{\text{index}}\left(\frac{3+\varepsilon_y^2}{4}, -\frac{1+\varepsilon_y}{2},0\right), F^{\text{index}}\left(\frac{1-\varepsilon_y}{2},1,0\right)\Bigg\}\Bigg\}.\end{aligned} \tag{5.5}$$

Recall that $\boldsymbol{v}^{\max,0}$ is the line of the change of basis matrix from the basis of eigenvectors for $M^{(0)}$ to the canonical basis for $\mathbb{R}^3$ in the position associated with $\lambda_{\max}$. As one entry of each M_q, $q=0,1$, is negative we have taken the lines of the matrices M_0 and $M^{(0)} = M_1 M_0$ into account in (5.5).

Simple algebra attests that $\boldsymbol{v}^{\max,0}$ is a constant multiple of the vector

$$\left(\frac{\lambda_1}{(\alpha-\lambda_1)^2+\beta^2}, \frac{\frac{4}{3+\varepsilon_y^2}\left[\left(\alpha+\frac{1+\varepsilon_y}{2}\right)^2+\beta^2\right]+\frac{1-\varepsilon_x}{2}}{(\alpha-\lambda_1)^2+\beta^2}, \frac{\frac{4}{3+\varepsilon_y^2}}{(\alpha-\lambda_1)^2+\beta^2}\right).$$

Therefore its entries are all non-negative for any $\varepsilon_x, \varepsilon_y \in (-1,1)$. Using Lemma 3.4.8

$$F^{\text{index}}\left(\boldsymbol{v}^{\max,0}\right) = F^{\text{index}}\left(\frac{1-\varepsilon_y}{2},1,0\right) = F^{\text{index}}(1,0,0) = +\infty.$$

On the other hand, we get

$$F^{\text{index}}\left(-\frac{1+\varepsilon_x}{2},0,1\right) = \frac{1-\varepsilon_x}{1+\varepsilon_x}$$

$$F^{\text{index}}\left(\frac{3+\varepsilon_y^2}{4},-\frac{1+\varepsilon_y}{2},0\right) = \frac{(1-\varepsilon_y)^2}{2(1+\varepsilon_y)}$$

and

$$F^{\text{index}}\left(\frac{-1-3\varepsilon_x-\varepsilon_y+\varepsilon_x\varepsilon_y}{4},\frac{1-\varepsilon_x}{2},1\right)=\begin{cases}+\infty & \text{if } -1-3\varepsilon_x-\varepsilon_y+\varepsilon_x\varepsilon_y\geq 0\\ \dfrac{(5-\varepsilon_y)(1-\varepsilon_x)}{1+3\varepsilon_x+\varepsilon_y-\varepsilon_x\varepsilon_y} & \text{if } -1-3\varepsilon_x-\varepsilon_y+\varepsilon_x\varepsilon_y<0.\end{cases}$$

It follows that

$$F^{\text{index}}\left(\frac{-1-3\varepsilon_x-\varepsilon_y+\varepsilon_x\varepsilon_y}{4},\frac{1-\varepsilon_x}{2},1\right)>F^{\text{index}}\left(-\frac{1+\varepsilon_x}{2},0,1\right)$$

for all $\varepsilon_x,\varepsilon_y\in(-1,1)$, and so

$$\sigma_{10}=\min\left\{\frac{1-\varepsilon_x}{1+\varepsilon_x},\frac{(1-\varepsilon_y)^2}{2(1+\varepsilon_y)}\right\}>0.$$

The rest of the proof for σ_{01} runs as before by interchanging ε_x and ε_y. □

We are thus led to the following consequence from Theorem 2.4.3.

Theorem 5.2.2. *Suppose that $\varepsilon_x,\varepsilon_y\in(-1,1)$. If $\varepsilon_x+\varepsilon_y<0$, then the C_0-cycle is e.a.s.*

The stability of the remaining heteroclinic cycles in the RSP quotient network is given in Theorems 5.2.3–5.2.6. The proofs are omitted because they are similar to that of Theorem 5.2.1 with the appropriate transition matrices in Appendix B.2. In the statement of these results it is useful to define

$$\begin{aligned}b_1(\varepsilon_x,\varepsilon_y)&=(5-\varepsilon_x)\varepsilon_y^2+\left(\varepsilon_x^2+10\varepsilon_x+1\right)\varepsilon_y-(1-\varepsilon_x)(4+5\varepsilon_x)\\ b_2(\varepsilon_x,\varepsilon_y)&=(5+\varepsilon_x)\varepsilon_y^2+\left(-\varepsilon_x^2+10\varepsilon_x-1\right)\varepsilon_y-(1+\varepsilon_x)(4-5\varepsilon_x).\end{aligned}$$

Theorem 5.2.3. *Suppose that $\varepsilon_x,\varepsilon_y\in(-1,1)$. The local stability indices for the C_1-cycle are:*

(a) if either $\varepsilon_x+\varepsilon_y<0$, or $b_1(\varepsilon_x,\varepsilon_y)<0$, or $\varepsilon_x-\varepsilon_y>0$, then $\sigma_{21}=\sigma_{12}=-\infty$ and the cycle is c.u;

(b) if $\varepsilon_x+\varepsilon_y>0$, and $b_1(\varepsilon_x,\varepsilon_y)>0$, and $\varepsilon_x-\varepsilon_y<0$, then

$$\begin{aligned}\sigma_{21}&=\frac{-4+\varepsilon_x+(3-\varepsilon_x)\varepsilon_y+\varepsilon_y^2}{(1-\varepsilon_x)(1+\varepsilon_y)}<0\\ \sigma_{12}&=\min\left\{\frac{\varepsilon_y-\varepsilon_x}{1-\varepsilon_y},\frac{1+2\varepsilon_x+\varepsilon_y^2}{2(1-\varepsilon_x)}\right\}>0\end{aligned}$$

and the cycle is f.a.s.

Theorem 5.2.4. *Suppose that $\varepsilon_x,\varepsilon_y\in(-1,1)$. The local stability indices for the C_2-cycle are:*

(a) if either $\varepsilon_x+\varepsilon_y<0$, or $b_2(\varepsilon_x,\varepsilon_y)<0$, or $\varepsilon_x-\varepsilon_y<0$, then $\sigma_{20}=\sigma_{02}=-\infty$ and the cycle is c.u;

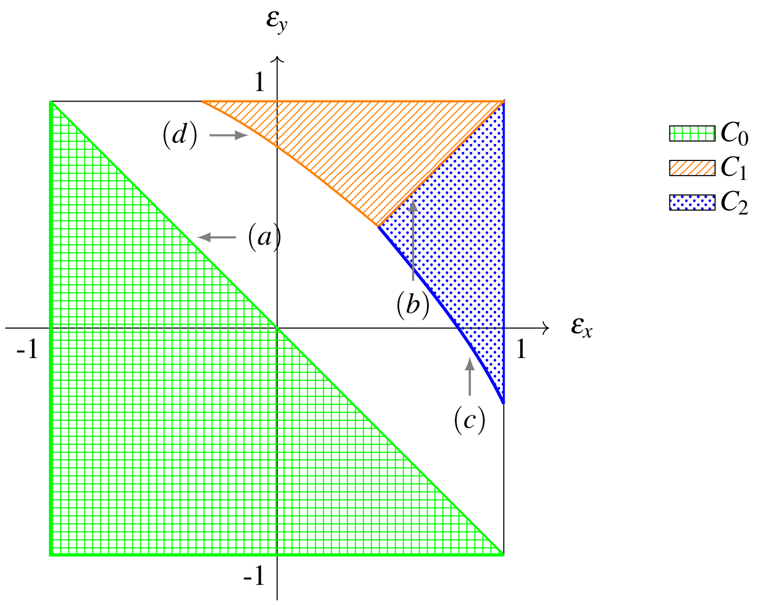

Fig. 5.2 Stability regions for the C_0-, C_1- and C_2-cycles in the two-parameter space. The lines in the interior are: (a) $\varepsilon_x+\varepsilon_y=0$; (b) $\varepsilon_x-\varepsilon_y=0$; (c) $\varepsilon_y=\frac{1-10\varepsilon_x+\varepsilon_x^2+\sqrt{81-24\varepsilon_x-2\varepsilon_x^2-40\varepsilon_x^3+\varepsilon_x^4}}{2(5+\varepsilon_x)}$; (d) $\varepsilon_y=\frac{-\left(1+10\varepsilon_x+\varepsilon_x^2\right)+\sqrt{81+24\varepsilon_x-2\varepsilon_x^2+40\varepsilon_x^3+\varepsilon_x^4}}{2(5-\varepsilon_x)}$.

(b) if $\varepsilon_x+\varepsilon_y>0$*, and* $b_2(\varepsilon_x,\varepsilon_y)>0$*, and* $\varepsilon_x-\varepsilon_y>0$*, then*

$$\sigma_{20}=\frac{-4+\varepsilon_y+(3-\varepsilon_y)\,\varepsilon_x+\varepsilon_x^2}{(1-\varepsilon_y)\,(1+\varepsilon_x)}<0$$

$$\sigma_{02}=\min\left\{\frac{\varepsilon_x-\varepsilon_y}{1-\varepsilon_x},\frac{1+2\varepsilon_y+\varepsilon_x^2}{2\,(1-\varepsilon_y)}\right\}>0$$

and the cycle is f.a.s.

Theorem 5.2.5. *Suppose that* $\varepsilon_x,\varepsilon_y\in(-1,1)$*. Then, the local stability indices for the* C_3*-cycle are all* $-\infty$ *and the cycle is c.u.*

Theorem 5.2.6. *Suppose that* $\varepsilon_x,\varepsilon_y\in(-1,1)$*. Then, the local stability indices for the* C_4*-cycle are all* $-\infty$ *and the cycle is c.u.*

Notice the C_3- and C_4-cycles never exhibit any kind of stability. This justifies their total absence from the numerical observations by Sato et al. [64]. The C_1- and C_2-cycles are not e.a.s making them difficult to detect in simulations. They are f.a.s in a subset of the complement of the stability region for the C_0-cycle in the two-parameter space. Figure 5.2 divides the entire two-parameter space $(-1,1)\times(-1,1)$ into admissible regions where the C_0-, C_1-, and C_2-cycles are attracting. Our analysis allows us to determine the exact expressions for the delimiting curves.

Recall that the two parameters, ε_x and ε_y, are the agents' payoffs when the outcome of their actions is a tie. They range from almost as bad as a loss to almost as good as a win. Under the C_0-cycle agents never tie. The associated dynamic behaviour is as stable as possible when the sum of payoffs for a tie is negative. In that case, a tie is not an attractive outcome for at least one agent for whom the payoff is negative and both avoid it unilaterally. The C_0-cycle models the existence of alternating dominance between two agents. On the other hand, either C_1 or C_2 involve a tie and a loss by a single agent. These cycles disclose some stability if the payoffs for a tie are high enough and its sum is itself positive. Here the agent that never wins is more rewarded than the other is penalised for the tie action. He has further an incentive to deviate and draws the game. The opponent not satisfied with the outcome tries to win successively.

We end with two brief comments concerning Lemma 4.9 in [5] that states that none of the heteroclinic cycles in the RSP network is e.a.s, and which must be incorrect in view of Theorem 5.2.2. The first comment is that the stability index provides a very powerful and systematic tool for the study of stability and it was not available at the time of [5]. The second is that the authors of [5] missed to take into account the permutation between consecutive cross sections.

5.3 An application to an economics problem

We show how the two-person RSP game provides a useful model to study strategic interactions in economics. The use of the game itself to support the cyclic behaviour of prices can be found in [35] and [51] among others. Price cycles were observed by Noel [51] in the Toronto retail gasoline market where major and independent firms alternate in charging the highest retail price (see Figure 1 therein). Firms undercut each other over subsequent periods to steal market share until prices reach a competitive level at which they make no profit. Margins become so low that some firm suddenly increases its price and the others follow it triggering the undercutting phase again. On the other hand, Hopkins and Seymour [35] address market price competition under seller and consumer learning. The existence of price dispersion where rival sellers offer the same good at different prices seems to depend on the absence of informed consumers.

We discuss the above-mentioned models in light of the results obtained for the two-person RSP game. Consider a market for a homogeneous good. In the model proposed by Noel [51] the agents are a major firm (Agent X) and an independent firm (Agent Y). We assume that they compete in a dynamic two-person RSP game by alternately setting prices. Firm's payoff corresponds to the current profit. In order to maximise it prices are chosen from three possible level:

R: *Low* **S**: *Intermediate* **P**: *High*

with a cyclical best-response structure. A Low price (R) beats an Intermediate price (S) because the higher number of consumers compensates for the loss in price. An Intermediate price (S) beats a High price (P) for the same reason. A High price (P) beats a Low price (R) because, even though it may attract less consumers, the price difference makes up for the reduction in sales.

Let us suppose that there are many consumers who seek to buy at most one unit of the good. Each firm takes as given consumer demand and the pricing strategies chosen by the opponent. Consumers have all relevant information about prices and product quality. In this regard they have a tendency to purchase from the cheapest firm. When faced with extreme prices they believe the good sold by the high-priced firm is of better quality. For example, brand-name products are more expensive than private labels but the former are typically associated to a higher level of quality.

Agent X (major firm) chooses	Agent Y (independent firm) chooses	Winner
Low price	High price	Y
Intermediate price	High price	X
Intermediate price	Low price	Y
High price	Low price	X
High price	Intermediate price	Y
Low price	Intermediate price	X
Low price	High price	Y

Table 5.2 Interpretation of the C_0-cycle in the context of Noel's model.

As we know long run equilibrium dynamics for our model consists of the heteroclinic network described by the C_0-, C_1- and C_2-cycles in Figure 5.1. According to the stability results in the previous section only C_0 can be empirically observed whenever the sum of the payoffs for a tie is negative. We see that the cycling phenomenon reported in [51] can be explained by the win-loss pattern of C_0. Indeed, this corresponds to the sequence of outcomes expressed in Table 5.2.

If the sum of the firms payoffs when they charge the same price is negative, then at least one firm earns a negative profit. This gives to both firms an incentive to deviate from equal prices. Suppose that X chooses Low. It is better for Y to choose High because the price war has become too costly. Then, X follows suit but chooses strategically an Intermediate price, and Y responds with Low to steal the market. Firm X next raises its price to a High level in the direction of exploiting profits. Undercutting starts again with Y fixing an Intermediate price and X lowers it further to its best advantage. In short, firms end up out of phase with respect to each other and alternate winning and losing each turn as the C_0-cycle predicts.

We look now to the Hopkins and Seymour [35] model where consumers engage in costly search for getting price quotations. Consider the following extension under the two-person RSP game: let a continuum of sellers be Agent X and a continuum of consumers be Agent Y. As before seller's payoff is its current profit. Consumer's payoff is the utility (or total satisfaction) from the good. At each point in time, sellers choose a level of price

R-s: *Low* **S-s**: *Intermediate* **P-s**: *High*

while consumers choose a level of information about prices

R-c: *Poor* **S-c**: *Reasonable* **P-c**: *Full.*

We assume that information is not freely available incurring in a search cost proportional to the attainable levels. Full information allows for knowledge of the whole distribution of price. Reasonable information says which sellers charge the highest price. Poor information does not distinguish sellers.

Within sellers, the relation among the possible actions is as suggested for the model of Noel [51]. Within consumers, being Poorly informed (R-c) beats being Reasonably informed (S-c) because the good might be bought anywhere spending the least on information. Being Reasonably informed (S-c) beats being Fully informed (P-c) for the same reason. Being Fully informed (P-c) beats being Poorly

Agent X (sellers) chooses	Agent Y (consumers) chooses	Winner
Low price	Fully informed	Y
Intermediate price	Fully informed	X
Intermediate price	Poorly informed	Y
High price	Poorly informed	X
High price	Reasonably informed	Y
Low price	Reasonably informed	X
Low price	Fully informed	Y

Table 5.3 Interpretation of the C_0-cycle in the context of Hopkins and Seymour model.

informed (R-c) because the good is always purchased at the lowest advertised price. The underlying goals behind the actions of the agents is based on the maximisation of their payoffs.

In our model suppose that sellers interact actively with consumers based on the dynamic driven by the two-person RSP game. We examine the C_0-cycle constituted by the choices in Table 5.3. The outcomes in each line are justified as follows. Given a market with Fully informed consumers and Low-price sellers it is eligible to say that

- R-s is beaten by P-c because Fully informed consumers cause the price charged by sellers to decrease.

Once markups are sufficiently small Low-price sellers have a greater incentive to raise their prices.

- S-s beats P-c because Intermediate-price sellers stay in business with Reasonably and Poorly informed consumers.

It is in the interest of Fully informed consumers to be Poorly informed to acquire the good without supporting search costs.

- S-s is beaten by R-c because Poorly informed consumers pay less for the good than they could.

Intermediate-price sellers make larger profits by charging a High price.

- P-s beats R-c because High-price sellers' clientele consists only of Poorly informed consumers.

Poorly informed consumers have an incentive to search for a lower price. They access Reasonable information at a relatively small cost.

- P-s is beaten by S-c because Reasonable informed consumers do not buy at a High price.

High-price sellers cut drastically the price in order to compete for all consumers and manage the losses.

- R-s beats S-c because Low-price sellers serve Reasonably and Fully informed consumers.

It is better for Reasonably informed consumers have Full information about prices to take best advantage of the current market. This initiates a new round of the joint seller-consumer interaction where Low-price sellers face Fully informed consumers.

Price dispersion appears here not because several sellers set different prices but because they choose different prices over time. Our price dispersion is then in line with the temporal price dispersion of Varian [66].

By way of conclusion, the description of our models by means of the RSP heteroclinic cycles may help to clarify real world retailing behaviour.

Chapter 6

Examples

The aim of the chapter is to work out two abstract examples for illustrating the practical use of the results achieved in Chapters 3 and 4.

We calculate the local stability indices for two particular heteroclinic networks involving a node in common. Both consist of two heteroclinic cycles of type Z, and so quasi-simple heteroclinic cycles. One is the Bowtie network with two heteroclinic cyles of type B_3^- in $\mathbb{R}^5$ and the other is the $\left(\mathrm{C}_2^-,\mathrm{C}_2^-\right)$-network in $\mathbb{R}^6$ whose name is self-explanatory.

The chapter is organised as follows. In Section 6.1 we study the stability of the heteroclinic cycles in the Bowtie network, and the stability of the heteroclinic network as a whole. We then employ the local stability index with respect to a heteroclinic cycle, the *c*-index, and with respect to the heteroclinic network, the *n*-index. The influence of a common node instead of a common heteroclinic connection regarding the stability properties is examined in comparison with the Kirk and Silber network in [39]. Section 6.2 provides the construction of the $\left(\mathrm{C}_2^-,\mathrm{C}_2^-\right)$-network by making use of the symmetry. We describe each heteroclinic cycle in term of the stability and relate the results to the ones of the $\left(\mathrm{B}_2^+,\mathrm{B}_2^+\right)$-network in [17]. We examine the shape of the range of the return map around the *R*-cycle and the occurrence of switching along the heteroclinic cycles. The main achievements are Proposition 6.1.2, Theorem 6.1.6, Proposition 6.2.1 and Lemma 6.2.2.

6.1 The Bowtie network

The Bowtie network is made up of two B_3^--cycles joined by one common node as depicted in Figure 4.16. This construction can be performed in $\mathbb{R}^5$ using the *simplex realisation* from [13] as follows. In the absence of noise we consider the vector field on $\boldsymbol{x} = (x_1,x_2,x_3,x_4,x_5) \in \mathbb{R}^5$ with

$$\dot{x}_j = x_j \left(1 + \sum_{i=1}^{5} (a_{ij}-1)\, x_i^2\right), \qquad j = 1,2,3,4,5, \tag{6.1}$$

which admits non-trivial equilibria ξ_j of saddle type on every x_j-axis. The system is equivariant under the symmetry group $\mathbb{Z}_2^5$ where each $\mathbb{Z}_2$ acts by a reflection $\gamma_j : x_j \mapsto -x_j$. All coordinate subspaces are fixed-point subspaces of appropriate isotropy subgroups and so invariant under the flow of (6.1).

In the notation of [39] we set

$$P_{ij} = \mathrm{Fix}\left(\mathbb{Z}_2^3\left(\gamma_k,\, k \neq i,j\right)\right) = \left\{\boldsymbol{x} \in \mathbb{R}^5 : x_k = 0 \text{ for all } k \neq i,j\right\} \qquad (i<j)$$

and

$$S_{ijk} = \mathrm{Fix}\left(\mathbb{Z}_2^2\left(\gamma_l,\, l \neq i,j,k\right)\right) = \left\{\boldsymbol{x} \in \mathbb{R}^5 : x_l = 0 \text{ for all } l \neq i,j,k\right\} \qquad (i<j<k)$$

for which $\dim(P_{ij}) = 2$ and $\dim\left(S_{ijk}\right) = 3$. The coefficients a_{ij} in (6.1) can be chosen such that there are two robust heteroclinic cycles

$$R = [\xi_1 \to \xi_2 \to \xi_3 \to \xi_1] \subset S_{123}$$
$$L = [\xi_2 \to \xi_4 \to \xi_5 \to \xi_2] \subset S_{245},$$

each with three nodes and three one-dimensional (saddle-sink) heteroclinic connections

$$\kappa_{1,2} = [\xi_1 \to \xi_2] \subset P_{12}, \qquad \kappa_{2,3} = [\xi_2 \to \xi_3] \subset P_{23}, \qquad \kappa_{3,1} = [\xi_3 \to \xi_1] \subset P_{13},$$
$$\kappa_{2,4} = [\xi_2 \to \xi_4] \subset P_{24}, \qquad \kappa_{4,5} = [\xi_4 \to \xi_5] \subset P_{45}, \qquad \kappa_{5,2} = [\xi_5 \to \xi_2] \subset P_{25}.$$

As both heteroclinic cycles lie entirely in a three-dimensional fixed-point subspace and $-I \in \mathbb{Z}_2^5$ they are of type B_3^-, and so of type Z. They are simple heteroclinic cycles and naturally fulfill the definition of quasi-simple heteroclinic cycle.

We are interested in the stability of the individual heteroclinic cycles and the Bowtie network as a whole. For this purpose, consider the construction of partial and full return maps in Appendix C.1 describing the flow near the network. Castro and Lohse [19] have strategically labelled the nodes of the Bowtie network to provide a correspondence with the parameters pertaining to the heteroclinic cycles in the original Kirk and Silber [39] network. The R-cycle is exactly the ξ_3-cycle in [39] in such a way that parameters coincide.

It is well known that contraction maps are an essential tool for evaluating attraction properties of dynamical systems. By contraction map we mean the following:

Consider a set $D \subset \mathbb{R}^n$ and a map $g : D \to \mathbb{R}^n$. We say that g is a *contraction* on D if

- $g(D) \subseteq D$;
- there exists $0 < q < 1$ such that $\|g(\boldsymbol{x}) - g(\boldsymbol{y})\| \leq q\,\|\boldsymbol{x} - \boldsymbol{y}\|$ for all $\boldsymbol{x}, \boldsymbol{y} \in D$.

We next discuss whether or not the return maps associated with each heteroclinic cycle can be contractions.

Lemma 6.1.1. *Suppose that $\tilde{\rho}, \rho > 1$ and $e_{23} > e_{24}$. If $\tilde{\delta} > 0$, then the return maps $\tilde{\pi}_j$ around the R-cycle in* (C.1)–(C.3) *are contractions. If $\delta > 0$, then the return maps π_j around the L-cycle in* (C.4)–(C.6) *are contractions.*

Proof. We prove the claim only for the R-cycle; analogous considerations apply to the L-cycle. As $\tilde{\rho} > 1$ and $\tilde{\delta} > 0$ we have

$$\tilde{\nu} = \frac{e_{24}}{e_{23}}(\tilde{\rho} - 1) + \frac{c_{21}}{e_{23}}\tilde{\delta} > 0 \tag{6.2}$$

and

$$\tilde{\tau} = \tilde{\sigma}(\tilde{\rho}-1) + \frac{c_{13}}{e_{12}}\frac{c_{21}}{e_{23}}\tilde{\delta} = -\tilde{\sigma} + \tilde{\rho}\frac{c_{34}}{c_{32}} > 0, \tag{6.3}$$

regardless the sign of $\tilde{\sigma}$.[1] Combining with $\tilde{\theta}$, $\tilde{\mu}$, $\tilde{\gamma} > 0$ we deduce that $\tilde{\pi}_j$ in (C.1)–(C.3) are contracting in each component. What is left is to show that the domains of definition of $\tilde{\pi}_j$ are mapped into themselves. The return map $\tilde{\pi}_3$ in (C.3) is well-defined in the entire $H_3^{in,2}$ when $\tilde{\delta} > 0$ and so this is immediate. Now

$$\begin{aligned}
\tilde{\pi}_1(x_2, x_4, x_5) \in \mathrm{dom}(\tilde{\pi}_1) &\Leftrightarrow 0 \le x_4 < x_2^{\tilde{\sigma}\tilde{\rho}-\tilde{\tau}} \\
\tilde{\pi}_2(x_3, x_4, x_5) \in \mathrm{dom}(\tilde{\pi}_2) &\Leftrightarrow 0 \le x_4 < x_3^{\frac{e_{24}}{e_{23}}\tilde{\rho}-\tilde{\nu}}
\end{aligned}$$

implies that the regions delimited by each inequality in (C.1) and (C.2) are mapped into themselves if

$$\begin{array}{ccccc}
x_2^{\tilde{\rho}\tilde{\sigma}-\tilde{\tau}} > x_2^{\tilde{\sigma}} & \Leftrightarrow & \tilde{\sigma}\tilde{\rho} - \tilde{\tau} < \tilde{\sigma} & \Leftrightarrow & -\dfrac{c_{13}}{e_{12}}\dfrac{c_{21}}{e_{23}}\tilde{\delta} < 0 \\
x_3^{\frac{e_{24}}{e_{23}}\tilde{\rho}-\tilde{\nu}} > x_3^{\frac{e_{24}}{e_{23}}} & \Leftrightarrow & \dfrac{e_{24}}{e_{23}}\tilde{\rho} - \tilde{\nu} < \dfrac{e_{24}}{e_{23}} & \Leftrightarrow & -\dfrac{c_{21}}{e_{23}}\tilde{\delta} < 0.
\end{array}$$

Hence every $\tilde{\pi}_j$ in (C.1)–(C.3) is a contraction mapping under the condition $\tilde{\delta} > 0$. □

We use σ_{ij} to denote the local stability index at a point on $\kappa_{i,j}$ with respect to the appropriate heteroclinic cycle.

Proposition 6.1.2. *Suppose that $e_{23} > e_{24}$.*

(a) The local stability indices for the R-cycle are:

- *if either $\tilde{\rho} < 1$ or $\tilde{\delta} < 0$, then $\sigma_{12} = \sigma_{23} = \sigma_{31} = -\infty$;*
- *if $\tilde{\rho} > 1$ and $\tilde{\delta} > 0$, then*

$$\begin{aligned}
\sigma_{12} &= F^{\mathrm{index}}\left(-\frac{e_{24}}{e_{23}}, 1, 0\right) = \frac{e_{23}}{e_{24}} - 1 > 0, \\
\sigma_{23} &= +\infty, \\
\sigma_{31} &= F^{\mathrm{index}}(-\tilde{\sigma}, 1, 0) = \begin{cases} +\infty & \text{if } \tilde{\sigma} \le 0 \\ \dfrac{1}{\tilde{\sigma}} - 1 > 0 & \text{if } 0 < \tilde{\sigma} < 1 \\ -\tilde{\sigma} + 1 < 0 & \text{if } \tilde{\sigma} > 1. \end{cases}
\end{aligned}$$

(b) The local stability indices for the L-cycle are:

- *if either $\rho < 1$ or $\delta < 0$, then $\sigma_{52} = \sigma_{24} = \sigma_{45} = -\infty$;*

[1] Recall that the transverse eigenvalues are negative when possible. Hence $c_{34} > 0$.

- *if* $\rho > 1$ *and* $\delta > 0$*, then*

$$\sigma_{52} = F^{\text{index}}\left(-\frac{e_{23}}{e_{24}}, 0, 1\right) = -\frac{e_{24}}{e_{23}} + 1 < 0,$$
$$\sigma_{24} = +\infty,$$
$$\sigma_{45} = F^{\text{index}}(-\sigma, 0, 1) = \begin{cases} +\infty & \textit{if } \sigma \le 0 \\ \dfrac{1}{\sigma} - 1 > 0 & \textit{if } 0 < \sigma < 1 \\ \sigma + 1 < 0 & \textit{if } \sigma > 1. \end{cases}$$

Proof. We prove case (a); calculations for case (b) are identical.

The procedure is to apply Theorem 3.4.9. On account of Lemma 3.4.5 we need to check conditions *(i)–(iii)* of Lemma 3.3.3 for the transition matrix $\widetilde{M}^{(3)}$ in (C.8). Since this is a lower triangular matrix its eigenvalues are the entries in the main diagonal: $\lambda_1 = \tilde{\rho}$, $\lambda_2 = 1$ and $\lambda_3 = 1$. The associated eigenvectors are $\boldsymbol{w}^{1,3} = \left(\tilde{\rho} - 1, \tilde{\delta}, \tilde{\gamma}\right)$, $\boldsymbol{w}^{2,3} = (0,1,0)$ and $\boldsymbol{w}^{3,3} = (0,0,1)$. We see that condition *(i)* is trivially fulfilled but either *(ii)* or *(iii)* do not hold when either $\tilde{\rho} < 1$ or $\tilde{\delta} < 0$. Under these inequalities part (a) of Theorem 3.4.9 gives $\sigma_{12} = \sigma_{23} = \sigma_{31} = -\infty$.

Now $\widetilde{M}^{(3)}$ satisfies *(i)–(iii)* of Lemma 3.3.3 with $\lambda_{\max} = \lambda_1$ and $\boldsymbol{w}^{\max,3} = \boldsymbol{w}^{1,3}$ if $\tilde{\rho} > 1$ and $\tilde{\delta} > 0$. We illustrate how to compute σ_{12} along the heteroclinic connection $\kappa_{1,2}$. By virtue of (3.14) the matrices describing the local basin of attraction near ξ_2 are $\widetilde{M}_2$, $\widetilde{M}_3\widetilde{M}_2$ and $\widetilde{M}^{(2)} = \widetilde{M}_1\widetilde{M}_3\widetilde{M}_2$. From those only $\widetilde{M}_2$ has a basic transition matrix with negative entries as first factor. Besides $\boldsymbol{v}^{\max,2}$ defined in (3.19) Lemma 3.4.6 establishes that F^{index} must be evaluated at the lines of the matrix M_2 such that

$$\sigma_{12} = \min\left\{F^{\text{index}}\left(\boldsymbol{v}^{\max,2}\right), \min\left\{F^{\text{index}}\left(\frac{c_{21}}{e_{23}}, 0, 0\right), F^{\text{index}}\left(-\frac{e_{24}}{e_{23}}, 1, 0\right), F^{\text{index}}\left(\frac{c_{25}}{e_{23}}, 0, 1\right)\right\}\right\}.$$

A trivial verification shows that for each $j = 1,2,3$ the vector $\boldsymbol{v}^{\max,j}$ is multiple of

$$\left(\frac{1}{\tilde{\rho} - 1}, 0, 0\right).$$

Therefore $\boldsymbol{v}^{\max,j}$ has non-negative entries whenever $\tilde{\rho} > 1$. Lemma 3.4.8 further attests

$$F^{\text{index}}\left(\boldsymbol{v}^{\max,j}\right) = F^{\text{index}}\left(\frac{c_{21}}{e_{23}}, 0, 0\right) = F^{\text{index}}\left(\frac{c_{25}}{e_{23}}, 0, 1\right) = +\infty$$

so that

$$\sigma_{12} = F^{\text{index}}\left(-\frac{e_{24}}{e_{23}}, 1, 0\right) = \frac{e_{23}}{e_{24}} - 1 > 0.$$

Similar arguments lead to

$$\sigma_{23} = \min\left\{F^{\text{index}}\left(\boldsymbol{v}^{\max,3}\right), \min\left\{F^{\text{index}}(\tilde{\rho}, 0, 0), F^{\text{index}}(\tilde{\nu}, 1, 0), F^{\text{index}}(\tilde{\mu}, 0, 1)\right\}\right\}$$

and

$$\sigma_{31} = \min\left\{F^{\text{index}}\left(\boldsymbol{v}^{\max,1}\right), \min\left\{F^{\text{index}}\left(\frac{c_{21}}{e_{23}}\frac{c_{13}}{e_{12}},0,0\right), F^{\text{index}}\left(-\tilde{\sigma},1,0\right), F^{\text{index}}\left(\frac{c_{15}}{e_{12}}+\frac{c_{25}}{e_{23}}\frac{c_{13}}{e_{12}},0,1\right)\right\}\right\}.$$

Here the arguments other than $\boldsymbol{v}^{\max,3}$ and $\boldsymbol{v}^{\max,1}$ are respectively the lines of the matrices $\widetilde{M}^{(3)} = \widetilde{M}_2\widetilde{M}_1\widetilde{M}_3$ and $\widetilde{M}_2\widetilde{M}_1$. Recall that $\tilde{v} > 0$ when $\tilde{\rho} > 1$ and $\tilde{\delta} > 0$ from (6.2). Therefore

$$F^{\text{index}}\left(\tilde{\rho},0,0\right) = F^{\text{index}}\left(\tilde{v},1,0\right) = F^{\text{index}}\left(\tilde{\mu},0,1\right) = +\infty$$

as well as

$$F^{\text{index}}\left(\frac{c_{21}}{e_{23}}\frac{c_{13}}{e_{12}},0,0\right) = F^{\text{index}}\left(\frac{c_{15}}{e_{12}}+\frac{c_{25}}{e_{23}}\frac{c_{13}}{e_{12}},0,1\right) = +\infty.$$

It follows that

$$\sigma_{23} = +\infty \quad \text{and} \quad \sigma_{31} = F^{\text{index}}\left(-\tilde{\sigma},1,0\right).$$

□

The results above are depicted in Figure 6.1 and comparable with Propositions 5.2 and 5.3 in [17] concerning the local stability indices for the Kirk and Silber network. By imposing the same assumptions the Bowtie network provides greater freedom of the parameters because the sign of $\tilde{\sigma}$ (resp. $\tilde{\delta}$) becomes independent of that of σ (resp. δ).

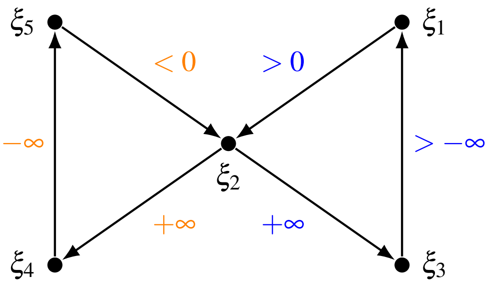

Fig. 6.1 The local stability indices for the Bowtie network when $\rho, \tilde{\rho} > 1$ and $\delta, \tilde{\delta} > 0$. The symbols "$< 0$" and "$> 0$" denote finite indices.

In the notation of [17] we have σ^n_{ij} to distinguish when the local stability index along $\kappa_{i,j}$ is calculated with respect to the whole heteroclinic network. The authors refer to it as an n-index.

Below we adhere to Footnote 4 in Chapter 3 introducing the factor $(1-\varepsilon)$ with $0 < \varepsilon < 1$ into the inequalities that define the domains of the local and return maps in Appendix C.1.

Proposition 6.1.3. *Suppose that $\tilde{\rho}, \rho > 1$ and $e_{23} > e_{24}$. If $\tilde{\delta} > 0$ and $\delta > 0$, then the local stability indices with respect to the Bowtie network are*

$$\sigma^n_{23} = \sigma^n_{24} = +\infty, \quad \sigma^n_{12},\ \sigma^n_{52} > 0, \quad \sigma^n_{31} = \begin{cases} +\infty & \text{if } \tilde{\sigma} \le 0 \\ > 0 & \text{if } \tilde{\sigma} > 0 \end{cases} \quad \text{and} \quad \sigma^n_{45} = \begin{cases} +\infty & \text{if } \sigma \le 0 \\ > 0 & \text{if } \sigma > 0. \end{cases}$$

Proof. Assume that $\tilde{\delta} > 0$ and $\delta > 0$. Lemma 2.4.6 together with Proposition 6.1.2 guarantee $\sigma_{23}^n = \sigma_{24}^n = +\infty$ and $\sigma_{12}^n > 0$. The remaining calculations run as in the proof of Lemma 5.4 of [17]. Return maps around both heteroclinic cycles are contractions by Lemma 6.1.1. Any trajectory that passes through their domains is then asymptotic to the corresponding heteroclinic cycle. It suffices to look at the set of points along each heteroclinic connection whose trajectories cross outside $\mathrm{dom}(\tilde{\pi}_2) \cup \mathrm{dom}(\pi_{RL}) \subset H_2^{in,1}$ or $\mathrm{dom}(\pi_2) \cup \mathrm{dom}(\pi_{LR}) \subset H_2^{in,5}$ whether starting near R or L, respectively.

We proceed by dealing with σ_{52}^n, σ_{45}^n and σ_{31}^n. For σ_{52}^n we examine the measure of $\mathscr{F}_0$ in $H_2^{in,5}$ across the heteroclinic connection $\kappa_{5,2}$ where

$$\begin{aligned}\mathscr{F}_0 &= \left\{(x_1,x_3,x_4) \in H_2^{in,5} : \ (x_1,x_3,x_4) \notin \mathrm{dom}(\pi_2) \cup \mathrm{dom}(\pi_{LR})\right\} \\ &= \left\{(x_1,x_3,x_4) \in H_2^{in,5} : \ (1-\varepsilon)^{-\frac{e_{23}}{e_{24}}} x_4^{\frac{e_{23}}{e_{24}}} \leq x_3 \leq (1-\varepsilon)\, x_4^{\frac{e_{23}}{e_{24}}}\right\}.\end{aligned} \tag{6.4}$$

Because this describes a thin cusp-shaped region we obtain $\sigma_{52}^n > 0$ and finite. To compute σ_{45}^n regard the set $\mathscr{G}_0$ in $H_5^{in,4}$ across the heteroclinic connection $\kappa_{4,5}$ where

$$\begin{aligned}\mathscr{G}_0 &= \left\{(x_1,x_2,x_3) \in H_5^{in,4} : \ g_5(x_1,x_2,x_3) \notin \mathrm{dom}(\pi_2) \cup \mathrm{dom}(\pi_{LR})\right\} \\ &= \left\{(x_1,x_2,x_3) \in H_5^{in,4} : \ (1-\varepsilon)^{-\frac{e_{23}}{e_{24}}} x_2^{\sigma} \leq x_3 \leq (1-\varepsilon)\, x_2^{\sigma}\right\}.\end{aligned} \tag{6.5}$$

It is clear that $\mathscr{G}_0$ is empty whenever $\sigma \leq 0$ and, in consequence, $\sigma_{45}^n = +\infty$. Otherwise $\sigma_{45}^n > 0$ and finite due to the fact that $\mathscr{G}_0$ depicts a thin cusp-shaped region for every $\sigma > 0$. Next σ_{31}^n is evaluated by means of the measure of $\mathscr{H}_0$ in $H_1^{in,3}$ across the heteroclinic connection $\kappa_{3,1}$ where

$$\begin{aligned}\mathscr{H}_0 &= \left\{(x_2,x_4,x_5) \in H_1^{in,3} : \ \tilde{g}_1(x_2,x_4,x_5) \notin \mathrm{dom}(\tilde{\pi}_2) \cup \mathrm{dom}(\pi_{RL})\right\} \\ &= \left\{(x_2,x_4,x_5) \in H_1^{in,3} : \ (1-\varepsilon)\, x_2^{\tilde{\sigma}} \leq x_4 \leq (1-\varepsilon)^{-\frac{e_{24}}{e_{23}}} x_2^{\tilde{\sigma}}\right\}.\end{aligned} \tag{6.6}$$

As before $\tilde{\sigma} \leq 0$ forces $\sigma_{31}^n = +\infty$, while $\tilde{\sigma} > 0$ forces $\sigma_{31}^n > 0$ and finite.

Notice also that σ_{12}^n is finite taking into account the region $\mathscr{I}_0$ in $H_2^{in,1}$ naturally excluded from the domains of $\tilde{\pi}_2$ and π_{RL}:

$$\begin{aligned}\mathscr{I}_0 &= \left\{(x_3,x_4,x_5) \in H_2^{in,1} : \ (x_1,x_4,x_5) \notin \mathrm{dom}(\tilde{\pi}_2) \cup \mathrm{dom}(\pi_{RL})\right\} \\ &= \left\{(x_3,x_4,x_5) \in H_2^{in,1} : \ (1-\varepsilon)\, x_3^{\frac{e_{24}}{e_{23}}} \leq x_4 \leq (1-\varepsilon)^{-\frac{e_{24}}{e_{23}}} x_3^{\frac{e_{24}}{e_{23}}}\right\}.\end{aligned} \tag{6.7}$$

□

Changing the sign of either $\tilde{\delta}$ or δ makes the Bowtie network less stable as shown next.

Proposition 6.1.4. *Suppose that $\tilde{\rho}, \rho > 1$ and $e_{23} > e_{24}$. If $\tilde{\delta}\delta < 0$, then the local stability indices with respect to the Bowtie network are*

- *if* $\tilde{\delta} < 0$ *and* $\delta > 0$, *then*

$$\sigma_{24}^n = +\infty, \quad \sigma_{23}^n,\, \sigma_{31}^n,\, \sigma_{12}^n,\, \sigma_{52}^n > 0 \quad \textit{and} \quad \sigma_{45}^n = \begin{cases} +\infty & \textit{if } \sigma \le 0 \\ > 0 & \textit{if } \sigma > 0; \end{cases}$$

- *if* $\tilde{\delta} > 0$ *and* $\delta < 0$, *then*

$$\sigma_{23}^n = +\infty, \quad \sigma_{24}^n,\, \sigma_{45}^n,\, \sigma_{12}^n,\, \sigma_{52}^n > 0 \quad \textit{and} \quad \sigma_{31}^n = \begin{cases} +\infty & \textit{if } \tilde{\sigma} \le 0 \\ > 0 & \textit{if } \tilde{\sigma} > 0. \end{cases}$$

Proof. Assume that $\tilde{\delta} < 0$ and $\delta > 0$. That $\sigma_{24}^n = +\infty$ follows directly from Lemma 2.4.6 and Proposition 6.1.2. Lemma 6.1.1 asserts that the return maps around the L-cycle are contractions. The values of σ_{52}^n and σ_{45}^n thus equal the ones in Proposition 6.1.3. All n-indices along the heteroclinic connections of the R-cycle can be handled in much the same way as in the proof of Lemma 3 of [39]. We must determine the set of points in each incoming cross section that are not attracted to the Bowtie network while trajectories through them move around R.

For σ_{31}^n we soon lose track of trajectories starting from $\mathscr{H}_0 \subset H_1^{in,3}$ in (6.6). Now $\mathscr{H}_0 \neq \emptyset$ as $\tilde{\sigma} > 0$ holds when $\tilde{\delta} < 0$. Given $k \in \mathbb{N}$ let us denote by $\mathscr{H}_k$ the kth preimage of $\mathscr{H}_0$ under $\tilde{\pi}_1$. We have

$$\begin{aligned} \mathscr{H}_1 &= \tilde{\pi}_1^{-1}(\mathscr{H}_0) \\ &= \left\{(x_2,x_4,x_5) \in H_1^{in,3} :\ (x_2,x_4,x_5) \in \operatorname{dom}(\tilde{\pi}_1) \text{ and } \tilde{\pi}_1(x_2,x_4,x_5) \in \mathscr{H}_0\right\} \\ &= \left\{(x_2,x_4,x_5) \in H_1^{in,3} :\ x_4 < (1-\varepsilon)x_2^{\tilde{\sigma}} \text{ and } (1-\varepsilon)x_2^{\tilde{\sigma}\tilde{\rho}-\tilde{\tau}} \le x_4 \le (1-\varepsilon)^{-\frac{e_{24}}{e_{23}}} x_2^{\tilde{\sigma}\tilde{\rho}-\tilde{\tau}}\right\}. \end{aligned} \tag{6.8}$$

Since $\tilde{\delta} < 0$, (6.3) shows that $\tilde{\sigma}\tilde{\rho} - \tilde{\tau} > \tilde{\sigma}$. The intersection of $\mathscr{H}_1$ with a sufficiently small neighbourhood of the origin is reduced to the second condition in (6.8). See Figure 6.2 where $\mathrm{Proj}_{2,4} : (x_2,x_4,x_5) \mapsto (x_2,x_4,0)$ denotes the projection mapping to the (x_2,x_4)-plane.

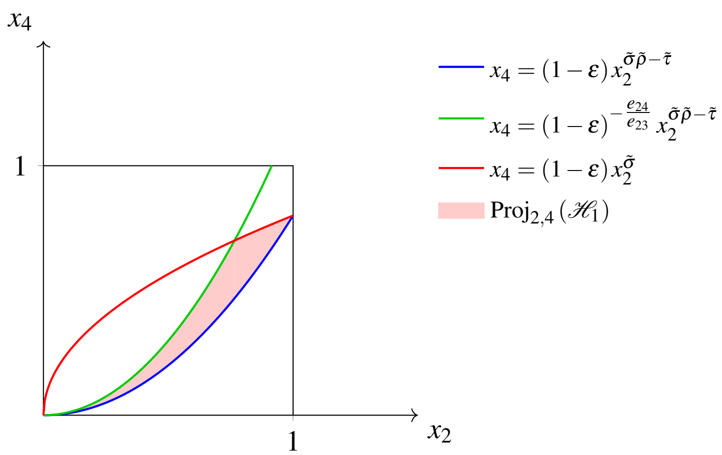

Fig. 6.2 Projection of $\mathscr{H}_1$ onto the (x_2,x_4)-plane within $H_1^{in,3}$.

Iteration of $\tilde{\pi}_1$ for $k \geq 2$ yields

$$\tilde{\pi}_1^k(x_2,x_4,x_5) = \left(x_2^{\tilde{\rho}^k}, x_4 x_2^{\tilde{\tau}\sum_{i=0}^{k-1}\tilde{\rho}^i}, x_5 x_2^{\tilde{\theta}\sum_{i=0}^{k-1}\tilde{\rho}^i} \right), \qquad 0 \leq x_4 < (1-\varepsilon)\, x_2^{\tilde{\sigma}\tilde{\rho}^{k-1}-\tilde{\tau}\sum_{i=0}^{k-2}\tilde{\rho}^i},$$

so that

$$\begin{aligned}
\mathscr{H}_k &= \tilde{\pi}_1^{-k}(\mathscr{H}_0) \\
&= \left\{ (x_2,x_4,x_5) \in H_1^{in,3} : \ (x_2,x_4,x_5) \in \mathrm{dom}\left(\tilde{\pi}_1^k\right) \text{ and } \tilde{\pi}_1^k(x_2,x_4,x_5) \in \mathscr{H}_0 \right\} \\
&= \Bigg\{ (x_2,x_4,x_5) \in H_1^{in,3} : \ x_4 < (1-\varepsilon)\, x_2^{\tilde{\sigma}\tilde{\rho}^{k-1}-\tilde{\tau}\sum_{i=0}^{k-2}\tilde{\rho}^i} \text{ and} \\
&\qquad (1-\varepsilon)\, x_2^{\tilde{\sigma}\tilde{\rho}^{k}-\tilde{\tau}\sum_{i=0}^{k-1}\tilde{\rho}^i} \leq x_4 \leq (1-\varepsilon)^{-\frac{e_{24}}{e_{23}}} x_2^{\tilde{\sigma}\tilde{\rho}^{k}-\tilde{\tau}\sum_{i=0}^{k-1}\tilde{\rho}^i} \Bigg\}.
\end{aligned}$$

All possible trajectories in $H_1^{in,3}$ that leave any neigbourhood of the Bowtie network are those that lie in $\bigcup_{k\in\mathbb{N}_0}\mathscr{H}_k$. The others belong to the basin of attraction of the heteroclinic network given by $\mathscr{B}(R\cup L)$ at which

$$\mathscr{B}(R\cup L)\cap B_\varepsilon(\mathbf{0}) = B_\varepsilon(\mathbf{0}) \setminus \bigcup_{k=0}^{\infty} \mathscr{H}_k$$

where $B_\varepsilon(\mathbf{0})$ is an open ε-ball around the origin in $H_1^{in,3}$. The sequence of exponents $(\alpha_k)_{k\in\mathbb{N}_0}$ with $\alpha_k = \tilde{\sigma}\tilde{\rho}^k - \tilde{\tau}\sum_{i=0}^{k-1}\tilde{\rho}^i$ is positive, monotonically increasing and unbounded because $\alpha_0 = \tilde{\sigma} > 0$ and

$$\begin{aligned}
\alpha_{k+1} - \alpha_k &= \tilde{\sigma}\tilde{\rho}^{k+1} - \tilde{\tau}\sum_{i=0}^{k}\tilde{\rho}^i - \left(\tilde{\sigma}\tilde{\rho}^k - \tilde{\tau}\sum_{i=0}^{k-1}\tilde{\rho}^i \right) \\
&= \tilde{\rho}^k(\tilde{\sigma}\tilde{\rho} - \tilde{\tau} - \tilde{\sigma}) \\
&= -\frac{c_{13}}{e_{12}}\frac{c_{21}}{e_{23}}\tilde{\delta}\tilde{\rho}^k > 0
\end{aligned}$$

whenever $\tilde{\rho} > 1$ and $\tilde{\delta} < 0$. Therefore we obtain $\sigma_{31}^n > 0$ by Lemma 2.4.7.

In the same manner to calculate σ_{12}^n we need the preimages of $\mathscr{I}_0 \subset H_2^{in,1}$ in (6.7) under the appropriate return map $\tilde{\pi}_2$. First

$$\begin{aligned}
\mathscr{I}_1 &= \tilde{\pi}_2^{-1}(\mathscr{I}_0) \\
&= \left\{ (x_3,x_4,x_5) \in H_2^{in,1} : \ (x_3,x_4,x_5) \in \mathrm{dom}(\tilde{\pi}_2) \text{ and } \tilde{\pi}_2(x_3,x_4,x_5) \in \mathscr{I}_0 \right\} \\
&= \left\{ (x_3,x_4,x_5) \in H_2^{in,1} : \ x_4 < (1-\varepsilon)\, x_3^{\frac{e_{24}}{e_{23}}} \text{ and } (1-\varepsilon)\, x_2^{\frac{e_{24}}{e_{23}}\tilde{\rho}-\tilde{\nu}} \leq x_4 \leq (1-\varepsilon)^{-\frac{e_{24}}{e_{23}}} x_2^{\frac{e_{24}}{e_{23}}\tilde{\rho}-\tilde{\nu}} \right\}.
\end{aligned}$$

With

$$\tilde{\pi}_2^k(x_3,x_4,x_5) = \left(x_3^{\tilde{\rho}^k}, x_4 x_3^{\tilde{\nu}\sum_{i=0}^{k-1}\tilde{\rho}^i}, x_5 x_3^{\tilde{\mu}\sum_{i=0}^{k-1}\tilde{\rho}^i} \right), \qquad 0 \leq x_4 < (1-\varepsilon)\, x_3^{\frac{e_{24}}{e_{23}}\tilde{\rho}^{k-1}-\tilde{\nu}\sum_{i=0}^{k-2}\tilde{\rho}^i},$$

we get

$$\begin{aligned}
\mathscr{I}_k &= \tilde{\pi}_2^{-k}(\mathscr{I}_0)\\
&= \left\{(x_3,x_4,x_5) \in H_2^{in,1} :\ (x_3,x_4,x_5) \in \mathrm{dom}\left(\tilde{\pi}_2^k\right) \text{ and } \tilde{\pi}_2^k(x_3,x_4,x_5) \in \mathscr{I}_0\right\}\\
&= \left\{ (x_3,x_4,x_5) \in H_2^{in,1} :\ x_4 < (1-\varepsilon)\, x_3^{\frac{e_{24}}{e_{23}}\tilde{\rho}^{k-1} - \tilde{\nu}\sum_{i=0}^{k-2}\tilde{\rho}^i} \text{ and} \right.\\
&\qquad \left. (1-\varepsilon)\, x_3^{\frac{e_{24}}{e_{23}}\tilde{\rho}^{k} - \tilde{\nu}\sum_{i=0}^{k-1}\tilde{\rho}^i} \le x_4 \le (1-\varepsilon)^{-\frac{e_{24}}{e_{23}}}\, x_3^{\frac{e_{24}}{e_{23}}\tilde{\rho}^{k} - \tilde{\nu}\sum_{i=0}^{k-1}\tilde{\rho}^i} \right\}.
\end{aligned}$$

But $(\beta_k)_{k\in\mathbb{N}_0}$ where $\beta_k = \dfrac{e_{24}}{e_{23}}\tilde{\rho}^k - \tilde{\nu}\sum_{i=0}^{k-1}\tilde{\rho}^i$ is an unbounded monotone increasing sequence since $\beta_0 = \dfrac{e_{24}}{e_{23}} > 0$ and

$$\begin{aligned}
\beta_{k+1} - \beta_k &= \frac{e_{24}}{e_{23}}\tilde{\rho}^{k+1} - \tilde{\nu}\sum_{i=0}^{k}\tilde{\rho}^i - \left(\frac{e_{24}}{e_{23}}\tilde{\rho}^{k} - \tilde{\nu}\sum_{i=0}^{k-1}\tilde{\rho}^i\right)\\
&= \tilde{\rho}^k\left(\frac{e_{24}}{e_{23}}\tilde{\rho} - \tilde{\nu} - \frac{e_{24}}{e_{23}}\right)\\
&= -\frac{c_{21}}{e_{23}}\tilde{\delta}\tilde{\rho}^k > 0.
\end{aligned}$$

Again by Lemma 2.4.7, it follows that $\sigma_{21}^n > 0$.

The last index remaining is σ_{23}^n. Similarly we determine the set $\mathscr{J}_0$ of points in $H_3^{in,2}$ that hit $H_2^{in,1}$ in neither $\mathrm{dom}(\tilde{\pi}_2)$ nor $\mathrm{dom}(\pi_{RL})$ and its preimages under $\tilde{\pi}_3$. We have

$$\begin{aligned}
\mathscr{J}_0 &= \left\{(x_1,x_4,x_5) \in H_3^{in,2} :\ \tilde{g}_1 \circ \tilde{g}_3(x_1,x_4,x_5) \notin \mathrm{dom}(\tilde{\pi}_2) \cup \mathrm{dom}(\pi_{RL})\right\}\\
&= \left\{(x_1,x_4,x_5) \in H_3^{in,2} :\ (1-\varepsilon)\, x_1^{-\tilde{\delta}} \le x_4 \le (1-\varepsilon)^{-\frac{e_{24}}{e_{23}}}\, x_1^{-\tilde{\delta}}\right\}
\end{aligned}$$

and

$$\begin{aligned}
\mathscr{J}_1 &= \tilde{\pi}_3^{-1}(\mathscr{J}_0)\\
&= \left\{(x_1,x_4,x_5) \in H_3^{in,2} :\ (x_1,x_4,x_5) \in \mathrm{dom}(\tilde{\pi}_3) \text{ and } \tilde{\pi}_3(x_1,x_4,x_5) \in \mathscr{J}_0\right\}\\
&= \left\{(x_1,x_4,x_5) \in H_3^{in,2} :\ x_4 < (1-\varepsilon)\, x_1^{-\tilde{\delta}} \text{ and } (1-\varepsilon)\, x_1^{-\tilde{\delta}\tilde{\rho}-\tilde{\delta}} \le x_4 \le (1-\varepsilon)^{-\frac{e_{24}}{e_{23}}}\, x_1^{-\tilde{\delta}\tilde{\rho}-\tilde{\delta}}\right\}.
\end{aligned}$$

For every $k \ge 2$ we write down

$$\tilde{\pi}_3^k(x_1,x_4,x_5) = \left(x_1^{\tilde{\rho}^k},\, x_4\, x_1^{\tilde{\delta}\sum_{i=0}^{k-1}\tilde{\rho}^i},\, x_5\, x_1^{\tilde{\gamma}\sum_{i=0}^{k-1}\tilde{\rho}^i}\right), \qquad 0 \le x_4 < (1-\varepsilon)\, x_1^{-\tilde{\delta}\sum_{i=0}^{k-1}\tilde{\rho}^i},$$

and so

$$
\begin{aligned}
\mathscr{J}_k &= \tilde{\pi}_3^{-k}\left(\mathscr{J}_0\right) \\
&= \left\{(x_1,x_4,x_5) \in H_3^{in,2} :\ (x_1,x_4,x_5) \in \operatorname{dom}\left(\tilde{\pi}_3^k\right) \text{ and } \tilde{\pi}_3^k(x_1,x_4,x_5) \in \mathscr{J}_0\right\} \\
&= \Bigg\{ (x_1,x_4,x_5) \in H_3^{in,2} :\ x_4 < (1-\varepsilon)\, x_1^{-\tilde{\delta}\sum_{i=0}^{k-1}\tilde{\rho}^i} \text{ and } \\
&\qquad\qquad (1-\varepsilon)\, x_1^{-\tilde{\delta}\sum_{i=0}^{k}\tilde{\rho}^i} \le x_4 \le (1-\varepsilon)^{-\frac{e_{24}}{e_{23}}}\, x_1^{-\tilde{\delta}\sum_{i=0}^{k}\tilde{\rho}^i} \Bigg\}.
\end{aligned}
$$

The sequence of exponents $(\gamma_k)_{k\in\mathbb{N}_0}$ with $\gamma_k = -\tilde{\delta}\sum_{i=0}^{k}\tilde{\rho}^i$ is positive and increases monotonically because $\gamma_0 = -\tilde{\delta} > 0$ and

$$
\begin{aligned}
\gamma_{k+1} - \gamma_k &= -\tilde{\delta}\sum_{i=0}^{k+1}\tilde{\rho}^i - \left(-\tilde{\delta}\sum_{i=0}^{k}\tilde{\rho}^i\right) \\
&= -\tilde{\delta}\tilde{\rho}^{k+1} > 0.
\end{aligned}
$$

Then, $\sigma_{23}^n > 0$ from Lemma 2.4.7.

The case $\tilde{\delta} > 0$ and $\delta < 0$ is analogous and we address it briefly. All return maps around the R-cycle are contractions according to Lemma 6.1.1. The associated n-indices are as in Proposition 6.1.3. For the L-cycle we compute σ_{52}^n, σ_{45}^n and σ_{24}^n using along each heteroclinic connection the sets of points whose trajectories next intersect the complement of $\operatorname{dom}(\pi_2) \cup \operatorname{dom}(\pi_{LR})$ in $H_2^{in,5}$. So they do not stay near the heteroclinic network any longer. These are, respectively, $\mathscr{F}_0 \subset H_2^{in,5}$ in (6.4), $\mathscr{G}_0 \subset H_5^{in,4}$ in (6.5) and

$$
\begin{aligned}
\mathscr{K}_0 &= \left\{(x_1,x_3,x_5) \in H_4^{in,2} :\ g_5 \circ g_4(x_1,x_3,x_5) \notin \operatorname{dom}(\pi_2) \cup \operatorname{dom}(\pi_{LR})\right\} \\
&= \left\{(x_1,x_3,x_5) \in H_4^{in,2} :\ (1-\varepsilon)\, x_5^{-\delta} \le x_3 \le (1-\varepsilon)^{-\frac{e_{23}}{e_{24}}}\, x_5^{-\delta}\right\}.
\end{aligned}
$$

In order to find all points that do not remain close to the heteroclinic network as they turn around L we take the preimages of the excluded sets under the appropriate return map. We have $\sigma > 0$ due to $\delta < 0$. By Lemma 2.4.7 we check at once that $\sigma_{52}^n, \sigma_{45}^n, \sigma_{24}^n > 0$. □

Proposition 6.1.5. *Suppose that $\tilde{\rho}, \rho > 1$ and $e_{23} > e_{24}$. If $\tilde{\delta} < 0$ and $\delta < 0$, then the local stability indices with respect to the Bowtie network are all positive and finite.*

Proof. Since $\tilde{\delta}$ and δ are independent the proof consists of joining the arguments applied to the R- and L-cycles in Proposition 6.1.4 given the imposed signs of the parameters. □

As a consequence of the last three results and Theorem 2.4.3 we establish the generic stability configuration of the Bowtie network.

Theorem 6.1.6. *Suppose that $\tilde{\rho}, \rho > 1$ and $e_{23} > e_{24}$. Then, the Bowtie network is e.a.s.*

The stability of the network as a whole is as robust a phenomenon in the Bowtie as in the Kirk and Silber network. In either case, it only depends on the magnitude of $\tilde{\rho}$ and ρ. However, unlike the Kirk and Silber network, in the Bowtie both heteroclinic cycles can be c.u while the whole heteroclinic network is e.a.s

6.2 The $\left(C_2^-, C_2^-\right)$-network

The $\left(C_2^-, C_2^-\right)$-network consists of two C_2^--cycles connected at two nodes related by symmetry, see Figure 6.3(a). It can be realised in $\mathbb{R}^6$ through the extension of the symmetry group that admits a single heteroclinic cycle of type C_2^- in $\mathbb{R}^4$, the latter found in [43, 56].

Consider a system of ordinary differential equations $\dot{\boldsymbol{x}} = f(\boldsymbol{x})$ where $\boldsymbol{x} = (x_1, x_2, x_3, x_4, x_5, x_6) \in \mathbb{R}^6$. We require $f : \mathbb{R}^6 \to \mathbb{R}^6$ to be a Γ-equivariant vector field with $\Gamma = \mathbb{Z}_2 \ltimes \mathbb{Z}_2^6$ generated by

$$\varphi : (x_1, x_2, x_3, x_4, x_5, x_6) \mapsto (x_4, x_5, x_6, x_1, x_2, x_3)$$

and

$$\gamma_j : x_j \mapsto -x_j, \quad j = 1, \ldots, 6.$$

The action of $\mathbb{Z}_2^6$ in $\mathbb{R}^6$ guarantees that each coordinate subspace is invariant under the flow. In particular, we only need to take the dynamics in the positive orthant. Let us denote

$$P_{ij} = \mathrm{Fix}\left(\mathbb{Z}_2^4(\gamma_k,\, k \neq i, j)\right) = \left\{\boldsymbol{x} \in \mathbb{R}^6 : x_k = 0 \text{ for all } k \neq i, j\right\} \qquad (i < j)$$

and

$$Q_{ijkl} = \mathrm{Fix}\left(\mathbb{Z}_2^2(\gamma_s,\, s \neq i, j, k, l)\right) = \left\{\boldsymbol{x} \in \mathbb{R}^6 : x_s = 0 \text{ for all } s \neq i, j, k, l\right\} \qquad (i < j < k < l).$$

We assume that there are six saddle-type equilibria ξ_j on the (positive) coordinate x_j-axes composing of two robust heteroclinic cycles

$$R = [\xi_1 \to \xi_2 \to \xi_4 \to \xi_5 \to \xi_1] \subset Q_{1245}$$
$$L = [\xi_2 \to \xi_3 \to \xi_5 \to \xi_6 \to \xi_2] \subset Q_{2356}.$$

Each heteroclinic connection $\kappa_{i,j} = [\xi_i \to \xi_j]$ belongs to the coordinate plane P_{ij} if $i < j$, or P_{ji} otherwise, such that ξ_j is a sink therein.

The heteroclinic cycles are invariant by the action of Γ. Given that $\xi_j = \varphi \xi_{j+3}$ we find the corresponding building blocks satisfying

$$\Gamma[\xi_1 \to \xi_2 \to \varphi\xi_1] = R$$
$$\Gamma[\xi_2 \to \xi_3 \to \varphi\xi_2] = L.$$

By construction, both heteroclinic cycles are contained in a four-dimensional fixed-point subspace of the form Q_{ijkl}. When restricting the representation of Γ to it they are of type C_2^- in the classification of [43]. We make use of the symmetry so that the original heteroclinic network quotients to a heteroclinic network with three nodes as illustrated in Figure 6.3(b). The quotient cycles are regarded as

$$R = [\xi_1 \to \xi_2 \to \xi_1]$$
$$L = [\xi_2 \to \xi_3 \to \xi_2].$$

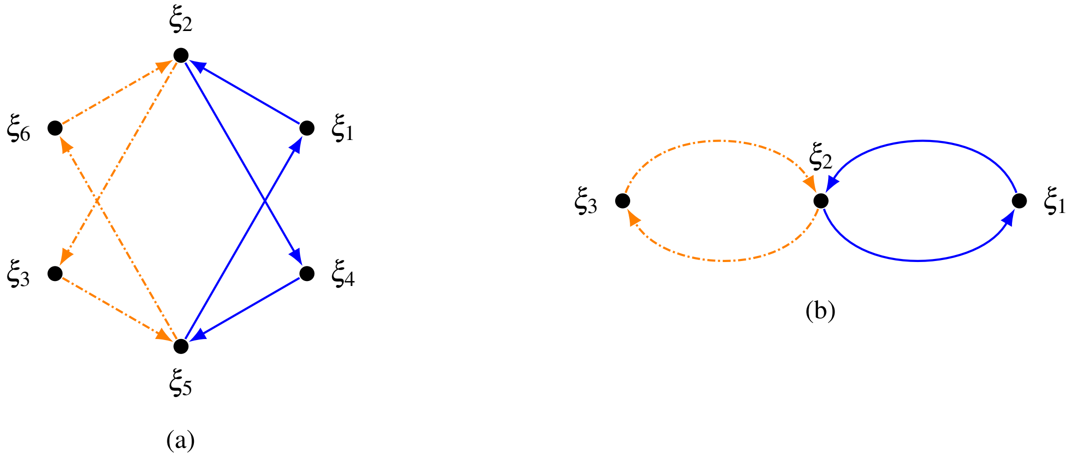

Fig. 6.3 (a) The $\left(\mathrm{C}_2^-,\mathrm{C}_2^-\right)$-network and (b) its quotient. The equilibria are such that $\xi_j = \varphi\xi_{j+3}$, $j = 1,2,3$, so the quotient network comprises of three relative equilibria.

All the information concerning the dynamic transitions near the $\left(\mathrm{C}_2^-,\mathrm{C}_2^-\right)$-network can be found in Appendix D.1. First we check Lemma 4.3.3 pointing out that all heteroclinic connections in this example are of type contracting-to-transverse. Write $F_{i,j,k}$ for the range of the local map $\phi_{i,j,k} : H_j^{in,i} \to H_j^{out,k}$ just as before. In $H_2^{out,4}$ we find

$$F_{1,2,4} = \left\{ (x_1,x_3,x_5,x_6) \in H_2^{out,4} : x_5 < x_1^{\frac{c_{25}}{c_{21}}} \text{ and } x_6 < x_1^{\frac{c_{26}}{c_{21}}} \right\}$$
$$F_{6,2,4} = \left\{ (x_1,x_3,x_5,x_6) \in H_2^{out,4} : x_1 < x_6^{\frac{c_{21}}{c_{26}}} \text{ and } x_5 < x_6^{\frac{c_{25}}{c_{26}}} \right\}.$$

Figure 6.4 shows how the F-sets are taken close to ξ_1 through $\phi_{5,1,2} \circ \psi_{2,1} : H_2^{out,4} \to H_1^{out,2}$. We consider the restriction of the sets to a convenient three-dimensional subspace. The transverse eigenspace at ξ_2 with respect to the R-cycle is spanned by x_3, x_5 and x_6. At the following node ξ_4 the expanding eigenspace is spanned by x_5. Every boundary of $F_{1,2,4}$ contained in the (x_1,x_3)- and (x_1,x_6)-faces are sent through $\phi_{5,1,2} \circ \psi_{2,1}$ to the origin of $H_1^{out,2}$. The cusp-shaped region that delimits $F_{1,2,4}$ in the (x_1,x_5)-face becomes a conic region in the (x_5,x_4)-face of $H_1^{out,2}$. A similar conclusion can be drawn for the transformation of $F_{6,2,4}$.

As the global map $\psi_{1,2} : H_1^{out,2} \to H_2^{in,1}$ is the identity we get directly the form of the range F_R under the return map $\pi_R \equiv \tilde{\pi}_2 : H_2^{in,1} \to H_2^{in,1}$ defined in (D.2). In fact, it corresponds to the blue cone-shaped region in Figure 6.4(b) and (d). Analytically, we have

$$F_R = \mathrm{im}\left(\tilde{g}_1\right) \cap \tilde{g}_1^*\left(\mathrm{im}\left(\tilde{g}_2\right)\right) = \psi_{1,2}\left(F_{5,1,2}\right) \cap \tilde{g}_1^*\left(\psi_{2,1}\left(F_{1,2,4}\right)\right).$$

The respective expressions in Appendix D.1 allow us to determine

$$\mathrm{im}\left(\tilde{g}_1\right) = \left\{ (x_3,x_4,x_5,x_6) \in H_2^{in,1} : x_3 < x_5^{\frac{c_{13}}{c_{15}}} \text{ and } x_4 < x_5^{\frac{c_{14}}{c_{15}}} \text{ and } x_6 < x_5^{\frac{c_{16}}{c_{15}}} \right\}$$
$$\tilde{g}_1^*\left(\mathrm{im}\left(\tilde{g}_2\right)\right) = \left\{ (x_3,x_4,x_5,x_6) \in H_2^{in,1} : x_4 > x_5^{\frac{c_{14}}{c_{15}} + \frac{e_{12}}{c_{15}}\frac{c_{21}}{c_{25}}} \text{ and } x_3 < x_4^{\frac{c_{26}}{c_{21}}} x_5^{\frac{c_{13}}{c_{15}} - \frac{c_{14}}{c_{15}}\frac{c_{26}}{c_{21}}} \right\}$$

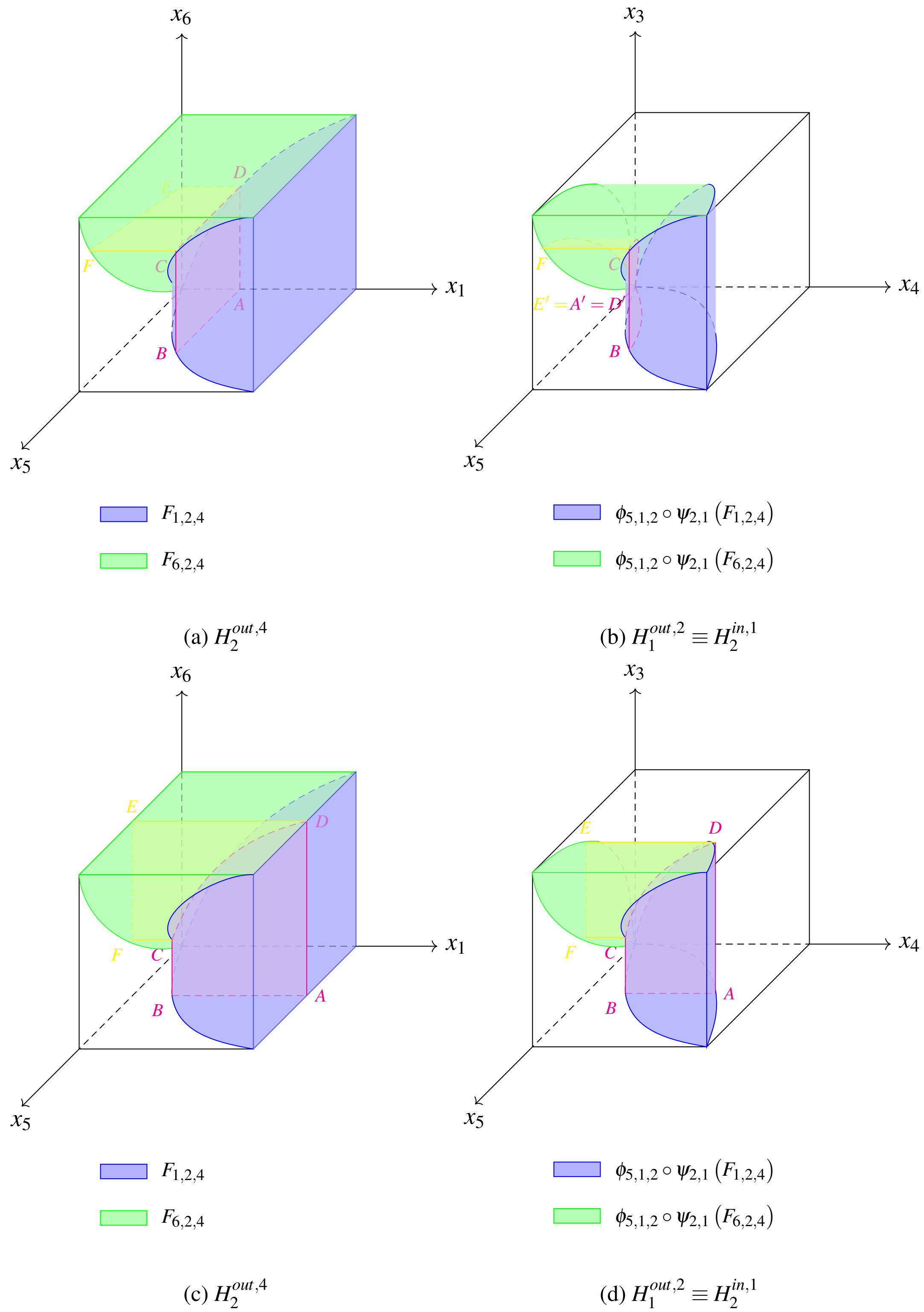

(a) $H_2^{out,4}$ (b) $H_1^{out,2} \equiv H_2^{in,1}$

(c) $H_2^{out,4}$ (d) $H_1^{out,2} \equiv H_2^{in,1}$

Fig. 6.4 Transformation of the F-sets near ξ_2 under $\phi_{5,1,2} \circ \psi_{2,1} : H_2^{out,4} \to H_1^{out,2}$ for the R-cycle in the $\left(C_2^-, C_2^-\right)$-network: the set $F_{1,2,4}$ of points coming from ξ_1 and the $F_{6,2,4}$ of points coming from ξ_6 on the left side, and their images under $\phi_{5,1,2} \circ \psi_{2,1}$ on the right side. (a) and (b) each square $[ABCD]$ on $x_1 = k$ is shrunk and transformed into a cusp-shaped surface $A'B'C'$ and each square $[CDEF]$ on $x_6 = k$ is shrunk and transformed into a cusp-shaped surface $C'D'F'$; (c) and (d) each surface $ABCD$ and $CDEF$ on $x_5 = k$ are shrunk and transformed into surfaces $A'B'C'D'$ and $C'D'E'F'$.

such that

$$F_R = \left\{ (x_3, x_4, x_5, x_6) \in H_2^{in,1} : x_3 < x_4^{\frac{c_{26}}{c_{21}}} x_5^{\frac{c_{13}}{c_{15}} - \frac{c_{14}}{c_{15}} \frac{c_{26}}{c_{21}}} \text{ and } x_5^{\frac{c_{14}}{c_{15}} + \frac{e_{12}}{c_{15}} \frac{c_{21}}{c_{25}}} < x_4 < x_5^{\frac{c_{14}}{c_{15}}} \text{ and } x_6 < x_5^{\frac{c_{16}}{c_{15}}} \right\}.$$

Figure 6.5 highlights F_R within $\operatorname{im}(\tilde{g}_1)$ restricted to the (x_3, x_4, x_5)-subspace of $H_2^{in,1}$. It is interesting to compare the set F_R with the analogous set for the Bowtie network in Figure 4.18. The shape of the sets is quite different and appears to depend on the type of the heteroclinic connections. Even so both are topologically identical to a cone.

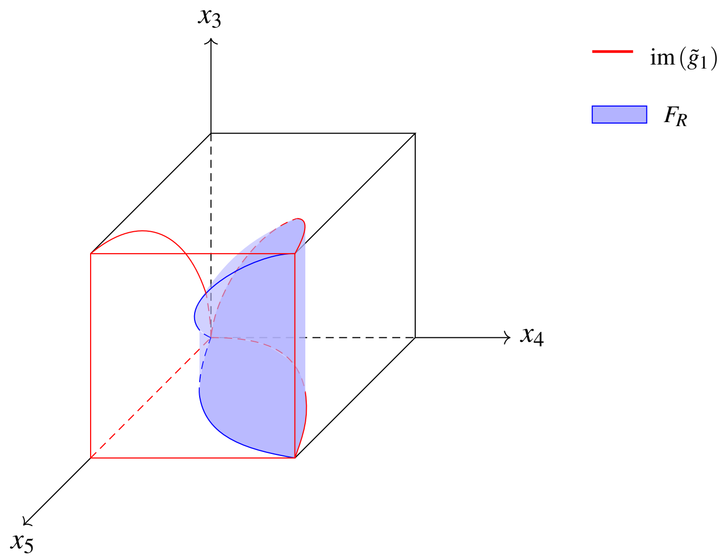

Fig. 6.5 The set F_R in $H_2^{in,1}$ for the $(\mathrm{C}_2^-, \mathrm{C}_2^-)$-network.

The following result provides the local stability indices of each heteroclinic cycle in the $(\mathrm{C}_2^-, \mathrm{C}_2^-)$-network. These are reproduced in Figure 6.6(a) when the indices are not all $-\infty$.

We continue to use σ_{ij} for the local stability index along the heteroclinic connection $\kappa_{i,j}$ with respect to the appropriate heteroclinic cycle.

Proposition 6.2.1. *Suppose that* $e_{23} < e_{24}$.

(a) The local stability indices for the R-cycle are:

- *if either*

$$\tilde{\alpha} + \frac{c_{21}}{e_{24}} < \min\left\{2, 1 + \frac{c_{21}}{e_{24}} \frac{c_{15}}{e_{12}}\right\},$$

  or $w_2^{\max,1} < 0$ *for the transition matrix* $\widetilde{M}^{(1)}$, *then* $\sigma_{12} = \sigma_{21} = -\infty$;

- *if*

$$\tilde{\alpha} + \frac{c_{21}}{e_{24}} > \min\left\{2, 1 + \frac{c_{21}}{e_{24}} \frac{c_{15}}{e_{12}}\right\},$$

and $w_4^{\max,1} > 0$ *for the transition matrix* $\widetilde{M}^{(1)}$*, then*

$$\sigma_{12} = F^{\text{index}}\left(1, -\frac{e_{23}}{e_{24}}, 0, 0\right) = \frac{e_{24}}{e_{23}} - 1 > 0$$

$$\sigma_{21} = F^{\text{index}}\left(\tilde{\delta}, 1, -\frac{e_{23}}{e_{24}}, 0\right) = \begin{cases} \dfrac{\tilde{\delta} + 1 - \dfrac{e_{23}}{e_{24}}}{\max\left\{\tilde{\delta}, 1\right\}} < 0 & \text{if } \tilde{\delta} + 1 - \dfrac{e_{23}}{e_{24}} < 0 \\ 0 & \text{if } \tilde{\delta} + 1 - \dfrac{e_{23}}{e_{24}} = 0 \\ \dfrac{-\tilde{\delta} - 1 + \dfrac{e_{23}}{e_{24}}}{\min\left\{\tilde{\delta}, -\dfrac{e_{23}}{e_{24}}\right\}} > 0 & \text{if } \tilde{\delta} + 1 - \dfrac{e_{23}}{e_{24}} > 0. \end{cases}$$

(b) The local stability indices for the L-cycle are:

- *if either*

$$\alpha + \frac{c_{26}}{e_{23}} < \min\left\{2, 1 + \frac{c_{26}}{e_{23}} \frac{c_{32}}{e_{35}}\right\},$$

or $w_1^{\max,3} < 0$ *for the transition matrix* $M^{(3)}$*, then* $\sigma_{32} = \sigma_{23} = -\infty$*;*

- *if*

$$\alpha + \frac{c_{26}}{e_{23}} > \min\left\{2, 1 + \frac{c_{26}}{e_{23}} \frac{c_{32}}{e_{35}}\right\},$$

and $w_2^{\max,3} > 0$ *for the transition matrix* $M^{(3)}$*, then*

$$\sigma_{32} = F^{\text{index}}\left(0, -\frac{e_{24}}{e_{23}}, 1, 0\right) = 1 - \frac{e_{24}}{e_{23}} < 0$$

$$\sigma_{23} = F^{\text{index}}\left(1, 0, \delta, -\frac{e_{24}}{e_{23}}\right) = \begin{cases} \dfrac{1 + \delta - \dfrac{e_{24}}{e_{23}}}{\max\left\{\delta, 1\right\}} < 0 & \text{if } 1 + \delta - \dfrac{e_{24}}{e_{23}} < 0 \\ 0 & \text{if } 1 + \delta - \dfrac{e_{24}}{e_{23}} = 0 \\ \dfrac{-1 - \delta + \dfrac{e_{24}}{e_{23}}}{\min\left\{\delta, -\dfrac{e_{24}}{e_{23}}\right\}} > 0 & \text{if } 1 + \delta - \dfrac{e_{24}}{e_{23}} > 0. \end{cases}$$

Proof. We give the proof only for the case (a); similar arguments apply to the case (b).

In line with Theorem 3.4.9 we must find when conditions *(i)–(iii)* of Lemma 3.3.3 for the transition matrix $\widetilde{M}^{(1)}$ in (D.3) are satisfied. The eigenvalues of $\widetilde{M}^{(1)}$ are the roots of the characteristic polynomial

$$p(\lambda) = (\lambda - 1)(\lambda + 1)\left[\lambda^2 - \left(\tilde{\alpha} + \frac{c_{21}}{e_{24}}\right)\lambda + \frac{c_{21}}{e_{24}}\tilde{\alpha} - \frac{c_{25}}{e_{24}}\tilde{\beta}\right]$$

with

$$\frac{c_{21}}{e_{24}}\tilde{\alpha} - \frac{c_{25}}{e_{24}}\tilde{\beta} = -\frac{c_{21}}{e_{24}}\frac{c_{15}}{e_{12}}.$$

They are $\lambda_1 = 1$, $\lambda_2 = -1$,

$$\lambda_3 = \frac{\tilde{\alpha} + \dfrac{c_{21}}{e_{24}} + \sqrt{\left(\tilde{\alpha} - \dfrac{c_{21}}{e_{24}}\right)^2 + 4\dfrac{c_{25}}{e_{24}}\tilde{\beta}}}{2}$$

and

$$\lambda_4 = \frac{\tilde{\alpha} + \dfrac{c_{21}}{e_{24}} - \sqrt{\left(\tilde{\alpha} - \dfrac{c_{21}}{e_{24}}\right)^2 + 4\dfrac{c_{25}}{e_{24}}\tilde{\beta}}}{2}.$$

Since $\tilde{\beta} > 0$ we have $\lambda_i \in \mathbb{R}$ for all $i = 1,2,3,4$, and condition *(i)* is immediate. The candidate for $\lambda_{\max}$, the maximum eigenvalue in absolute value of $\widetilde{M}^{(1)}$, is λ_3. In particular, $\lambda_3 > |\lambda_4|$ because $\tilde{\alpha} + \dfrac{c_{21}}{e_{24}} > 0$. Observe that λ_3 and λ_4 are also the eigenvalues of the 2×2 submatrix

$$\begin{bmatrix} \tilde{\alpha} & \dfrac{c_{25}}{e_{24}} \\ \tilde{\beta} & \dfrac{c_{21}}{e_{24}} \end{bmatrix}.$$

By Lemma B.2 in [53] we know that $\lambda_3 > 1$ if and only if

$$\max\left\{\frac{\tilde{\alpha} + \dfrac{c_{21}}{e_{24}}}{2}, \tilde{\alpha} + \frac{c_{21}}{e_{24}} - \frac{c_{21}}{e_{24}}\frac{c_{15}}{e_{12}}\right\} > 1, \tag{6.9}$$

which is equivalent to

$$\tilde{\alpha} + \frac{c_{21}}{e_{24}} > \min\left\{2, 1 + \frac{c_{21}}{e_{24}}\frac{c_{15}}{e_{12}}\right\}.$$

Denote by $\boldsymbol{w}^{3,1} = \left(w_1^{3,1}, w_2^{3,1}, w_3^{3,1}, w_4^{3,1}\right)$ the eigenvector of $\widetilde{M}^{(1)}$ associated with the eigenvalue λ_3. Simple algebra attests that

$$\begin{aligned}
w_1^{3,1} &= \frac{c_{25}}{e_{24}}\left(\lambda_3^2 - 1\right) \\
w_2^{3,1} &= \frac{c_{25}}{e_{24}}\left(\tilde{\delta} + \lambda_3\tilde{\eta}\right) + (\lambda_3 - \tilde{\alpha})\left(-\frac{e_{23}}{e_{24}} + \frac{c_{26}}{e_{24}}\lambda_3\right) \\
w_3^{3,1} &= (\lambda_3 - \tilde{\alpha})\left(\lambda_3^2 - 1\right) \\
w_4^{3,1} &= \frac{c_{25}}{e_{24}}\left(\lambda_3\tilde{\delta} + \tilde{\eta}\right) + (\lambda_3 - \tilde{\alpha})\left(-\frac{e_{23}}{e_{24}}\lambda_3 + \frac{c_{26}}{e_{24}}\right)
\end{aligned}$$

and

$$\lambda_3 - \tilde{\alpha} = \frac{-\tilde{\alpha} + \dfrac{c_{21}}{e_{24}} + \sqrt{\left(\tilde{\alpha} - \dfrac{c_{21}}{e_{24}}\right)^2 + 4\dfrac{c_{25}}{e_{24}}\tilde{\beta}}}{2} > \frac{-\tilde{\alpha} + \dfrac{c_{21}}{e_{24}} + \left|\tilde{\alpha} - \dfrac{c_{21}}{e_{24}}\right|}{2} \geq 0.$$

Hence the first and third components of $\boldsymbol{w}^{3,1}$ are always positive whenever $\lambda_3 > 1$. The same is not so obvious for the second and fourth components of $\boldsymbol{w}^{3,1}$. But, from the relation $\widetilde{M}^{(1)}\boldsymbol{w}^{3,1} = \lambda_3 \boldsymbol{w}^{3,1}$, we have seen that

$$\tilde{\eta} w_1^{3,1} + \frac{c_{26}}{e_{24}} w_3^{3,1} + w_4^{3,1} = \lambda_3 w_2^{3,1}.$$

If $\lambda_3 > 1$, then $\tilde{\eta} w_1^{3,1} + \frac{c_{26}}{e_{24}} w_3^{3,1} > 0$ and $w_4^{3,1} > 0$ implies $w_2^{3,1} > 0$. We deduce that condition *(iii)* of Lemma 3.3.3 is violated for either $\lambda_3 < 1$, namely (6.9) does not hold, or $w_2^{3,1} < 0$. These restrictions leads to $\sigma_{12} = \sigma_{21} = -\infty$ according to part (a) of Theorem 3.4.9.

On the contrary, $\widetilde{M}^{(1)}$ satisfies *(i)–(iii)* of Lemma 3.3.3 with $\lambda_{\max} = \lambda_3$ and $\boldsymbol{w}^{\max,1} = \boldsymbol{w}^{3,1}$ provided (6.9) is true and $w_4^{3,1} > 0$. We further calculate the local stability indices along the heteroclinic connections of R. For σ_{12} we consider the matrices $\widetilde{M}_2$ and $\widetilde{M}^{(2)} = \widetilde{M}_1 \widetilde{M}_2$ whose transition starts near ξ_2. Lemma 3.4.6 states that

$$\begin{aligned}\sigma_{12} = \min\Bigg\{ & F^{\text{index}}\left(\boldsymbol{v}^{\max,2}\right), \\ & \min\left\{F^{\text{index}}\left(0, \frac{c_{25}}{e_{24}}, 1, 0\right), F^{\text{index}}\left(0, \frac{c_{26}}{e_{24}}, 0, 1\right), F^{\text{index}}\left(0, \frac{c_{21}}{e_{24}}, 0, 0\right), \right. \\ & \left. F^{\text{index}}\left(1, -\frac{e_{23}}{e_{24}}, 0, 0\right)\right\}\Bigg\},\end{aligned}$$

where $\boldsymbol{v}^{\max,2}$ is the vector defined in (3.19) and the remaining arguments are the lines of the matrix $\widetilde{M}_2$. It is easy to check that $\boldsymbol{v}^{\max,2}$ is multiple of

$$\left(0, \frac{e_{12}}{c_{14}} \frac{\tilde{\mu} - \lambda_4}{(\lambda_3 - \lambda_4)\left(\lambda_3^2 - 1\right)}, \frac{1}{(\lambda_3 - \lambda_4)\left(\lambda_3^2 - 1\right)}, 0\right).$$

By similarity $\widetilde{M}^{(1)}$ and $\widetilde{M}^{(2)}$ have equal eigenvalues in such a way that λ_i, $i = 3, 4$, is also expressed as

$$\lambda_{3,4} = \frac{\tilde{\mu} + \frac{c_{15}}{e_{12}} \pm \sqrt{\left(\tilde{\mu} - \frac{c_{15}}{e_{12}}\right)^2 + 4\frac{c_{14}}{e_{12}}\tilde{\rho}}}{2}.$$

Then,

$$\tilde{\mu} - \lambda_4 = \frac{\tilde{\mu} - \frac{c_{15}}{e_{12}} + \sqrt{\left(\tilde{\mu} - \frac{c_{15}}{e_{12}}\right)^2 + 4\frac{c_{14}}{e_{12}}\tilde{\rho}}}{2} > \frac{\tilde{\mu} - \frac{c_{15}}{e_{12}} + \left|\tilde{\mu} - \frac{c_{15}}{e_{12}}\right|}{2} \geq 0.$$

We can certainly take $\boldsymbol{v}^{\max,2}$ with non-negative entries because $\lambda_3 > \lambda_4$. We now employ Lemma 3.4.8 yielding

$$F^{\text{index}}\left(\boldsymbol{v}^{\max,2}\right) = F^{\text{index}}\left(0, \frac{c_{25}}{e_{24}}, 1, 0\right) = F^{\text{index}}\left(0, \frac{c_{26}}{e_{24}}, 0, 1\right) = F^{\text{index}}\left(0, \frac{c_{21}}{e_{24}}, 0, 0\right) = +\infty$$

and

$$\sigma_{12} = F^{\text{index}}\left(1, -\frac{e_{23}}{e_{24}}, 0, 0\right) = \frac{e_{24}}{e_{23}} - 1 > 0.$$

In the same manner we find

$$\sigma_{21} = \min\Big\{F^{\text{index}}\left(\boldsymbol{v}^{\max,1}\right),\\ \min\Big\{F^{\text{index}}\left(\tilde{\alpha},0,\frac{c_{25}}{e_{24}},0\right),F^{\text{index}}\left(\tilde{\eta},0,\frac{c_{26}}{e_{24}},1\right),F^{\text{index}}\left(\tilde{\beta},0,\frac{c_{21}}{e_{24}},0\right),\\ F^{\text{index}}\left(\tilde{\delta},1,-\frac{e_{23}}{e_{24}},0\right)\Big\}\Big\},$$

the vector $\boldsymbol{v}^{\max,1}$ being multiple of

$$\left(\frac{e_{24}}{c_{25}}\frac{\tilde{\alpha}-\lambda_4}{(\lambda_3-\lambda_4)\left(\lambda_3^2-1\right)},0,\frac{1}{(\lambda_3-\lambda_4)\left(\lambda_3^2-1\right)},0\right)$$

with

$$\tilde{\alpha}-\lambda_4 = \frac{\tilde{\alpha}-\frac{c_{21}}{e_{24}}+\sqrt{\left(\tilde{\alpha}-\frac{c_{21}}{e_{24}}\right)^2+4\frac{c_{25}}{e_{24}}\tilde{\beta}}}{2} > \frac{\tilde{\alpha}-\frac{c_{21}}{e_{24}}+\left|\tilde{\alpha}-\frac{c_{21}}{e_{24}}\right|}{2} \geq 0.$$

As a result

$$F^{\text{index}}\left(\boldsymbol{v}^{\max,1}\right) = F^{\text{index}}\left(\tilde{\alpha},0,\frac{c_{25}}{e_{24}},0\right) = F^{\text{index}}\left(\tilde{\eta},0,\frac{c_{26}}{e_{24}},1\right) = F^{\text{index}}\left(\tilde{\beta},0,\frac{c_{21}}{e_{24}},0\right) = +\infty$$

and

$$\sigma_{21} = F^{\text{index}}\left(\tilde{\delta},1,-\frac{e_{23}}{e_{24}},0\right).$$

□

The graph in Figure 6.3(b) may represent the translated $\left(\mathrm{B}_2^+,\mathrm{B}_2^+\right)$-network of Section 3.5 wherein the shared heteroclinic connection is reduced to a node. Fix here $\xi_b = \xi_2$. Its existence is supported in $\mathbb{R}^5$ by the cylinder realisation in [13] as well. The local stability indices for the new R and L-cycles coincide respectively with the ones for the so-called C_2 and C_3-cycles in Lemma 3.5.1. The same graph describes two heteroclinic networks whose corresponding heteroclinic cycles can hold different levels of attraction. In fact, under the stability of the heteroclinic cycles the indices σ_{21} an σ_{23} for the $\left(\mathrm{C}_2^-,\mathrm{C}_2^-\right)$-network assign any value in $(-\infty,+\infty)$. Those exhibit the strongest form of local stability

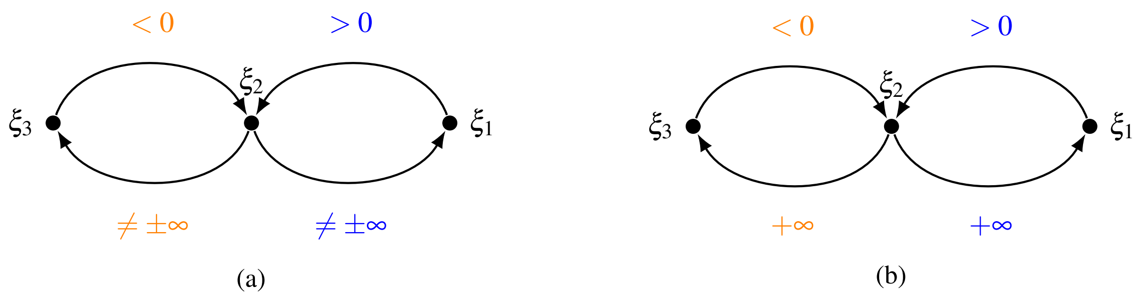

Fig. 6.6 The local stability indices for (a) the $\left(\mathrm{C}_2^-,\mathrm{C}_2^-\right)$-network in Proposition 6.2.1 and (b) the translated $\left(\mathrm{B}_2^+,\mathrm{B}_2^+\right)$-network in Lemma 3.5.1. The symbols "< 0" and "> 0" denote finite indices.

in the presence of heteroclinic cycles of type B_2^+, see Figure 6.6(b). Calculations in [53] suggest that single type-B and type-C cycles in $\mathbb{R}^4$ distinguish themselves by its local stability indices.

We end this section by examining the conditions that induce switching along one heteroclinic cycle in the $\left(\mathrm{C}_2^-,\mathrm{C}_2^-\right)$-network, say the R-cycle.

Lemma 6.2.2. *There is switching along the R-cycle in the* $\left(\mathrm{C}_2^-,\mathrm{C}_2^-\right)$*-network if and only if*

$$\frac{c_{13}}{c_{14}} < \frac{e_{23}}{e_{24}} < \frac{\tilde{\theta}}{\tilde{\mu}} \qquad \text{or} \qquad \frac{\tilde{\theta}}{\tilde{\mu}} < \frac{e_{23}}{e_{24}} < \frac{c_{13}}{c_{14}}.$$

Proof. Switching along the R-cycle occurs if and only if $\tilde{g}_1\left(\psi_{2,1}\left(F_{i,2,4}\right)\right) \cap C_{1,2,k} \neq \emptyset$ with $i = 1,6$ and $k = 3,4$. Using information of Appendix D.1 we find

$$C_{1,2,3} = \left\{ (x_3,x_4,x_5,x_6) \in H_2^{in,1} : x_4 < x_3^{\frac{e_{24}}{e_{23}}} \right\}$$
$$C_{1,2,4} = \left\{ (x_3,x_4,x_5,x_6) \in H_2^{in,1} : x_3 < x_4^{\frac{e_{23}}{e_{24}}} \right\}$$

and

$$\tilde{g}_1\left(\psi_{2,1}\left(F_{1,2,4}\right)\right) = \left\{ (x_3,x_4,x_5,x_6) \in H_2^{in,1} : x_3 < x_4^{\frac{c_{26}}{c_{21}}} x_5^{\frac{c_{13}}{c_{15}} - \frac{c_{14}}{c_{15}}\frac{c_{26}}{c_{21}}} \right.$$
$$\left. \text{and } x_5^{\frac{c_{14}}{c_{15}} + \frac{e_{12}}{c_{15}}\frac{c_{21}}{c_{25}}} < x_4 < x_5^{\frac{c_{14}}{c_{15}}} \text{ and } x_6 < x_5^{\frac{c_{16}}{c_{15}}} \right\}$$
$$\tilde{g}_1\left(\psi_{2,1}\left(F_{6,2,4}\right)\right) = \left\{ (x_3,x_4,x_5,x_6) \in H_2^{in,1} : x_4 < x_3^{\frac{c_{21}}{c_{26}}} x_5^{\frac{c_{14}}{c_{15}} - \frac{c_{13}}{c_{15}}\frac{c_{21}}{c_{26}}} \right.$$
$$\left. \text{and } x_5^{\frac{c_{13}}{c_{15}} + \frac{e_{12}}{c_{15}}\frac{c_{26}}{c_{25}}} < x_3 < x_5^{\frac{c_{13}}{c_{15}}} \text{ and } x_6 < x_5^{\frac{c_{16}}{c_{15}}} \right\}.$$

It is worth pointing out that $C_{1,2,4}$ and $\tilde{g}_1\left(\psi_{2,1}\left(F_{1,2,4}\right)\right)$ are respectively the domain and the range of the return map $\pi_R \equiv \tilde{\pi}_2 = \tilde{g}_1 \circ \tilde{g}_2 : H_2^{in,1} \to H_2^{in,1}$ around R. Moreover, the sets $\tilde{g}_1\left(\psi_{2,1}\left(F_{1,2,4}\right)\right)$ and

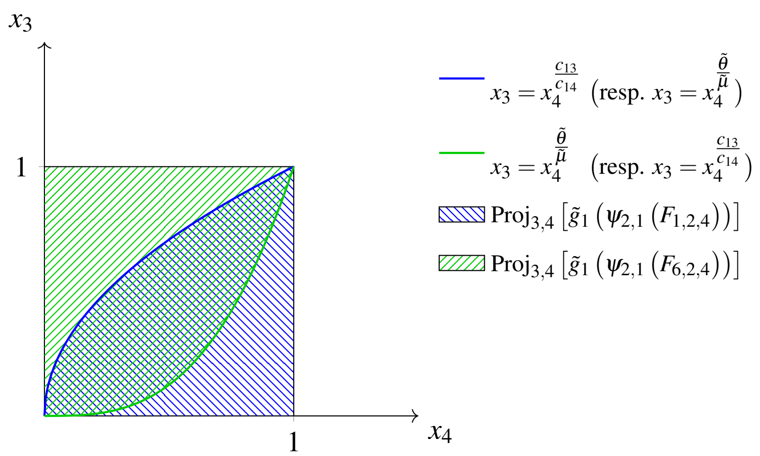

Fig. 6.7 Projection of $\tilde{g}_1\left(\psi_{2,1}\left(F_{i,2,4}\right)\right)$, $i = 1,6$, onto the (x_3,x_4)-plane within $H_2^{in,1}$.

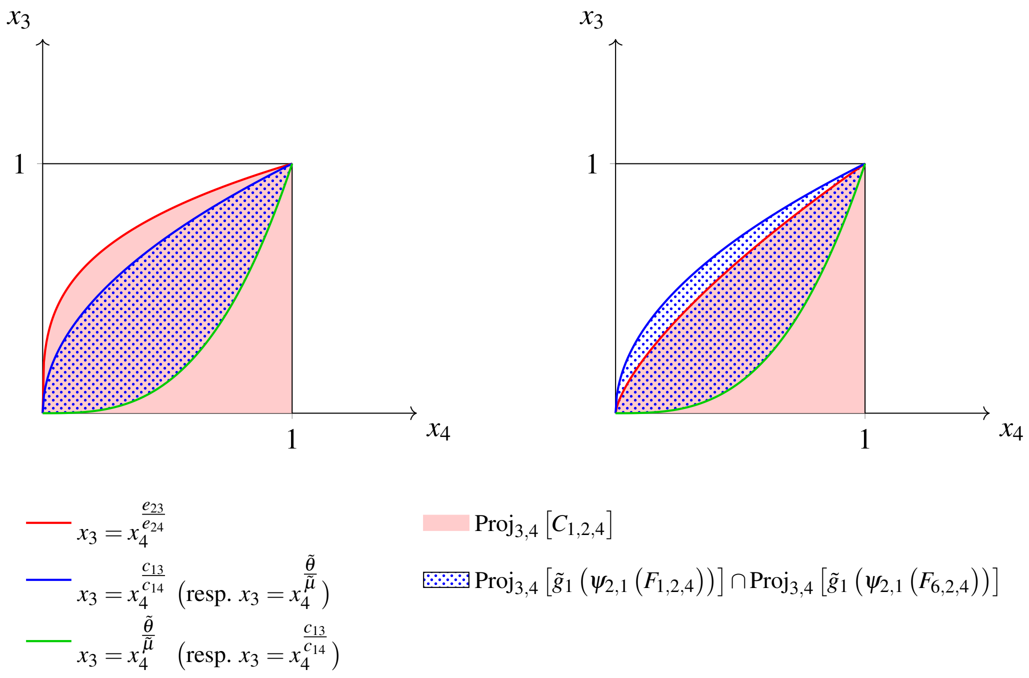

Fig. 6.8 Intersection of the projected sets $\tilde{g}_1\left(\psi_{2,1}\left(F_{1,2,4}\right)\right)$ and $\tilde{g}_1\left(\psi_{2,1}\left(F_{6,2,4}\right)\right)$ with $C_{1,2,4}$ on the (x_3,x_4)-plane within $H_2^{in,1}$. On the left side $\tilde{g}_1\left(\psi_{2,1}\left(F_{1,2,4}\right)\right)$ is contained in $C_{1,2,4}$ and then $\tilde{g}_1\left(\psi_{2,1}\left(F_{1,2,4}\right)\right) \cap C_{1,2,3} = \emptyset$. On the right side $\tilde{g}_1\left(\psi_{2,1}\left(F_{i,2,4}\right)\right) \cap C_{1,2,k} \neq \emptyset$, $i = 1,6$ and $k = 3,4$.

$\tilde{g}_1\left(\psi_{2,1}\left(F_{6,2,4}\right)\right)$ coincide geometrically with the blue and green cone-shaped regions in Figure 6.4(b) and (d).

In order to determine the desired intersections we project on the (x_3,x_4)-plane the boundary curves that separate $\tilde{g}_1\left(\psi_{2,1}\left(F_{1,2,4}\right)\right)$ from $\tilde{g}_1\left(\psi_{2,1}\left(F_{6,2,4}\right)\right)$ inside $H_2^{in,1}$. The latter are

$$\begin{cases} x_3 = x_4^{\frac{c_{26}}{c_{21}}} x_5^{\frac{c_{13}}{c_{15}} - \frac{c_{14}}{c_{15}}\frac{c_{26}}{c_{21}}} \\ x_4 = x_5^{\frac{c_{14}}{c_{15}} + \frac{e_{12}}{c_{15}}\frac{c_{21}}{c_{25}}} \end{cases} \Leftrightarrow x_3 = x_4^{\frac{\tilde{\theta}}{\tilde{\mu}}} \qquad \text{and} \qquad \begin{cases} x_3 = x_4^{\frac{c_{26}}{c_{21}}} x_5^{\frac{c_{13}}{c_{15}} - \frac{c_{14}}{c_{15}}\frac{c_{26}}{c_{21}}} \\ x_4 = x_5^{\frac{c_{14}}{c_{15}}} \end{cases} \Leftrightarrow x_3 = x_4^{\frac{c_{13}}{c_{14}}}.$$

Regardless of the relation between such curves the projection of $\tilde{g}_1\left(\psi_{2,1}\left(F_{i,2,4}\right)\right)$, $i = 1,6$, on the (x_3,x_4)-plane has the configuration of Figure 6.7. Let $\mathrm{Proj}_{3,4} : (x_3,x_4,x_5,x_6) \mapsto (x_3,x_4,0,0)$ be the projection mapping to the (x_3,x_4)-subspace. It suffices to check when $\mathrm{Proj}_{3,4}\left[\tilde{g}_1\left(\psi_{2,1}\left(F_{1,2,4}\right)\right)\right] \cap \mathrm{Proj}_{3,4}\left[\tilde{g}_1\left(\psi_{2,1}\left(F_{6,2,4}\right)\right)\right] \cap \mathrm{Proj}_{3,4}\left[C_{1,2,4}\right] \neq \emptyset$ because we take $C_{1,2,3}$ as the complement of $C_{1,2,4}$ in $H_2^{in,1}$. Figure 6.8 depicts two possible situations. Of course the one capable of inducing switching along the R-cycle is that on the right. This occus whenever

$$x_4^{\frac{\tilde{\theta}}{\tilde{\mu}}} < x_4^{\frac{e_{23}}{e_{24}}} < x_4^{\frac{c_{13}}{c_{14}}} \Leftrightarrow \frac{\tilde{\theta}}{\tilde{\mu}} > \frac{e_{23}}{e_{24}} > \frac{c_{13}}{c_{14}}$$

or

$$x_4^{\frac{c_{13}}{c_{14}}} < x_4^{\frac{e_{23}}{e_{24}}} < x_4^{\frac{\tilde{\theta}}{\tilde{\mu}}} \Leftrightarrow \frac{c_{13}}{c_{14}} > \frac{e_{23}}{e_{24}} > \frac{\tilde{\theta}}{\tilde{\mu}}.$$

$\square$

In Lemma 4.3.10 we have seen that switching along the R-cycle in the Bowtie network occurs whenever the condition $\tilde{\delta} < 0$ is satisfied. This implies that the R-cycle is c.u from Proposition 6.1.2. We notice that, unlike for the Bowtie network, the conditions for the existence of switching in Lemma 6.2.2 appear to be unrelated to those for the stability of each heteroclinic cycle.

Chapter 7

Conclusions and Prospects

We conclude this work by answering to our research questions:

Q1. YES **Q2.** NO

Our first aim was to provide a systematic study of the stability of robust heteroclinic cycles made up of one-dimensional heteroclinic connections and hyperbolic non-resonant saddle equilibria (Chapter 3). In the context of systems with symmetry such heteroclinic cycles are known as simple heteroclinic cycles. We started by introducing a new class of heteroclinic cycles bringing together the desired chacteristics in other settings than the symmetric one. We called it quasi-simple heteroclinic cycles. In order to address the stability of a quasi-simple heteroclinic cycle we quantified the stability of the individual heteroclinic connections using the local stability index of Podvigina and Ashwin [53]. Application of this tool in heteroclinic dynamics has been actually limited to simple heteroclinic cycles in dimension four. We then took advantage of its potential and showed that the calculations can be performed for a much wider collection of heteroclinic cycles. To be specific we developed a method that, under one mild assumption, yields an explicit expression for the values of the local stability index at a point of a heteroclinic connection in a quasi-simple heteroclinic cycle. Assumption 3.2.1 guarantees that the dynamics between incoming cross sections at consecutive nodes can be accurately approximated using basic transition matrices.[1] They are crucial to implement the methodical procedure. In fact, our results still hold as long as such a matricial representation exists whether or not the assumption is satisfied. We constructed a function that assigns to each vector the local stability index of a flow-invariant set whose basin of attraction is locally bounded by a power curve. Its exponents are the entries of the vector output. According to the geometry of the local basin of attraction of a quasi-simple heteroclinic cycle we obtained the local stability index along one of its heteroclinic connections by applying this function to the rows of some transition matrices. These are at most as many as the number of heteroclinic connections.

We have confirmed the views of [53, p. 910] in that "transition matrices can be used to study the stability of simple cycles in higher-dimensional systems" while contradicting their expectation that "we expect such a classification to be so complex that the results can hardly be enlightening". Of course our method recovers results previously obtained by other authors for simple heteroclinic cycles in dimension four.

[1] The form of a basic transition matrix is given in (3.8).

Our second aim was to prove the absence of infinite switching near a heteroclinic network involving a finite number of hyperbolic non-resonant saddle equilibria whose linearisation has only real eigenvalues (Chapter 4). It was achieved by looking at the different form of stability of a heteroclinic cycle within a heteroclinic network and of the whole heteroclinic network. Along the way, we addressed the construction of quasi-simple heteroclinic cycles according to the type of their heteroclinic connections. This provides quite simple examples of interesting dynamics and allows us to compose them in heteroclinic networks. The absence of infinite switching does not preclude weaker forms of switching. Considering two quasi-simple heteroclinic cycles connected either by a heteroclinic connection or by a node we examined the occurrence of switching at nodes, along heteroclinic connections, and along an entire heteroclinic cycle.

We illustrated our results with a two-person parametrised RSP game (Chapter 5) and two abstract examples (Chapter 6). The former was in fact the motivation behind this work. We saw that the dynamics and stability properties of the RSP cycles in the quotient network depend strongly on the parameters describing the rewards for ties. We proved that only the heteroclinic cycle where the two agents alternate in winning and losing can be e.a.s. This is in accordance with the numerical simulations of Sato et al. [64], which show this heteroclinic cycle as possessing some attracting properties (see Figure 15 on the top therein). An interpretation of the results adds to the understanding of the game and its applications. However those are so far constrained to a single population of individuals rather than the strategic interaction of two (or more) independent individuals or populations. We then proposed an application to a real-world economic problem of the two-person RSP game. We hope that this first approach and its results can open the door to further research in this context.

This work has a potentially novel and useful contribution to the stability and dynamics of robust heteroclinic cycles in systems with or without symmetry. Examples of heteroclinic cycles falling into quasi-simple but not simple category are abundant in the literature, namely from game theory, population dynamics, winnerless competition or Lotka-Volterra-type models, and coupled cells systems. Many interesting questions concerning dynamics have a natural starting point in the study of stability. For example, stability can provide a description of the dynamics near a heteroclinic cycle in a heteroclinic network. Stability is also essential in the study of bifurcations from heteroclinic cycles. We believe that our results may give insight to others working on stability and dynamics in nonlinear dynamical systems.

Some suggestions for future work concern the following comments and open questions:

1. Roslan and Ashwin [62] have distinguished the stability index of an attractor at a point from the global stability index of an attractor as a set. For a class of piecewise expanding linear skew product maps Corrolary 2.1 in [62] relates these two measures. Can we relate similarly the stability index of a heteroclinic cycle at a point with the global stability index of the heteroclinic cycle as a whole? We guess that an e.a.s heteroclinic cycle would be equivalent to a positive global stability index.

2. Assumption 3.2.1 can be weakened such that the global maps consist of a linear transformation. This is satisfied, for instance, by simple heteroclinic cycles of type A. It would be interesting to extend our results in such a case for understanding the stability of those heteroclinic cycles.

3. We have focused on real eigenvalues at nodes. Can we calculate systematically the local stability index for heteroclinic connections of a heteroclinic cycle or network involving at least one node with complex eigenvalues?

4. We have supported the construction of quasi-simple heteroclinic cycles in the simplex and cylinder realisations of [13]. Specifically in the latter heteroclinic connections are contained in different coordinate planes such that the entire heteroclinic cycle is embedded in a vector space of dimension one plus the number of heteroclinic connections. How can we optimise the cylinder method in order to use the minimum number of planes?

5. The design of an algorithm to compute directly the local stability index along a heteroclinic connection in line with our method would be very useful mainly for systems in higher dimensions.

References

[1] Afraimovich, V. S., Rabinovich, M. I., and Varona, P. (2004a). Heteroclinic contours in neural ensembles and the winnerless competition principle. *International Journal of Bifurcation and Chaos*, 14(04):1195–1208.

[2] Afraimovich, V. S., Zhigulin, V. P., and Rabinovich, M. I. (2004b). On the origin of reproducible sequential activity in neural circuits. *Chaos: An Interdisciplinary Journal of Nonlinear Science*, 14(4):1123–1129.

[3] Aguiar, M. A. D. (2011). Is there switching for replicator dynamics and bimatrix games? *Physica D: Nonlinear Phenomena*, 240(18):1475–1488.

[4] Aguiar, M. A. D., Ashwin, P., Dias, A., and Field, M. J. (2010a). Dynamics of coupled cell networks: Synchrony, heteroclinic cycles and inflation. *Journal of Nonlinear Science*, 21(2):271–323.

[5] Aguiar, M. A. D. and Castro, S. B. S. D. (2010). Chaotic switching in a two-person game. *Physica D: Nonlinear Phenomena*, 239(16):1598–1609.

[6] Aguiar, M. A. D., Castro, S. B. S. D., and Labouriau, I. S. (2005). Dynamics near a heteroclinic network. *Nonlinearity*, 18(1):391–414.

[7] Aguiar, M. A. D., Labouriau, I. S., and Rodrigues, A. A. P. (2010b). Switching near a network of rotating nodes. *Dynamical Systems*, 25(1):75–95.

[8] Armbruster, D., Stone, E., and Kirk, V. (2003). Noisy heteroclinic networks. *Chaos*, 13(1):71–79.

[9] Arnold, L. G. (2000). Stability of the market equilibrium in Romer's model of endogenous technological change: A complete characterization. *Journal of Macroeconomics*, 22(1):69–84.

[10] Ashwin, P. and Chossat, P. (1998). Attractors for robust heteroclinic cycles with continua of connections. *Journal of Nonlinear Science*, 8(2):103–129.

[11] Ashwin, P. and Field, M. J. (1999). Heteroclinic networks in coupled cell systems. *Archive for Rational Mechanics and Analysis*, 148(2):107–143.

[12] Ashwin, P., Karabacak, O., and Nowotny, T. (2011). Criteria for robustness of heteroclinic cycles in neural microcircuits. *The Journal of Mathematical Neuroscience*, 1(1):13.

[13] Ashwin, P. and Postlethwaite, C. M. (2013). On designing heteroclinic networks from graphs. *Physica D: Nonlinear Phenomena*, 265:26–39.

[14] Ashwin, P. and Postlethwaite, C. M. (2015). Designing heteroclinic and excitable networks in phase space using two populations of coupled cells. *Journal of Nonlinear Science*, 26(2):345–364.

[15] Brannath, W. (1994). Heteroclinic networks on the tetrahedron. *Nonlinearity*, 7(5):1367–1384.

[16] Busse, F. H. and Heikes, K. E. (1980). Convection in a rotating layer: A simple case of turbulence. *Science*, 208(4440):173–175.

[17] Castro, S. B. S. D. and Lohse, A. (2014). Stability in simple heteroclinic networks in $\mathbb{R}^4$. *Dynamical Systems*, 29(4):451–481.

[18] Castro, S. B. S. D. and Lohse, A. (2016a). Construction of heteroclinic networks in $\mathbb{R}^4$. *Nonlinearity*, 29(12):3677–3695.

[19] Castro, S. B. S. D. and Lohse, A. (2016b). Switching in heteroclinic networks. *SIAM Journal on Applied Dynamical Systems*, 15(2):1085–1103.

[20] Chossat, P., Krupa, M., Melbourne, I., and Scheel, A. (1997). Transverse bifurcations of homoclinic cycles. *Physica D: Nonlinear Phenomena*, 100(1-2):85–100.

[21] Chossat, P., Krupa, M., Melbourne, I., and Scheel, A. (1999). Magnetic dynamos in rotating convection - a dynamical systems approach. *Dynamics of Continuous, Discrete and Impulsive Systems*, 5:327–340.

[22] Chossat, P. and Lauterbach, R. (2000). *Methods in Equivariant Bifurcations and Dynamical Systems (Advanced Series in Nonlinear Dynamics)*. World Scientific Publishing Company.

[23] Field, M. (1980). Equivariant dynamical systems. *Transactions of the American Mathematical Society*, 259(1):185–205.

[24] Field, M. and Swift, J. W. (1991). Stationary bifurcation to limit cycles and heteroclinic cycles. *Nonlinearity*, 4(4):1001–1043.

[25] Field, M. J. (2015). Heteroclinic networks in homogeneous and heterogeneous identical cell systems. *Journal of Nonlinear Science*, 25(3):779–813.

[26] Field, M. J. (2017). Patterns of desynchronization and resynchronization in heteroclinic networks. *Nonlinearity*, 30(2):516–557.

[27] Garrido-da-Silva, L. and Castro, S. B. S. D. (2018a). Cyclic dominance in a two-person Rock-Scissors-Paper game. *arXiv:1607.08748*, pages 1–30.

[28] Garrido-da-Silva, L. and Castro, S. B. S. D. (2018b). Stability of quasi-simple heteroclinic cycles. *Dynamical Systems*, 0(0):1–26.

[29] Golubitsky, M., Stewart, I., and Schaeffer, D. G. (1988). *Singularities and Groups in Bifurcation Theory*, volume II. Springer New York.

[30] Guckenheimer, J. and Holmes, P. (1988). Structurally stable heteroclinic cycles. *Mathematical Proceedings of the Cambridge Philosophical Society*, 103(1):189–192.

[31] Hawker, D. and Ashwin, P. (2005). Classification of robust heteroclinic cycles for vector fields with symmetry. *Journal of Physics A: Mathematical and General*, 38(39):8319–8335.

[32] Hofbauer, J. (1994). Heteroclinic cycles in ecological differential equations. In Brunovský, P. and Medved', M., editors, *Proceedings of the EQUADIFF 8*, volume 4, pages 105–116. Tatra Mountains Mathematical Publications.

[33] Hofbauer, J. and Sigmund, K. (1998). *Evolutionary games and population dynamics*. Cambridge University Press, Cambridge.

[34] Homburg, A. J. and Knobloch, J. (2010). Switching homoclinic networks. *Dynamical Systems*, 25(3):351–358.

[35] Hopkins, E. and Seymour, R. M. (2002). The stability of price dispersion under seller and consumer learning. *International Economic Review*, 43(4):1157–1190.

[36] Keller, G. (2014). Stability index for chaotically driven concave maps. *Journal of the London Mathematical Society*, 89(2):603–622.

[37] Kirk, V., Lane, E., Postlethwaite, C. M., Rucklidge, A. M., and Silber, M. (2010). A mechanism for switching near a heteroclinic network. *Dynamical Systems*, 25(3):323–349.

[38] Kirk, V. and Rucklidge, A. M. (2008). The effect of symmetry breaking on the dynamics near a structurally stable heteroclinic cycle between equilibria and a periodic orbit. *Dynamical Systems*, 23(1):43–74.

[39] Kirk, V. and Silber, M. (1994). A competition between heteroclinic cycles. *Nonlinearity*, 7(6):1605–1621.

[40] Krupa, M. (1997). Robust heteroclinic cycles. *Journal of Nonlinear Science*, 7(2):129–176.

[41] Krupa, M. and Melbourne, I. (1995a). Asymptotic stability of heteroclinic cycles in systems with symmetry. *Ergodic Theory and Dynamical Systems*, 15(01):121–147.

[42] Krupa, M. and Melbourne, I. (1995b). Nonasymptotically stable attractors in $O(2)$ mode interactions. In *Normal forms and homoclinic chaos (Waterloo, ON, 1992)*, volume 4 of *Fields Inst. Commun.*, pages 219–232. Amer. Math. Soc., Providence, RI.

[43] Krupa, M. and Melbourne, I. (2004). Asymptotic stability of heteroclinic cycles in systems with symmetry II. *Proceedings of the Royal Society of Edinburgh: Section A Mathematics*, 134(06):1177–1197.

[44] Labouriau, I. S. and Rodrigues, A. A. P. (2012). Global generic dynamics close to symmetry. *Journal of Differential Equations*, 253(8):2527–2557.

[45] Lohse, A. (2014). *Attraction properties and non-asymptotic stability of simple heteroclinic cycles and networks in* $\mathbb{R}^4$. PhD thesis, University of Hamburg.

[46] Lohse, A. (2015). Stability of heteroclinic cycles in transverse bifurcations. *Physica D: Nonlinear Phenomena*, 310:95–103.

[47] May, R. M. and Leonard, W. J. (1975). Nonlinear aspects of competition between three species. *SIAM Journal on Applied Mathematics*, 29(2):243–253.

[48] Melbourne, I. (1991). An example of a nonasymptotically stable attractor. *Nonlinearity*, 4(3):835–844.

[49] Melbourne, I., Proctor, M., and Rucklidge, A. (2001). A heteroclinic model of geodynamo reversals and excursions. In Chossat, P., Ambruster, D., and Oprea, I., editors, *Dynamo and Dynamics, a Mathematical Challenge*, pages 363–370. Springer Netherlands, Dordrecht.

[50] Noel, M. D. (2007a). Edgeworth price cycles, cost-based pricing, and sticky pricing in retail gasoline markets. *The Review of Economics and Statistics*, 89(2):324–334.

[51] Noel, M. D. (2007b). Edgeworth price cycles: Evidence from the Toronto retail gasoline market. *The Journal of Industrial Economics*, 55(1):69–92.

[52] Podvigina, O. (2012). Stability and bifurcations of heteroclinic cycles of type Z. *Nonlinearity*, 25(6):1887–1917.

[53] Podvigina, O. and Ashwin, P. (2011). On local attraction properties and a stability index for heteroclinic connections. *Nonlinearity*, 24(3):887–929.

[54] Podvigina, O., Castro, S. B. S. D., and Labouriau, I. S. (2018). Stability of a heteroclinic network and its cycles: a case study from Boussinesq convection. *Dynamical Systems*, 0(0):1–37.

[55] Podvigina, O. and Chossat, P. (2015). Simple heteroclinic cycles in $\mathbb{R}^4$. *Nonlinearity*, 28(4):901–926.

[56] Postlethwaite, C. M. (2010). A new mechanism for stability loss from a heteroclinic cycle. *Dynamical Systems*, 25(3):305–322.

[57] Postlethwaite, C. M. and Dawes, J. H. P. (2005). Regular and irregular cycling near a heteroclinic network. *Nonlinearity*, 18(4):1477–1509.

[58] Reis, G. L. d. (1978). Structural stability of equivariant vector fields. *Anais da Academia Brasileira de Ciencias*, 50(3):273–276.

[59] Rodrigues, A. A. (2013). Persistent switching near a heteroclinic model for the geodynamo problem. *Chaos, Solitons & Fractals*, 47:73–86.

[60] Rodrigues, A. A. P. (2016). Is there switching without suspended horseshoes? In Patrício, J. P., das Neves, J. S., and Florentino, C., editors, *Boletim da Sociedade Portuguesa de Matemática*, volume 74, pages 61–80. Sociedade Portuguesa de Matemática, Lisboa.

[61] Rodrigues, A. A. P. and Labouriau, I. S. (2014). Spiralling dynamics near heteroclinic networks. *Physica D: Nonlinear Phenomena*, 268:34–49.

[62] Roslan, U. A. M. and Ashwin, P. (2016). Local and global stability indices for a riddled basin attractor of a piecewise linear map. *Dynamical Systems*, 31(3):375–392.

[63] Ruelle, D. (1989). *Elements of Differentiable Dynamics and Bifurcation Theory*. Academic Press.

[64] Sato, Y., Akiyama, E., and Crutchfield, J. P. (2005). Stability and diversity in collective adaptation. *Physica D: Nonlinear Phenomena*, 210(12):21–57.

[65] Sinervo, B. and Lively, C. M. (1996). The rock–paper–scissors game and the evolution of alternative male strategies. *Nature*, 380:240–243.

[66] Varian, H. R. (1980). A model of sales. *The American Economic Review*, 70(4):651–659.

Appendix A

The function F^{index}

A.1 Proof of Lemma 3.4.8

Consider a return map $\pi \equiv \pi_1 : \mathbb{R}^N \to \mathbb{R}^N$ associated with a point on a heteroclinic connection that intersects H_1^{in}. For small $\delta > 0$, let $\mathscr{B}_\delta^\pi$ be the δ-local basin of attraction of $\mathbf{0} \in \mathbb{R}^N$ for the map π.

Given $\boldsymbol{\alpha} = (\alpha_1, \alpha_2, \ldots, \alpha_N) \in \mathbb{R}^N$, suppose that $\mathscr{B}_\delta^\pi$ in H_1^{in} in the new coordinates (3.5) is $U_R(\boldsymbol{\alpha}; \mathbf{0}; \ldots; \mathbf{0})$ for some large $R < 0$. Since the measure of a set is always regarded as its measure in the original variables, we represent the latter set in original coordinates $(w, \boldsymbol{z}) = (x_1, x_2, \ldots, x_N) \equiv \boldsymbol{x}$ as $\tilde{U}_R(\boldsymbol{\alpha})$. Then,

$$\tilde{U}_R(\boldsymbol{\alpha}) = \left\{ \boldsymbol{x} \in \tilde{U}_R : \left| x_1^{\alpha_1} x_2^{\alpha_2} \cdots x_N^{\alpha_N} \right| < 1 \right\}. \tag{A.1}$$

where

$$\tilde{U}_R = \left\{ \boldsymbol{x} : \max_i \; |x_i| < \mathrm{e}^R \right\}.$$

In particular, the set $\tilde{U}_R$ is an open ball of radius $\varepsilon = \mathrm{e}^R > 0$ centred at $\mathbf{0} \in \mathbb{R}^N$ for the maximum norm. Hence, by virtue of Definition 3.4.7, the value of $F^{\text{index}}(\boldsymbol{\alpha}) = F^+(\boldsymbol{\alpha}) - F^-(\boldsymbol{\alpha})$ quantifies the local extent of $\tilde{U}_R(\boldsymbol{\alpha})$ such that

$$F^-(\boldsymbol{\alpha}) = \lim_{R \to -\infty} \frac{\ln(\Sigma_R)}{R}, \qquad F^+(\boldsymbol{\alpha}) = \lim_{R \to -\infty} \frac{\ln(1 - \Sigma_R)}{R}$$

with

$$\Sigma_R = \frac{\ell\left(\tilde{U}_R(\boldsymbol{\alpha})\right)}{\ell\left(\tilde{U}_R\right)}.$$

Notice that the region in $\mathbb{R}^N$ determined by the whole $\tilde{U}_R(\boldsymbol{\alpha})$ is invariant with respect to the reflections $x_j \mapsto -x_j$, $j = 1, \ldots, N$. Thus, we only consider $\boldsymbol{x} \in \mathbb{R}_+^N$. Define $\alpha_{\min} = \min_{i=1,\ldots,N} \alpha_i$. The construction of F^+ proceeds in three cases.

Case 1: If $\alpha_{\min} \geq 0$, then $\alpha_i \geq 0$ for all $i = 1, \ldots, N$. Given (A.1), we have $\alpha_i > 0$ for at least one $i = 1, \ldots, N$. Then, for sufficiently large negative R, $\tilde{U}_R(\boldsymbol{\alpha})$ is reduced to $\tilde{U}_R$. Thus, $\Sigma_R = 1$ and $F^+(\boldsymbol{\alpha}) = +\infty$.

Case 2: If $\alpha_{\min} < 0$ and $\sum_{i=1}^{N} \alpha_i > 0$, then there exist $K \geq 1$ and $i_1, \ldots, i_K \in \{1, \ldots, N\}$ such that $\alpha_{i_1}, \ldots, \alpha_{i_K} < 0$ and $\alpha_i \geq 0$ for any $i \neq i_1, \ldots, i_K$ or $\alpha_{i_1}, \ldots, \alpha_{i_K} \geq 0$ and $\alpha_i < 0$ for any $i \neq i_1, \ldots, i_K$. We provide the proof when $K = i_K = 1$ as the technique remains the same but the calculations are unnecessarily complicated.

Suppose first that $\alpha_1 < 0$, $\alpha_i \geq 0$ for all $i = 2, \ldots, N$. Then, $\alpha_{\min} = \alpha_1$. Given $\boldsymbol{x} \in \tilde{U}_R(\boldsymbol{\alpha})$, we have $\boldsymbol{x} \in \tilde{U}_R$ and

$$\begin{aligned} &x_1 > x_2^{-\frac{\alpha_2}{\alpha_1}} x_3^{-\frac{\alpha_3}{\alpha_1}} \cdots x_N^{-\frac{\alpha_N}{\alpha_1}} \\ &x_i < x_{i_1}^{-\frac{\alpha_{i_1}}{\alpha_i}} x_{i_2}^{-\frac{\alpha_{i_2}}{\alpha_i}} \cdots x_{i_{N-1}}^{-\frac{\alpha_{i_{N-1}}}{\alpha_i}}, \quad i = 2, \ldots, N;\ i \neq i_l,\ l = 1, \ldots, N-1, \end{aligned}$$

so that

$$\begin{aligned} \ell\left(\tilde{U}_R \backslash \tilde{U}_R(\boldsymbol{\alpha})\right) &= \int_0^{\varepsilon} \int_0^{\varepsilon} \cdots \int_0^{\varepsilon} \int_0^{x_2^{-\frac{\alpha_2}{\alpha_1}} x_3^{-\frac{\alpha_3}{\alpha_1}} \cdots x_N^{-\frac{\alpha_N}{\alpha_1}}} dx_1 dx_2 \ldots dx_{N-1} dx_N \\ &= \frac{\varepsilon^{N - \frac{1}{\alpha_1} \sum_{i=1}^{N} \alpha_i}}{\prod_{i=2}^{N} \left(-\frac{\alpha_i}{\alpha_1} + 1\right)} \end{aligned}$$

and

$$1 - \Sigma_R = \frac{\ell\left(\tilde{U}_R \backslash \tilde{U}_R(\boldsymbol{\alpha})\right)}{\ell\left(\tilde{U}_R\right)} = \frac{\frac{\varepsilon^{N - \frac{1}{\alpha_1} \sum_{i=1}^{N} \alpha_i}}{\prod_{i=2}^{N} \left(-\frac{\alpha_i}{\alpha_1} + 1\right)}}{\varepsilon^N} = \frac{\varepsilon^{-\frac{1}{\alpha_1} \sum_{i=1}^{N} \alpha_i}}{\prod_{i=2}^{N} \left(-\frac{\alpha_i}{\alpha_1} + 1\right)}.$$

Therefore

$$\frac{\ln(1 - \Sigma_R)}{R} = -\frac{1}{\alpha_1} \sum_{i=1}^{N} \alpha_i - \frac{\ln\left(\prod_{i=2}^{N} \left(-\frac{\alpha_i}{\alpha_1} + 1\right)\right)}{R}$$

and

$$F^+(\boldsymbol{\alpha}) = -\frac{1}{\alpha_1} \sum_{i=1}^{N} \alpha_i - \lim_{R \to -\infty} \frac{\ln\left(\prod_{i=2}^{N} \left(-\frac{\alpha_i}{\alpha_1} + 1\right)\right)}{R} = -\frac{1}{\alpha_{\min}} \sum_{i=1}^{N} \alpha_i > 0.$$

Suppose now that $\alpha_1 \geq 0$, $\alpha_i < 0$ for all $i = 2, \ldots, N$. If $\boldsymbol{x} \in \tilde{U}_R(\boldsymbol{\alpha})$, then $\boldsymbol{x} \in \tilde{U}_R$ and

$$\begin{aligned} &x_1 < x_2^{-\frac{\alpha_2}{\alpha_1}} x_3^{-\frac{\alpha_3}{\alpha_1}} \cdots x_N^{-\frac{\alpha_N}{\alpha_1}} \\ &x_i > x_{i_1}^{-\frac{\alpha_{i_1}}{\alpha_i}} x_{i_2}^{-\frac{\alpha_{i_2}}{\alpha_i}} \cdots x_{i_{N-1}}^{-\frac{\alpha_{i_{N-1}}}{\alpha_i}}, \quad i = 2, \ldots, N;\ i \neq i_l,\ l = 1, \ldots, N-1. \end{aligned}$$

In calculating the measure of the set determined by these inequalities, we must take into account how the respective boundaries intersect the boundaries of $\tilde{U}_R$. These intersections lead to a splitting of the integral that expresses the measure of $\tilde{U}_R \backslash \tilde{U}_R(\boldsymbol{\alpha})$ (and of $\tilde{U}_R(\boldsymbol{\alpha})$) which was not necessary before.

Accordingly, the integrals that follow have a rather daunting aspect. Indeed,

$$\begin{aligned}
&\ell\left(\tilde{U}_R \setminus \tilde{U}_R(\boldsymbol{\alpha})\right) = \\
&= \int_0^{\varepsilon}\int_0^{\varepsilon}\int_0^{\min\left\{\varepsilon,\varepsilon^{-\sum_{i=4}^{N}\frac{\alpha_i}{\alpha_3}}x_1^{-\frac{\alpha_1}{\alpha_3}}x_2^{-\frac{\alpha_2}{\alpha_3}}\right\}}\int_0^{\min\left\{\varepsilon,\varepsilon^{-\sum_{i=5}^{N}\frac{\alpha_i}{\alpha_4}}x_1^{-\frac{\alpha_1}{\alpha_4}}x_2^{-\frac{\alpha_2}{\alpha_4}}x_3^{-\frac{\alpha_3}{\alpha_4}}\right\}}\dots \\
&\dots\int_0^{\min\left\{\varepsilon,\varepsilon^{-\frac{\alpha_N}{\alpha_{N-1}}}x_1^{-\frac{\alpha_1}{\alpha_{N-1}}}\dots x_{N-2}^{-\frac{\alpha_{N-2}}{\alpha_{N-1}}}\right\}}\int_0^{\min\left\{\varepsilon,x_1^{-\frac{\alpha_1}{\alpha_N}}\dots x_{N-1}^{-\frac{\alpha_{N-1}}{\alpha_N}}\right\}} dx_N dx_{N-1}\dots dx_4 dx_3 dx_2 dx_1 \\
&= \int_0^{\varepsilon}\left\{\int_0^{\varepsilon^{-\sum_{i=3}^{N}\frac{\alpha_i}{\alpha_2}}x_1^{-\frac{\alpha_1}{\alpha_2}}}\int_0^{\varepsilon}\cdots\int_0^{\varepsilon} dx_N\dots dx_3 dx_2 + \right. \\
&+\int_{\varepsilon^{-\sum_{i=3}^{N}\frac{\alpha_i}{\alpha_2}}x_1^{-\frac{\alpha_1}{\alpha_2}}}^{\varepsilon}\int_0^{\varepsilon^{-\sum_{i=4}^{N}\frac{\alpha_i}{\alpha_3}}x_1^{-\frac{\alpha_1}{\alpha_3}}x_2^{-\frac{\alpha_2}{\alpha_3}}}\int_0^{\varepsilon}\cdots\int_0^{\varepsilon} dx_N\dots dx_4 dx_3 dx_2 + \\
&+\int_{\varepsilon^{-\sum_{i=3}^{N}\frac{\alpha_i}{\alpha_2}}x_1^{-\frac{\alpha_1}{\alpha_2}}}^{\varepsilon}\int_{\varepsilon^{-\sum_{i=4}^{N}\frac{\alpha_i}{\alpha_3}}x_1^{-\frac{\alpha_1}{\alpha_3}}x_2^{-\frac{\alpha_2}{\alpha_3}}}^{\varepsilon}\int_0^{\varepsilon^{-\sum_{i=5}^{N}\frac{\alpha_i}{\alpha_4}}x_1^{-\frac{\alpha_1}{\alpha_4}}x_2^{-\frac{\alpha_2}{\alpha_4}}x_3^{-\frac{\alpha_3}{\alpha_4}}} \\
&\qquad\int_0^{\varepsilon}\cdots\int_0^{\varepsilon} dx_N\dots dx_5 dx_4 dx_3 dx_2 + \\
&+\cdots+ \\
&+\int_{\varepsilon^{-\sum_{i=3}^{N}\frac{\alpha_i}{\alpha_2}}x_1^{-\frac{\alpha_1}{\alpha_2}}}^{\varepsilon}\cdots\int_{\varepsilon^{-\sum_{i=N-1}^{N}\frac{\alpha_i}{\alpha_{N-2}}}x_1^{-\frac{\alpha_1}{\alpha_{N-2}}}\dots x_{N-3}^{-\frac{\alpha_{N-3}}{\alpha_{N-2}}}}^{\varepsilon} \\
&\qquad\int_0^{\varepsilon^{-\frac{\alpha_N}{\alpha_{N-1}}}x_1^{-\frac{\alpha_1}{\alpha_{N-1}}}\dots x_{N-2}^{-\frac{\alpha_{N-2}}{\alpha_{N-1}}}}\int_0^{\varepsilon} dx_N dx_{N-1} dx_{N-2}\dots dx_2 + \\
&+\int_{\varepsilon^{-\sum_{i=3}^{N}\frac{\alpha_i}{\alpha_2}}x_1^{-\frac{\alpha_1}{\alpha_2}}}^{\varepsilon}\cdots\int_{\varepsilon^{-\sum_{i=N-1}^{N}\frac{\alpha_i}{\alpha_{N-2}}}x_1^{-\frac{\alpha_1}{\alpha_{N-2}}}\dots x_{N-3}^{-\frac{\alpha_{N-3}}{\alpha_{N-2}}}}^{\varepsilon} \\
&\left.\int_{\varepsilon^{-\frac{\alpha_N}{\alpha_{N-1}}}x_1^{-\frac{\alpha_1}{\alpha_{N-1}}}\dots x_{N-2}^{-\frac{\alpha_{N-2}}{\alpha_{N-1}}}}^{\varepsilon}\int_0^{x_1^{-\frac{\alpha_1}{\alpha_N}}\dots x_{N-1}^{-\frac{\alpha_{N-1}}{\alpha_N}}} dx_N dx_{N-1} dx_{N-2}\dots dx_2\right\} dx_1 \\
&= \frac{\varepsilon^{N-\frac{1}{\alpha_2}\sum_{i=1}^{N}\alpha_i}}{\prod_{i=1,i\neq 2}^{N}\left(-\frac{\alpha_i}{\alpha_2}+1\right)} + \frac{\varepsilon^{N-\frac{1}{\alpha_3}\sum_{i=1}^{N}\alpha_i}}{\prod_{i=1,i\neq 3}^{N}\left(-\frac{\alpha_i}{\alpha_3}+1\right)} + \cdots + \frac{\varepsilon^{N-\frac{1}{\alpha_N}\sum_{i=1}^{N}\alpha_i}}{\prod_{i=1,i\neq N}^{N}\left(-\frac{\alpha_i}{\alpha_N}+1\right)}
\end{aligned}$$

and

$$1-\Sigma_R = \frac{\ell\left(\tilde{U}_R \setminus \tilde{U}_R(\boldsymbol{\alpha})\right)}{\ell\left(\tilde{U}_R\right)} = \sum_{j=2}^{N}\frac{\varepsilon^{-\frac{1}{\alpha_j}\sum_{i=1}^{N}\alpha_i}}{\prod_{i=1\neq j}^{N}\left(-\frac{\alpha_i}{\alpha_j}+1\right)}.$$

Consequently, $\frac{\ln(1-\Sigma_R)}{R} \underset{R\to-\infty}{\longrightarrow} \frac{\infty}{\infty}$. Using L'Hôpital's rule, we obtain

$$\frac{\frac{d}{dR}\ln(1-\Sigma_R)}{\frac{d}{dR}R} = \frac{\sum_{j=2}^{N}\left(-\frac{1}{\alpha_j}\sum_{i=1}^{N}\alpha_i\right)\frac{\varepsilon^{-\frac{1}{\alpha_j}\sum_{i=1}^{N}\alpha_i}}{\prod_{i=1\neq j}^{N}\left(-\frac{\alpha_i}{\alpha_j}+1\right)}}{\sum_{j=2}^{N}\frac{\varepsilon^{-\frac{1}{\alpha_j}\sum_{i=1}^{N}\alpha_i}}{\prod_{i=1\neq j}^{N}\left(-\frac{\alpha_i}{\alpha_j}+1\right)}}. \tag{A.2}$$

Since $R<0$ is sufficiently large and therefore $\varepsilon = e^R > 0$ is sufficiently small, the highest power of ε in (A.2) is the one with lowest exponent, that is,

$$\max_{j=2,\dots,N}\left\{\varepsilon^{-\frac{1}{\alpha_j}\sum_{i=1}^N \alpha_i}\right\} = \varepsilon^{\min_{j=2,\dots,N}\left\{-\frac{1}{\alpha_j}\sum_{i=1}^N \alpha_i\right\}} = \varepsilon^{-\frac{1}{\alpha_{\min}}\sum_{i=1}^N \alpha_i}.$$

For $R\to-\infty$, i.e. $\varepsilon = e^R \to 0$, (A.2) becomes asymptotically close to

$$-\frac{1}{\alpha_{\min}}\sum_{i=1}^N \alpha_i,$$

which yields

$$F^+(\boldsymbol{\alpha}) = -\frac{1}{\alpha_{\min}}\sum_{i=1}^N \alpha_i > 0.$$

Case 3: If $\sum_{i=1}^N \alpha_i < 0$, then $\alpha_i \le 0$ for all $i=1,\dots,N$ or there exist $K\ge 1$ and $i_1,\dots,i_K\in\{1,\dots,N\}$ such that either $\alpha_{i_1},\dots,\alpha_{i_K}\le 0$ and $\alpha_i<0$ for any $i\ne i_1,\dots,i_K$ or $\alpha_{i_1},\dots,\alpha_{i_K}>0$ and $\alpha_i\le 0$ for any $i\ne i_1,\dots,i_K$. From the two previous cases and the fact that $F^+(-\boldsymbol{\alpha}) = F^-(\boldsymbol{\alpha})$, we have immediately $F^+(\boldsymbol{\alpha})=0$ and $F^-(\boldsymbol{\alpha})>0$.

Observe that if $\sum_{i=1}^N \alpha_i = 0$, then $F^+(\boldsymbol{\alpha}) = F^-(\boldsymbol{\alpha}) = 0$ in Cases 2 and 3.

A.2 The function F^{index} when $N=3$

We see at once that the function $F^+(\boldsymbol{\alpha})$ is invariant under permutations of α_i, $i=1,\dots,N$. In particular, for $N=3$, it follows that

$$F^+(\alpha_1,\alpha_2,\alpha_3) = \begin{cases} +\infty, & \text{if } \min\{\alpha_1,\alpha_2,\alpha_3\}\ge 0 \\ 0, & \text{if } \alpha_1+\alpha_2+\alpha_3\le 0 \\ -\dfrac{\alpha_1+\alpha_2+\alpha_3}{\min\{\alpha_1,\alpha_2,\alpha_3\}}, & \text{if } \min\{\alpha_1,\alpha_2,\alpha_3\}<0 \text{ and } \alpha_1+\alpha_2+\alpha_3\ge 0 \end{cases}$$

and

$$F^-(\alpha_1,\alpha_2,\alpha_3) = \begin{cases} +\infty, & \text{if } \max\{\alpha_1,\alpha_2,\alpha_3\}\le 0 \\ 0, & \text{if } \alpha_1+\alpha_2+\alpha_3\ge 0 \\ -\dfrac{\alpha_1+\alpha_2+\alpha_3}{\max\{\alpha_1,\alpha_2,\alpha_3\}}, & \text{if } \max\{\alpha_1,\alpha_2,\alpha_3\}>0 \text{ and } \alpha_1+\alpha_2+\alpha_3\le 0 \end{cases}$$

such that

$$F^{\text{index}}(\alpha_1, \alpha_2, \alpha_3) = \begin{cases} +\infty, & \text{if } \min\{\alpha_1, \alpha_2, \alpha_3\} \geq 0 \\ -\infty, & \text{if } \max\{\alpha_1, \alpha_2, \alpha_3\} \leq 0 \\ 0, & \text{if } \alpha_1 + \alpha_2 + \alpha_3 = 0 \\ \dfrac{\alpha_1 + \alpha_2 + \alpha_3}{\max\{\alpha_1, \alpha_2, \alpha_3\}}, & \text{if } \max\{\alpha_1, \alpha_2, \alpha_3\} > 0 \text{ and } \alpha_1 + \alpha_2 + \alpha_3 < 0 \\ -\dfrac{\alpha_1 + \alpha_2 + \alpha_3}{\min\{\alpha_1, \alpha_2, \alpha_3\}}, & \text{if } \min\{\alpha_1, \alpha_2, \alpha_3\} < 0 \text{ and } \alpha_1 + \alpha_2 + \alpha_3 > 0. \end{cases}$$

Appendix B

Transitions near the RSP cycles

In this section we describe the construction of Poincaré maps (also called return maps) from and to cross sections of the flow near each equilibrium once around the entire heteroclinic cycle. The Poincaré maps are the composition of local and global maps. The local maps approximate the flow in a neighbourhood of an equilibrium. The global maps approximate the flow along a heteroclinic connection between two consecutive equilibria.

Near ξ_j, we introduce an incoming cross section $H_j^{in,i}$ across the heteroclinic connection $[\xi_i \to \xi_j]$ and an outgoing cross section $H_j^{out,k}$ across the heteroclinic connection $[\xi_j \to \xi_k]$, $j \neq i,k$. By definition, these are five-dimensional subspaces in $\mathbb{R}^6$. However, Krupa and Melbourne [43] show that not all dimensions are important in the study of stability as followed.

B.1 Poincaré maps

Assume that the flow is linearisable about each equilibrium. Locally at ξ_j, we denote by $-c_{ji} < 0$ the eigenvalue in the stable direction through the heteroclinic connection $[\xi_i \to \xi_j]$ and $e_{jk} > 0$ the eigenvalue in the unstable direction through the heteroclinic connection $[\xi_j \to \xi_k]$. Each equilibrium actually has two outgoing connections emanating from it and two incoming connections leading to it. Looking at ξ_j from the point of view of the sequence of heteroclinic connections $[\xi_i \to \xi_j \to \xi_k]$, we say that $-c_{ji}$ is *contracting*, e_{jk} is *expanding*, $-c_{jl}$ and e_{jm} are *transverse* with $j \neq i,k,l,m$, $i \neq l$ and $k \neq m$ (see [27, 43, 52, 53]). The linearised flow in relevant local coordinates near ξ_j is given by

$$\begin{aligned}
\dot{v} &= -c_{ji}v \\
\dot{w} &= e_{jk}w \\
\dot{z}_1 &= -c_{jl}z_1 \\
\dot{z}_2 &= e_{jm}z_2,
\end{aligned} \tag{B.1}$$

such that v, w and (z_1, z_2) correspond, respectively, to the contracting, expanding and transverse directions. Table B.1 provides all eigenvalues restricted to those directions for the three equilibria ξ_0, ξ_1 and ξ_2.

ξ_0	$e_{01} = 1$	$e_{02} = \dfrac{1+\varepsilon_x}{2}$	$-c_{01} = -1$	$-c_{02} = -\dfrac{1-\varepsilon_y}{2}$
ξ_1	$e_{12} = \dfrac{1+\varepsilon_y}{2}$	$e_{10} = 1$	$-c_{12} = -\dfrac{1-\varepsilon_x}{2}$	$-c_{10} = 1$
ξ_2	$e_{20} = \dfrac{1-\varepsilon_y}{2}$	$e_{21} = \dfrac{1-\varepsilon_x}{2}$	$-c_{20} = -\dfrac{1+\varepsilon_x}{2}$	$-c_{21} = -\dfrac{1-\varepsilon_x}{2}$

Table B.1 Eigenvalues of the linearisation of the flow about each equilibrium in a system of local coordinates in the basis of the associated contracting, expanding and transverse eigenvectors.

The cross sections above are reduced to a three-dimensional subspace and can be expressed as

$$H_j^{in,i} = \{(1, w, z_1, z_2) : \ 0 < w, z_1, z_2 < 1\}$$
$$H_j^{out,k} = \{(v, 1, z_1, z_2) : \ 0 < v, z_1, z_2 < 1\}.$$

We construct *local maps* $\phi_{ijk} : H_j^{in,i} \to H_j^{out,k}$ near each ξ_j, *global maps* $\psi_{jk} : H_j^{out,k} \to H_k^{in,j}$ near each heteroclinic connection $[\xi_j \to \xi_k]$ and their compositions $g_j = \psi_{jk} \circ \phi_{ijk} : H_j^{in,i} \to H_k^{in,j}$, $j \neq i,k$. Composing the latter in the correct order gives *Poincaré maps* $\pi_j : H_j^{in,i} \to H_j^{in,i}$, one for each heteroclinic connection belonging to the heteroclinic cycle.

Integrating (B.1) we find

$$\phi_{ijk}(w, z_1, z_2) = \left(w^{\frac{c_{ji}}{e_{jk}}}, \ z_1 w^{\frac{c_{jl}}{e_{jk}}}, \ z_2 w^{-\frac{e_{jm}}{e_{jk}}} \right), \quad \text{for } 0 < z_2 < w^{\frac{e_{jm}}{e_{jk}}}.$$

Expressions for global maps depend both on which heteroclinic connection and heteroclinic cycle one considers. Following [5, Remark, p. 1603], in the leading order any global map ψ_{jk} is well represented by a permutation.

We describe the details for the heteroclinic cycle $C_0 = [\xi_0 \to \xi_1 \to \xi_0]$. The other cases are similar and therefore we omit the calculations. Notice that

$$\Gamma((\mathrm{R},\mathrm{P}) \to (\mathrm{S},\mathrm{P}) \to (\mathrm{S},\mathrm{R})) = C_0.$$

We pick, respectively, the heteroclinic connections $[(\mathrm{R},\mathrm{P}) \to (\mathrm{S},\mathrm{P})]$ and $[(\mathrm{S},\mathrm{P}) \to (\mathrm{S},\mathrm{R})]$ as representatives of $[\xi_0 \to \xi_1]$ and $[\xi_1 \to \xi_0]$, see Table 5.1. Considering the flow linearised about each representative heteroclinic connection, the global maps have the form

$$\psi_{01} : H_0^{out,1} \to H_1^{in,0}, \qquad \psi_{10}(v, z_1, z_2) = (z_1, z_2, v)$$
$$\psi_{10} : H_1^{out,0} \to H_0^{in,1}, \qquad \psi_{01}(v, z_1, z_2) = (z_1, z_2, v).$$

The pairwise composite maps $g_0 = \psi_{01} \circ \phi_{101}$ and $g_1 = \psi_{10} \circ \phi_{010}$ are

$$\begin{aligned}
g_0 : H_0^{in,1} \to H_1^{in,0}, \qquad & g_0(w,z_1,z_2) = \left(z_1 w^{\frac{1-\varepsilon_y}{2}},\, z_2 w^{-\frac{1+\varepsilon_x}{2}},\, w \right), \\
& \text{for } 0 < z_2 < w^{\frac{1+\varepsilon_x}{2}}, \\
g_1 : H_1^{in,0} \to H_0^{in,1}, \qquad & g_1(w,z_1,z_2) = \left(z_1 w^{\frac{1-\varepsilon_x}{2}},\, z_2 w^{-\frac{1+\varepsilon_y}{2}},\, w \right), \\
& \text{for } 0 < z_2 < w^{\frac{1+\varepsilon_y}{2}}.
\end{aligned} \tag{B.2}$$

The dynamics in the vicinity of the C_0-cycle is accurately approximated by the two Poincaré maps $\pi_0 = g_1 \circ g_0$ and $\pi_1 = g_0 \circ g_1$ with

$$\begin{aligned}
&\pi_0 : H_0^{in,1} \to H_0^{in,1}, \\
&\pi_0(w,z_1,z_2) = \left(z_2 z_1^{\frac{1-\varepsilon_x}{2}} w^{\frac{-1-3\varepsilon_x-\varepsilon_y+\varepsilon_x\varepsilon_y}{4}},\, z_1^{-\frac{1+\varepsilon_y}{2}} w^{\frac{3+\varepsilon_y^2}{4}},\, z_1 w^{\frac{1-\varepsilon_y}{2}} \right),
\end{aligned} \tag{B.3}$$

for $0 < z_2 < w^{\frac{1+\varepsilon_x}{2}}$ and $z_1 > w^{\frac{3+\varepsilon_y^2}{2(1+\varepsilon_y)}}$,

$$\begin{aligned}
&\pi_1 : H_1^{in,0} \to H_1^{in,0}, \\
&\pi_1(w,z_1,z_2) = \left(z_2 z_1^{\frac{1-\varepsilon_y}{2}} w^{\frac{-1-\varepsilon_x-3\varepsilon_y+\varepsilon_x\varepsilon_y}{4}},\, z_1^{-\frac{1+\varepsilon_x}{2}} w^{\frac{3+\varepsilon_x^2}{4}},\, z_1 w^{\frac{1-\varepsilon_x}{2}} \right),
\end{aligned} \tag{B.4}$$

for $0 < z_2 < w^{\frac{1+\varepsilon_y}{2}}$ and $z_1 > w^{\frac{3+\varepsilon_x^2}{2(1+\varepsilon_x)}}$.

B.2 Transition matrices

Consider the change of coordinates

$$\boldsymbol{\eta} \equiv (\eta_1, \eta_2, \eta_3) = (\ln v, \ln z_1, \ln z_2). \tag{B.5}$$

The maps $g_j : H_j^{in,i} \to H_k^{in,j}$, $j \neq i,k$, become linear such that

$$g_j(\boldsymbol{\eta}) = M_j \boldsymbol{\eta},$$

where M_j are called the *basic transition matrices*. For the Poincaré maps $\pi_j : H_j^{in,i} \to H_j^{in,i}$ the transition matrices are the product of basic transition matrices in the appropriate order. We denote them by $M^{(j)}$.

In particular, the basic transition matrices of the maps g_0 and g_1 in (B.2) with respect to C_0 are

$$M_0 = \begin{bmatrix} \frac{1-\varepsilon_y}{2} & 1 & 0 \\ -\frac{1+\varepsilon_x}{2} & 0 & 1 \\ 1 & 0 & 0 \end{bmatrix}, \quad M_1 = \begin{bmatrix} \frac{1-\varepsilon_x}{2} & 1 & 0 \\ -\frac{1+\varepsilon_y}{2} & 0 & 1 \\ 1 & 0 & 0 \end{bmatrix}. \tag{B.6}$$

Then, the products $M^{(0)} = M_1 M_0$ and $M^{(1)} = M_0 M_1$ provide the transition matrices of the Poincaré maps π_0 in (B.3) and π_1 in (B.4):

$$\begin{aligned} M^{(0)} &= \begin{bmatrix} \frac{-1-3\varepsilon_x-\varepsilon_y+\varepsilon_x\varepsilon_y}{4} & \frac{1-\varepsilon_x}{2} & 1 \\ \frac{3+\varepsilon_y^2}{4} & -\frac{1+\varepsilon_y}{2} & 0 \\ \frac{1-\varepsilon_y}{2} & 1 & 0 \end{bmatrix} \\ M^{(1)} &= \begin{bmatrix} \frac{-1-\varepsilon_x-3\varepsilon_y+\varepsilon_x\varepsilon_y}{4} & \frac{1-\varepsilon_y}{2} & 1 \\ \frac{3+\varepsilon_x^2}{4} & -\frac{1+\varepsilon_x}{2} & 0 \\ \frac{1-\varepsilon_x}{2} & 1 & 0 \end{bmatrix}. \end{aligned} \tag{B.7}$$

Analogously, this process yields the transition matrices for the remaining heteroclinic cycles. We use different accents according to the heteroclinic cycle: for C_1,

$$\begin{aligned} \widetilde{M}^{(1)} &: H_1^{in,2} \to H_1^{in,2}, \qquad \widetilde{M}^{(1)} = \widetilde{M}_2 \widetilde{M}_1 \\ \widetilde{M}^{(2)} &: H_2^{in,1} \to H_2^{in,1}, \qquad \widetilde{M}^{(2)} = \widetilde{M}_1 \widetilde{M}_2 \end{aligned}$$

where

$$\widetilde{M}_1 = \begin{bmatrix} \frac{2}{1+\varepsilon_y} & 1 & 0 \\ \frac{1-\varepsilon_x}{1+\varepsilon_y} & 0 & 0 \\ -\frac{2}{1+\varepsilon_y} & 0 & 1 \end{bmatrix}, \quad \widetilde{M}_2 = \begin{bmatrix} -\frac{1-\varepsilon_y}{1-\varepsilon_x} & 0 & 1 \\ \frac{1+\varepsilon_x}{1-\varepsilon_x} & 1 & 0 \\ \frac{1+\varepsilon_y}{1-\varepsilon_x} & 0 & 0 \end{bmatrix};$$

for C_2,

$$\begin{aligned} \widetilde{\widetilde{M}}^{(0)} &: H_0^{in,2} \to H_0^{in,2}, \qquad \widetilde{\widetilde{M}}^{(0)} = \widetilde{\widetilde{M}}_2 \widetilde{\widetilde{M}}_0 \\ \widetilde{\widetilde{M}}^{(2)} &: H_2^{in,0} \to H_2^{in,0}, \qquad \widetilde{\widetilde{M}}^{(2)} = \widetilde{\widetilde{M}}_0 \widetilde{\widetilde{M}}_2 \end{aligned}$$

where

$$\widetilde{\widetilde{M}}_0 = \begin{bmatrix} \frac{2}{1+\varepsilon_x} & 1 & 0 \\ \frac{1-\varepsilon_y}{1+\varepsilon_x} & 0 & 0 \\ -\frac{2}{1+\varepsilon_x} & 0 & 1 \end{bmatrix}, \quad \widetilde{\widetilde{M}}_2 = \begin{bmatrix} -\frac{1-\varepsilon_x}{1-\varepsilon_y} & 0 & 1 \\ \frac{1+\varepsilon_y}{1-\varepsilon_y} & 1 & 0 \\ \frac{1+\varepsilon_x}{1-\varepsilon_y} & 0 & 0 \end{bmatrix};$$

for C_3,

$$\begin{aligned} \widehat{M}^{(1)} &: H_1^{in,0} \to H_1^{in,0}, & \widehat{M}^{(1)} &= \widehat{M}_2\widehat{M}_0\widehat{M}_1 \\ \widehat{M}^{(2)} &: H_2^{in,1} \to H_2^{in,1}, & \widehat{M}^{(2)} &= \widehat{M}_0\widehat{M}_1\widehat{M}_2 \\ \widehat{M}^{(0)} &: H_0^{in,2} \to H_0^{in,2}, & \widehat{M}^{(0)} &= \widehat{M}_1\widehat{M}_2\widehat{M}_0 \end{aligned}$$

where

$$\widehat{M}_1 = \begin{bmatrix} -\frac{2}{1+\varepsilon_y} & 0 & 1 \\ \frac{1-\varepsilon_x}{1+\varepsilon_y} & 1 & 0 \\ \frac{2}{1+\varepsilon_y} & 0 & 0 \end{bmatrix}, \quad \widehat{M}_2 = \begin{bmatrix} \frac{1+\varepsilon_x}{1-\varepsilon_y} & 1 & 0 \\ \frac{1+\varepsilon_y}{1-\varepsilon_y} & 0 & 0 \\ -\frac{1-\varepsilon_x}{1-\varepsilon_y} & 0 & 1 \end{bmatrix}, \quad \widehat{M}_0 = \begin{bmatrix} 1 & 1 & 0 \\ -\frac{1+\varepsilon_x}{2} & 0 & 1 \\ \frac{1-\varepsilon_y}{2} & 0 & 0 \end{bmatrix};$$

and, for C_4,

$$\begin{aligned} \widehat{\widehat{M}}^{(0)} &: H_0^{in,1} \to H_0^{in,1}, & \widehat{\widehat{M}}^{(0)} &= \widehat{\widehat{M}}_2\widehat{\widehat{M}}_1\widehat{\widehat{M}}_0 \\ \widehat{\widehat{M}}^{(2)} &: H_2^{in,0} \to H_2^{in,0}, & \widehat{\widehat{M}}^{(2)} &= \widehat{\widehat{M}}_1\widehat{\widehat{M}}_0\widehat{\widehat{M}}_2 \\ \widehat{\widehat{M}}^{(1)} &: H_1^{in,2} \to H_1^{in,2}, & \widehat{\widehat{M}}^{(1)} &= \widehat{\widehat{M}}_0\widehat{\widehat{M}}_2\widehat{\widehat{M}}_1 \end{aligned}$$

where

$$\widehat{\widehat{M}}_0 = \begin{bmatrix} -\frac{2}{1+\varepsilon_x} & 0 & 1 \\ \frac{1-\varepsilon_y}{1+\varepsilon_x} & 1 & 0 \\ \frac{2}{1+\varepsilon_x} & 0 & 0 \end{bmatrix}, \quad \widehat{\widehat{M}}_2 = \begin{bmatrix} \frac{1+\varepsilon_y}{1-\varepsilon_x} & 1 & 0 \\ \frac{1+\varepsilon_x}{1-\varepsilon_x} & 0 & 0 \\ -\frac{1-\varepsilon_y}{1-\varepsilon_x} & 0 & 1 \end{bmatrix}, \quad \widehat{\widehat{M}}_1 = \begin{bmatrix} 1 & 1 & 0 \\ -\frac{1+\varepsilon_y}{2} & 0 & 1 \\ \frac{1-\varepsilon_x}{2} & 0 & 0 \end{bmatrix}.$$

Appendix C

Transitions near the Bowtie network

C.1 Maps between cross sections

The dynamics near the Bowtie network was already studied in [19]. We recall their general setting and terminology.

Ensuring that all transverse eigenvalues are negative whenever possible, the linearisation of the flow at ξ_3, for instance, is assumed to be given by

$$\begin{aligned}
\dot{x}_1 &= e_{31} x_1 \\
\dot{x}_2 &= -c_{32} x_2 \\
\dot{x}_3 &= -r_3 x_3 \\
\dot{x}_4 &= -c_{34} x_4 \\
\dot{x}_5 &= -c_{35} x_5
\end{aligned}$$

for some positive constants e_{31}, c_{32}, r_3, c_{34}, c_{35}. Similar equations define the flow linearised about the other nodes labeling the associated eigenvalues accordingly.

We introduce cross sections $H_j^{in,i}$ and $H_j^{out,k}$ at incoming and outgoing connections near each ξ_j as in (4.1)–(4.2). Near ξ_3 these are

$$\begin{aligned}
H_3^{in,2} &= \{(x_1, x_4, x_5) : 0 \leq x_1, x_4, x_5 < 1\} \\
H_3^{out,1} &= \{(u_2, u_4, u_5) : 0 \leq u_2, u_4, u_5 < 1\}
\end{aligned}$$

after selecting the relevant coordinates.

Local and global maps are constructed in the standard way. We list the former in order to ease of reference; for the R-cycle,

$$\begin{aligned}
&\phi_{3,1,2} : H_1^{in,3} \to H_1^{out,2}, \qquad \phi_{3,1,2}(x_2, x_4, x_5) = \left(x_2^{\frac{c_{13}}{e_{12}}}, x_4 x_2^{\frac{c_{14}}{e_{12}}}, x_5 x_2^{\frac{c_{15}}{e_{12}}} \right) \\
&\phi_{1,2,3} : H_2^{in,1} \to H_2^{out,3}, \qquad \phi_{1,2,3}(x_3, x_4, x_5) = \left(x_3^{\frac{c_{21}}{e_{23}}}, x_4 x_3^{-\frac{e_{24}}{e_{23}}}, x_5 x_3^{\frac{c_{25}}{e_{23}}} \right), \qquad 0 \leq x_4 < x_3^{\frac{e_{24}}{e_{23}}} \\
&\phi_{2,3,1} : H_3^{in,2} \to H_3^{out,1}, \qquad \phi_{2,3,1}(x_1, x_4, x_5) = \left(x_1^{\frac{c_{32}}{e_{31}}}, x_4 x_1^{\frac{c_{34}}{e_{31}}}, x_5 x_1^{\frac{c_{35}}{e_{31}}} \right)
\end{aligned}$$

for the L-cycle,

$$\begin{aligned}
&\phi_{5,2,4}: H_2^{in,5} \to H_2^{out,4}, && \phi_{5,2,4}\left(x_1,x_3,x_4\right) = \left(x_1 x_4^{\frac{c_{21}}{e_{24}}}, x_3 x_4^{-\frac{e_{23}}{e_{24}}}, x_4^{\frac{c_{25}}{e_{24}}}\right), && 0 \leq x_3 < x_4^{\frac{e_{23}}{e_{24}}} \\
&\phi_{2,4,5}: H_4^{in,2} \to H_4^{out,5}, && \phi_{2,4,5}\left(x_1,x_3,x_5\right) = \left(x_1 x_5^{\frac{c_{41}}{e_{45}}}, x_5^{\frac{c_{42}}{e_{45}}}, x_3 x_5^{\frac{c_{43}}{e_{45}}}\right) \\
&\phi_{4,5,2}: H_5^{in,4} \to H_5^{out,2}, && \phi_{4,5,2}\left(x_1,x_2,x_3\right) = \left(x_1 x_2^{\frac{c_{51}}{e_{52}}}, x_3 x_2^{\frac{c_{53}}{e_{52}}}, x_2^{\frac{c_{54}}{e_{52}}}\right)
\end{aligned}$$

and, for the transition between cycles,

$$\begin{aligned}
&\phi_{1,2,4}: H_2^{in,1} \to H_2^{out,4}, && \phi_{1,2,4}\left(x_3,x_4,x_5\right) = \left(x_4^{\frac{c_{21}}{e_{24}}}, x_3 x_4^{-\frac{e_{23}}{e_{24}}}, x_5 x_4^{\frac{c_{25}}{e_{24}}}\right), && 0 \leq x_3 < x_4^{\frac{e_{23}}{e_{24}}} \\
&\phi_{5,2,3}: H_2^{in,5} \to H_2^{out,3}, && \phi_{5,2,3}\left(x_1,x_3,x_4\right) = \left(x_1 x_3^{\frac{c_{21}}{e_{23}}}, x_4 x_3^{-\frac{e_{24}}{e_{23}}}, x_3^{\frac{c_{25}}{e_{23}}}\right), && 0 \leq x_4 < x_3^{\frac{e_{24}}{e_{23}}}.
\end{aligned}$$

Following the usual notation $\psi_{j,k}: H_j^{out,k} \to H_k^{in,j}$ stands for the global map along the connection $\kappa_{j,k}$. They can be taken as the identity due to the $\mathbb{Z}_2^5$ symmetry. See [43] and [52] for more details. Thus $H_j^{out,k}$ and $H_k^{in,j}$ are freely identified with each other. We compose the local and global maps pairwise to give

$$\begin{aligned}
&\tilde{g}_1: H_1^{in,3} \to H_2^{in,1}, && \tilde{g}_1 = \psi_{1,2} \circ \phi_{3,1,2} \\
&\tilde{g}_2: H_2^{in,1} \to H_3^{in,2}, && \tilde{g}_2 = \psi_{2,3} \circ \phi_{1,2,3} \\
&\tilde{g}_3: H_3^{in,2} \to H_1^{in,3}, && \tilde{g}_3 = \psi_{3,1} \circ \phi_{2,3,1}
\end{aligned}$$

about the R-cycle, and

$$\begin{aligned}
&g_2: H_2^{in,5} \to H_4^{in,2}, && g_2 = \psi_{2,4} \circ \phi_{5,2,4} \\
&g_4: H_4^{in,2} \to H_5^{in,4}, && g_4 = \psi_{4,5} \circ \phi_{2,4,5} \\
&g_5: H_5^{in,4} \to H_2^{in,5}, && g_5 = \psi_{5,2} \circ \phi_{4,5,2}
\end{aligned}$$

about the L-cycle. From one cycle to the other we obtain

$$\begin{aligned}
&g_{RL}: H_2^{in,1} \to H_4^{in,2}, && g_{RL} = \psi_{2,4} \circ \phi_{1,2,4} \\
&g_{LR}: H_2^{in,5} \to H_3^{in,2}, && g_{LR} = \psi_{2,3} \circ \phi_{5,2,3}.
\end{aligned}$$

Of course their expressions match those of the local maps involved. Composition of the resulting maps in the correct order yields the full return maps $\tilde{\pi}_1$, $\tilde{\pi}_2$, $\tilde{\pi}_3$ around R and π_2, π_4, π_5 around L:

$$\tilde{\pi}_1 = \tilde{g}_3 \circ \tilde{g}_2 \circ \tilde{g}_1: H_1^{in,3} \to H_1^{in,3}, \qquad \tilde{\pi}_1\left(x_2,x_4,x_5\right) = \left(x_2^{\tilde{\rho}}, x_4 x_2^{\tilde{\tau}}, x_5 x_2^{\tilde{\theta}}\right), \qquad 0 \leq x_4 < x_2^{\tilde{\sigma}} \tag{C.1}$$

$$\tilde{\pi}_2 = \tilde{g}_1 \circ \tilde{g}_3 \circ \tilde{g}_2: H_2^{in,1} \to H_2^{in,1}, \qquad \tilde{\pi}_2\left(x_3,x_4,x_5\right) = \left(x_3^{\tilde{\rho}}, x_4 x_3^{\tilde{\nu}}, x_5 x_3^{\tilde{\mu}}\right), \qquad 0 \leq x_4 < x_3^{\frac{e_{24}}{e_{23}}} \tag{C.2}$$

$$\tilde{\pi}_3 = \tilde{g}_2 \circ \tilde{g}_1 \circ \tilde{g}_3: H_3^{in,2} \to H_3^{in,2}, \qquad \tilde{\pi}_3\left(x_1,x_4,x_5\right) = \left(x_1^{\tilde{\rho}}, x_4 x_1^{\tilde{\delta}}, x_5 x_1^{\tilde{\gamma}}\right), \qquad 0 \leq x_4 < x_1^{-\tilde{\delta}} \tag{C.3}$$

and

$$\pi_2 = g_5 \circ g_4 \circ g_2 : H_2^{in,5} \to H_2^{in,5}, \qquad \pi_2\left(x_1,x_3,x_4\right) = \left(x_1 x_4^{\mu}, x_3 x_4^{\nu}, x_4^{\rho}\right), \qquad 0 \le x_3 < x_4^{\frac{e_{23}}{e_{24}}} \tag{C.4}$$

$$\pi_4 = g_2 \circ g_5 \circ g_4 : H_4^{in,2} \to H_4^{in,2}, \qquad \pi_4\left(x_1,x_3,x_5\right) = \left(x_1 x_5^{\gamma}, x_3 x_5^{\delta}, x_5^{\rho}\right), \qquad 0 \le x_3 < x_5^{-\delta} \tag{C.5}$$

$$\pi_5 = g_4 \circ g_2 \circ g_5 : H_5^{in,4} \to H_5^{in,4}, \qquad \pi_5\left(x_1,x_2,x_3\right) = \left(x_1 x_2^{\theta}, x_2^{\rho}, x_3 x_2^{\tau}\right), \qquad 0 \le x_3 < x_2^{\sigma} \tag{C.6}$$

where

$$\begin{aligned}
\tilde{\rho} &= \frac{c_{21}}{e_{23}}\frac{c_{32}}{e_{31}}\frac{c_{13}}{e_{12}} > 0 & \rho &= \frac{c_{42}}{e_{45}}\frac{c_{54}}{e_{52}}\frac{c_{25}}{e_{24}} > 0 \\
\tilde{\nu} &= -\frac{e_{24}}{e_{23}} + \frac{c_{21}}{e_{23}}\frac{c_{34}}{e_{31}} + \frac{c_{21}}{e_{23}}\frac{c_{32}}{e_{31}}\frac{c_{14}}{e_{12}} & \nu &= -\frac{e_{23}}{e_{24}} + \frac{c_{25}}{e_{24}}\frac{c_{43}}{e_{45}} + \frac{c_{25}}{e_{24}}\frac{c_{42}}{e_{45}}\frac{c_{53}}{e_{52}} \\
\tilde{\mu} &= \frac{c_{25}}{e_{23}} + \frac{c_{21}}{e_{23}}\frac{c_{35}}{e_{31}} + \frac{c_{21}}{e_{23}}\frac{c_{32}}{e_{31}}\frac{c_{15}}{e_{12}} > 0 & \mu &= \frac{c_{21}}{e_{24}} + \frac{c_{25}}{e_{24}}\frac{c_{41}}{e_{45}} + \frac{c_{25}}{e_{24}}\frac{c_{42}}{e_{45}}\frac{c_{51}}{e_{52}} > 0 \\
\tilde{\delta} &= \frac{c_{34}}{e_{31}} + \frac{c_{32}}{e_{31}}\frac{c_{14}}{e_{12}} - \frac{c_{32}}{e_{31}}\frac{c_{13}}{e_{12}}\frac{e_{24}}{e_{23}} & \delta &= \frac{c_{43}}{e_{45}} + \frac{c_{42}}{e_{45}}\frac{c_{53}}{e_{52}} - \frac{c_{42}}{e_{45}}\frac{c_{54}}{e_{52}}\frac{e_{23}}{e_{24}} \\
\tilde{\gamma} &= \frac{c_{35}}{e_{31}} + \frac{c_{32}}{e_{31}}\frac{c_{15}}{e_{12}} + \frac{c_{32}}{e_{31}}\frac{c_{13}}{e_{12}}\frac{c_{25}}{e_{23}} > 0 & \gamma &= \frac{c_{41}}{e_{45}} + \frac{c_{42}}{e_{45}}\frac{c_{51}}{e_{52}} + \frac{c_{42}}{e_{45}}\frac{c_{54}}{e_{52}}\frac{c_{21}}{e_{24}} > 0 \\
\tilde{\tau} &= \frac{c_{14}}{e_{12}} - \frac{c_{13}}{e_{12}}\frac{e_{24}}{e_{23}} + \frac{c_{13}}{e_{12}}\frac{c_{21}}{e_{23}}\frac{c_{34}}{e_{31}} & \tau &= \frac{c_{53}}{e_{52}} - \frac{c_{54}}{e_{52}}\frac{e_{23}}{e_{24}} + \frac{c_{54}}{e_{52}}\frac{c_{25}}{e_{24}}\frac{c_{43}}{e_{45}} \\
\tilde{\theta} &= \frac{c_{15}}{e_{12}} + \frac{c_{13}}{e_{12}}\frac{e_{25}}{e_{23}} + \frac{c_{13}}{e_{12}}\frac{c_{21}}{e_{23}}\frac{c_{35}}{e_{31}} > 0 & \theta &= \frac{c_{51}}{e_{52}} + \frac{c_{54}}{e_{52}}\frac{e_{21}}{e_{24}} + \frac{c_{54}}{e_{52}}\frac{c_{25}}{e_{24}}\frac{c_{41}}{e_{45}} > 0 \\
\tilde{\sigma} &= \frac{c_{13}}{e_{12}}\left(\frac{e_{24}}{e_{23}} - \frac{c_{14}}{c_{13}}\right), & \sigma &= \frac{c_{54}}{e_{52}}\left(\frac{e_{23}}{e_{24}} - \frac{c_{53}}{c_{54}}\right).
\end{aligned} \tag{C.7}$$

In addition the behaviour of trajectories that start close to one cycle and visit the other is modelled by the maps

$$\pi_{RL} = g_5 \circ g_4 \circ g_{RL} : H_2^{in,1} \to H_2^{in,5}, \quad \pi_{RL}\left(x_3,x_4,x_5\right) = \left(x_4^{\mu} x_5^{\alpha}, x_3 x_4^{\nu} x_5^{\beta}, x_4^{\rho} x_5^{\frac{e_{24}}{c_{25}}\rho}\right), \quad 0 \le x_3 < x_4^{\frac{e_{23}}{e_{24}}}$$

$$\pi_{LR} = \tilde{g}_1 \circ \tilde{g}_3 \circ g_{LR} : H_2^{in,5} \to H_2^{in,1}, \quad \pi_{LR}\left(x_1,x_3,x_4\right) = \left(x_1^{\frac{e_{23}}{c_{21}}\tilde{\rho}} x_1^{\tilde{\rho}}, x_1^{\tilde{\beta}} x_3^{\tilde{\nu}} x_4, x_1^{\tilde{\alpha}} x_3^{\tilde{\mu}}\right), \quad 0 \le x_4 < x_3^{\frac{e_{24}}{e_{23}}}$$

where

$$\begin{aligned}
\tilde{\alpha} &= \frac{c_{35}}{e_{31}} + \frac{c_{32}}{e_{31}}\frac{c_{15}}{e_{12}} > 0 & \alpha &= \frac{c_{41}}{e_{45}} + \frac{c_{42}}{e_{45}}\frac{c_{51}}{e_{52}} > 0 \\
\tilde{\beta} &= \frac{c_{34}}{e_{31}} + \frac{c_{32}}{e_{31}}\frac{c_{14}}{e_{12}} > 0, & \beta &= \frac{c_{43}}{e_{45}} + \frac{c_{42}}{e_{45}}\frac{c_{53}}{e_{52}} > 0.
\end{aligned}$$

Our choice of label for the parameters above-mentioned comes originally from [19] and [39].

C.2 Transition matrices

By applying the transformation (3.5) to the maps $\tilde{g}_j$ and g_j we find the respective basic transition matrices $\widetilde{M}_j$ and M_j regarding each cycle. These are, for R,

$$\widetilde{M}_1 = \begin{bmatrix} \frac{c_{13}}{e_{12}} & 0 & 0 \\ \frac{c_{14}}{e_{12}} & 1 & 0 \\ \frac{c_{15}}{e_{12}} & 0 & 1 \end{bmatrix}, \qquad \widetilde{M}_2 = \begin{bmatrix} \frac{c_{21}}{e_{23}} & 0 & 0 \\ -\frac{e_{24}}{e_{23}} & 1 & 0 \\ \frac{c_{25}}{e_{23}} & 0 & 1 \end{bmatrix}, \qquad \widetilde{M}_3 = \begin{bmatrix} \frac{c_{32}}{e_{31}} & 0 & 0 \\ \frac{c_{34}}{e_{31}} & 1 & 0 \\ \frac{c_{35}}{e_{31}} & 0 & 1 \end{bmatrix}$$

and, for L,

$$M_2 = \begin{bmatrix} 1 & 0 & \frac{c_{21}}{e_{24}} \\ 0 & 1 & -\frac{e_{23}}{e_{24}} \\ 0 & 0 & \frac{c_{25}}{e_{24}} \end{bmatrix}, \qquad M_4 = \begin{bmatrix} 1 & 0 & \frac{c_{41}}{e_{45}} \\ 0 & 0 & \frac{c_{42}}{e_{45}} \\ 0 & 1 & \frac{c_{43}}{e_{45}} \end{bmatrix}, \qquad M_5 = \begin{bmatrix} 1 & \frac{c_{51}}{e_{52}} & 0 \\ 0 & \frac{c_{53}}{e_{52}} & 1 \\ 0 & \frac{c_{54}}{e_{52}} & 0 \end{bmatrix}.$$

In the same manner let $\widetilde{M}^{(j)}$ and $M^{(j)}$ denote the transition matrices for the return maps $\tilde{\pi}_j$ and π_j. Then,

$$\begin{aligned} \widetilde{M}^{(1)} = \widetilde{M}_3\widetilde{M}_2\widetilde{M}_1 &= \begin{bmatrix} \tilde{\rho} & 0 & 0 \\ \tilde{\tau} & 1 & 0 \\ \tilde{\theta} & 0 & 1 \end{bmatrix} & \qquad M^{(2)} = M_5M_4M_2 &= \begin{bmatrix} 1 & 0 & \mu \\ 0 & 1 & \nu \\ 0 & 0 & \rho \end{bmatrix} \\ \widetilde{M}^{(2)} = \widetilde{M}_1\widetilde{M}_3\widetilde{M}_2 &= \begin{bmatrix} \tilde{\rho} & 0 & 0 \\ \tilde{\nu} & 1 & 0 \\ \tilde{\mu} & 0 & 1 \end{bmatrix} & \qquad M^{(4)} = M_2M_5M_4 &= \begin{bmatrix} 1 & 0 & \gamma \\ 0 & 1 & \delta \\ 0 & 0 & \rho \end{bmatrix} \\ \widetilde{M}^{(3)} = \widetilde{M}_2\widetilde{M}_1\widetilde{M}_3 &= \begin{bmatrix} \tilde{\rho} & 0 & 0 \\ \tilde{\delta} & 1 & 0 \\ \tilde{\gamma} & 0 & 1 \end{bmatrix}, & \qquad M^{(5)} = M_4M_2M_5 &= \begin{bmatrix} 1 & \theta & 0 \\ 0 & \rho & 0 \\ 0 & \tau & 1 \end{bmatrix}. \end{aligned} \tag{C.8}$$

Appendix D

Transitions near the $\left(\mathrm{C}_2^-,\mathrm{C}_2^-\right)$-network

D.1 Maps between cross sections

We describe the construction of the return maps around the two heteroclinic cycles comprising of the $\left(C_2^-,C_2^-\right)$-network:

$$R=[\xi_1\to\xi_2\to\xi_4\to\xi_5\to\xi_1]\equiv[\xi_1\to\xi_2\to\xi_1]$$
$$L=[\xi_2\to\xi_3\to\xi_5\to\xi_6\to\xi_2]\equiv[\xi_2\to\xi_3\to\xi_2]\,.$$

To this end we write down the local and global maps, which approximate the dynamics of trajectories close to each heteroclinic cycle. As usual we assume that all transverse eigenvalues are negative whenever possible. Restricting to the relevant coordinates, local maps are, for the R-cycle,

$$\phi_{5,1,2}:H_1^{in,5}\to H_1^{out,2},\qquad \phi_{5,1,2}\left(x_2,x_3,x_4,x_6\right)=\left(x_3x_2^{\frac{c_{13}}{e_{12}}},x_4x_2^{\frac{c_{14}}{e_{12}}},x_2^{\frac{c_{15}}{e_{12}}},x_6x_2^{\frac{c_{16}}{e_{12}}}\right)$$

$$\phi_{1,2,4}:H_2^{in,1}\to H_2^{out,4},\qquad \phi_{1,2,4}\left(x_3,x_4,x_5,x_6\right)=\left(x_4^{\frac{c_{21}}{e_{24}}},x_3x_4^{-\frac{e_{23}}{e_{24}}},x_5x_4^{\frac{c_{25}}{e_{24}}},x_6x_4^{\frac{c_{26}}{e_{24}}}\right),\qquad 0\le x_3<x_4^{\frac{e_{23}}{e_{24}}},$$

for the L-cycle,

$$\phi_{6,2,3}:H_2^{in,6}\to H_2^{out,3},\qquad \phi_{6,2,3}\left(x_1,x_3,x_4,x_5\right)=\left(x_1x_3^{\frac{c_{21}}{e_{23}}},x_4x_3^{-\frac{e_{24}}{e_{23}}},x_5x_3^{\frac{c_{25}}{e_{23}}},x_3^{\frac{c_{26}}{e_{23}}}\right),\qquad 0\le x_4<x_3^{\frac{e_{24}}{e_{23}}}$$

$$\phi_{2,3,5}:H_3^{in,2}\to H_3^{out,5},\qquad \phi_{2,3,5}\left(x_1,x_4,x_5,x_6\right)=\left(x_1x_5^{\frac{c_{31}}{e_{35}}},x_5^{\frac{c_{32}}{e_{35}}},x_4x_5^{\frac{c_{34}}{e_{35}}},x_6x_5^{\frac{c_{36}}{e_{35}}}\right)$$

and, for the transition between cycles,

$$\phi_{1,2,3}:H_2^{in,1}\to H_2^{out,3},\qquad \phi_{1,2,3}\left(x_3,x_4,x_5,x_6\right)=\left(x_3^{\frac{c_{21}}{e_{23}}},x_4x_3^{-\frac{e_{24}}{e_{23}}},x_5x_3^{\frac{c_{25}}{e_{23}}},x_6x_3^{\frac{c_{26}}{e_{23}}}\right),\qquad 0\le x_4<x_3^{\frac{e_{24}}{e_{23}}}$$

$$\phi_{6,2,4}:H_2^{in,6}\to H_2^{out,4},\qquad \phi_{6,2,4}\left(x_1,x_3,x_4,x_5\right)=\left(x_1x_4^{\frac{c_{21}}{e_{24}}},x_3x_4^{-\frac{e_{23}}{e_{24}}},x_5x_4^{\frac{c_{25}}{e_{24}}},x_4^{\frac{c_{26}}{e_{24}}}\right),\qquad 0\le x_3<x_4^{\frac{e_{23}}{e_{24}}}.$$

We derive the global maps by means of the symmetries. The equivariance of the vector field under $\mathbb{Z}_2^6$ implies that to leading order they are the identity map. Recall that the nodes are pairwise related by the symmetry $\varphi\left(x_1,x_2,x_3,x_4,x_5,x_6\right)=\left(x_4,x_5,x_6,x_1,x_2,x_3\right)$. We further use it to go back to the representative cross section in view of $H_4^{in,2}=\gamma H_1^{in,5}$ and $H_5^{in,3}=\gamma H_2^{in,6}$. For each heteroclinic connection the global maps take the form

$$\begin{aligned} \psi_{1,2}: H_1^{out,2} \to H_2^{in,1}, \qquad & \psi_{1,2}\left(x_3,x_4,x_5,x_6\right)=\left(x_3,x_4,x_5,x_6\right) \\ \psi_{2,1}: H_2^{out,4} \to H_1^{in,5}, \qquad & \psi_{2,1}\left(x_1,x_3,x_5,x_6\right)=\left(x_5,x_6,x_1,x_3\right) \end{aligned}$$

along the R-cycle, and

$$\begin{aligned} \psi_{2,3}: H_2^{out,3} \to H_3^{in,2}, \qquad & \psi_{2,3}\left(x_1,x_4,x_5,x_6\right)=\left(x_1,x_4,x_5,x_6\right) \\ \psi_{3,2}: H_3^{out,5} \to H_2^{in,6}, \qquad & \psi_{3,2}\left(x_1,x_2,x_4,x_6\right)=\left(x_4,x_6,x_1,x_2\right) \end{aligned}$$

along the L-cycle. We define the composition of the above-mentioned maps yielding for R

$$\begin{aligned} \tilde{g}_1: H_1^{in,5} \to H_2^{in,1}, \qquad & \tilde{g}_1=\psi_{1,2}\circ\phi_{5,1,2} \\ \tilde{g}_2: H_2^{in,1} \to H_1^{in,5}, \qquad & \tilde{g}_2=\psi_{2,1}\circ\phi_{1,2,4}, \end{aligned}$$

for L,

$$\begin{aligned} g_2: H_2^{in,6} \to H_3^{in,2}, \qquad & g_2=\psi_{2,3}\circ\phi_{6,2,3} \\ g_3: H_3^{in,2} \to H_2^{in,6}, \qquad & g_3=\psi_{3,2}\circ\phi_{2,3,5}, \end{aligned}$$

and, from one heteroclinic cycle to the other,

$$\begin{aligned} g_{RL}: H_2^{in,1} \to H_3^{in,2}, \qquad & g_{RL}=\psi_{2,3}\circ\phi_{1,2,3} \\ g_{LR}: H_2^{in,6} \to H_1^{in,5}, \qquad & g_{LR}=\psi_{2,1}\circ\phi_{6,2,4}. \end{aligned}$$

Then, the return maps around the R- and L-cycles are, respectively, given by

$$\begin{aligned} \tilde{\pi}_1=\tilde{g}_2\circ\tilde{g}_1: H_1^{in,5}\to H_1^{in,5}, \qquad & \tilde{\pi}_1\left(x_2,x_3,x_4,x_6\right)=\left(x_4^{\frac{c_{25}}{e_{24}}}x_2^{\tilde{\alpha}},\, x_6x_4^{\frac{c_{26}}{e_{24}}}x_2^{\tilde{\eta}},\, x_4^{\frac{c_{21}}{e_{24}}}x_2^{\tilde{\beta}},\, x_3x_4^{-\frac{e_{23}}{e_{24}}}x_2^{\tilde{\delta}}\right), \\ & 0\leq x_3<x_4^{\frac{e_{23}}{e_{24}}}x_2^{-\tilde{\delta}}, \end{aligned} \tag{D.1}$$

$$\begin{aligned} \tilde{\pi}_2=\tilde{g}_1\circ\tilde{g}_2: H_2^{in,1}\to H_2^{in,1}, \qquad & \tilde{\pi}_2\left(x_3,x_4,x_5,x_6\right)=\left(x_6x_5^{\frac{c_{13}}{e_{12}}}x_4^{\tilde{\theta}},\, x_5^{\frac{c_{14}}{e_{12}}}x_4^{\tilde{\mu}},\, x_5^{\frac{c_{15}}{e_{12}}}x_4^{\tilde{\rho}},\, x_3x_5^{\frac{c_{16}}{e_{12}}}x_4^{\tilde{\nu}}\right), \\ & 0\leq x_3<x_4^{\frac{e_{23}}{e_{24}}} \end{aligned} \tag{D.2}$$

and

$$\begin{aligned} \pi_2=g_3\circ g_2: H_2^{in,6}\to H_2^{in,6}, \qquad & \pi_2\left(x_1,x_3,x_4,x_5\right)=\left(x_4x_5^{\frac{c_{34}}{e_{35}}}x_3^{\nu},\, x_5^{\frac{c_{36}}{e_{35}}}x_3^{\mu},\, x_1x_5^{\frac{c_{31}}{e_{35}}}x_3^{\theta},\, x_5^{\frac{c_{32}}{e_{35}}}x_3^{\rho}\right), \\ & 0\leq x_4<x_3^{\frac{e_{24}}{e_{23}}}, \end{aligned}$$

$$\begin{aligned} \pi_3=g_2\circ g_3: H_3^{in,2}\to H_3^{in,2}, \qquad & \pi_3\left(x_1,x_4,x_5,x_6\right)=\left(x_4x_6^{\frac{c_{21}}{e_{23}}}x_5^{\eta},\, x_1x_6^{-\frac{e_{24}}{e_{23}}}x_5^{\delta},\, x_6^{\frac{c_{25}}{e_{23}}}x_5^{\alpha},\, x_6^{\frac{c_{26}}{e_{23}}}x_5^{\beta}\right), \\ & 0\leq x_1<x_6^{\frac{e_{24}}{e_{23}}}x_5^{-\delta} \end{aligned}$$

where

$$\tilde{\rho} = \frac{c_{25}}{e_{24}}\frac{c_{15}}{e_{12}} > 0 \qquad \rho = \frac{c_{25}}{e_{23}}\frac{c_{32}}{e_{35}} > 0$$

$$\tilde{\nu} = -\frac{e_{23}}{e_{24}} + \frac{c_{25}}{e_{24}}\frac{c_{16}}{e_{12}} \qquad \nu = -\frac{e_{24}}{e_{23}} + \frac{c_{25}}{e_{23}}\frac{c_{34}}{c_{35}}$$

$$\tilde{\mu} = \frac{c_{21}}{e_{24}} + \frac{c_{25}}{e_{24}}\frac{c_{14}}{e_{12}} > 0 \qquad \mu = \frac{c_{26}}{e_{23}} + \frac{c_{25}}{e_{23}}\frac{c_{36}}{e_{35}} > 0$$

$$\tilde{\delta} = \frac{c_{13}}{e_{12}} - \frac{c_{14}}{e_{12}}\frac{e_{23}}{e_{24}} \qquad \delta = \frac{c_{31}}{e_{35}} - \frac{c_{36}}{e_{35}}\frac{e_{24}}{e_{23}}$$

$$\tilde{\theta} = \frac{c_{26}}{e_{24}} + \frac{c_{25}}{e_{24}}\frac{c_{13}}{e_{12}} > 0 \qquad \theta = \frac{c_{21}}{e_{23}} + \frac{c_{25}}{e_{23}}\frac{c_{31}}{e_{35}} > 0$$

$$\tilde{\eta} = \frac{c_{16}}{e_{12}} + \frac{c_{14}}{e_{12}}\frac{c_{26}}{e_{24}} > 0 \qquad \eta = \frac{c_{34}}{e_{35}} + \frac{c_{36}}{e_{35}}\frac{c_{21}}{e_{23}} > 0$$

$$\tilde{\alpha} = \frac{c_{15}}{e_{12}} + \frac{c_{14}}{e_{12}}\frac{c_{25}}{e_{24}} > 0 \qquad \alpha = \frac{c_{32}}{e_{35}} + \frac{c_{36}}{e_{35}}\frac{c_{25}}{e_{23}} > 0$$

$$\tilde{\beta} = \frac{c_{14}}{e_{12}}\frac{c_{21}}{e_{24}} > 0, \qquad \beta = \frac{c_{36}}{e_{35}}\frac{c_{26}}{e_{23}} > 0.$$

We describe the visit to each heteroclinic cycle starting close to the other through the maps

$$\pi_{RL} = g_3 \circ g_{RL} : H_2^{in,1} \to H_2^{in,6}, \quad \pi_{RL}(x_3, x_4, x_5, x_6) = \left(x_4 x_5^{\frac{c_{34}}{e_{35}}} x_3^{\mu}, x_6 x_5^{\frac{c_{36}}{e_{35}}} x_3^{\nu}, x_5^{\frac{c_{31}}{e_{35}}} x_3^{\theta}, x_5^{\frac{c_{32}}{e_{35}}} x_3^{\rho} \right),$$
$$0 \leq x_4 < x_3^{\frac{e_{24}}{e_{23}}},$$

$$\pi_{LR} = \tilde{g}_1 \circ g_{LR} : H_2^{in,6} \to H_2^{in,1}, \quad \pi_{LR}(x_1, x_3, x_4, x_5) = \left(x_5^{\frac{c_{13}}{e_{12}}} x_4^{\tilde{\theta}}, x_1 x_5^{\frac{c_{14}}{e_{12}}} x_4^{\tilde{\mu}}, x_5^{\frac{c_{15}}{e_{12}}} x_4^{\tilde{\rho}}, x_3 x_5^{\frac{c_{13}}{e_{12}}} x_4^{\tilde{\nu}} \right),$$
$$0 \leq x_3 < x_4^{\frac{e_{23}}{e_{24}}}.$$

D.2 Transition matrices

In the new coordinates (3.5) the maps $\tilde{g}_j$ and g_j become linear, their structure being represented by basic transition matrices $\widetilde{M}_j$ and M_j. These are, for R,

$$\widetilde{M}_1 = \begin{bmatrix} \frac{c_{13}}{e_{12}} & 1 & 0 & 0 \\ \frac{c_{14}}{e_{12}} & 0 & 1 & 0 \\ \frac{c_{15}}{e_{12}} & 0 & 0 & 0 \\ \frac{c_{16}}{e_{12}} & 0 & 0 & 1 \end{bmatrix}, \qquad \widetilde{M}_2 = \begin{bmatrix} 0 & \frac{c_{25}}{e_{24}} & 1 & 0 \\ 0 & \frac{c_{26}}{e_{24}} & 0 & 1 \\ 0 & \frac{c_{21}}{e_{24}} & 0 & 0 \\ 1 & -\frac{e_{23}}{e_{24}} & 0 & 0 \end{bmatrix}$$

and, for L,

$$M_2 = \begin{bmatrix} 1 & \frac{c_{21}}{e_{23}} & 0 & 0 \\ 0 & -\frac{e_{24}}{e_{23}} & 1 & 0 \\ 0 & \frac{c_{25}}{e_{23}} & 0 & 1 \\ 0 & \frac{c_{26}}{e_{23}} & 0 & 0 \end{bmatrix}, \qquad M_3 = \begin{bmatrix} 0 & 1 & \frac{c_{34}}{e_{35}} & 0 \\ 0 & 0 & \frac{c_{36}}{e_{35}} & 1 \\ 1 & 0 & \frac{c_{31}}{e_{35}} & 0 \\ 0 & 0 & \frac{c_{32}}{e_{35}} & 0 \end{bmatrix}.$$

Transition matrices of the return maps $\tilde{\pi}_j$ and π_j are the products of the basic transition matrices of the form

$$\widetilde{M}^{(1)} = \widetilde{M}_2\widetilde{M}_1 = \begin{bmatrix} \tilde{\alpha} & 0 & \frac{c_{25}}{e_{24}} & 0 \\ \tilde{\eta} & 0 & \frac{c_{26}}{e_{24}} & 1 \\ \tilde{\beta} & 0 & \frac{c_{21}}{e_{24}} & 0 \\ \tilde{\delta} & 1 & -\frac{e_{23}}{e_{24}} & 0 \end{bmatrix}, \qquad \widetilde{M}^{(2)} = \widetilde{M}_1\widetilde{M}_2 = \begin{bmatrix} 0 & \tilde{\theta} & \frac{c_{13}}{e_{12}} & 1 \\ 0 & \tilde{\mu} & \frac{c_{14}}{e_{12}} & 0 \\ 0 & \tilde{\rho} & \frac{c_{15}}{e_{12}} & 0 \\ 1 & \tilde{\nu} & \frac{c_{16}}{e_{12}} & 0 \end{bmatrix} \tag{D.3}$$

and

$$M^{(2)} = M_3M_2 = \begin{bmatrix} 0 & \nu & 1 & \frac{c_{34}}{e_{35}} \\ 0 & \mu & 0 & \frac{c_{36}}{e_{35}} \\ 1 & \theta & 0 & \frac{c_{31}}{e_{35}} \\ 0 & \rho & 0 & \frac{c_{32}}{e_{35}} \end{bmatrix}, \qquad M^{(3)} = M_2M_3 = \begin{bmatrix} 0 & 1 & \eta & \frac{c_{21}}{e_{23}} \\ 1 & 0 & \delta & -\frac{e_{24}}{e_{23}} \\ 0 & 0 & \alpha & \frac{c_{25}}{e_{23}} \\ 0 & 0 & \beta & \frac{c_{26}}{e_{23}} \end{bmatrix},$$

respectively.